RICE UNIVERSITY

Insights into Peroxisome Matrix Protein Import and IBA Metabolism Through Analysis of IBA-response Mutants

by

Naxhiely Martinez

A THESIS SUBMITTED IN
PARTIAL FULFILLMENT OF THE
REQUIREMENTS FOR THE DEGREE

Doctor of Philosophy

APPROVED, THESIS COMMITTEE:

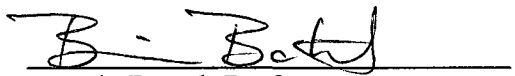

Bonnie Bartel, Professor
Biochemistry and Cell Biology

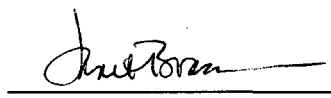

Janet Braam, Professor, Chair
Biochemistry and Cell Biology

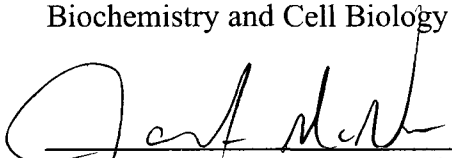

James McNew, Associate Professor
Biochemistry and Cell Biology

Michael Stern, Professor
Biochemistry and Cell Biology

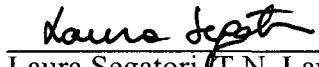

Laura Segatori, T.N. Law Assistant Professor; Assistant Professor, Bioengineering/Chemical and Biomolecular Engineering

Houston, TX
January 2010

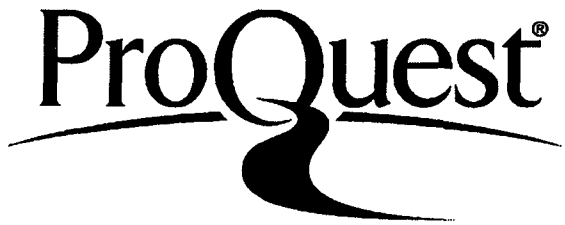

ProQuest LLC
789 East Eisenhower Parkway
P.O. Box 1346
Ann Arbor, MI 48106-1346

ABSTRACT

Insights into Peroxisome Matrix Protein Import and IBA Metabolism Through Analysis of IBA-response Mutants

by

Naxhiely Martínez

Peroxisomes are single membrane-bound organelles that function to compartmentalize certain metabolic reactions critical to plant and animal development. I have studied peroxisomal processes in the model plant *Arabidopsis thaliana,* with a focus on the import of matrix proteins from the cytoplasm into the organelle matrix and the metabolism of the plant hormone indole-3-butryic acid (IBA). In this thesis, I describe my characterization of *Arabidopsis thaliana* peroxisome defective mutants isolated through forward and reverse genetic screens in physiological and biochemical assays.

Peroxisome import depends on more than a dozen peroxin (PEX) proteins, with PEX5 and PEX7 serving as receptors that shuttle proteins bearing a peroxisome targeting sequence (PTS) into the organelle. PEX5 is the PTS1 receptor, PEX7 is the PTS2 receptor, and in both plants and mammals, PEX7 depends upon PEX5 binding to deliver PTS2 cargo into the peroxisome. I found a *pex7* missense mutation, *pex7-2*, that disrupts PEX7-cargo binding and PEX7-PEX5 interactions in yeast, as well as PEX7 accumulation in plants. I examined localization of peroxisomally-targeted GFP derivatives in light-grown *pex7* mutants and, surprisingly, observed defects not only in PTS2 import, but also in PTS1 protein import. These PTS1 import defects were accompanied by a decrease in PEX5 accumulation in light-grown *pex7* mutants. Together, these data suggest that PEX5 and PTS1 import depend on the PEX7 PTS2 receptor in *Arabidopsis* and reveal a role for the environment in modulating peroxin function.

Genetic evidence suggests that indole-3-butyric acid (IBA) is converted to the auxin indole-3-acetic acid (IAA) in *Arabidopsis* peroxisomes. The IBR1, IBR3, and IBR10 proteins contain peroxisomal targeting signals and are candidates for catalyzing the various steps of IBA β-oxidation. My analysis of the *ibr* mutants has provided evidence for the importance of the IBR enzymes and insight into the roles of IAA that derives from IBA β-oxidation.

In humans, deficiencies in peroxins underlie the peroxisomal biogenesis disorders, which are frequently lethal in early infancy. Advancing our understanding of peroxisome biogenesis and metabolism in a genetically distinct model system will allow the continued refinement of our understanding of these essential organelles.

ACKNOWLEDGEMENTS

There are many people who helped contribute to my success as a graduate student. I would like to thank:

My advisor Dr. Bonnie Bartel—Thank you for being an exceptional mentor, teacher, and boss. I know that my extremely positive graduate school experience is due to her dedication as a mentor and the wonderful work environment that she creates for us. She has always been actively involved in all of the research going on in the lab and is thus always available when advice is needed. I would like to thank her also for all the encouragement, reassurance, understanding, and for posting random anecdotes about research on the lab door throughout all the ups and downs of being in graduate school and working in research. Thank you Bonnie for investing in my education as a researcher and helping me become comfortable with the fact that the more I learn, the less I know!

My coworkers, past and present—Thank you to Bethany Zolman who showed me the ropes and guided me through my first research project in the lab. Thank you to Dereth Phillips, Sarah Ratzel, Kristen Rogers, Erica Solís, and Lucia Strader for not just being extremely helpful coworkers but also wonderful friends. Thank you to Andrew Woodward and Melanie Monroe-Augustus for all the insight on the PEX projects and the many entertaining lunch conversations. Thank you to Rebekah Rampey for the sunshine she brought into my life every summer that she came back to the lab. Thank you to Jeanne Rasbery and Diana Dugas, the senior graduate students when I started out, for always being eager to answer my questions and for all the countless advice about graduate school. I would like to thank rotation students Tyler Moss (assisted with the creation of the PED1 constructs), Neda Nikravan (assisted in the mapping of B1017/*pex7-2*), and Kalie Van Ree (assisted with isolation of doubles) for assistance on

the PEX7 project. Thank you to graduate student Sarah Christensen and undergraduate students Karie Runcie and Arthur Millius for all their help.

My family and friends—Thank you for all your love, support, and encouragement. A special thanks goes out to Angela Martinez, my youngest sister, who worked with me in the lab in the summer of 2008, and to my husband, Michael Ramón, for putting up with my weird work schedule and helping me harvest and water plants on occasion.

Last, but certainly not least, I would like to thank my committee members for sharing their wisdom and new ideas and guiding me in the right direction these past five years.

TABLE OF CONTENTS

FIGURES

TABLES

ABBREVIATIONS

2,4-D	2,4-dichlorophenoxyacetic acid
2,4-DB	2,4-dichlorophenoxybutyric acid
4-CL-like	4-coumarate:CoA-ligase-like
BLAST	Basic Local Alignment Search Tool
AIM	abnormal inflorescence meristem
ACX	acyl-CoA oxidase
Col-0	Columbia
DTT	dithiothreitol
EDTA	ethylenediaminetetraacetic acid
EMS	ethyl methane sulfonate
F1, F2, etc.	filial generation 1, 2, etc,
FG	forward genetics
GFP	green fluorescent protein
IAA	indole-3-acetic acid
IBA	indole-3-butyric acid
ibr	IBA response
ICapA	indole-3-caproic acid
KAT	3-ketoacyl-CoA thiolase
LACS	long-chain acyl CoA synthetase
L*er*	Landsberg *erecta*
M1, M2, etc.	mutagenized plant generation 1, 2, etc.
MFP	multifunctional protein
NAA	1-napthalacetic acid
PCR	polymerase chain reaction
PED	peroxisome defective
PEX	peroxin

PN	plant nutrient medium
PNS	plant nutrient medium supplemented with sucrose
PTS1/PTS2	peroxisome targeting signal type 1 and 2
RG	reverse genetics
T-DNA	transfer-DNA
T1, T2, etc.	transformant generation 1, 2, etc.
TILLING	Targeting Induced Local Lesions in Genomes
Tris	Tris Hydroxymethylaminoethane
Triton	octylpheoxypolyethoxyethanol polyethylene glycol-*p*-isooctylphenyl ether
UBC	ubiquitin-conjugating
Ws	Wassilewskija
Wt	wild type

Chapter 1: Introduction

1.1. Peroxisomes

Peroxisomes compartmentalize certain metabolic reactions, perhaps to protect cytoplasmic proteins from oxidative stress. Two processes common to peroxisomes in all eukaryotes studied are fatty acid β-oxidation and hydrogen peroxide decomposition. Peroxisomes are also the destination for other processes, many involving oxidation, that vary by species and developmental stage or cell type.

1.1.A. Mammalian peroxisomes

In mammals, peroxisomes house the biosynthesis of various compounds such as cholesterol and fatty acids (Hodge et al., 1991; Baes et al., 2000). Mammalian peroxisomes are also the site for the degradation of compounds such as prostaglandins and polyamines (Reddy and Hashimoto, 2001). Defects in peroxisome biogenesis can lead to severe genetic disorders in humans. Mutations in the gene that encodes a peroxisome receptor *PEX5* cause diseases such as Zellweger syndrome and neonatal adrenoleukodystrophy (Dodt et al., 1995). Defects in *PEX7*, another peroxisome receptor, lead to the development of infantile refsum disease (van den Brink et al., 2003) and rhizomelic chondrodysplasia punctata (Braverman et al., 1997; Motley et al., 1997; Purdue et al., 1997). These peroxisome disorders are characterized by deficiencies in peroxisome formation or function leading to developmental abnormalities that are generally fatal in early infancy.

1.1.B. Fungal peroxisomes

In yeasts and other fungi, peroxisomes are required for utilization of certain carbon sources such as fatty acids (Erdmann et al., 1989; Cregg et al., 1990). Fungal peroxisomes are involved in the biosynthesis of penicillin and lysine as well as the degradation of amino acids and methanol (reviewed in Michels et al., 2005). Much of

what we know about peroxisome biogenesis has emerged from screens for yeast mutants unable to grow on carbon sources that require peroxisomes for utilization.

1.1.C. Plant peroxisomes

Plant peroxisomes are implicated in the biosynthesis of several phytohormones, house certain photorespiration enzymes, and participate in various degradative processes (reviewed in Hayashi and Nishimura, 2003). In plants, peroxisomes are required for germination, seed oil quality, photosynthetic efficiency, and plant defense. Null mutations in *Arabidopsis* PEX2, PEX10, and PEX12 are embryo lethal (Hu et al., 2002; Schumann et al., 2003; Sparkes et al., 2003; Fan et al., 2005), implying an essential role for plant peroxisomes during embryonic development.

1.2. Peroxisome biogenesis

Peroxin (PEX) proteins are defined as being necessary for peroxisome biogenesis and function. More than 30 peroxins have been identified in yeasts and mammals (reviewed in Wanders and Waterham, 2004). Forward and reverse genetics approaches, as well as sequence similarity analyses, have helped identify the plant peroxins summarized in Table 1-1. Genetic studies have revealed that these plant peroxins are involved in many processes including embryogenesis, seedling establisment, photomorphogeneis, and photorespiration (reviewed in Hayashi and Nishimura, 2003).

Peroxisome biogenesis can be divided into three stages: 1) insertion of peroxisomal membrane proteins, 2) import of peroxisomal matrix proteins, and 3) peroxisome proliferation (reviewed in Brown and Baker, 2003). Though peroxisomal processes have been studied extensively, many questions remain about the biogenesis of peroxisomes. Moreover, many of the studies of peroxisome function have been conducted in fungal or animal systems, and whether plant peroxisomes function similarly has not been fully explored. This project is concentrated on developing a more complete

Table 1-1. *Arabidopsis PEX* genes and mutants isolated through forward and reverse genetics

Name	Gene	Mutant	Isolation	References
PEX1	At5g08470	*pex1i*	RG (RNAi)	(Nito et al., 2007)
PEX2	At1g79810	*ted3*	FG (EMS)	(Hu et al., 2002)
		pex2	RG (T-DNA)	(Hu et al., 2002)
		pex2i	RG (RNAi)	(Nito et al., 2007)
PEX3.1	At1g48640			
		pex3-1/3-2i	RG (RNAi)	(Nito et al., 2007)
PEX3.2	At3g18160			
PEX4	At5g25760	*pex4-1*	FG (EMS)	(Zolman et al., 2005)
PEX5	At5g56290	*pex5-1*	FG (EMS)	(Zolman et al., 2000)
		pex5i	RG (RNAi)	(Hayashi et al., 2005)
		pex5-10	RG (T-DNA)	(Zolman et al., 2005)
PEX6	At1g03000	*pex6-1*	FG (EMS)	(Zolman and Bartel, 2004)
PEX7	At1g29260	*pex7-1*	RG (T-DNA)	(Woodward and Bartel, 2005)
		pex7i	RG (RNAi)	(Hayashi et al., 2005)
		pex7-2	FG (EMS)	This study
PEX10	At2g26350	*pex10*	RG (T-DNA)	(Schumann et al., 2003; Sparkes et al., 2003)
PEX11.1	At1g47750	PEX11aRNAi,		
		PEX11bRNAi,	RG (RNAi)	(Nito et al., 2007)
PEX11.2	At3g47430	*PEX11a/11bi*		
PEX11.3	At1g01820	PEX11cRNAi,		
PEX11.4	At2g45740	PEX11dRNAi,	RG (RNAi)	(Nito et al., 2007)
		PEX11eRNAi,		
PEX11.5	At3g61070	*PEX11c/11d/11ei*		
PEX12	At3g04460	*apm4*	FG (EMS)	(Mano et al., 2006)
		pex12	RG (T-DNA)	(Fan et al., 2005)
		pex12i	RG (RNAi)	(Nito et al., 2007)
PEX13	At3g07560	*apm2*	FG (EMS)	(Mano et al., 2006)
		pex13i	RG (RNAi)	(Nito et al., 2007)
PEX14	At5g62810	*ped2*	FG (EMS)	(Hayashi et al., 2000)
PEX16	At2g45690	*sse1*	FG (T-DNA)	(Lin et al., 2004)
		pex16i	RG (RNAi)	(Nito et al., 2007)
PEX17	At4g18195	--		
	At4g18197	--		
	At4g18205	--		
PEX19.1	At3g03490	*pex19-1i*	RG (RNAi)	(Nito et al., 2007)
PEX19.2	At5g17550	*pex19-2i*	RG (RNAi)	(Nito et al., 2007)
PEX22	At3g21865	*pex22-1*	RG (T-DNA)	(Zolman et al., 2005)

FG, forward genetics from EMS-mutagenized seeds; FG (TDNA), forward genetics from T-DNA inserted mutants; RG, reverse genetics; (Modified from Hayashi and Nishimura, 2006).

understanding of peroxisomal matrix protein import in the model plant *Arabidopsis thaliana*.

1.3. Peroxisomal matrix protein import

Because peroxisomes lack DNA, all necessary proteins are encoded in the nucleus and imported posttranslationally from the cytosol. A remarkable feature that distinguishes peroxisomal import from most organellar import is that peroxisomes can import oligomeric and fully folded proteins (McNew and Goodman, 1994; Kato et al., 1999). There are two well-characterized signals that can direct proteins to enter the peroxisome matrix. The peroxisome targeting signal 1, or PTS1, consists of variants of a Ser-Lys-Leu (SKL) sequence at the extreme carboxyl terminus of the protein (Gould et al., 1989; Mullen, 2002; Neuberger et al., 2004). The second signal, PTS2, is an amino-terminal nonapeptide variant of an Arg-Leu-$(X)_5$-His-Leu sequence in the first ~30 amino acids of the protein (Osumi et al., 1991; Flynn et al., 1998). In *Arabidopsis*, there are nine major ("present in at least ten sequences in three different orthologous groups"; (Reumann, 2004; Reumann et al., 2004) PTS1 tripeptides, with SKL and SRL occurring most commonly, and 11 minor ("present in at least two sequences"; (Reumann, 2004; Reumann et al., 2004) PTS1 tripeptides (Reumann, 2004; Reumann et al., 2004). *Arabidopsis* also has two major PTS2 peptides, Arg-Leu-$(X)_5$-His-Leu and Arg-Ile-$(X)_5$-His-Leu, and nine minor PTS2 peptides (Reumann, 2004; Reumann et al., 2004).

Although PTS1-containing proteins are more common than PTS2-containing proteins in all examined organisms, PTS2 proteins appear to comprise about 26% of plant peroxisomal proteins (Kamada et al., 2003; Reumann et al., 2004), including several enzymes necessary for fatty acid β-oxidation that are essential for normal seedling development (Hayashi et al., 1998; Hooks et al., 1999; Eastmond et al., 2000; Adham et al., 2005; Pracharoenwattana et al., 2005; Pracharoenwattana et al., 2007).

There are two PTS receptors that bind and escort cargo proteins from the cytoplasm to the peroxisome for import: PEX5 and PEX7. PEX5 recognizes PTS1-containing proteins (Brocard et al., 1994; Dodt et al., 1995; Fransen et al., 1995) and PEX7 is the receptor for proteins with a PTS2 (Rehling et al., 1996). Both receptor and cargo bind a docking complex composed of the membrane proteins PEX13 and PEX14 (reviewed in Brown and Baker, 2008) and are then translocated to the peroxisome (Dammai and Subramani, 2001) in a manner dependent on the zinc-finger proteins PEX2, PEX10, and PEX12 (Dodt and Gould, 1996), where the cargo dissociates from the receptors (Dammai and Subramani, 2001). Upon entrance into the peroxisomal matrix, PTS2 proteins, such as 3-ketoacyl-CoA thiolase (thiolase), are processed into a mature form in animals and plants by removal of the N-terminal recognition sequence (Preisig-Muller and Kindl, 1993; Kato et al., 1996). The receptors are recycled back to the cytoplasm through a process involving PEX1, PEX2, PEX6, PEX10, and PEX12 in mammals and PEX1, PEX2, PEX4, PEX6, PEX8, and PEX22 in yeast, where they are free to undergo further rounds of import (reviewed in Titorenko and Rachubinski, 2001)

1.4. The PEX5 and PEX7 matrix protein receptors

1.4.A. PEX5.

PEX5 is made up of multiple C-terminal tetratricopeptide and N-terminal pentapeptide repeats that are involved in PTS1 recognition (Figure 1.1; Dodt et al., 1995; Terlecky et al., 1995; Gatto et al., 2000) and PEX13/PEX14 binding (Schliebs et al., 1999), respectively. A PEX7 binding domain lies within the pentapeptide repeat region in mammalian and plant PEX5 (Figure 1.1).

1.4.B. PEX7.

PEX7 was first discovered in *S. cerevisiae* (Marzioch et al., 1994) and is a member of the WD-40 repeat family (Figure 1.2). WD-40 proteins usually consist of

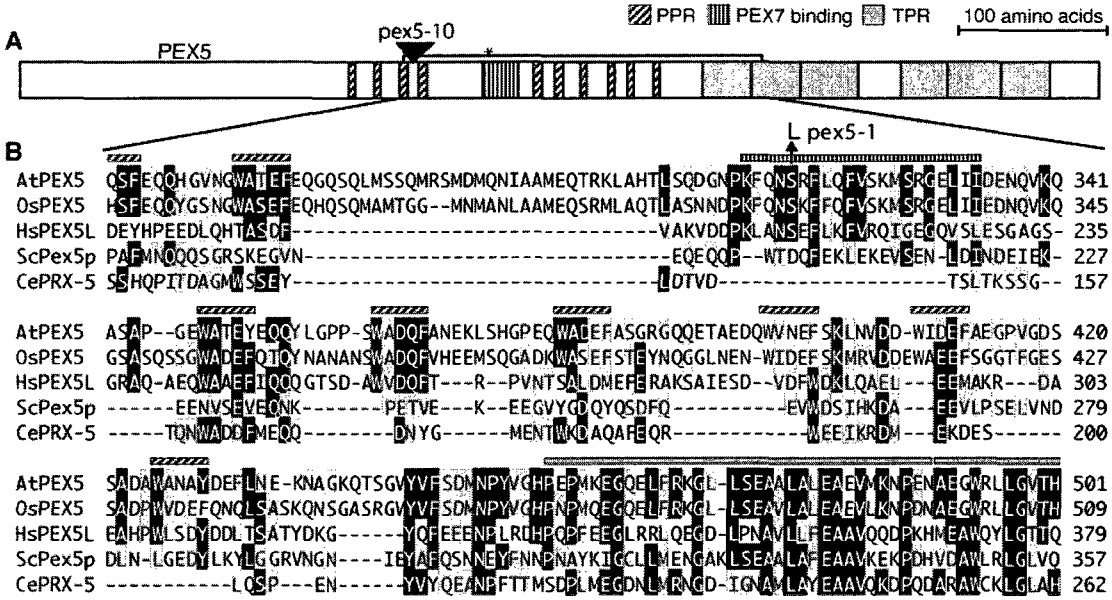

Figure 1.1. PEX5 domain structure and alignment.

A. Schematic showing domain architecture of PEX5. The region within the bracket is the region represented in B, the asterisk marks the Ser to Leu mutation in *pex5-1*. B. Amino acid alignment of PEX5 proteins from *Arabidopsis thaliana* (At), rice (*Oryza sativa*, Os), human (Hs), *Saccharomyces cerevisiae* (Sc), and *Caenorhabditis elegans* (Ce). The PEX7 binding domain lies within the pentapeptide repeat region. The *pex5-1* mutant contains a serine to leucine mutation in the presumed PEX7 binding site. *pex5-10* contains a T-DNA insertion in exon 5. Black and gray shading denote conserved residues and similar residues, respectively. (Figure modified from Woodward and Bartel, 2005)

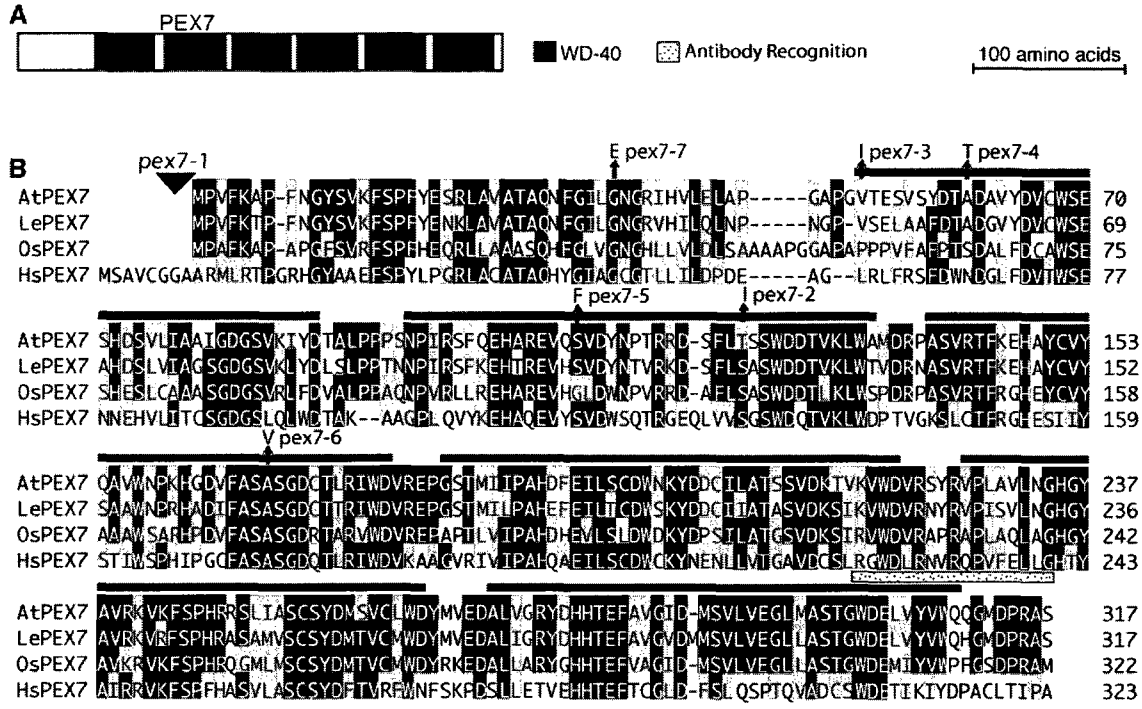

Figure 1.2. PEX7 alignment.

A. Schematic showing domain architecture of PEX7. PEX7 is comprised of six WD-40 domains, indicated by black bars. B. Amino acid alignment of PEX7 proteins from *Arabidopsis* (At), tomato (Le), rice (Os), and human (Hs). *pex7-1* contains a T-DNA insertion (triangle) 95 bp upstream of the initiator ATG. *pex7-2* contains a threonine to isoleucine missense (arrow *pex7-2*) mutation in the coding region. Five TILLING mutants have been isolated (arrows *pex7-3–pex7-7*). Our PEX7 antibody was raised against a peptide comprising the C-terminal 17 amino acids of PEX7 (stippled bar). Black and gray shading denote conserved residues and similar residues, respectively. (Figure modified from Woodward and Bartel, 2005).

seven ~40 amino acid stretches that often end in Trp-Asp (Neer et al., 1994). Although the crystal structure of PEX7 has not been reported, other WD-40 proteins fold into β-propeller structures and serve as scaffolds for protein-protein interactions (Chothia et al., 1997; Smith et al., 1999).

1.5. Receptor-cargo recognition

Receptor-cargo recognition differs between mammals and yeast. Some of these differences can be explained by the observation that mammals have long (PEX5L) and short (PEX5S) isoforms of PEX5 that result from alternative splicing; both isoforms can bind the PTS1, but only PEX5L binds to PEX7 and functions in PTS2 import (Figure 1.3; Braverman et al., 1998; Otera et al., 1998). *Arabidopsis* appears to only encode a PEX5L isoform, which is required for both PTS1 and PTS2 import (Figure 1.3.A; Neer et al., 1994; Wanders and Waterham, 2004; Hayashi et al., 2005; Woodward and Bartel, 2005). Like humans, rice has two PEX5 splice isoforms, and only the longer isoform binds PEX7 (Figure 1.3.C; Lee et al., 2006). Yeast PEX5 resembles PEX5S; the PEX7-binding domain of mammalian PEX5L is similar to the PEX7-binding region in *S. cerevisiae* proteins PEX18 and PEX21 (Dodt et al., 2001; Otera et al., 2002), functionally redundant proteins that are believed to play the role in the yeast PTS2 import pathway that is served by PEX5L in other organisms (Figure 1.3.D; Stein et al., 2002). In other fungi, such as *Neurospora crassa* and *Yarrowia lipolytica*, PEX18 and PEX21 are replaced by a single PEX20 protein (Figure 1.3.E; Sichting et al., 2003), which in *Hansenula polymorpha* has been shown to bind PTS2 sequences (Otzen et al., 2005). No interaction between PEX18/PEX21 and PTS2 has been demonstrated. Interestingly, the nematode *C. elegans* completely lacks PEX7 and the corresponding PTS2 import pathway; proteins that contain a PTS2 in other organisms are PTS1-targeted in *C. elegans* (Figure 1.3.B; Gurvitz et al., 2000; Motley et al., 2000).

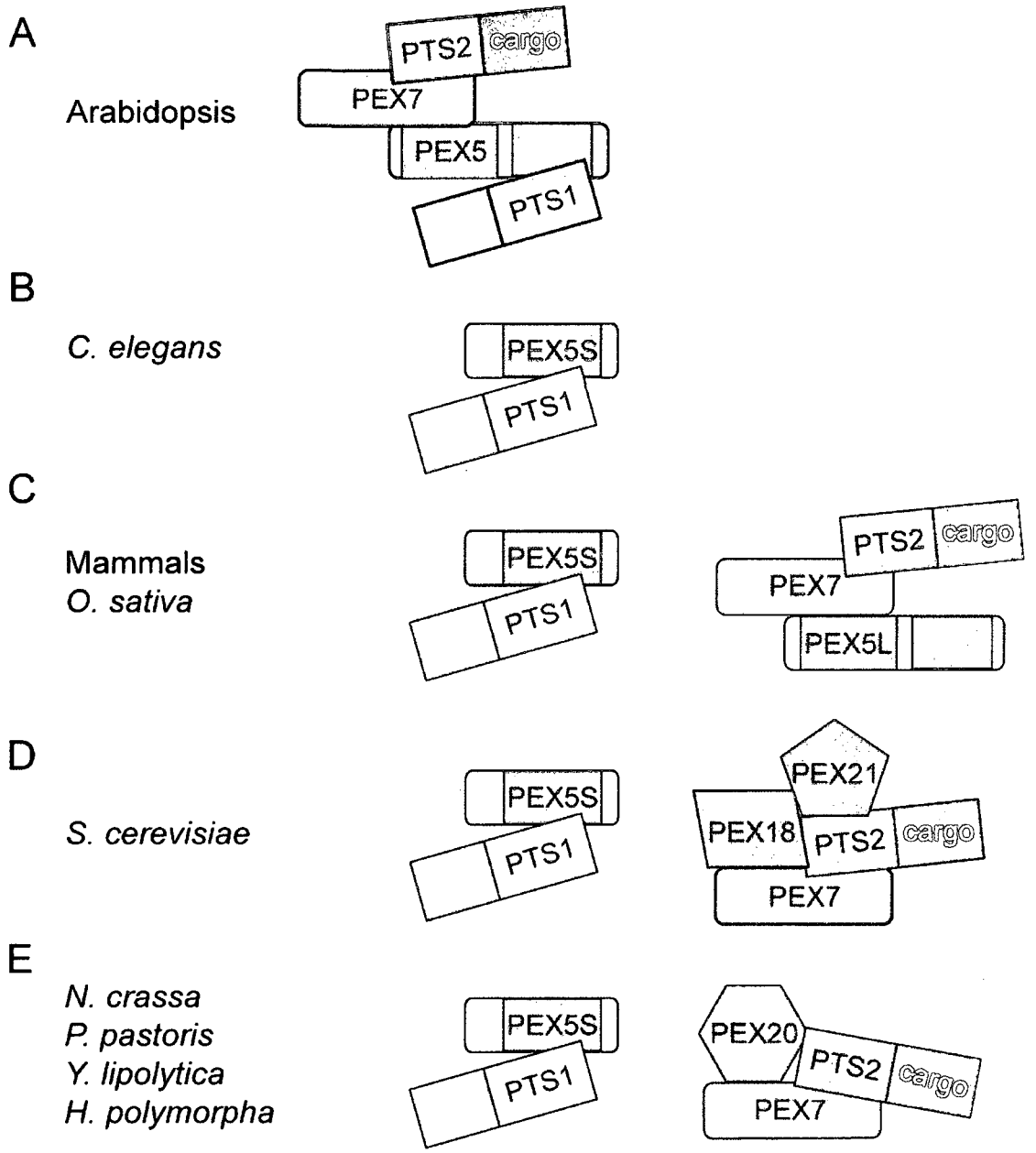

Figure 1.3. A comparison of receptor cargo recognition in different organisms.

A. *Arabidopsis* PEX7 is dependent on PEX5 for entrance into the peroxisome. B. *C. elegans* has no PEX7 and all peroxisomal proteins are targeted via PEX5. C. Mammals and rice (*O. sativa*) have long (L) and short (S) isoforms of PEX5 that result from alternative splicing. D. *S. cerevisiae* PEX18 and PEX21 have a PEX7 binding domain similar to the PEX5L mammalian isoform and serve as co-receptors with PEX7. E. Other fungi replace PEX18 and PEX21 with the single PEX20 chaperone. (Redrawn from Brown and Baker, 2008).

1.6. Membrane docking

In addition to differences in interactions between the receptors, the binding of the PEX5 and PEX7 with the membrane peroxins comprising the docking complex also differs in various species. In mammals, plants, and some yeasts, PEX13 and PEX14 make up the docking complex (Figure 1.4). PEX17 is also part of the docking complex in *S. cerevisiae*.

Yeast PEX5 interacts with PEX13 and PEX14 in yeast two-hybrid assays (Elgersma et al., 1996; Albertini et al., 1997). *In vitro* binding assays have shown that yeast PEX5 has a higher binding affinity to PEX14 than PEX13 and that binding to PEX13 is dramatically reduced when PEX5 is cargo-bound (Urquhart et al., 2000). In *P. pastoris*, the PEX7 chaperone protein PEX20 binds PEX14 through the same motif required in PEX5 for PEX14 binding (Leon et al., 2006).

Yeast PEX7 interacts with PEX13, PEX14, and thiolase in yeast two-hybrid assays and coimmunoprecipitates with PEX14 and PEX5 (Elgersma et al., 1996; Albertini et al., 1997; Stein et al., 2002). Yeast PEX14 possesses two independent PEX5 binding sites and one PEX7 binding site (Niederhoff et al., 2005). Moreover, PEX14, but not PEX13, binds thiolase, and this interaction is disrupted in a yeast *pex7* deletion mutant, implying that PEX14 is critical for PTS2 protein import in yeast (Stein et al., 2002).

In contrast to what occurs in yeast, where PEX5 and PEX7 appear to independently interact with the docking peroxins, human PEX7 depends on PEX5 for docking at the peroxisome (Braverman et al., 1998; Matsumura et al., 2000; Dodt et al., 2001; Sparkes and Baker, 2002; Johnson and Olsen, 2003). In mammals, PEX7 coimmunoprecipitates with PEX5 (Matsumura et al., 2000; Otera et al., 2000) and *in vitro* studies have shown that PEX5 bridges the binding of PEX7 and its cargo to PEX14 (Otera et al., 2000). Similarly, *Arabidopsis* PEX7 binds PEX5, but not PEX14, in a yeast

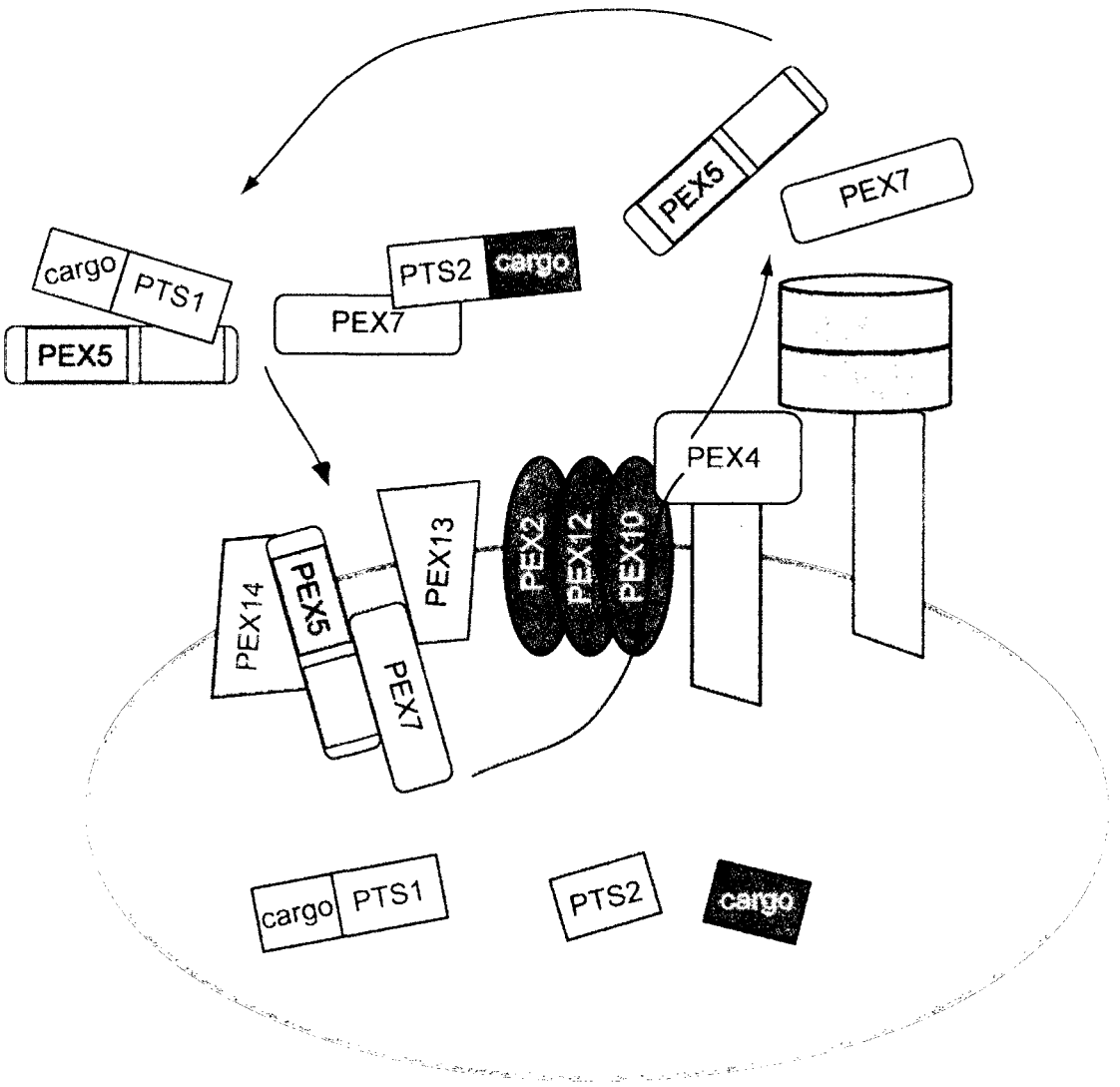

Figure 1.4 Model of PTS1 and PTS2 import in plants based on what is known in mammals, fungi, and plants.

Upon recognition of cargo, the PEX5 and PEX7 receptors bind the membrane docking complex consisting of PEX13 and PEX14. The receptors are translocated into the peroxisome where they release their cargo. Receptor recycling is dependent on the RING finger complex made up of PEX2, PEX10, and PEX12, which, in yeast, is anchored to the docking complex via PEX8. PEX5 is monoubiquitinated by the E2 ubiquitin conjugating enzyme PEX4, anchored to the peroxisomal membrane via PEX22, prior to release from the membrane. Little is known about PEX7 recycling. Receptor recycling also requires the action of the AAA-proteins PEX1 and PEX6, which are anchored to the peroxisome membrane via PEX15 in yeast and PEX26 in mammals. After the receptors are recycled back out into the cytosol, they are free to undergo further rounds of import. The PTS2 peptide is removed following import in plants and mammals.

two-hybrid assay (Figure 1.4; Nito et al., 2002); unlike yeast, there is no demonstrated PEX14-PEX7 interaction in mammals or plants. The N-terminal portion of *Arabidopsis* PEX13 interacts with PEX7, but not PEX5, in the yeast two-hybrid assay (Figure 1.4; Mano et al., 2006). However, mutations in PEX14 (Hayashi et al., 2000) and PEX13 (Mano et al., 2006) have deficiencies in both PTS1 and PTS2 import, implying that although PEX7 and PEX5 do not bind both membrane proteins in yeast two-hybrid assays, PEX7 and PEX5 may still depend on both proteins for translocation into the peroxisome.

1.7. Translocation and receptor recycling

Although both PEX5 and PEX7 appear to enter the peroxisome, it is still unclear whether the two proteins remain membrane bound (simple shuttle hypothesis) when they release their cargo to the peroxisome matrix or whether they are completely released into the peroxisome matrix (extended shuttle hypothesis) (Figure 1.4). Regardless of how completely the receptors enter the peroxisome, both proteins are cycled back out into the cytosol for further rounds of import (Figure 1.4). The details of both translocation and recycling also reveal differences among different species.

1.7.A. PEX5 and PEX7 co-receptor recycling

S. cerevisiae PEX5 (Rehling et al., 2000) and PEX20 (Smith and Rachubinski, 2001) interact with the intraperoxisomal PEX8 protein, suggesting translocation into the peroxisome. *H. polymorpha* PEX8 may also play a role in cargo release (Wang et al., 2003). However, PEX8 homologs are not found in animals or plants. Mammalian PEX5 data are consistent with the extended shuttle mechanism (Dammai and Subramani, 2001). There is no evidence for PEX18 and PEX21 entering the peroxisome and little is known about how PEX5 is translocated into *Arabidopsis* peroxisomes.

PEX5 recycling (Figure 1.4) back out into the cytosol requires the membrane RING finger peroxins PEX2, PEX10, and PEX12, the E2 ubiquitin conjugating (UBC)

enzyme PEX4, and the interacting AAA-ATPases PEX1 and PEX6. PEX4 is linked to the peroxisome membrane via PEX22 in yeast and plants (Koller et al., 1999; Zolman et al., 2005). PEX4 and PEX22 have not been identified in mammals, but a cytosolic UBC that plays the role of PEX4 in mammals has been described (Grou et al., 2008). PEX1 and PEX6 are anchored to the peroxisome via PEX15 in yeast (Birschmann et al., 2003) and PEX26 in mammals (Matsumoto et al., 2003). No *Arabidopsis* homolog for PEX15/PEX26 has been identified.

The PEX2/10/12 RING complex, which is likely serving the role of an E3 ubiquitin ligase (Lazarow, 2003), combined with the UBC enzyme PEX4, facilitates monoubiquitination of PEX5 and the PEX7 co-receptors PEX18 and PEX20 (reviewed in Brown and Baker, 2008). Yeast PEX12 (Platta et al., 2009), PEX1, and PEX6 may also be involved in recognition of monoubiquitinated PEX5 and subsequent removal from the membrane (reviewed in Brown and Baker, 2008).

In the absence of efficient removal from the peroxisome membrane, PEX5, PEX18, and PEX20 can be polyubiquitinated through the action of UBC1/4/5 (reviewed in Brown and Baker, 2008) and PEX2 (yeast) (Platta et al., 2009). These polyubiquitinated proteins may be degraded by the 26S proteasome (Figure 1.5).

1.7.B. PEX7 recycling

Although PEX7 translocates in and out of yeast peroxisomes (Nair et al., 2004), the molecular details of how this process occurs remain obscure. *Arabidopsis pex4* and *pex6* mutants have PTS2 import defects, suggesting a role for these proteins in PEX7 recycling (Zolman and Bartel, 2004; Zolman et al., 2005). A recent study has shown that *Arabidopsis* PEX7 interacts with the RING-finger protein PEX12 (Singh et al., 2009); PEX12 has been implicated in monoubiquitination of PEX5 in yeast (Platta et al., 2009). Although no evidence of PEX7 ubiquitination has been reported, PEX7 co-receptors (PEX5, PEX18, PEX20) are known to be ubiquitinated and recycled (reviewed in

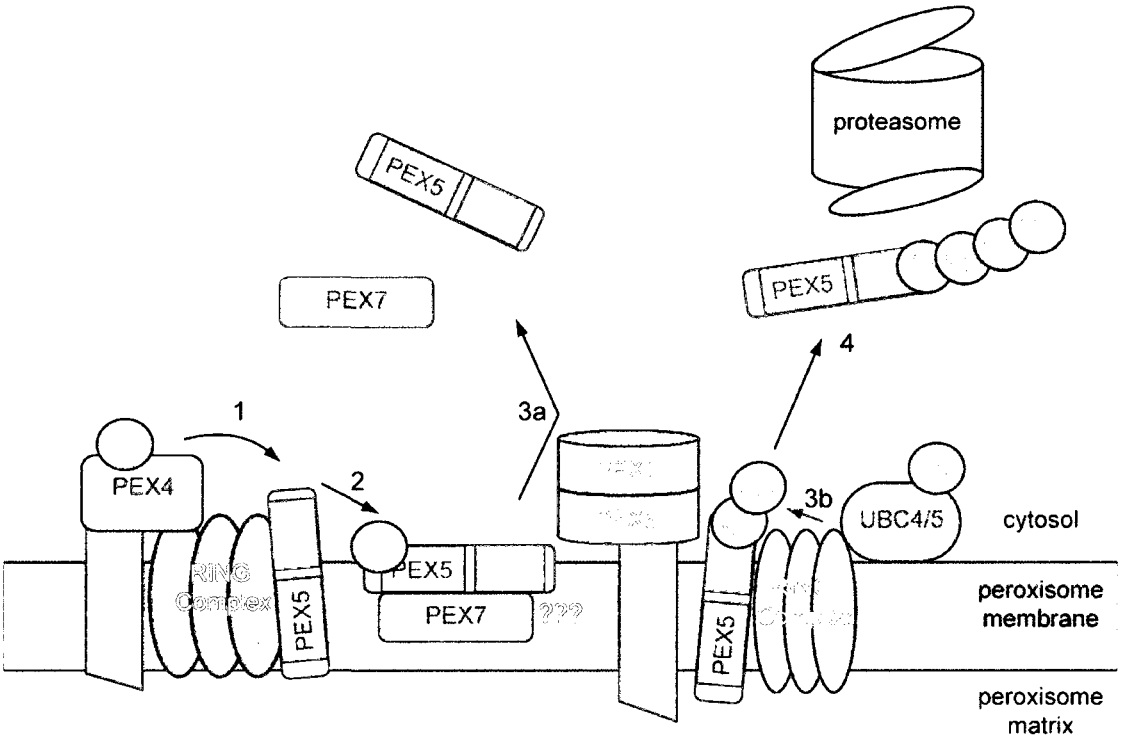

Figure 1.5. Model for PEX5 and PEX7 receptor recycling.

After cargo release (1 and 2), PEX5 is monoubiquitinated by the E2 protein PEX4 and perhaps the PEX2, PEX10, and PEX12 RING complex, which likely plays the role of an E3 ligase. (3a) PEX1 and PEX6, which are tethered to the membrane by PEX15/26, recognize the monoubiquitinated PEX5 and facilitate its release to the cytosol. (3b) In an alternative pathway, yeast PEX5 can be polyubiquitinated by Ubc4p and Ubc5p. (4) Polyubiquitinated PEX5 can be sent to the proteasome for degradation. Recent work in yeast indicates that PEX12 is the RING protein required for PEX5 monoubiquitination and PEX2 is required for PEX5 polyubiquitination (Platta et al., 2009).

(reviewed in Brown and Baker, 2008). It is possible that PEX7 is recycled back to the cytosol through its association with the co-receptors. Moreover, PEX7 may assist the co-receptors in associating with the recycling components through its association with PEX12.

1.8. Tools for studying peroxisome biogenesis and function in *Arabidopsis*

We are studying peroxisome biogenesis and function by isolating and characterizing mutants defective in peroxisomal processes. Because the peroxisome is the site of fatty acid β-oxidation and is implicated in metabolism of the auxin precursor indole-3-butyric acid (IBA), isolating mutants defective in these processes can lead to insights into peroxisomal biogenesis and function.

1.8.A. Fatty acid β-oxidation

Fatty acids are broken down through the process of β-oxidation to provide a source of energy. β-oxidation is the sequential removal of two carbon units in the form of acetyl-CoA (Figure 1.6). In animals, peroxisomal enzymes shorten long-chain fatty acids. Further shortening of medium-chain and short-chain fatty acids takes place in mitochondria. In plants, the process of β-oxidation occurs predominantly, if not exclusively, in peroxisomes (Kindl, 1993). *Arabidopsis* is an oilseed plant. During germination, before photosynthesis begins, oilseed plants use fatty acid β-oxidation to convert stored fatty acids into sugar, a usable energy source; failure to β-oxidize fatty acids leads to an inability to convert stored energy into sugar. This defect can be assayed by germinating seedlings on media with and without sucrose. Mutants defective in fatty acid β-oxidation (summarized in Table 1-2) are unable to grow on medium without sucrose because they are incapable of converting stored fats to sugar (Hayashi et al., 1998).

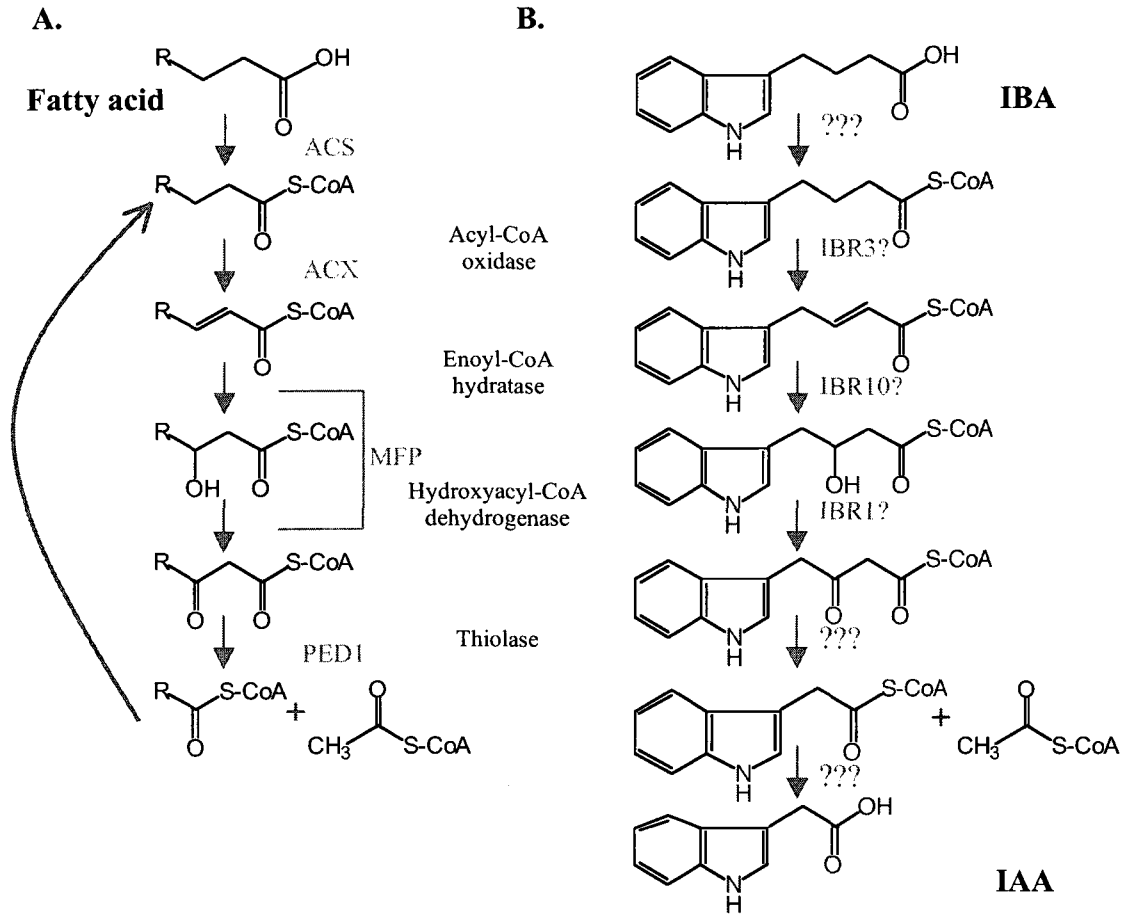

Figure 1.6. Fatty acid β-oxidation versus a model for IBA β-oxidation.

A. Fatty acid β-oxidation is carried out by the sequential action of acyl-CoA synthetases (ACS), acyl-CoA oxidases (ACX), multifunctional proteins (MFP) responsible for two different enzymatic activities, and thiolases including PED1 (peroxisome defective). B. A proposed pathway for IBA to IAA conversion may involve the proteins IBR3, a putative acyl-CoA dehydrogenase, IBR10, a putative enoyl-CoA hydratase, and IBR1, a putative hydroxyacyl-CoA dehydrogenase.

Table 1-2. *Arabidopsis* β-oxidation enzymes

Gene	Enzyme	PTS	Mutant Phenotype*	Reference
LACS6	Acyl-CoA synthetase	PTS2	*lacs6* and *lacs7* not suc. dep.; *lacs6 lacs7* is suc. dep., not IBA^R	(Fulda et al., 2002; Shockey et al., 2002; Shockey et al., 2003)
LACS7	Acyl-CoA synthetase	PTS1, PTS2		
ACX1	Long-chain acyl-CoA oxidase	PTS1	IBA^R, not suc. dep.; *acx1acx2* is suc. dep.	(Hooks et al., 1999; Adham et al., 2005)
ACX2	Very long-chain acyl-CoA oxidase	PTS2	not IBA^R, not suc. dep.	(Hooks et al., 1999; Adham et al., 2005)
ACX3	Medium-chain acyl-CoA oxidase	PTS2	IBA^R, not suc. dep.	(Eastmond et al., 2000; Froman et al., 2000; Adham et al., 2005)
ACX4	Short-chain acyl-CoA oxidase	PTS1	IBA^R, suc. dep. in light	(Hayashi et al., 1999; Adham et al., 2005)
ACX5	Acyl-CoA oxidase-like	PTS1	not IBA^R, not suc. dep.	(Adham et al., 2005)
ACX6	Acyl-CoA oxidase-like	PTS2	not IBA^R, not suc. dep.	(Adham et al., 2005)
AIM1	Multifunctional protein	PTS1	IBA^R, not suc. dep.	(Richmond and Bleecker, 1999)
MFP2	Multifunctional protein	PTS1	not IBA^R, suc. dep.	(Richmond and Bleecker, 1999; Rylott et al., 2006)
PED1/KAT2	Thiolase	PTS2	IBA^R, suc. dep.	(Hayashi et al., 1998; Germain et al., 2001)
KAT1	Thiolase	PTS2	None reported	
KAT5	Thiolase	PTS2	None reported	

*IBA^R, IBA-resistant root elongation; suc. dep., sucrose dependent for normal seedling development following germination.

Acyl-CoA synthetases. The first step of peroxisomal β-oxidation involves the activation of a precursor through the addition of a CoA group. In *Arabidopsis*, two long chain acyl-CoA synthetases, LACS6 and LACS7 are peroxisomal enzymes that activate fatty acids (Fulda et al., 2002; Shockey et al., 2003). *lacs6* and *lacs7* do not exhibit fatty acid metabolism defects as single mutants but when combined, the double mutant is sucrose dependent (Fulda et al., 2002; Shockey et al., 2003).

Acyl-CoA oxidases. ACX enzymes catalyze the step of fatty acid β-oxidation that follows activation. There are six apparent ACX isozymes in *Arabidopsis*, with varying chain-length specificities (Table 1-2). Three mutants, *acx1*, *acx2*, and *acx4*, defective in acyl-CoA oxidases, have been implicated in fatty acid metabolism. *acx4* and the *acx1 acx2* double mutant are sucrose dependent (Adham et al., 2005). Mutations in *ACX3*, *AXC5*, and *ACX6* do not lead to sucrose-dependent phenotypes, suggesting their respective protein products are not required for fatty acid metabolism (Hooks et al., 1999; Eastmond et al., 2000; Froman et al., 2000; Adham et al., 2005).

Multifunctional proteins. Following acyl-CoA oxidase activity, the multifunctional proteins catalyze the next step of fatty acid β-oxidation. *Arabidopsis* has two predicted multifunctional proteins: AIM1 (abnormal inflorescence meristem) and MFP2 (Richmond and Bleecker, 1999). Although AIM1 has enoyl-CoA hydratase activity, *aim1* mutant seedlings are not sucrose dependent (Richmond and Bleecker, 1999). In contrast, the *mfp2* mutant is sucrose-dependent (Rylott et al., 2006). Combining *aim1* with *mfp2* causes embryo lethality (Rylott et al., 2006), suggesting that these two proteins have partially redundant functions.

Thiolase. The final step of fatty acid β-oxidation is catalyzed by thiolase. *Arabidopsis* has three genes that encode peroxisomal 3-ketoacyl-CoA thiolase enzymes: *KAT2/PED1*, *KAT1*, and *KAT5*. These enzymes act during the last step of fatty acid β-oxidation to cleave ketoacyl-CoA to acetyl-CoA and fatty acyl-CoA. The *ped1* mutant is

sucrose dependent (Hayashi et al., 1998), suggesting that *PED1/KAT2* is the most important thiolase isozyme during seedling development.

1.8.B. IBA and IAA

The plant hormones most relevant to this thesis are called auxins. Auxins are characterized by the presence of an indole ring and are important in many plant growth and developmental processes. IBA and IAA are two endogenous auxins, characterized by the presence of an indole ring; the only structural difference between the two compounds is two additional carbon units in the form of butyric acid on the side chain of IBA versus the shorter acetic acid side chain of IAA (Figure 1.7). There is evidence that IBA and IAA can be interconverted (Fawcett et al., 1960; Epstein and Lavee, 1984; Ludwig-Müller and Epstein, 1991; Nordström et al., 1991; van der Krieken et al., 1992; Baraldi et al., 1993). Free IAA and IBA are of similar abundance in *Arabidopsis* (Ludwig-Müller et al., 1993). IBA initiates lateral roots more efficiently than IAA, because for IAA to initiate a similar number of roots as IBA, IAA must be used at concentrations that dramatically inhibit root elongation (Zolman et al., 2000). Moreover, IBA is more stable than IAA (Robbins et al., 1988; Nissen and Sutter, 1990; Nordström et al., 1991). Although there are some reports that IBA may act on its own via its own receptors through IAA-independent pathways (Poupart and Waddell, 2000), the genetic evidence discussed below indicates that the majority of IBA responses in *Arabidopsis* appear to stem from its conversion to IAA.

1.8.C. 2,4-DB and 2,4-D

The synthetic IBA analog 2,4-dichlorophenoxybutyric acid (2,4-DB) (Figure 1.7) differs from the synthetic IAA analog 2,4-dichlorophenoxyacetic acid (2,4-D) (Figure 1.7) by two carbon units and is thought to be converted to 2,4-D in a process similar to fatty acid β-oxidation (Wain and Wightman, 1954). Both 2,4-DB and 2,4-D initiate lateral roots and inhibit primary root elongation similarly to IBA and IAA.

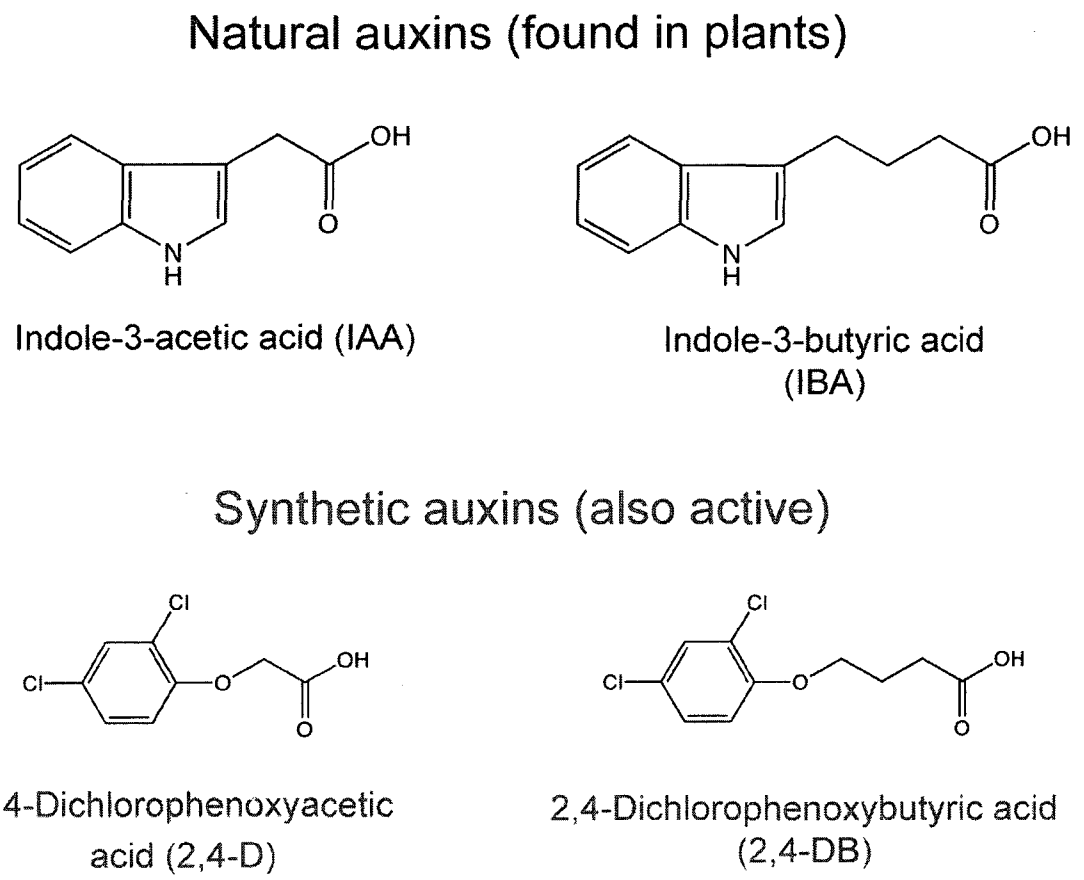

Figure 1.7. Natural and synthetic auxins.

IBA is likely converted to IAA through β-oxidation. Similarly 2,4-DB is converted to 2,4-D through β-oxidation.

1.8.D. IBA β-oxidation

Figure 1.6 summarizes a proposed pathway for IBA to IAA conversion. Although all of the genetic evidence is consistent with the possibility, IBA to IAA conversion within peroxisomes has never actually been demonstrated. The process begins when a CoA is added to the side chain of IBA by a hypothetical acyl-CoA synthetase. The IBA-CoA may then go through dehydrogenation by an acyl-CoA oxidase or dehydrogenase.The two following proposed steps, hydration and oxidation, may be catalyzed by a multifunctional protein, or by separate enzymes. Finally, a ketoacyl-CoA thiolase could be involved in releasing acetyl-CoA and IAA-CoA, and a thioester hydrolase could be responsible for cleaving IAA-CoA and releasing the free form of IAA.

1.8.E. *IBA-response* (*ibr*) mutants

Several mutants have been isolated that are defective in IBA responsiveness. Defects attributed to the conversion pathway are characterized by plants that have long roots on media with exogenously applied IBA (IBA resistant) while maintaining a wild-type response to IAA (IAA sensitive). Because IBA to IAA conversion is likely a peroxisomal process, *ibr* mutants are useful instruments in our exploration of how peroxisomes are made and how they function. We have used both forward and reverse genetic approaches to isolate and characterize various *ibr* mutants.

Three of these mutants are discussed in detail in Chapter 7. *ibr3*, *ibr10*, and *ibr1* display an IBA-resistant, IAA-sensitive phenotype without any apparent defect in fatty acid β-oxidation (Zolman et al., 2000; Zolman et al., 2008). *IBR3*, *IBR10*, and *IBR1* encode proteins similar to three proteins involved in fatty acid β-oxidation: an acyl-CoA oxidase/dehydrogenase, an enoyl-CoA hydratase, and a hydroxyacyl-CoA dehydrogenase, respectively (Zolman et al., 2007; Zolman et al., 2008). Thus the IBR3, IBR10, and IBR1 proteins are candidates for catalyzing sequential steps of IBA β-oxidation (Figure 1.6).

1.8.F. A role for fatty acid β-oxidation enzymes in IBA β-oxidation

In addition to the *ibr3*, *ibr1*, and *ibr10* mutants, several of the fatty acid β-oxidation mutants listed in Table 1-2 can be classified as *ibr* mutants and have therefore been implicated in IBA metabolism.

The *lacs6 lacs7* double mutant responds normally to IBA and 2,4-DB (Fulda et al., 2002; Shockey et al., 2002; Shockey et al., 2003), indicating that LACS6 and LACS7 are unlikely to act on auxin precursors. In Appendix B, I describe my use of reverse genetic analysis to study the role of 4-CoA Ligase-like proteins in IBA metabolism, and how I uncovered two enzymes that may redundantly act in IBA activation.

Three mutants, *acx1*, *acx3*, and *acx4*, have been isolated that are defective in acyl-CoA oxidases and are resistant to the effects of IBA. Double mutant analysis has implicated ACX2 and ACX5 in IBA responses as well (Adham et al., 2005).

The *aim1* mutant is IBA-resistant (Zolman et al., 2000), and 2,4-DB-resistant (Richmond and Bleecker, 1999) suggesting a role for AIM1 in IBA and 2,4-DB β-oxidation. However, the *mfp2* mutant is not 2,4-DB-resistant (Rylott et al., 2006) or IBA-resistant (unpublished).

The *ped1* mutant was isolated as being resistant to 2,4-DB (Hayashi et al., 1998) and is also resistant to IBA (Zolman et al., 2000). These results suggest a shared role for PED1 in fatty acid and IBA metabolism.

1.8.G. A role for an acyl-activating enzyme in 2,4-DB β-oxidation

Most *Arabidopsis* mutants resistant to IBA are similarly resistant to 2,4-DB, suggesting that the enzymes that act in the metabolism of these auxins are shared. Recently, a study of the acyl-activating enzyme AAE18 showed that an *aae18* mutant is resistant to the effects of 2,4-DB while retaining response to IBA (Wiszniewski et al., 2008). This is the first report of an enzyme that may act solely on 2,4-DB conversion.

Because some fatty β-oxidation mutant phenotypes point to a relationship between IBA biosynthesis and fatty acid metabolism, the question follows of whether the

enzymes acting in fatty acid β-oxidation (Figure 1.6.A) are the same as those used IBA to IAA conversion (Figure 1.6.B). If there are shared enzymes, it is possible that the enzymes used in fatty acid metabolism also act directly on IBA-CoA and its derivatives. *ped1*, *aim1*, and *acx* mutants are deficient not only in fatty acid β-oxidation, but also in IBA β-oxidation, suggesting that there are shared factors between the two processes (Hayashi et al., 1998; Zolman et al., 2000; Adham et al., 2005). However, evidence to support the possibility that enzymes exist that act solely on IBA-CoA independently of fatty acid metabolism has arisen with the isolation of *ibr3*, *ibr10*, and *ibr1* that are deficient in IBA responses but lack defects in fatty acid β-oxidation (Zolman et al., 2000). This paradox has led to the suggestion that some of the fatty acid β-oxidation mutants may be disrupting IBA β-oxidation indirectly, perhaps by sequestration of needed cofactors (Adham et al., 2005). The ultimate resolution of this paradox will require *in vitro* enzyme assays comparing activities with the proposed precursors.

1.8.H. *Arabidopsis pex7-1* and *pex5* mutants.

Arabidopsis peroxisomal receptor mutants also fall under the category of *ibr* mutants. Chapters 3 through 6 detail my characterization of mutations in the PEX7 and PEX5 receptors. These mutants also display IBA-resistant, IAA-sensitive phenotypes.

Two *Arabidopsis* mutants defective in PTS2 import have been isolated and characterized in the Bartel lab, *pex7-1* and *pex5-1* (Figures 1.4 and 1.5). The first *Arabidopsis PEX7* mutant, *pex7-1*, was characterized in 2005 (Woodward and Bartel, 2005). *pex7-1* contains a T-DNA insertion (SALK_005354) 95 bp upstream of the *PEX7* start codon in the 5' untranslated region (UTR). Localization studies using a peroxisomally targeted version of GFP (PTS2-GFP) revealed a defect in PTS2 protein import in seedling root hairs (Woodward and Bartel, 2005). However, examination of thiolase processing indicated that substantial PTS2 import still occurs in *pex7-1* (Woodward and Bartel, 2005).

Two *Arabidopsis pex5* mutants have been described (Figure 1.4). *pex5-10* is a T-DNA insertion mutant believed to be a null based on western blot analysis (Zolman et al., 2005). In the *pex5-1* mutant, a serine to leucine mutation (Zolman et al., 2000) in the presumed PEX7 binding site of PEX5 leads to a deficiency in PTS2 import but leaves PTS1 import unaffected (Woodward and Bartel, 2005). In fact, the PTS2 defect in *pex5-1* is magnified compared to *pex7-1*, as judged by PTS2-GFP localization and thiolase processing (Woodward and Bartel, 2005). Western analyses indicated that PEX5 protein was present in *pex5-1*, *pex7-1*, and *pex5-1 pex7-1* mutants (Woodward and Bartel, 2005). The mutated serine in *pex5-1* is analogous to a mutated serine in a CHO cell line that is deficient in PTS2 import due to inefficient PEX7 binding (Matsumura et al., 2000). The combined evidence suggests an important role for serine 318 in PEX7 binding.

pex5-1 pex7-1 double mutants have enhanced physiological phenotypes compared to either single mutant and completely blocked thiolase PTS2 processing (Woodward and Bartel, 2005). The double mutant also has severe developmental abnormalities (Woodward and Bartel, 2005). We hypothesize that these severe defects are caused by the combination of reduced PEX7 accumulation in *pex7-1* and reduced PEX7 binding in *pex5-1*. PTS-GFP import in the double mutants is described in Chapter 5. Another question that remains to be answered is whether the severe phenotypes observed in the double mutant result from reduced PEX7 binding to pex5-1. This question was explored using yeast two-hybrid analysis and bypass experiments in Chapters 4 and 6.

In this thesis, I describe a detailed characterization of the physiological and molecular defects in the peroxisomal mutants *pex7-1*, *pex7-2*, *pex5-1*, and *pex5-10* (Chapters 3 through 6), as well as *ibr1*, *ibr3*, and *ibr10* (Chapter 7). I also describe the isolation and preliminary characterization of new putative *ibr* mutants (Appendix A) and how I used a reverse genetics approach to look at candidates for IBA activation (Appendix B).

Chapter 2: Materials and Methods

2.1. Plant materials and growth conditions

pex7-2 was isolated as an *IBA-response* (*ibr*) mutant from progeny of EMS-mutagenized Col-0 seeds (Lehle Seeds, Round Rock, TX) as previously described (Adham et al., 2005; Zolman et al., 2008) and was backcrossed once prior to phenotypic analyses. The *pex7-1* (Woodward and Bartel, 2005) and *pex5-10* (Zolman et al., 2005) T-DNA insertion mutants and the *pex5-1* missense allele (Zolman et al. 2000) are in the Columbia (Col-0) accession. *ped1-1* (Hayashi et al., 1998) is in the Landsberg *erecta* (L*er*) background.

For phenotypic assays, seeds were surface-sterilized, stratified three days at 4°C or as indicated, and plated on plant nutrient media (PN) (Haughn and Somerville, 1986) supplemented with 0.5% sucrose (PNS), hormones, kanamycin, or Basta (glufosinate-ammonium) as indicated. Hormone stocks were dissolved in ethanol, and the volume of added ethanol was normalized for hormone-supplemented medium and unsupplemented controls. Seedlings were grown at 22°C under continuous white or yellow-filtered light (Stasinopoulos and Hangarter, 1990).

2.2. Phenotypic analyses

2.2.A. Root and hypocotyl elongation

Seedlings were grown for eight days on PN or PNS supplemented with hormones as indicated. Roots and hypocotyls were measured to nearest millimeter and means and standard errors were calculated using Microsoft Excel.

2.2.B. Lateral root proliferation

Seedlings grown on PNS for four days under white light at 22°C were transferred to new plates containing hormone or an equal volume of ethanol for the no hormone

control. Roots were measured to the nearest millimeter and lateral roots were counted using a dissecting microscope. The quotient of lateral roots per millimeter was calculated for each seedling and the mean of this value and standard errors were calculated using Microsoft Excel.

2.2.C. Sucrose dependence in the dark

Seedlings were plated on PN and PNS and grown for one day under white light at 22°C then plates were wrapped in foil and incubated for an additional 4 or 5 days as indicated at 22°C in the dark. Plants were grown vertically or horizontally as indicated. The foil was then removed from the plates, seedlings were removed from the agar using forceps, and hypocotyls were measured to the nearest millimeter and means and standard errors were calculated using Microsoft Excel.

2.2.D. Seed development and morphology

pex5-1, *pex7-1*, *pex7-2*, progeny of *pex5-1/pex5-1 pex7-2/PEX7*, and progeny of *pex5-10/PEX5 pex7-2/pex7-2* were grown on PNS and transferred to soil. Plants were genotyped in soil and those with the same genotype as the parents were selected for analysis. Siliques of varying ages were opened with forceps and a razor blade and developing seeds were photographed using a dissecting microscope.

Mature siliques from the same plants were harvested and the seeds were placed on a Petri plate and photographed. The numbers of shrunken and filled seeds were counted.

2.2.E. Adult analysis

Seedlings grown for 26 days on PNS under white light were moved to soil where they continued to grow under continuous white light at 22°C. When the plants were 55 days old they were removed from the soil for photography.

2.3. Genetic Analysis of mutants

2.3.A. Mapping

DNA was isolated from IBA-resistant plants selected from F_2 progeny of *pex7-2* crossed to L*er tt4*. Mapping with PCR-based molecular markers (Konieczny and Ausubel, 1993; Bell and Ecker, 1994) localized the lesion to chromosome 1. Fine mapping with additional markers F28N24 (PCR amplification with primers F28N24-1, CTTGATGCAAATCCATAGGAAGTGAGTCA, and F28N24-2, CCGTTTGCAGGCATGATATAAACCTGTCA, yielded a 257-bp product in Col-0 and a 219-bp product in L*er*), F27G20 (Fujibe et al., 2006), F6N18 (PCR amplification with primers F6N18-2, ATTGATTTCTAACTCCAACTCTACATAGC, and F6N18-4, GTTTGTGTTCTTTGTTGTTTTCTTTTAG, yielded a 202-bp product in Col-0 and a 181-bp product in L*er*), and T9L6 (Magidin, 2002) localized the defect between F27G20 and the F28N24. The At1g29260 gene was PCR-amplified from genomic DNA prepared from the mutant and the resultant amplicon was sequenced directly.

2.3.B. Plant DNA isolation

DNA was obtained from plant tissue as described (Celenza et al., 1995). Briefly, a green leaf was placed in a 1.5 ml microcentrifuge tube and snap-frozen on dry ice. Frozen tissue was ground with a pestle and 10 µL of 0.5 N NaOH was added. Tissue was allowed to thaw at room temperature before placing at 100°C in a sand bath for 30 seconds. Tissue was neutralized using 100 µL of 0.2 M Tris pH 8.0 with 1 mM EDTA, pH 8.0.

2.3.C. Yeast DNA isolation

One yeast colony per strain was resuspended in 100 µL of sterile water. Five µL of the resuspended colony was used was used as a template for PCR to verify the presence of the desired construct. The details of construct verification are summarized in Table 2-1.

Table 2-1. Primer pairs and product sizes for yeast two-hybrid construct verification.

Primers[1]	Expected Product Size	Program Used	pBI770/pBI771 Inserts detected
PEX7-QRTF + ADC-1	341 bp	SSLP	PEX7 PEX7SKL pex7-2 pex7-2-SKL
PED1-5 + ADC-1	337 bp	SSLP	PED1 tPED1 PED1SKL
GAL4-1 + PEX5-13	322 bp	SSLP	PEX5 tPEX5 pex5-1 tpex5-1
PEX7-N9 + PEX7-N12	294 bp	SSLP	PEX7 PEX7SKL pex7-2 pex7-2-SKL

[1]Primer sequences are listed in Table 2-3.
[2]PCR program parameters listed in Table 2-2.

Table 2-2. PCR programs used in this study.

Program	Cycles	Denaturation	Annealing	Elongation
SSLP	40	15 sec at 94°C	15 sec at 55°C	1 min at 72°C
CAPS	40	30 sec at 95°C	15 sec at 56°C	3 min at 72°C
Mutate	30	1 min at 95°C	1 min at 55°C	5 min at 65°C
TPMSTR25	25	20 sec at 94°C	15 sec at 55°C	2 min at 72°C
CAPSGRAD	40	30 sec at 95°C	30 sec at 56°C	3 min at 72°C
TPMSTR8K	35	20 sec at 95°C	15 sec at 55°C	8 min at 72°C

(Modified from Zolman, 2002)

2.3.D. *pex7* complementation

pex7-2 was crossed to *pex7-1* plants and F_1 seed was harvested. F_1 seedlings were assayed for IBA resistance in root elongation. *pex7-2* was transformed with *35S-PEX7* using the floral dip method (Clough and Bent, 1998). T1 plants were selected on 7.5 μg/mL glufosinate ammonium and homozygous plants were selected from subsequent generations by analyzing the pattern of seedling glufosinate ammonium resistance.

2.3.E. Overexpression and yeast two-hybrid constructs

PEX7 and pex7-2. *PEX7* and *pex7-2* cDNAs with an in-frame SalI site 5' of the ATG and a NotI site immediately downstream of the stop was made by PCR-amplifying a *PEX7* cDNA clone APZ50H10R (Asamizu et al., 2000) or *pex7-2* mutant genomic DNA, respectively, using Ex-Taq (TaKaRa Bio Inc.) with PEX7-SalI-F and PEX7-NotI-R (Table 2-3). Amplicons were cloned into pCR4-TOPO (Invitrogen) to give pCR4-PEX7 and pCR4-pex7-2.

To make *35S-PEX7*, the *PEX7* coding sequence was subcloned as a SalI/NotI fragment from pCR4-*PEX7* into XhoI/NotI-cut 35SpBARN (LeClere and Bartel, 2001) to give *35S-PEX7c* in which *PEX7* was driven by the strong 35S promoter. To make yeast two-hybrid constructs, inserts from these pCR4-PEX7 and pCR4-pex7-2 were subcloned into SalI/NotI-cut pBI770 to make pBI770-PEX7 and pBI770-pex7-2, respectively.

PEX7-SKL and pex7-2-SKL. *PEX7*-SKL and *pex7-2*-SKL constructs were made with an in-frame SalI site 5' of the ATG and a SKL-NotI site immediately downstream of the stop was made by PCR-amplifying a *PEX7* cDNA clone APZ50H10R (Asamizu et al., 2000) or *pex7-2* mutant genomic DNA, respectively, using Ex-Taq with PEX7-SalI-F and PEX7-SKL-NotI-R (Table 2-3). The resultant amplicons were cloned into pCR4-TOPO to give pCR4-*PEX7*-SKL and pCR4-*pex7-2*-SKL. The inserts from these plasmids were subcloned into XhoI/NotI-cut 35SpBARN (LeClere and Bartel,

2001) and SalI/NotI-cut pBI770 and pBI771 to give *35S-PEX7*-SKL, 35S-*pex7-2*-SKL, pBI770-*PEX7*-SKL, pBI770-*pex7-2*-SKL, pBI771-*PEX7*-SKL and pBI771-*pex7-2*-SKL.

***PEX5* and *pex5-1*.** A *PEX5* cDNA with an in-frame SalI site 5' of the ATG was made using Quikchange site-directed mutagenesis (Stratagene) with the primer PEX5-SalI-F (Table 2-3) on a PEX5 cDNA in the NotI site of pBluescript KS (pKS-PEX5; Zolman et al., 2000) to make pKS-PEX5b3. A *pex5-1* cDNA was similarly made from the same template using the primers PEX5-SalI-F and PEX5-mutant (Table 2-3) and the PCR program MUTATE to introduce a 5' SalI site and a C to T mutation that causes the serine to leucine missense amino acid change present in the *pex5-1* mutant. This plasmid is called pKS-PEX5b5. The SalI/Not1 *PEX5* fragment from pKS-PEX5b3 was ligated into XhoI/NotI cut 35SpBARN (LeClere and Bartel, 2001) to make 35SPEX5. The SalI/Not1 *PEX5* and *pex5-1* fragments from pKS-PEX5b3 and pKS-PEX5b5 were ligated into SalI/Not1-cut pBI771 to make pBI771-*PEX5* and pBI771-*pex5-1*.

Truncated *PEX5* and truncated *pex5-1*. Truncated *PEX5* and *pex5-1* cDNAs containing a 5' SalI site and a 3' NotI site and lacking the TPR domain (PTS1-binding region) were made using oligo-mutagenesis. pKS-*PEX5* and pKS-*pex5-1* were PCR-amplified with PEX5-SalI-F and PEX5-Stop-R (Table 2-3) using Ex-Taq and the program TPMSTR8K (Table 2-2). Gel-purified PCR products were cloned into pCR4-TOPO to make pCR4-*tPEX5* and pCR4-*tpex5-1*. SalI/NotI *tPEX5* and *tpex5-1* fragments were ligated into SalI/NotI-cut pBI770 and pBI771 to make pBI770-*tPEX5*, pBI770-*tpex5-1*, pBI771-*tPEX5*, and pBI771-*tpex5-1*. SalI/NotI-cut *tPEX5* was also ligated into XhoI/NotI-cut 35SpBARN (LeClere and Bartel, 2001) to make 35S-*tPEX5*.

Full length and truncated *PED1*. A *PED1* cDNA flanked by an in-frame SalI site 5' of the ATG and a NotI site immediately 3' of the stop codon was PCR-amplified from *PED1* cDNA U09045 (Yamada et al., 2003) using Triple Master Taq DNA polymerase (Eppendorf) with PED1-SalI-F1 and PED1-NotI-R (Table 2-3). A truncated *PED1* cDNA lacking the PTS2 was similarly amplified using PED1-SalI-F2 (Table 2-3)

and PED1-NotI-R. Amplicons were cloned into pCR4-TOPO to make pCR4-*PED1* and pCR4-*tPED1*. Inserts from these plasmids were subcloned into SalI/NotI-cut pBI771 to make pBI771-*PED1* and pBI771-*tPED1*. The SalI/Not1 *PED1* and *tPED1* fragments from pCR4-*PED1* and pCR4-*tPED1* were ligated into XhoI/NotI-cut 35SpBARN (LeClere and Bartel, 2001) to make 35S-*PED1* and 35S-*tPED1*.

PED1-SKL. To make the 35S-PED1-SKL construct, a *PED1* cDNA flanked by an in-frame SalI site 5' of the ATG and an SKL-NotI site immediately 3' of the stop codon was PCR-amplified from *PED1* cDNA U09045 (Yamada et al., 2003) using Triple Master Taq DNA polymerase with PED1-SalI-F1 and PED1-SKL-NotI-R. The resultant amplicon was cloned into pCR4-TOPO to make pCR4-PED1-SKL. The insert from this plasmid was subcloned into SalI/NotI-cut pBI770 and pBI771 to make pBI770-PED1-SKL and pBI771-*PED1*-SKL. To make 35S-*PED1*-SKL, the SalI/NotI *PED1*-SKL fragment from pCR4-*PED1*-SKL was ligated into XhoI/NotI-cut 35SpBARN (LeClere and Bartel, 2001).

Table 2-3. Sequences of oligonucleotides used to make DNA constructs.

Name	Sequence (5' to 3')
35S-F	AAGGGATGACGCACAATCCCACTATCC
NOS-R	GATAATCATCGCAAGAGCCGGCAACAG
PED1-5	GGGACTTGACCCAGAGAAAATCAATGTCAACGG
PEX7-QRTF	TGGCTGTGCTTAATGGTCATG
PEX7-N12	GGAGATTGTACTTTAAGGATTTGGGATGTT
GAL4-1	CTATCTATTCGATGATGAAGATACC
ADC-1	CGACAACCTTGATTGGAGACTTGACC
PEX7-1	CTCGAATTTAGATTTCTCTCTCACTTTTA
PEX7-2	CTTCTCGAAGATTCAATTCAACGAT
PEX7-SalI-F	GTCGACAAGAAGCTATGCCGGTGTTCAAAGCT
PEX7-SKL-NotI-R	GCGGCCGCTCAAAGCTTACTACTGGCTCTAGGATCCAT
PEX7-NotI-R	GCGGCCGCTCAACTGGCTCTAGGATCC
PED1-SalI-F1	GTCGACCGGAAAAAATGGAGAAAGCGATCGAG
PED1-SalI-F2	GTCGACCGGAAAAAATGTTGGCTGGGGACAGTGCT
PED1-SKL-NotI-R	GCGGCCGCCTAAAGCTTACTGCGAGCGTCCTTGGACAA
PED1-NotI-R	GCGGCCGCCTAGCGAGCGTCCTT
PEX5-SalI-F	GCGGAGGAGTAGAAACCCGGTCGACACATGGCGATGAGAG
PEX5-Mutant	CCGAAATTTCAGAATTTAAGATTCCTTCAGTTTGTTTCC
PEX5-Stop-R	CCACATAAGGATTCAGCGGCCGCGAATTCAGACACCACTGGTTT
PEX7-N8	CTCCAGAAGCAGAAGCAAACACATCAC
PEX7-N9	GACGGCTCAGTGAAGATTTACGAC
PEX5-13	AAGTGGCTGATCTAACTCAGA

Table 2-4. Bartel lab stock numbers for plasmids used in this study.

Insert	Vector (cells)					
	Bluescript (*E. coli*)	TOPO (*E. coli*)	pBI770 (*E. coli*)	pBI771 (*E. coli*)	35SpBARN (*E. coli*)	35SpBARN (*A. tumefacians*)
PEX7		2101, 2102	2136	2258	2203	2215
pex7-2		2103	2137	2260		
PEX7SKL		2104	2138	2259	2204	2217
pex7-2SKL		2220, 2221	2222, 2223	2293	2261	2262
PED1		2109	2148	2149	2205	2218
tPED1		2096, 2097	2369, 2370	2150	2295	2297
PED1SKL		2094, 2095	2209	2294	2206	2216
PEX5	2112			2140	2207	2214
pex5-1	2214			2141		
tPEX5[1]		2287	2289	2290	2296	2298
tpex5-1		2288	2291	2292		

[1]The tPEX5 construct was found to have a frameshift mutation.

2.4. Yeast two-hybrid analysis

Inserts for the yeast two-hybrid constructs were fused to Gal4-DNA-binding domain using the pBI770 "bait" vector or the Gal4-activation domain using the pBI771 "prey" vector (Kohalmi et al., 1998). All inserts and junctions were verified by sequencing.

Plasmids were transformed (Gietz and Schiestl, 1995) into the AH109 (*MAT***a**, *trp1-901*, *leu2-3, 112*, *ura3-52*, *his3-200*, *gal4*Δ, *gal80*Δ, *LYS2::GAL1*$_{UAS}$*-GAL1*$_{TATA}$*-HIS3*, *GAL2UAS-GAL2TATA-ADE2*, *URA3::MEL1UAS-MEL1TATA-lacZ*, *MEL1*; Clontech) *Saccharomyces cervesiae* yeast strain. Strains were grown on synthetic complete (SC) media lacking Leu and Trp or lacking Leu, Trp, and His and supplemented with 2 mM 3-aminotriazole.

2.5. *Escherichia coli* transformation and growth conditions

XL-10 Gold (Stratagene), NEB5-α (New England Biolabs) and TOP10 (Invitrogen) chemically competent cells were used in this study. Strains were stored at -80°C. Transformed cells were grown at 37°C on LB agar plates containing selective antibiotics.

XL-10 Gold cells were transformed using the recommended protocol from the Stratagene QuikChange site-directed mutagenesis kit with several modifications. Cells were thawed on ice and 45 μL of cells per reaction were aliquoted into snap-cap tubes. Two μL of β-mercaptoethanol were added to each tube. Cells were swirled every two minutes for ten minutes on ice before adding 1.5 μL of DNA and incubating for 30 minutes on ice. Cells were heat shocked at 41°C for 30 seconds then incubated on ice for two minutes. 500 μL of room temperature SOC was added to each tube and cells were recovered for one hour at 37°C while gently shaking.

NEB5-α and TOP10 cells were thawed on ice and one to five μL of DNA was added to cells. Cells were incubated for 10 minutes on ice. Transformation mixtures were heat shocked at 42°C for 30 seconds then placed on ice for two minutes. 250 μL SOC was added to the mixture and cells were allowed to recover for one hour at 30°C while gently shaking.

Cells were plated on three plates (1%, 10%, and 89% of the total). Cells transformed with 35SpBARN constructs were selected on kanamycin and cells transformed with TOPO and pBI770/771 constructs were selected on carbenicillin. Cells were grown overnight at 37°C.

2.6. *Agrobacterium tumefacions* transformation and growth

All plant transformation vectors were transformed into *Agrobacterium tumefacians* strain GV3101 (Koncz et al., 1992) using electroporation (Ausubel et al., 1995). Transformants were selected for kanamycin and gentamycin resistance after growing several days at room temperature. Bacterial strains were stored at -80°C in 50% glycerol.

2.7. Yeast transformation and growth

A YPD culture was inoculated with the AH109 yeast strain and grown at 30°C overnight to an OD of 1.0 or higher. For each transformation (Gietz and Schiestl, 1995), 0.5 mL of culture was aliquoted into a 1.5 mL microcentrifuge tube and centrifuged for 10 seconds at full speed. The pellet was resuspended in 50 μL of sterile water by vortexing. Carrier DNA (X mg/mL salmon sperm DNA) was boiled at 100°C prior to adding 10 μL to each transformation tube. Two μL of each plasmid to be transformed was added to each transformation tube and cells were mixed gently by vortexing. 500 μl of transformation buffer (40% PEG 3350, 0.1 M lithium acetate, 10 mM Tris pH 7.5, 1 mM EDTA, and 0.1 M DTT) was added to each tube and the cells were allowed to

incubate at room temperature overnight. The transformation cell mixture was then centrifuged for 10 seconds and resuspended in 200 µL of sterile water by vortexing. Transformation reactions were spread on SC –Leu –Trp plates by shaking with sterile glass beads and grown at 30°C for 2 days. Yeast strains were stored at -80°C in 50% glycerol.

2.8. *Arabidopsis thaliana* transformation and growth

Wild type Col-0, *pex7-1*, *pex7-2*, *pex5-1*, *pex5-10*, and *ped1-1* plants were transformed with GV3101 strains transformed with plasmids of interest by floral dipping (Clough and Bent, 1998). Prior to transformation plants were grown five per pot under continuous white light at 22°C. Primary bolts were cut once to promote prolific production of inflorescences. Once secondary bolts were produced, plants were dipped, covered in saran wrap, and kept in the dark overnight. Saran wrap was then removed and plants were grown under continuous white light.

2.8.A. Identification of transformed plants

T_1 transformants were selected on plant nutrient (PN) medium supplemented with 7.5 µg/mL BASTA. BASTA resistant T_1 transformants were transferred to soil and PCR on leaf DNA was used to confirm the presence of the insert. T_2 plants positive for the insert were plated on medium supplemented with 7.5 µg/mL BASTA and plant lines that had 75% or higher BASTA resistance were transferred to soil for spraying with BASTA. T_3 lines were checked for BASTA resistance and used in western and phenotypic analyses.

2.8.B. Mutant rescue and overexpression

Overexpression of the 35S constructs was confirmed in the T_2 and T_3 lines via western blotting with PEX7, PEX5, and PED1 antibodies. Rescue analysis was completed by analyzing IBA resistance and PTS2 processing.

2.9. Double mutant generation and identification

pex7-2 was crossed with *pex5-1*, *pex5-10*, and Col-0. *pex7-1* was crossed with *pex5-10*. F_1 seeds were grown on PNS under white light at 22°C for at least 8 days before transferring to soil. F_1 plants were grown to produce seed under continuous white light in soil. F_2 seeds were harvested and grown on medium containing 0.5% sucrose then transferred to soil prior to PCR-based determination of genotypes.

2.10. Reporter analysis

2.10.A. Visualization of matrix protein import using green fluorescent protein

Col-0 expressing *35S-GFP-PTS1* (Zolman and Bartel, 2004) or *35S-PTS2-GFP* (Woodward and Bartel, 2005; Zolman et al., 2005) were crossed to *pex7-2* and *pex7-1 pex5-1* and lines homozygous for the mutant allele(s) and transgene were selected in the subsequent generations. *pex5-1* and *pex7-1* expressing *35S-GFP-PTS1* or *35S-PTS2-GFP* were described previously (Woodward and Bartel, 2005). Plant lines expressing GFP were grown on PNS at 22°C for 7 days under white light or for 1 day in the light under white light and 4 days on vertically-oriented plates in the dark. Prior to imaging, dark-grown seedlings were soaked in 10 μg/mL propidium iodide for no less than ten minutes to stain cell walls. Samples were mounted in sterile MilliQ water. Confocal images of cotyledon cells were obtained using a Zeiss multiphoton laser scanning microscope 510 META NLO equipped with a 63x oil immersion lens. GFP and propidium iodide were excited using a 488 nm argon laser. Bandpass emission filters of 500-530 nm and 650-710 nm were used to detect GFP and propidium iodide fluorescence, respectively.

2.10.B. DR5-GUS expression analysis

Wild type and *ibr10* lines homozygous for the DR5-GUS transgene (Guilfoyle, 1999)were grown for four days on medium supplemented with 0.5% sucrose then

transferred to medium containing no hormone, IBA, or NAA and grown for an additional one to four days. Seedlings were removed from the agar and stained for 3 days at 37°C with 0.5 mg/mL 5-bromo-4-chloro-3-indolyl-β-D-glucuronide (Bartel and Fink, 1994).

2.11. Western blot analysis

Protein was extracted from seedlings grown under continuous white light at 22°C in sterile water for 2 days or on PN supplemented with 0.5% sucrose for 4 or 8 days by grinding in NuPAGE 2x loading buffer (Invitrogen, Carlsbad, CA). Protein was extracted from 5 mL yeast cell cultures grown overnight at 30°C to an OD of 0.8-1.0 by resuspending in 2 volumes of NuPAGE 2x loading buffer then adding half a volume of glass beads followed by boiling 2.5 minutes at 100°C, vortexing on high for 1 minute, then boiling again 2.5 minutes. Following centrifugation, the supernatant was moved to a fresh tube with 1/10 volume of 0.5 M DTT and then boiled for 5 min. 5 µL of supernatant was loaded onto NuPAGE 10% Bis-Tris gels (Invitrogen) next to broad range prestained protein markers (P7708S, New England Biolabs, Beverly, MA) and Cruz Markers (Santa Cruz Biotechnology, Santa Cruz, CA) and transferred for 35 minutes at 24 V to a Hybond ECL nitrocellulose membrane (Amersham Pharmacia Biotech, Piscataway, NJ) using NuPAGE transfer buffer (Invitrogen). Membranes were blocked with 8% non-fat dry milk in Tween Tris-Buffered Saline (Ausubel et al., 1999) and incubated at 4°C with rabbit anti-PEX5 (1:100 dilution; Zolman and Bartel, 2004), rabbit anti-PEX7 (1:2500 dilution; generated and affinity purified against a peptide corresponding to the C-terminal 17 amino acids of PEX7 by Bethyl Laboratories, Montgomery, TX), rabbit anti-PED1 (1:2000 dilution; Lingard et al., 2009), or rabbit anti-PMDH2 (1:2000 dilution; Pracharoenwattana et al., 2007) as a primary antibody followed by incubation with a horseradish peroxidase-linked goat anti-rabbit IgG secondary antibody (sc-2030, Santa Cruz Biotechnology). As a loading control, membranes were incubated with mouse anti-HSC70 (1:5000 dilution, Stressgen

Bioreagents SPA-817) followed by horseradish peroxidase-linked anti-mouse IgG secondary antibody (sc-2031, Santa Cruz Biotechnology). Horseradish peroxidase was visualized using LumiGLO (Cell Signaling Technology, Danvers, MA) according to the manufacturer's instructions.

Chapter 3: Phenotypic Characterization of *pex7-2* and other PTS receptor mutants

This chapter summarizes my characterization of the physiological defects in *Arabidopsis pex7* and *pex5* mutants. The alleles under investigation are depicted in Figure 3.1. I compared the *pex7-2* mutant to the *pex7-1* mutant (Woodward and Bartel, 2005) and two mutants defective in the PTS1 receptor PEX5, the *pex5-1* missense allele (Zolman et al., 2000) and the *pex5-10* T-DNA insertion allele (Zolman and Bartel, 2004).

3.1. *pex7-2* isolation

Because peroxisomes are the site of fatty acid β-oxidation and metabolism of the auxin precursor indole-3-butyric acid (IBA), sucrose dependence and IBA resistance can be used to assess peroxisome function in *Arabidopsis* seedlings (Zolman et al., 2000). To identify new peroxisome defective mutants, we screened for mutants with IBA-resistant root elongation to isolate *IBA-response* (*ibr*) mutants that remain sensitive to the active auxin indole-3-acetic acid (IAA). Arthur Millius and Ana Raquel Adham originally identified B1017, a mutant that was IBA resistant and sucrose dependent during early seedling growth. Rotation student Neda Nikravan and I used recombination mapping to localize the lesion in one such mutant to a region on chromosome 1 north of the centromere (Figure 3.2.A.). This region contains *PEX7* (*At1g29260*), which encodes the *Arabidospis* PTS2 receptor. Because the previously characterized *pex7-1* insertion mutant also displays reduced IBA response (Woodward and Bartel, 2005), I PCR-amplified and sequenced the *PEX7* coding region from mutant DNA. We found a C to T base change at position 371 (where the A of the ATG start codon is position 1) that results in a threonine to isoleucine amino acid change in the second WD-40 repeat of PEX7 (Figure 3.2.A), and we named this new allele *pex7-2*.

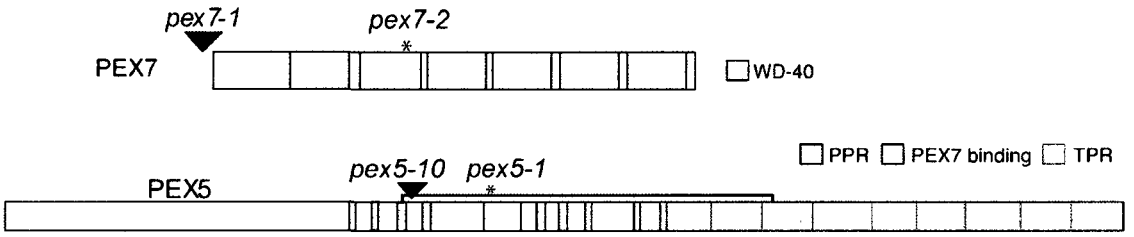

Figure 3.1. Genes and mutants under investigation.

pex7-1 contains a T-DNA insertion (triangle) 95 bp upstream of the start site. *pex7-2* contains a threonine to isoleucine missense mutation in the coding region. The *pex5-1* mutant contains a serine to leucine mutation in the presumed PEX7 binding site. *pex5-10* contains a T-DNA insertion in exon 5. Triangles designate positions of T-DNA inserts, and asterisks indicate point mutations.

To determine whether the IBA-resistant root elongation of *pex7-2* was caused by the mutation in the *PEX7* gene, we conducted a complementation test with *pex7-1*. I found that *pex7-2* was recessive, demonstrated by the wild-type sensitivity of *pex7-2/PEX7* F_1 seedlings to IBA (Figure 3.2.B.), and that *pex7-2* failed to complement the *pex7-1* resistance to IBA (Figure 3.2.B.), confirming that the lesion that I identified in the *PEX7* gene was responsible for the *pex7-2* mutant phenotypes. Moreover, we could fully restore *pex7-2* mutant defects by expressing a wild-type version of the *PEX7* open reading frame from the cauliflower mosaic virus 35S promoter in the *pex7-2* mutant (Figure 3.2.C. and 3.2.D.). Because *pex7-1* is a partial loss-of-function allele (Woodward and Bartel, 2005) that is not in the coding sequence (Figure 3.1.), this new allele allowed a more extensive characterization of PEX7 function in plants.

3.2. *pex7-2* β-oxidation defects

I used physiological assays that require peroxisomal metabolism to compare the extent of peroxisomal deficiency in the various *pex7* and *pex5* mutants. *pex7-2* displayed resistance to inhibition of root elongation by IBA similar to *pex5-1* and *pex7-1*. Like *pex5-1* and *pex7-1*, *pex7-2* seedlings responded to IBA at higher concentrations, whereas the severe *pex5-10* insertion allele appeared unresponsive to IBA in this assay (Figure 3.3.A. and 3.3.B.). *pex7-2* was more resistant to the promotion of lateral roots by IBA than *pex7-1*, but like other *pex* mutants, still responded robustly to the promotion of lateral roots by the synthetic auxin 1-naphthaleneacetic acid (NAA) (Figure 3.4.A. and 3.4.B.), implicating conversion of the IBA protoauxin to active IAA rather than the ability to form lateral roots as the *pex7-2* mutant defect.

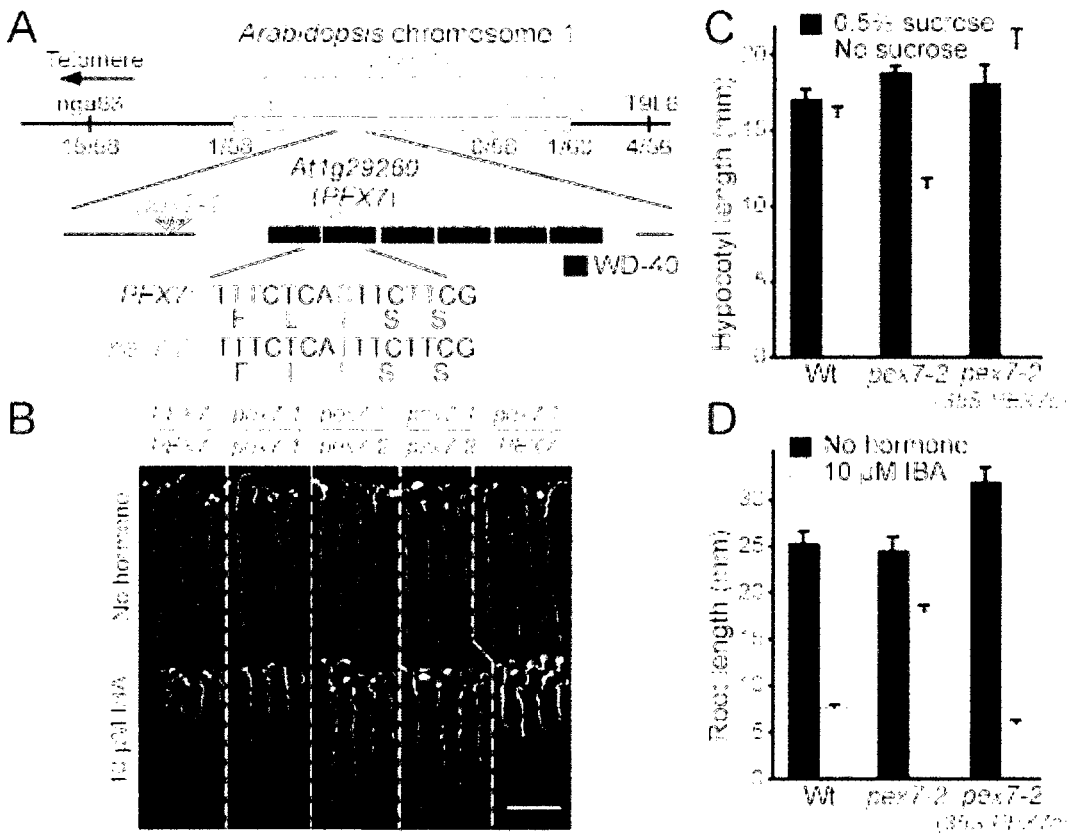

Figure 3.2. Positional cloning of the gene defective in *pex7-2*.

A. Mapping with PCR-based markers nga63, F28N24, F27G20, F6N18, and T9L6 localized the defect between F27G20 and the F28N24. Examination of genes in this region revealed the *PEX7* gene (*At1g29260*), which encodes the PTS2 receptor, a WD-40 repeat protein. *pex7-2* has a C to T mutation at position 371 (where 1 is the A in the initiator ATG) that causes a threonine to isoleucine missense mutation in the second WD-40 repeat. B. *pex7-2* fails to complement *pex7-1*. Roots of eight-day-old seedlings grown under yellow-filtered light on 10 μM IBA or medium containing no hormone were removed from the agar for photography. Col-0 plants were used as wild type (*PEX7/PEX7*). Four seedlings representing the range of observed responses were arranged on a new plate for photography. Scale bar represents 1 cm. C. *35S-PEX7* rescues *pex7-2* sucrose dependence. Roots of seedlings grown under white light for 1 day and transferred to the dark for five additional days of growth on medium containing 0.5% sucrose or no sucrose were removed from the agar and hypocotyl lengths were measured. Bars show mean + SE; $n \geq 9$. D. *35S-PEX7* rescues *pex7-2* IBA resistant root elongation. Eight-day-old seedlings grown under yellow-filtered light on 10 μM IBA or medium containing no hormone were removed from the agar and roots were measured. Bars show mean + SE; $n \geq 10$.

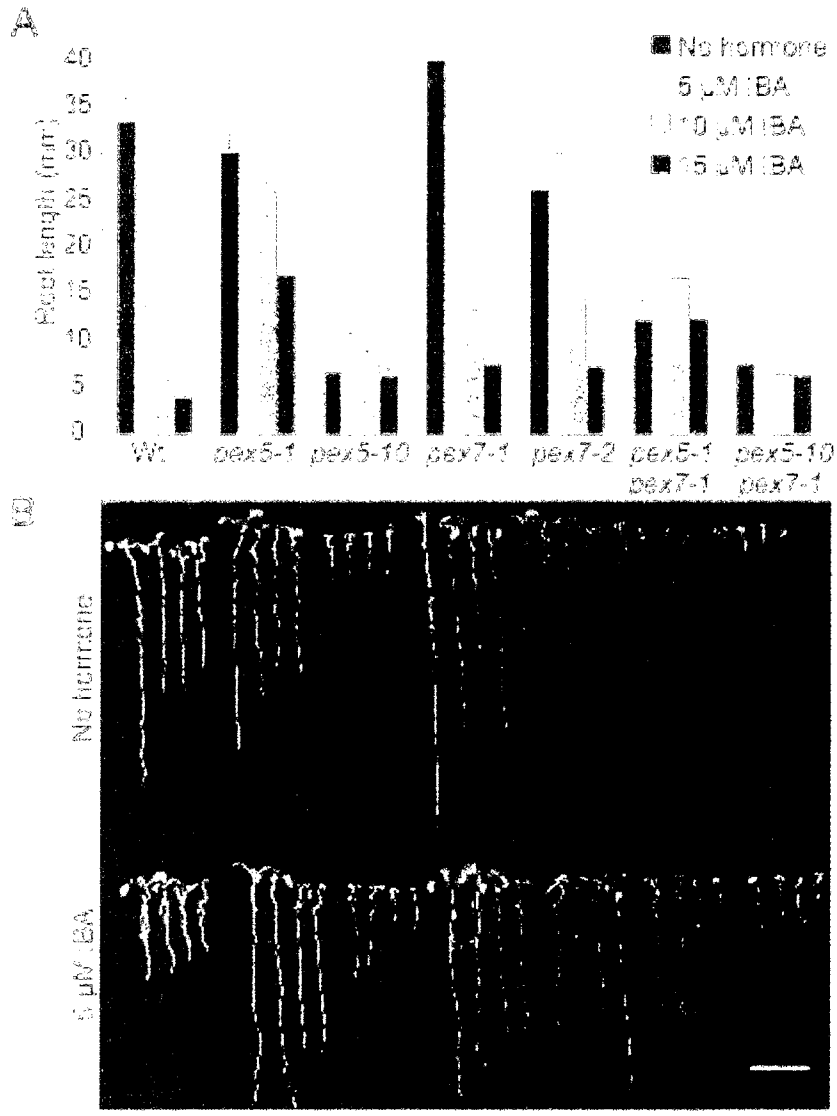

Figure 3.3. *pex* mutants are resistant to root elongation inhibition by IBA.

A. Seedlings stratified 3 days at 4°C then grown for 8 days under yellow-filtered light on medium without hormone or supplemented with IBA were removed from the agar and roots were measured. Bars show mean + SE; $n \geq 8$. B. Four seedlings representing the range of observed responses were arranged on a new plate for photography; scale bar represents 1 cm.

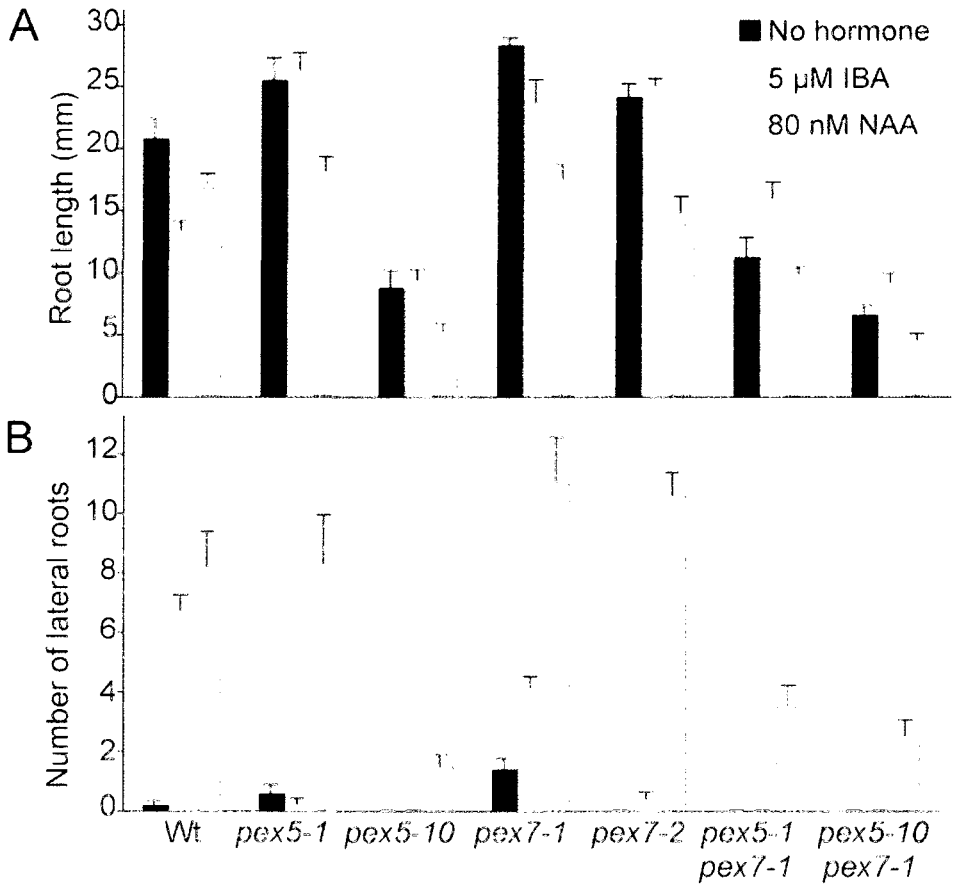

Figure 3.4. *pex* mutants are resistant to lateral root promotion by IBA.

Four-day-old seedlings were transferred from hormone-free medium to medium containing IBA, the synthetic auxin NAA, or no hormone. After 4 additional days, plants were removed from the agar and root length was measured (A) and lateral roots emerged from the primary root were counted (B). Bars show mean + SE; $n \geq 10$.

In addition to IBA response defects, peroxisome-defective mutants often fail to efficiently β-oxidize seed storage fatty acids following germination, resulting in developmental arrest or delays that can be restored by the provision of sucrose (Hayashi et al., 1998; Zolman et al., 2000). I found that *pex7-2*, unlike *pex7-1*, was markedly sucrose dependent in the dark, similar to *pex5-1* but not as severe as *pex5-10* (Figure 3.5.A. and 3.5.B.). When grown in the light, however, *pex7-2* was severely sucrose dependent, whereas *pex5-1* and *pex7-1* resembled wild type (Figure 3.5.C. and 3.5.D.).

3.3. *pex7-2* is developmentally delayed

When grown on sucrose in the light, *pex7-2* seedlings were smaller than *pex7-1* and *pex5-1*, which resembled wild type, but not as small as *pex5-10* (Figure 3.6.A.). Although *pex7-2* and *pex5-10* are developmentally delayed as seedlings, they eventually produce healthy, fertile adult plants (Figure 3.6.B.).

3.4. Severe *pex* receptor mutants are resistant to paraquat

Because *pex* mutants have deficient peroxisomes, we expected that the ability of these mutants to neutralize oxidative stress might be impaired. I analyzed the response of *pex7* and *pex5* mutants to conditions of high oxidative stress by growing the mutants in the presence of paraquat, an herbicide that produces superoxide radicals through inhibition of photosynthesis (Asada, 1996). Based on Joseph Faust's preliminary results showing that Drosophila *pex3* RNAi lines are paraquat super-sensitive, I expected to see enhanced sensitivity to paraquat in *pex7* and *pex5* mutants. However, the more severe *pex* mutants *pex5-10* and *pex7-2* displayed resistance to paraquat in a root elongation assay (Figure 3.7).

We can envision several possibilities that might explain the enhanced resistance of the *pex* mutants to paraquat. Reduced photosynthetic efficiency in plants causes

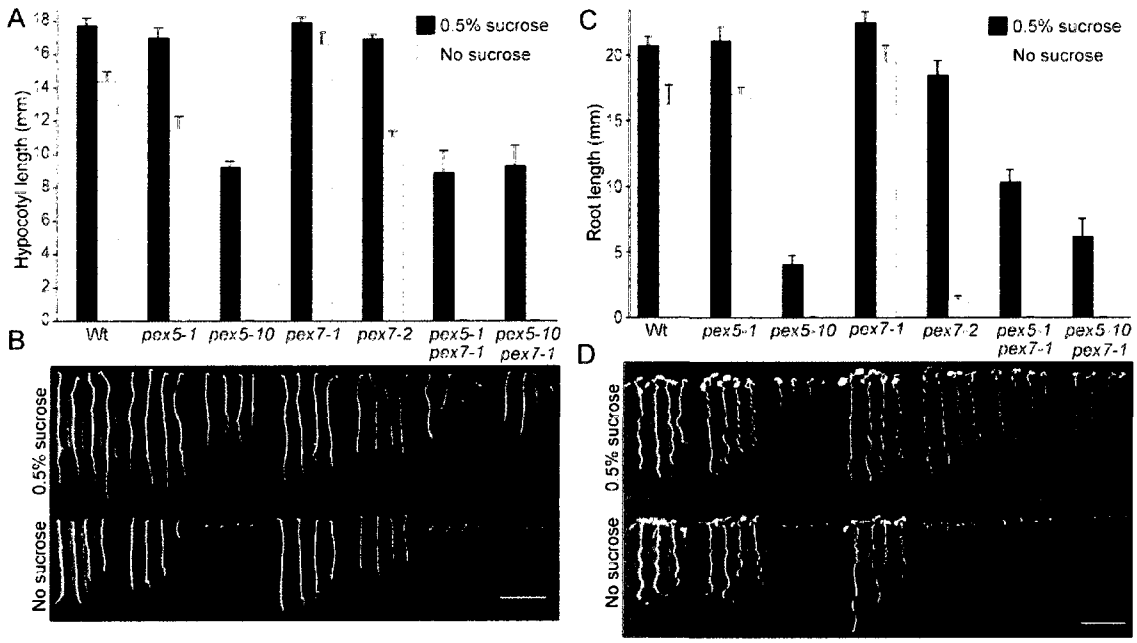

Figure 3.5. *pex7-2* sucrose dependence suggests defects in fatty acid metabolism.

A. Hypocotyl lengths of seedlings grown on sucrose-free medium for 1 day in the light and 5 days vertically in darkness compared to plants grown on 0.5% sucrose. Bars show mean + SE; $n \geq 9$. B. Four seedlings representing the range of observed hypocotyl lengths in panel A were arranged on a new plate for photography; scale bar represents 1 cm. C-D. Sucrose dependence of light-grown *pex* mutants. C. Root lengths of seedlings grown for 8 days on sucrose-free medium under white light compared to plants grown on medium supplemented with 0.5% sucrose. Bars show mean + SE; $n \geq 10$. D. Four seedlings representing the range of observed responses in panel C were arranged on a new plate for photography; scale bar represents 1 cm.

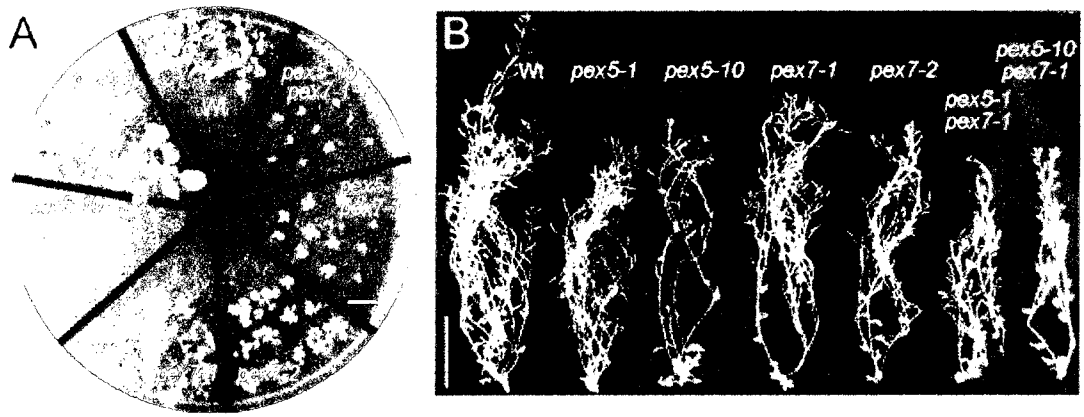

Figure 3.6. Developmental defects of *pex5* and *pex7* mutant plants.

A. *pex5-10, pex7-2,* and *pex5 pex7-1* double mutants are developmentally delayed. Seedlings were grown for 26 days on medium supplemented with 0.5% sucrose under white light. Bar, 1 cm. B. *pex5* and *pex7* mutants produce relatively healthy and fertile adult plants. Plants from panel *A* were transferred to soil and grown under constant white light. Representative 55-day-old plants are shown. Scale bar represents 10 cm.

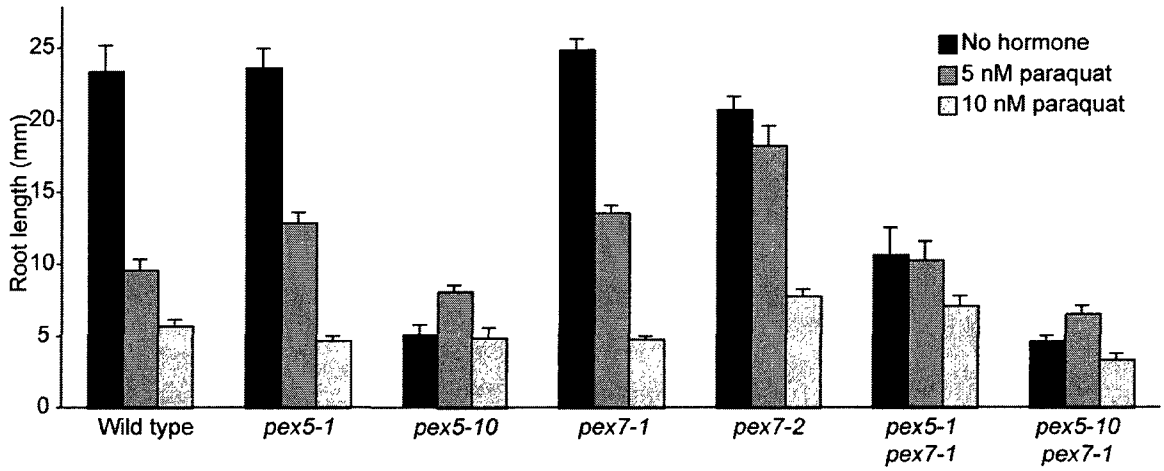

Figure 3.7. Severe *pex* mutants are resistant to paraquat.

Roots of eight-day-old seedlings grown under yellow-filtered light on paraquat or unsupplemented medium were removed from the agar and root length was measured. Bars show mean + SE; $n \geq 8$.

resistance to paraquat (Chase et al., 1998). Some photorespiration mutants have reduced photosynthesis (Somerville and Ogren, 1980; Somerville and Ogren, 1981). Severe *pex* mutants are pale when grown in the light suggesting a deficiency in photorespiration. Thus, it is possible that the reduced photorespiration in severe *pex* mutants is causing resistance to paraquat through a reduction in photosynthetic efficiency. An alternative hypotheis, is that, perhaps, in peroxisome import mutants, catalase remains in the cytosol in a stable and active form, as in some patients with peroxisome biogenesis disorders (Fujiwara et al., 2000; Akiyama et al., 2002), and can therefore fight off superoxide radicals in the cytosol. Additional experiments will be needed to distinguish amongst these possibilities.

3.5. Enhanced peroxisome-defective phenotypes in *pex7 pex5* double mutants

The phenotypically weak *pex7-1* mutation dramatically enhances *pex5-1* phenotypes, consistent with the finding that both single mutants confer partial defects in PTS2 import (Woodward and Bartel, 2005). In contrast to *pex7-1*, I was unable to recover viable *pex5-1 pex7-2* or *pex5-10 pex7-2* double mutants. For example, I analyzed the progeny of *pex5-1/pex5-1 pex7-2/PEX7* individuals and found 69% (18/26) *pex5-1/pex5-1 pex7-2/PEX7* plants and 31% (8/26) *pex5-1/pex5-1 PEX7/PEX7* plants, suggesting that the *pex5-1 pex7-2* double mutant is lethal. Similarly, in the progeny of *pex5-10/PEX5 pex7-2/pex7-2* plants, I observed 62% (8/13) *pex5-10/PEX5 pex7-2/pex7-2* plants and 38% (5/13) *PEX5/PEX5 pex7-2/pex7-2* plants, suggesting that *pex5-10 pex7-2* is also lethal.

Altogether, I analyzed 343 progeny of *pex5-1* x *pex7-2* crosses and 91 progeny of *pex5-10* x *pex7-2* crosses without recovering either double mutant. I analyzed developing seeds in *pex5-1/pex5-1 pex7-2/PEX7* and *pex5-10/PEX5 pex7-2/pex7-2* siliques and found that these plants generate approximately 9% (16/184) and 10% (24/249) shrunken seeds, respectively (Figure 3.8.B). I concluded that combining *pex7-2*

with either *pex5-1* or *pex5-10* confers embryonic lethality, confirming that peroxisome matrix protein import is essential for *Arabidopsis* embryogenesis. Moreover, our inability to recover the *pex5-10 pex7-2* double mutant strongly suggests that the *pex5-10* allele does not completely abolish PEX5 function, despite the presence of a T-DNA in exon five (Zolman and Bartel, 2004).

In contrast to the inviability of the *pex5 pex7-2* double mutants, I was able to isolate the *pex5-10 pex7-1* double mutant. The *pex5-10 pex7-1* mutant resembled *pex5-10*; it did not germinate without sucrose (Figure 3.5.A-D) and displayed similar IBA resistance as *pex5-10* in root elongation (Figure 3.3.A and B) and lateral root initiation (Figure 3.4.A and B) assays. The general growth and development of *pex5-10 pex7-1* also was similar to that of *pex5-10*; both mutants were slow to develop when grown with sucrose in the light or the dark (Figure 3.5.A-D and 3.6.A), but eventually produced relatively healthy, fertile adult plants (Figure 3.6.B). The viability of *pex5 pex7-1* double mutants coupled with the inviability of *pex5 pex7-2* double mutants is consistent with our phenotypic analyses of the relative defects in the *pex7-1* and *pex7-2* single mutants, which also suggest that *pex7-2* more completely blocks *PEX7* function than *pex7-1*.

3.6. Conclusions

The sucrose dependence and IBA resistance defects in the *pex* receptor mutants suggest that the mutants have defective peroxisomes (Figure 3.5). The resistance of the strong receptor mutants *pex7-2*, *pex5-10*, and the *pex5-1 pex7-1* and *pex5-10 pex7-1* double mutants to the effects of paraquat (Figure 3.7) could be due to reduced photosynthesis efficiency. The enhanced phenotypes seen in the *pex5 pex7-2* doubles support the hypothesis that *Arabidopsis PEX7* functions in a manner that is not entirely dependent on *PEX5*. The following chapters will describe my exploration of the molecular defects underlying the physiological defects that I have observed.

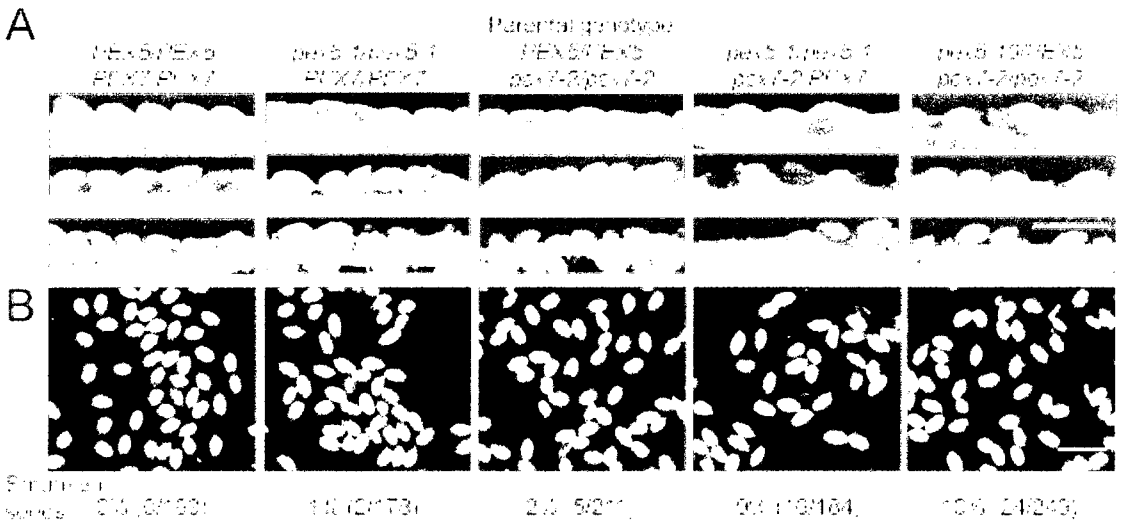

Figure 3.8. *pex7-2* confers embryo lethality in combination with *pex5* mutants.

A. Valves were removed from siliques of the indicated genotypes to reveal developing seeds. Images are arranged in order of increasing silique maturity (top to bottom). B. Mature seed phenotypes of lines in panel *A*; the fraction of shrunken versus filled seeds is shown below the images. Bar, 1 mm.

Chapter 4: Characterization of PEX7 and PEX5 interactions

Nito et al. have shown in *Arabidopsis* that the region in which *pex5-1* is mutated is necessary but not sufficient for PEX5 binding to PEX7 (2002). Studies of human PEX5, however, implicate the same region in the *Arabidopsis pex5-1* mutant as being sufficient to bind PEX7 (Braverman et al., 1998; Otera et al., 1998). The *pex7-2* mutation could be detrimental to the formation of a PEX5-PEX7 complex or may bind PEX5 but not cargo PTS2 proteins. I used directed yeast 2-hybrid experiments using *pex7-2* and *pex5-1* to determine whether the residues that are mutated in either mutant are vital to the protein binding domains. I generated PEX7, pex7-2, PEX5, pex5-1, PEX7-SKL, pex7-2-SKL, PED1, and PED1-SKL constructs fused to the Gal4 activation domain using the pBI771 "prey" vector (Kohalmi et al., 1998) or to the Gal4 DNA-binding domain using the pBI770 "bait" vector (Kohalmi et al., 1998). Various construct combinations (Table 4-1 and Figure 4.1) were transformed into the AH109 yeast strain following standard procedures (Gietz and Schiestl, 1995).

4.1. pex7-2-PEX5 interactions

In plants and mammals, PEX7 must bind both PTS2 cargo and the PTS1 receptor PEX5 to deliver PTS2 cargo to peroxisomes (Braverman et al., 1998; Otera et al., 1998; Nito et al., 2002; Hayashi et al., 2005; Woodward and Bartel, 2005). I used directed yeast two-hybrid assays to determine whether one or both of these functions was altered in pex7-2. As previously demonstrated (Nito et al., 2002), I found that *Arabidopsis* PEX7 and PEX5 interacted in the yeast two-hybrid assay. However, pex7-2 did not interact with PEX5 in this assay (Figure 4.2.A). Because pex7-2 protein efficiently accumulated in yeast (Figure 4.2.B), a failure to grow suggests a deficiency in receptor binding.

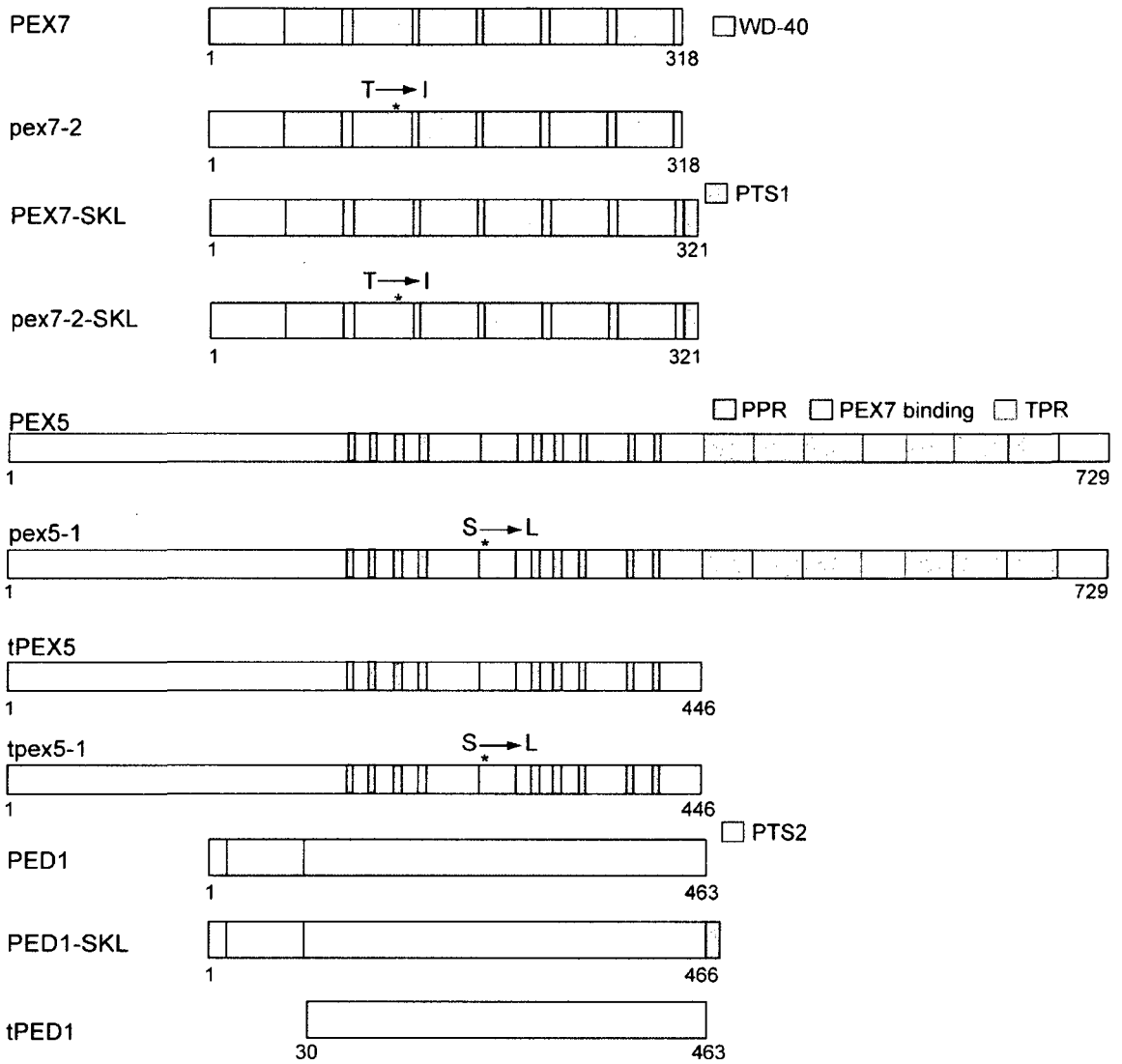

Figure 4.1. Peroxin and thiolase constructs used in yeast two-hybrid analysis.

The PEX7 constructs were all fused to the Gal4-DNA binding domain (BD), PEX5 constructs were fused to the Gal4-activation domain (AD), and PED1 constructs were fused to both the Gal4-DNA BD and Gal4-AD. TPR, tetratricopeptide repeat; PPR, pentapeptide repeat; PTS1/2, peroxisome targeting signal 1/2. Numbers below schematics indicate amino acid residues in the corresponding proteins. Asterisks denote the location of point mutations.

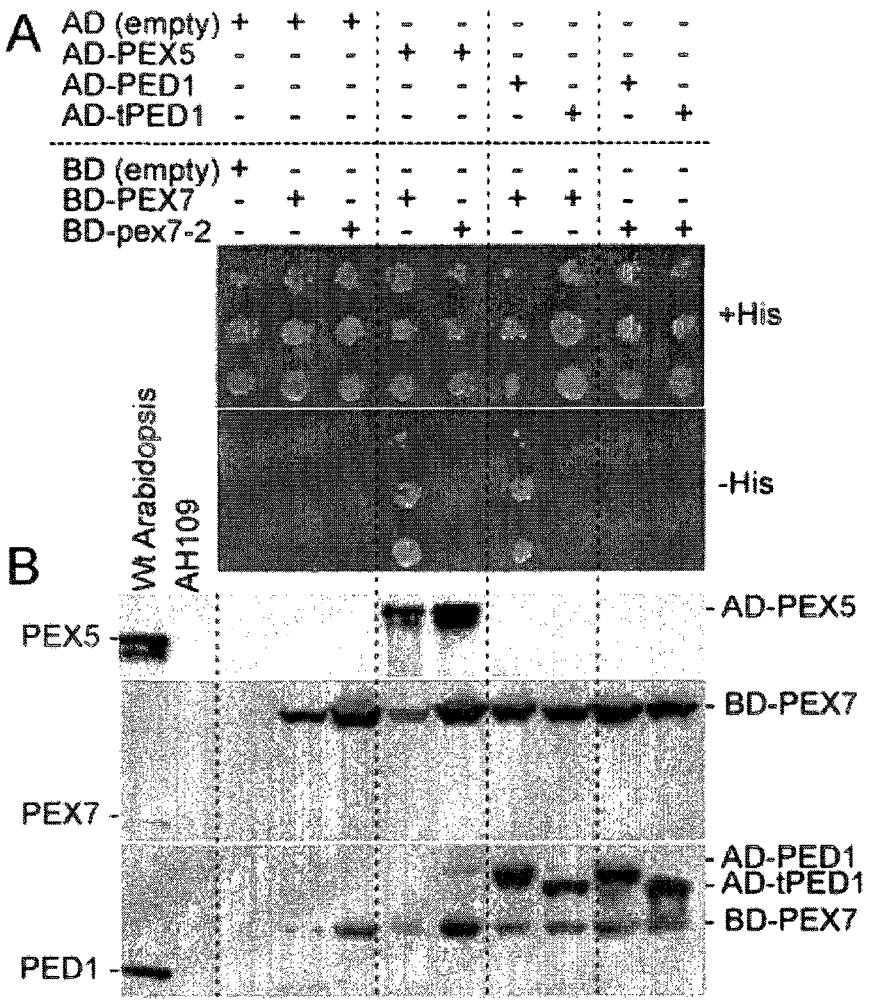

Figure 4.2. The pex7-2 lesion disrupts PEX5 and PTS2-cargo binding in yeast.

A. Yeast two-hybrid assays were conducted with PEX7 and pex7-2 fused to the GAL4-DNA binding domain (BD) and PEX5, PED1 (a PTS2 protein), and tPED1 (without the PTS2 region) fused to the GAL4 activation domain (AD). See Figure 4.1. for a description of the constructs. Serial dilutions spotted onto permissive plates (+His) and plates on which growth requires interaction (-His) are shown after incubation at 30°C for 2 days. B. Proteins extracted from yeast strains in panel *A* were separated using SDS-PAGE and immunoblots were sequentially probed with the indicated antibodies generated against PEX5 (top), PEX7 (middle), and PED1 (bottom). Extracts from 8-day-old wild-type *Arabidopsis* seedlings and the untransformed AH109 yeast were included as controls (left two lanes).

4.2. pex7-2-cargo interactions

To determine if the pex7-2 mutation disrupted cargo binding, I also compared PEX7 and pex7-2 interactions with the PTS2 protein thiolase (PED1). As expected, PEX7 interacted with PED1 but not with a N-terminally truncated version of PED1 (tPED1) lacking the PTS2 region (Figure 4.2.A). In contrast, I found that pex7-2 paired with PED1 did not grow on selective medium (Figure 4.2.A). Because the Gal4-pex7-2 and Gal4-PEX7 proteins accumulated similarly in yeast (Figure 4.2.B), our yeast two-hybrid results suggest that the pex7-2 mutation disrupts both PEX5 and PTS2 cargo binding. This result may mean that the pex7-2 mutation alters folding in such a way that impedes all PEX7 interactions. Alternatively, PEX7 may need to bind cargo to bind PEX5, or PEX7 may need to bind PEX5 to bind cargo, and a direct disruption of one of these interactions impairs the other as well.

4.3. PEX5-cargo interactions

The *pex5-1* mutant displays reduced levels of PTS2 protein import into peroxisomes (Woodward and Bartel, 2005). One hypothesis to explain this defect is that pex5-1 impairs PEX7 binding. If this hypothesis is correct it may be possible to rescue pex5-1 phenotypes by making PTS2 proteins recognizable to PEX5 through addition of a PTS1. To test the feasibility of this idea, I generated a PED1-PTS1 construct (PED1-SKL) fused to the GAL4-DNA binding domain and expressed it in yeast along with PEX5 and pex5-1 fused to the GAL4 activation domain. I found that PED1-SKL did in fact bind to PEX5 and pex5-1 (Figure 4.3), whereas the control PED1 construct did not bind PEX5, as expected (Figure 4.3). Because we have a construct that will bind pex5-1, it will be interesting to see if transforming PED1-SKL into *pex5-1* plants will rescue mutant phenotypes. This result also supports the conclusion that *pex5-1* is not deficient in GFP-PTS1 import (Woodward and Bartel, 2005) because it is still able to interact with a PTS1-containing protein.

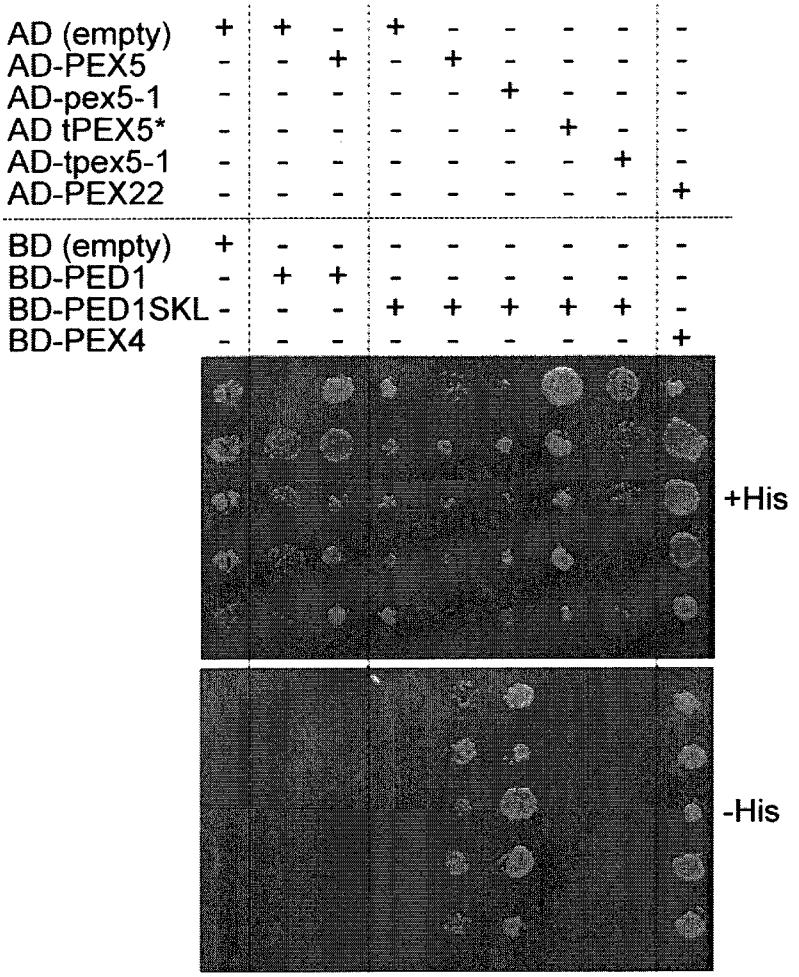

Figure 4.3. Full-length and truncated PEX5-cargo interaction.

A yeast two-hybrid assay was conducted with PED1 and PED1-SKL fused to GAL4-DNA binding domain (BD) and PEX5 and pex5-1 fused to the GAL4 activation domain (AD). The PEX4-PEX22 interaction was used as the positive control (Zolman et al., 2005). Colony replicates were spotted onto permissive plates (+His) and plates on which growth requires interaction (-His). Plates were incubated at 30°C for 2 days. The AD-tPEX5 construct contains a frameshift mutation and thus strains containing AD-tPEX5 cannot grow on –His.

4.4. pex5-1-PEX7 interactions

The *pex5-1* mutant has a defect in PTS2-GFP import and not GFP-PTS1 import (Woodward and Bartel, 2005). Because *pex5-1* contains a mutation in the presumed PEX7 binding site, we hypothesized that the reason for the disruption in PTS2 import in this mutant could be due to a disruption of interaction with PEX7. Surprisingly, I found that strains coexpressing pex5-1 and PEX7 were able to grown on –His, suggesting that interaction between these two proteins is not disrupted by the Ser to Leu mutation (Figure 4.4). Because pex7-2 was not able to interact with PEX5 (Figure 4.2.A), I did not expect to see pex7-2 interaction with pex5-1. Indeed, pex7-2 did not grow on –His when paired with pex5-1 (Figure 4.4). It is possible that although pex5-1 still interacts with PEX7, it may have a weaker interaction that the yeast two-hybrid is not sensitive enough to detect. Another possibility is that the pex5-1 mutation may actually strengthen the interaction with PEX7 causing PEX7 to be unable to release from PEX5 and somehow disrupting PEX7 function. In the future, β-galactosidase assays may assist in distinguishing between stronger and weaker binding interactions. I will discuss my exploration of a third possible explanation in the following sections.

4.5. Truncated pex5-1-PEX7 interactions

The existence of a yeast protein or proteins possessing both a PTS1 and PTS2 that bridges pex5-1 and PEX7 could explain the ability of pex5-1 to bind to PEX7 in the yeast two-hybrid assay. A few Arabidopsis peroxisomal proteins contain both a PTS1 and a PTS2 (Fulda et al., 2002; Shockey et al., 2002) and such proteins may bridge the interaction between PEX5 and PEX7. Pex8p in the yeast *Hansenula polymorpha* possesses both a PTS1 and PTS2 (Waterham et al., 1994). Similary, *S. cerevisiae* Pex8p possesses a PTS1 that is not essential for peroxisomal targeting, suggesting that it may

possess another localization signal (Waterham et al., 1994; Rehling et al., 2000; Wang et al., 2004).

To test the hypothesis that yeast proteins containing both a PTS1 and PTS2 could be bridging the interaction between *pex5-1* and PEX7, I created truncated PEX5 and pex5-1 constructs so that they would lack the TPR repeat-containing cargo-binding region (Figure 4.1) and coexpressed these truncated versions with the PEX7 construct. Surprisingly, PEX7 no longer interacted with tPEX5 (data not shown), suggesting that PEX5 may need to bind cargo to bind PEX7. However, strains containing tpex5-1 coexpressed with PEX7 were still able to grow on –His medium (data not shown). When I sequenced the tPEX5 construct, I discovered a stop codon early in the coding sequence, explaining why tPEX5 could not bind PEX7 but tpex5-1 could.

4.6. Truncated pex5-1-cargo interactions

As expected, when I coexpressed tpex5-1 with PED1-SKL the strain was unable to grown on –His suggesting that the truncated version of pex5-1 successfully disrupts interaction with PTS1-cargo (Figure 4.3).

4.7. Engineering an alternate PEX5-PEX7 interaction

We had originally expected that pex5-1 would show reduced binding to PEX7, and therefore I engineered PEX7 with a C-terminal PTS1 (PEX7-SKL) to provide an alternate means for PEX7 to bind to pex5-1 and perhaps deliver PTS2 cargo to the peroxisome. Indeeed, PEX7-SKL binds pex5-1 in the yeast two-hybrid, but so does PEX7 (Figure 4.4), so this experiment was not informative.

When I examined a pex7-2-SKL construct in these assays, I found that unlike pex7-2, slight growth was observed for the pex7-2-SKL/PEX5 and pex7-2-SKL/pex5-1 pairs (Figure 4.4), suggesting that the SKL was able to direct binding of pex7-2-SKL to the PEX5 cargo-binding region, and supporting the conclusion that pex5-1 is not

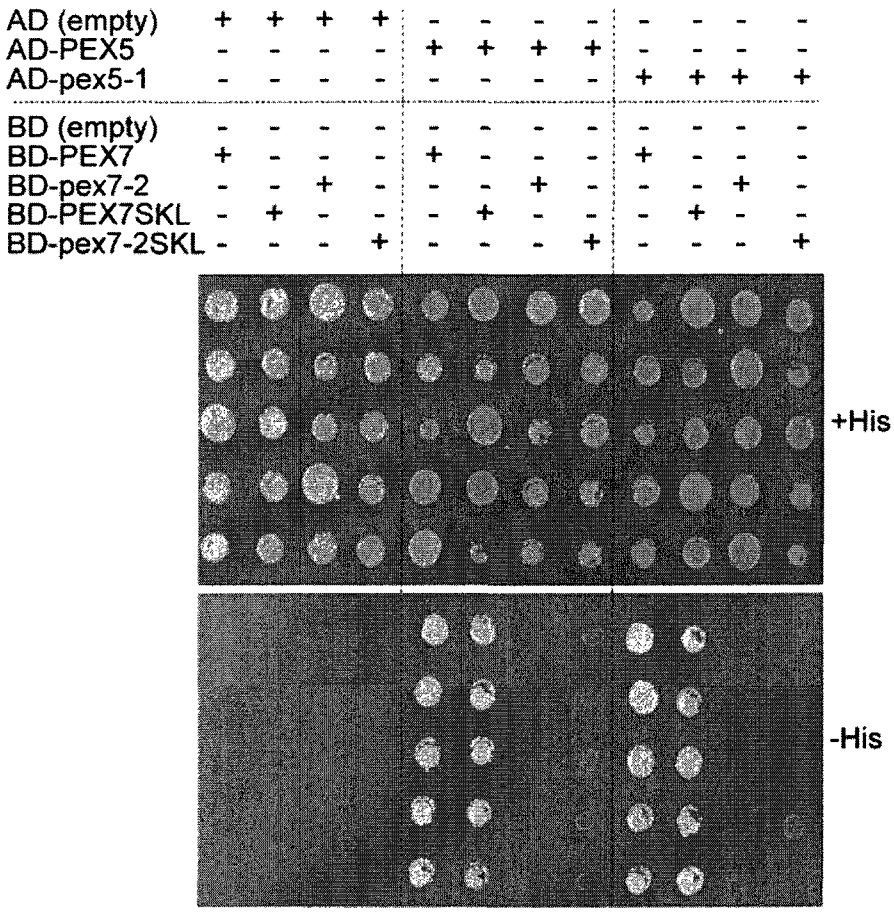

Figure 4.4. Rescue receptor interaction.

A yeast two-hybrid assay was conducted with PEX7 and pex7-2SKL fused to GAL4-DNA binding domain (BD) and PEX5 and pex5-1 fused to the GAL4 activation domain (AD). Colony replicates were spotted onto permissive plates (+His) and plates on which growth requires interaction (-His). Plates were incubated at 30°C for 2 days.

deficient in PTS1 binding. The growth on –His in the pex7-2-SKL/pex5-1 pair (Figure 4.4), however, is much weaker than the PED1-SKL/pex5-1 pair (Figure 4.3) or the PEX7-SKL/pex5-1 pair (Figure 4.4) further implying that the pex7-2 mutation somehow hinders binding to PEX5.

4.8. Conclusions

My yeast two-hybrid analysis revealed that pex7-2 disrupts interaction with cargo and PEX5 and furthermore, that these interactions can be partially restored through the addition of a C-terminal PTS1. I unexpectedly found that pex5-1 did not disrupt interaction with cargo or PEX7 and, in this case, my assays were not sensitive enough to distinguish whether these interactions were in fact weaker than those with PEX5. Through the use of a truncated pex5-1 version, I was able to eliminate the possibility that a yeast protein possessing both a PTS1 and PTS2 could be bridging the interaction of pex5-1 with PEX7. Chapter 5 describes my determination of the effects these disrupted interactions might have in vivo.

Table 4-1. Summary of yeast strains used in this study.

Strain	pBI770 (BD)	pBI771 (AD)	Stock number	-His growth
1	PEX7	PED1	2228	++
2	PEX7	tPED1	2229	no
3	PEX7	PEX5	2230	+++
4	PEX7	pex5-1	2231	+++
5	pex7-2	PED1	2232	no
6	pex7-2	PEX5	2233	no
7	pex7-2	pex5-1	2234	no
8	PEX7SKL	pex5-1	2235	+++
9	PED1SKL	pex5-1	2236	+++
10	PEX4	PEX22	2237	+++
11	pBI770	pBI771	2238	no
12	PEX7	pBI771	2239	no
13	pex7-2	pBI771	2240	no
14	PEX7SKL	pBI771	2241	no
15	PED1SKL	pBI771	2242	no
16	pBI770	PED1	2243	no
17	pBI770	tPED1	2244	no
18	pBI770	PEX5	2245	no
19	pBI770	pex5-1	2246	no
20	PED1	PEX5	2247	no
21	PED1	pex5-1	2248	no
22	pex7-2-SKL	pBI771	2249	no
23	pex7-2-SKL	pex5-1	2250	no
24	PED1	pBI771	2252	no
25	PED1SKL	PEX5	2253	+++
26	PEX7SKL	PED1	2254	no
27	pex7-2-SKL	PED1	2255	no
28	PEX7SKL	PEX5	2256	+++
29	pex7-2-SKL	PEX5	2257	+
30	PEX7	PEX7	2263	no
31	PED1	PEX7	2264	no
32	PED1	pex7-2	2265	no
33	PED1	PEX7SKL	2266	+
34	pBI770	PEX7	2267	no

[1]We discovered that the tPEX5 construct has a frameshift mutation. Any yeast two-hybrid results from strains containing tPEX5 therefore are not shown.
[2]pBI770-PEX5 (Nito et al., 2002) and pBI770-tpex5-1 self activate. Any yeast two-hybrid results from strains containing pBI770-tpex5-1 were deemed unreliable and are not shown.

Table 4-1. (cont.)

Strain	pBI770 (BD)	pBI771 (AD)	Stock number	-His growth
35	pBI770	pex7-2	2268	no
36	pBI770	PEX7SKL	2269	no
37	PED1SKL	PEX7	2270	no
38	PED1SKL	pex7-2	2271	no
39	PED1SKL	PEX7SKL	2272	no
40	pex7-2	PEX7	2273	no
41	pex7-2	pex7-2	2274	no
42	pex7-2	PEX7SKL	2275	no
43	PEX7	PEX7SKL	2276	no
44	PEX7	pex7-2	2277	no
45	PEX7SKL	PEX7	2278	no
46	PEX7SKL	pex7-2	2279	no
47	PEX7SKL	PEX7SKL	2280	no
48	pex7-2SKL	PEX7	2281	no
49	pex7-2SKL	pex7-2	2282	no
50	pex7-2SKL	PEX7SKL	2283	no
51	PEX7	PED1SKL	2304	+++
52	pex7-2	PED1SKL	2305	no
53	PEX7SKL	PED1SKL	2306	+++
54[1]	tPEX5	pBI771	2307	no
59[2]	tpex5-1	pBI771	2312	+++
70[1]	pBI770	tPEX5	2323	no
75	pBI770	tpex5-1	2328	no
76	PEX7	tpex5-1	2329	+++
77	pex7-2	tpex5-1	2330	no
78	PEX7SKL	tpex5-1	2331	+++
79	pex7-2SKL	tpex5-1	2332	no
83	PED1	tpex5-1	2335	no
84	tPED1	tpex5-1	2372	
85	PED1SKL	tpex5-1	2336	no
86	pBI770	PED1SKL	2373	
87	pBI770	pex7-2SKL	2374	
88	pex7-2	tPED1	2375	no
89	tPED1	pBI771	2376	

Chapter 5: Molecular Analysis of *pex7-2*

This chapter describes my characterization of the molecular defects that underlie *pex7* and *pex5* phenotypes. I used western blotting to monitor protein accumulation and to indirectly assess defects in PTS2 protein import. GFP analysis helped me to directly assess defects in both PTS1 and PTS2 import in the mutants.

5.1. Matrix Protein Import Analysis

5.1.A. PTS2-protein processing

I indirectly assessed PTS2 cargo import into *pex7* peroxisomes by using immunoblotting to monitor removal of the PTS2 signal from thiolase and peroxisomal malate dehydrogenase (PMDH). PTS2 processing occurs after import and requires the action of the peroxisomally localized PTS2-processing protease DEG15, which is a PTS1 protein (Helm et al., 2007; Schuhmann et al., 2008). Similar to previous reports of thiolase processing defects in *pex7-1, pex5-10,* and *pex7-1 pex5-1* (Woodward and Bartel, 2005; Zolman et al., 2005), I found that thiolase and PMDH were fully processed in wild type, partially processed in the *pex7-1*, *pex7-2*, and *pex5-1* single mutants, and only minimally processed in *pex5-10* and the double mutants (Figure 5.1). I found similar thiolase processing defects in light- and dark-grown seedlings, although some defects appeared somewhat more severe when seedlings were grown in the light (Figure 5.1). For example, about half of the thiolase was processed in dark-grown *pex7-2* seedlings, whereas thiolase was almost completely unprocessed in light-grown *pex7-2* seedlings. PMDH does not accumulate in dark-grown seedlings (data not shown).

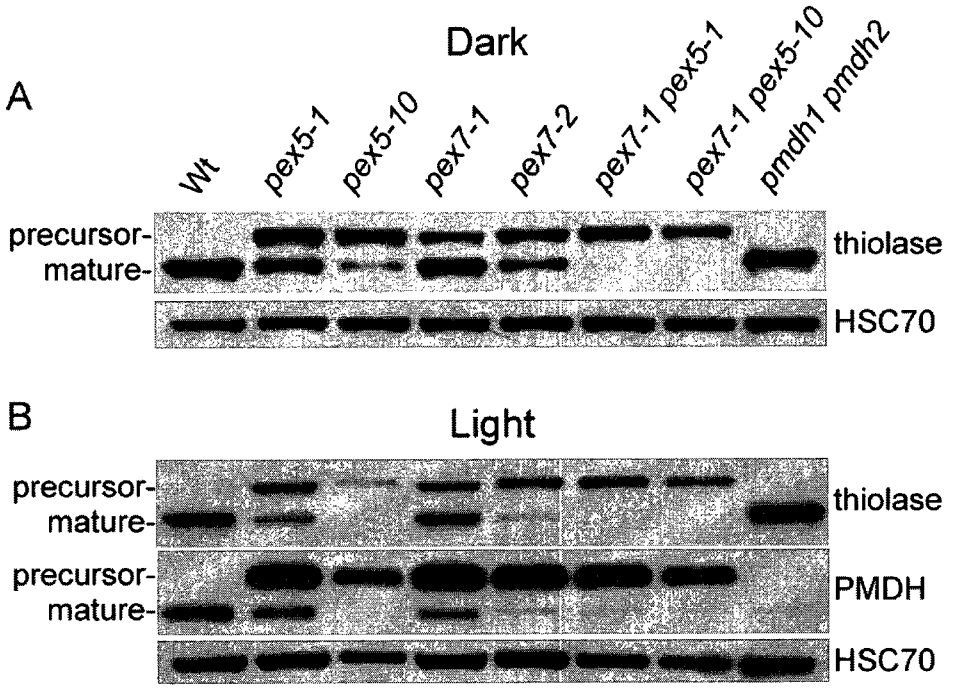

Figure 5.1. *pex7* and *pex5* single and double mutants have PTS2 processing defects.

A. Dark-grown *pex7* mutants have PTS2 processing defects. Proteins were extracted from seedlings grown 1 day in light and 4 days in darkness on 0.5% sucrose and analyzed by immunoblotting with the indicated antibodies. B. Light-grown *pex7* mutants have PTS2 processing defects. Proteins extracted from 7-day-old seedlings grown on 0.5% sucrose under white light were analyzed by immunoblotting. The *pmdh1pmdh2* double mutant, which contains T-DNAs inserted in both of the genes encoding peroxisomal malate dehydrogenase isozymes (Pracharoenwattana et al., 2007), is included as a control for the PMDH antibody.

5.1.B. Peroxisomally-targeted GFP analysis

To directly analyze the effects of the *pex7-2* mutation on matrix protein import, we crossed *pex7-2* to transgenic lines containing peroxisome-targeted green fluorescent protein (GFP) derivatives and I examined the resultant homozygous plants using confocal fluorescence microscopy. The PTS2-GFP construct contains the first 147 base pairs from the PED1 thiolase isoform, which includes the PTS2 sequence, fused to the N-terminus of GFP (Woodward and Bartel, 2005). Whereas wild-type cotyledon cells efficiently imported PTS2-GFP into punctate structures diagnostic of peroxisomes, I found that in *pex7-2* cotyledons, PTS2-GFP displayed some cytosolic fluorescence in the dark and mostly cytosolic fluorescence in the light (Figure 5.2). This localization confirmed that, although not completely blocked, PTS2 import is defective in *pex7-2*.

I also examined a PTS1 reporter (Zolman and Bartel, 2004), and found that GFP-PTS1 displayed the expected punctate peroxisomal fluorescence pattern in cotyledons of dark-grown *pex7* seedlings (Figure 5.3). Surprisingly, however, GFP-PTS1 displayed primarily cytosolic fluorescence in light-grown *pex7-2* seedlings, indicating a defect in GFP-PTS1 import into peroxisomes (Figure 5.3.). This PTS1 import defect was apparent in multiple cell types, including cotyledon epidermal cells and the underlying mesophyll cells (Figure 5.3). To assess whether this defect in PTS1-GFP was unique to *pex7-2*, I also examined cotyledons of the weaker *pex7-1* allele and in the *pex5-1 pex7-1* double mutant. In both cases I detected substantial cytosolic GFP-PTS1 in light-, but not dark-grown seedlings (Figure 5.3), confirming that reduced PTS1 import can result from decreased PEX7 function.

5.2. Protein accumulation analysis

The cytosolic fluorescence pattern of GFP-PTS1 in light-grown *pex7* mutants suggested that PTS1 import, and by extension PEX5, depends on PEX7. To further understand the basis of the *pex7* PTS1 import defects, I analyzed peroxin protein levels in

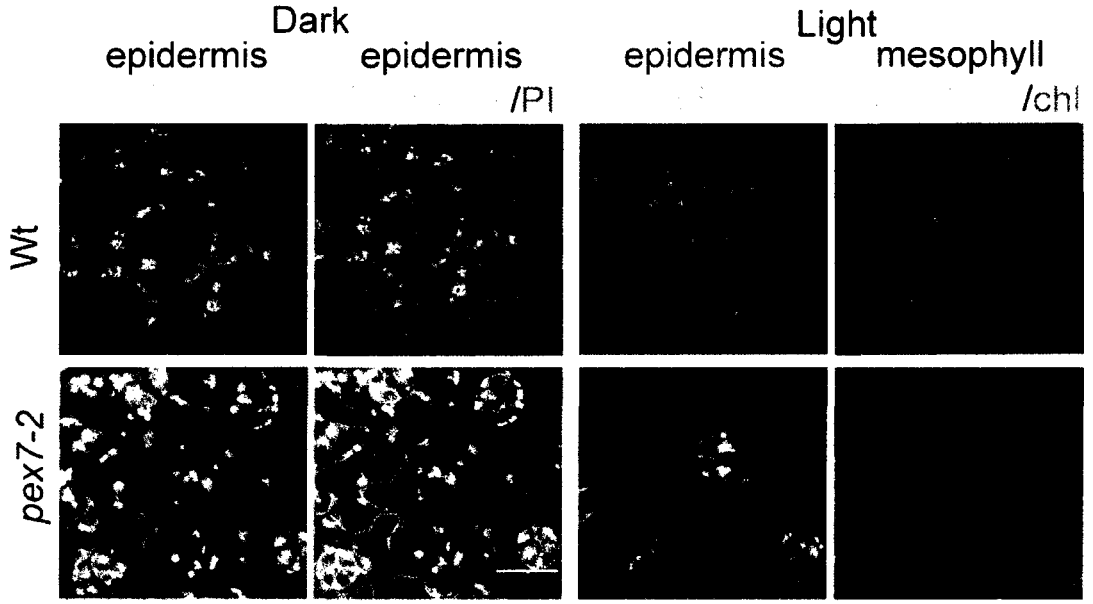

Figure 5.2. *pex7-2* has defective PTS2-GFP import.

Cotyledons of 7-day-old light-grown seedlings or of seedlings grown 1 day in the light and 4 days in the dark on 0.5% sucrose were analyzed using confocal fluorescence microscopy. Matrix protein import defects were visualized by imaging fluorescence from a GFP derivative (PTS2-GFP) carrying the N-terminal peroxisome targeting sequence from PED1 (Woodward and Bartel, 2005). Dark-grown cotyledons were briefly stained with propidum iodide, which stains cell walls, before visualization of epidermal cells; the second column from the left shows merged images of GFP (green; third column) and propidium iodide (red) fluorescence. Epidermal cells (third column) and the underlying mesophyll cells (last column) were imaged from light grown seedlings. The mesophyll column shows merged images of GFP (green) and chlorophyll (red) fluorescence. Because of the large central vacuole of expanded plant cells, most of the cytosol is consolidated at the cell margins. Scale bar represents 20 μm.

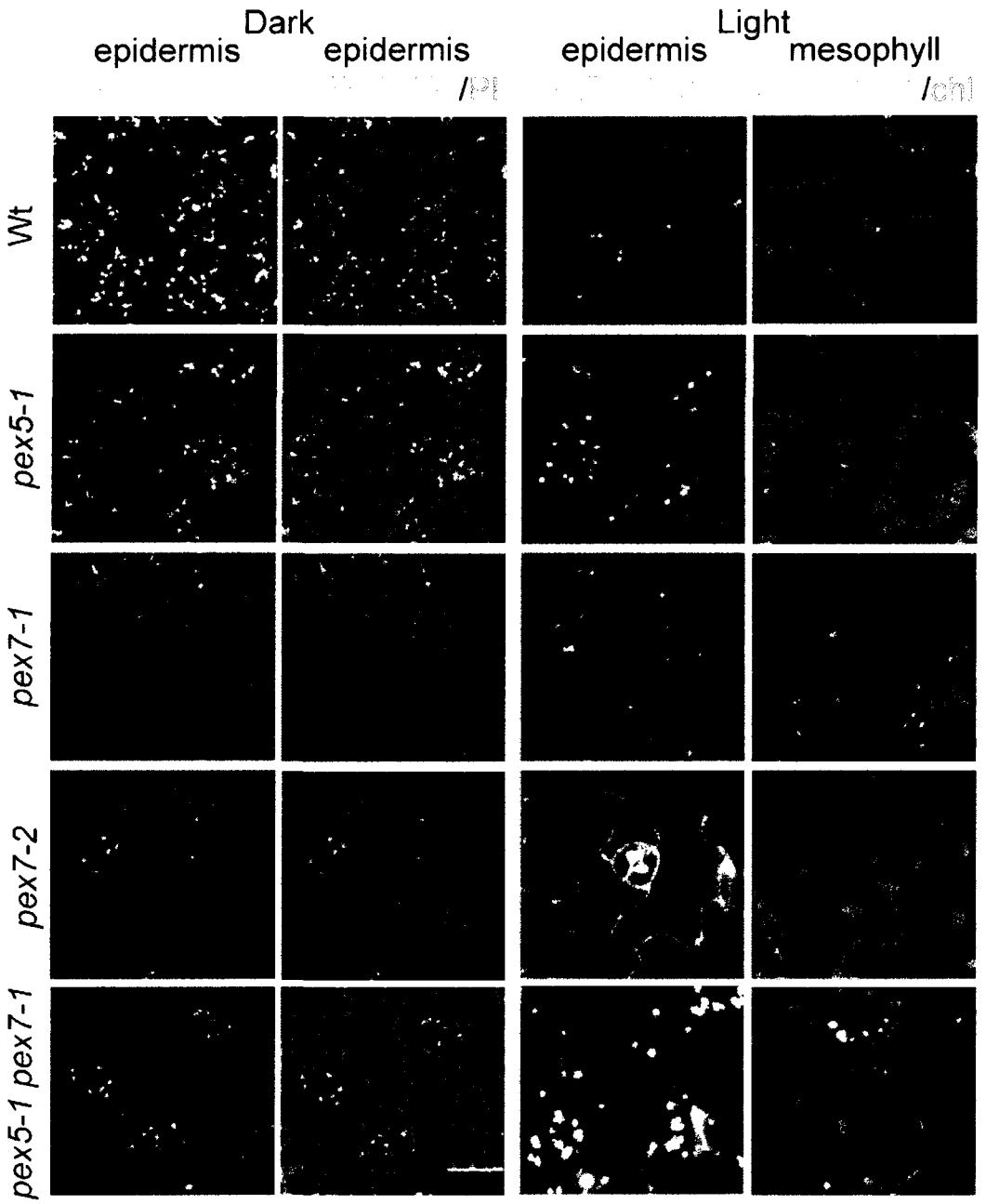

Figure 5.3. *pex7-2* has defective GFP-PTS1 protein import in the light.

Cotyledons of seedlings grown as in Figure 5.2 were analyzed using confocal fluorescence microscopy as in Figure 5.2. Matrix protein import defects were visualized by imaging fluorescence from a GFP derivative (GFP-PTS1) carrying the a C-terminal PTS1 (Zolman and Bartel, 2004). Scale bar represents 20 μm.

mutant seedlings. I found that PEX7 levels were similar to wild type in both *pex5* alleles but were reduced in both *pex7* alleles (Figure 5.4), consistent with the reduced *PEX7* mRNA level in *pex7-1* (Woodward and Bartel, 2005) and suggesting that the *pex7-2* lesion might impair PEX7 stability in seedlings in addition to disrupting PEX5 and cargo interactions (Figure 4.2.A). As previously reported (Woodward and Bartel, 2005; Zolman et al., 2005), *pex5-1* and *pex5-10* mutants accumulated normal and undetectable levels of full-length PEX5, respectively. Although PEX5 levels were nearly normal in *pex7* mutants grown in the dark (Figure 5.4.A), both *pex7* mutant alleles accumulated substantially less PEX5 than wild type in light-grown seedlings (Figure 5.4.B). This result suggested that the unexpected defects in GFP-PTS1 import displayed by the *pex7* mutants could be explained by the reduced accumulation of PEX5 in these mutants and that PEX5 might depend on PEX7 for stability in light-grown seedlings.

5.3. Conclusions

In this chapter, I have described direct and indirect evidence that *pex* receptor mutants have defects in PTS2 protein import. These defects seem to be enhanced when seedlings are grown in the light versus the dark, implying a direct or indirect effect of light conditions on peroxisome development. In *pex7* mutants, protein accumulation analysis revealed that low PEX7 levels probably contribute to the PTS2 defects I observed. In Chapter 4, I demonstrated that pex5-1 did not disrupt interaction with cargo or PEX7 in the yeast two-hybrid assay, and in this chapter, I found that *pex5-1* had no obvious effect on PEX5 or PEX7 protein accumulation, so it is still unclear what is causing the *pex5-1* PTS2 defects. Unexpectedly, I observed a defect in PTS1 protein import in light-grown *pex7* mutants. Protein accumulation analysis revealed that this PTS1 defect is accompanied by a decrease in PEX5 levels in the light, suggesting the possibility that restoring PEX5 levels might ameliorate *pex7* phenotypes. In Chapter 6, I

describe my attempts to rescue the *pex* receptor mutant phenotypes by overexpressing each receptor in each mutant.

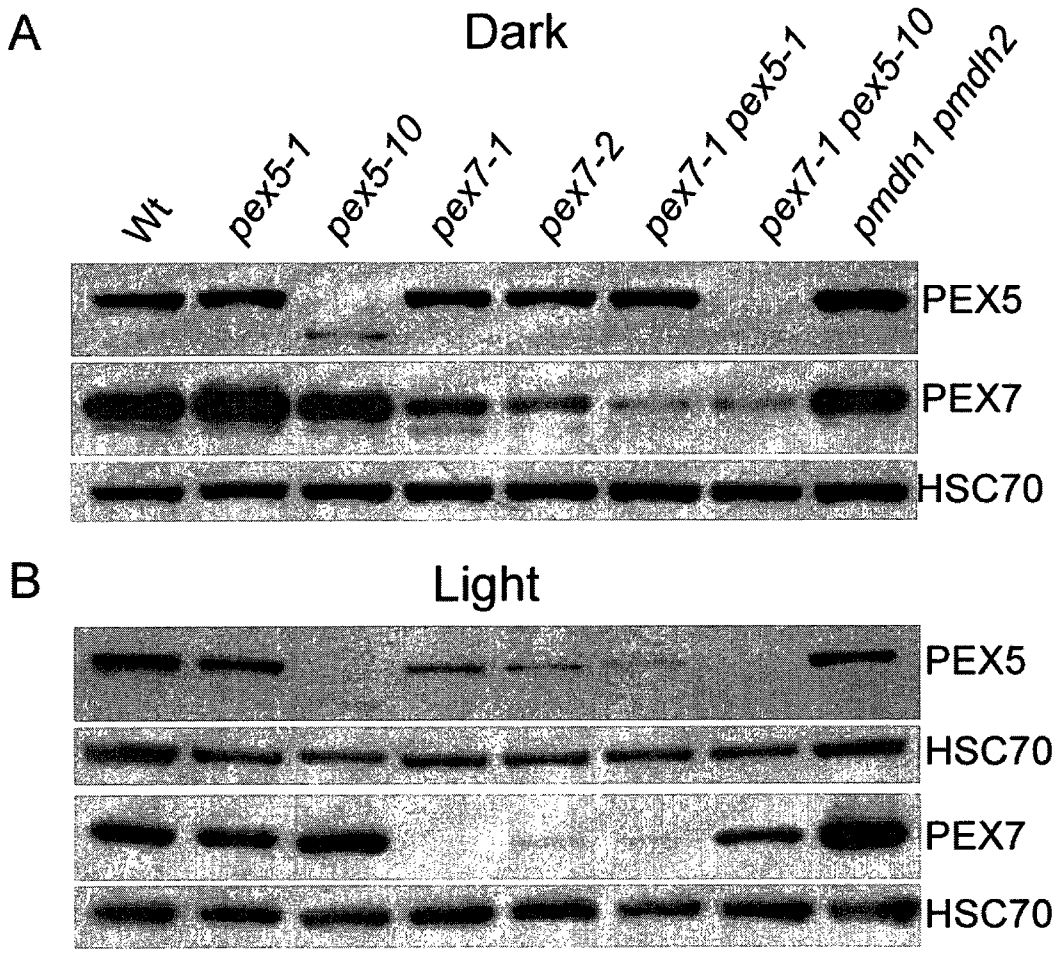

Figure 5.4. PEX7 and PEX5 accumulation in *pex7* and *pex5* single and double mutants.

A. Dark-grown *pex7* mutants have PEX7 accumulation defects. Proteins were extracted from seedlings grown 1 day in light and 4 days in darkness on 0.5% sucrose and analyzed by immunoblotting with the indicated antibodies. B. Light-grown *pex7* mutants have reduced PEX7 and PEX5 accumulation. Proteins extracted from 7-day-old seedlings grown on 0.5% sucrose under white light were analyzed by immunoblotting. The *pmdh1pmdh2* double mutant, which contains T-DNAs inserted in both of the genes encoding peroxisomal malate dehydrogenase isozymes (Pracharoenwattana et al., 2007), is included as a control for the PMDH antibody.

Chapter 6: Overexpression analysis of *pex* mutants

In Chapter 5, I described a decrease in PEX5 and PEX7 protein accumulation in *pex7* mutants. This deficiency in protein levels may contribute to the physiological phenotypes as well as the defects in PTS1 and PTS2-GFP import I observed. I also confirmed that *pex5* mutants have deficiencies in PTS2 processing and import. In this chapter, I describe my attempts to rescue physiological and molecular defects in both *pex5* and *pex7* mutants by overexpressing various proteins in these mutants. As outlined below, I found that *35S-PEX7* partially rescued *pex5-1*, but that *35S-PEX5* did not rescue *pex7-1* or *pex7-2* phenotypes. These results are summarized in Tables 6-1 and 6-2.

I generated constructs in which *PEX5*, *PEX7*, and *PED1* cDNAs are driven by the 35S promoter as described in Chapter 2. I also created PTS1-tagged versions of *PEX7*, *PED1*, and *pex7-2*. All constructs (Tables 6-1 and 6-2) were transformed into wild type to assess whether they had no deleterious effects on physiological and molecular phenotypes, and into various mutants to assess phenotypic rescue.

6.1. PEX5 overexpression

6.1.A. PEX5 overexpression in wild type

Receptor levels in the light and dark. I used western blotting with anti-PEX5 antibody to monitor PEX5 levels. The wild type (*35S-PEX5*) transgenic line (Col (*35S-PEX5*)) had significantly higher PEX5 levels than untransformed wild type in both the light and the dark, indicating successful PEX5 overexpression (Figure 6.1). *35S-PEX5* had no effect on PEX7 levels in wild-type transgenic lines (Figure 6.1).

Table 6-1. Summary of results for receptor overexpression analysis.

Construct	Plant line	PEX7 levels	PEX5 levels	PTS2 processing	IBA response	sucrose dependence
35S-PEX5	Wild type	no change	elevated	no change	no change	no change
	pex5-1	no change	elevated	rescued	rescued	rescued
	pex5-10	no change	elevated	rescued	rescued	not tested
	pex7-1	no change	elevated (dark)	no change	no change	no change
	pex7-2	no change	elevated (dark)	no change	no change	no change
35S-PEX7	Wild type	no change	no change	no change	no change	no change
	pex5-1	elevated	no change	partial	no change	partial
	pex7-1	restored	no change	rescued	rescued	rescued
	pex7-2	restored	no change	rescued	rescued	rescued
35S-PEX7-SKL	Wild type	no change	no change	no change	defective	not tested
	pex5-1	no change	no change	rescued	partial	not tested
	pex7-1	no change	no change	partial	rescued	not tested
	pex7-2	no change	no change	partial	partial	not tested
35S-pex7-2-SKL	Wild type	no change	no change	no change	no change	not tested
	pex7-1	no change	no change	partial	rescued	not tested
	pex7-2	no change	no change	partial	partial	not tested

Table 6-2. Summary of results for PED1 and PED1-SKL overexpression analysis.

Construct	Plant line	PED1 levels	PEX7 levels	PEX5 levels	PTS2 processing	IBA response	sucrose dependence
35S-PED1	Wild type	no change	no change	no change	no change	no change	not tested
	pex7-1	no change	no change	no change	no change	partial	not tested
	ped1-1	elevated	no change	no change	rescued	rescued	not tested
35S-PED1-SKL	Wild type	elevated	no change	no change	no change	no change	not tested
	pex5-1	elevated	no change	no change	partial	partial	not tested
	pex7-1	no change	restored	no change	rescued	partial	not tested
	ped1-1	restored	no change	no change	rescued	rescued	not tested

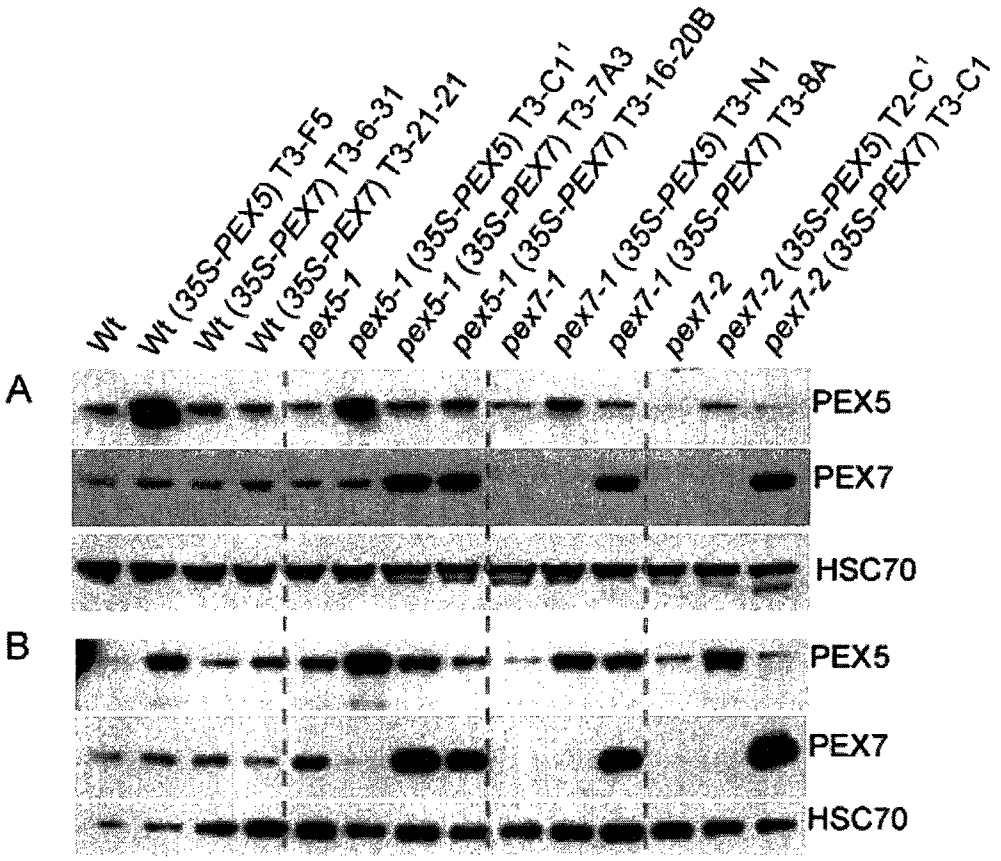

Figure 6.1. Receptor accumulation in overexpression lines.

A. PEX5 and PEX7 accumulation in light-grown seedlings. Seeds were surface-sterilized prior to plating for growth on PNS. Seedlings were grown for seven days under white light at 22°C. Each lane contains protein from at least ten seedlings. B. PEX5 and PEX7 accumulation in dark grown seedlings. Seedlings were grown under white light for 1 day at 22°C then transferred to the dark and grown vertically for 4 days at 22°C. Each lane contains protein from between 10 to 15 seedlings. Proteins were separated by SDS-PAGE and analyzed by western blotting with the indicated antibodies. [1]Plant lines segregating for the transgene.

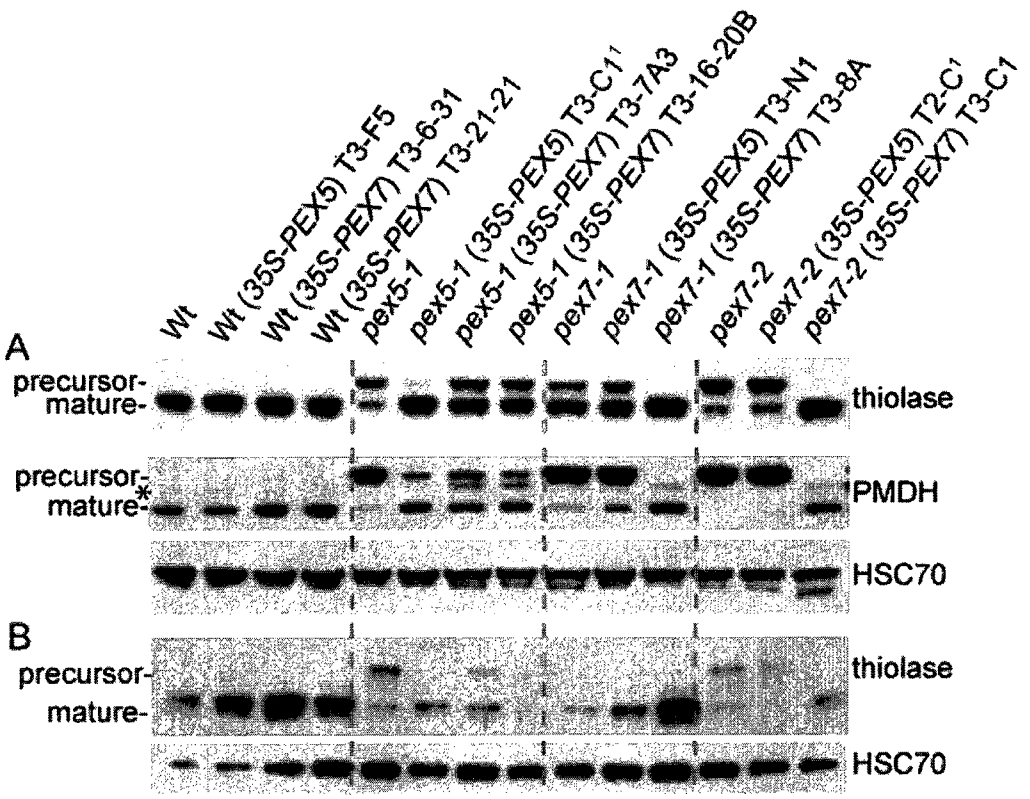

Figure 6.2. PTS2 processing in overexpression lines.

A. Thiolase and PMDH processing in light-grown seedlings. Seeds were surface-sterilized prior to plating for growth on PNS. Seedlings were grown for seven days under white light at 22°C. Each lane contains protein from at least ten seedlings. The PMDH panel was probed with PMDH antibody after the PEX7 antibody. Residual PEX7 signal is seen between the precursor and mature PMDH in the *35S-PEX7* lanes (marked with an asterisk; compare to second panel in Figure 6.1.A). B. Thiolase processing in dark grown seedlings. Seedlings were grown under white light for 1 day at 22°C then transferred to the dark and grown vertically for 4 days at 22°C. Each lane contains protein from between 10 to 15 seedlings. Proteins were separated by SDS-PAGE and analyzed by western-blotting with the indicated antibodies. [1]Plant lines segregating for the transgene.

PTS2 processing in the light and dark. I analyzed processing of thiolase in the light and dark and PMDH in the light in wild type (*35S-PEX5*) (Figure 6.2). *35S-PEX5* had no observable effect on thiolase and PMDH processing in wild-type plants (Figure 6.2).

IBA resistance and sucrose dependence. Wild type (*35S-PEX5*) plants remained sucrose independent in the dark (Figure 6.3) and retained IBA responsive primary root elongation (Figure 6.4). Together these experiments demonstrated that increasing PEX5 levels in wild-type plants does not detectably alter peroxisome functioning.

6.1.B. PEX5 overexpression in *pex5-1* and *pex5-10*

Western receptor levels in the light and dark. In the light and in the dark, *pex5-1* (*35S-PEX5*) had increased PEX5 accumulation compared to untransformed *pex5-1* (Figure 6.1). *pex5-10* (*35S-PEX5*) also displayed elevated levels of full-length PEX5 in the light (Figure 6.5).

PTS2 processing in the light and dark. *pex5-1* (*35S-PEX5*) lines displayed a clear reversal of the ratio of processed PTS2 protein to unprocessed PTS2 protein compared to untransformed lines (Figure 6.2). The residual unprocessed thiolase and PMDH in *pex5-1* (*35S-PEX5*) (Figure 6.2) was probably due to the fact that the line was segregating for the transgene.

IBA resistance and sucrose dependence. To avoid skewing the data with segregating lines, I measured all seedlings in each transformed line, and then transferred them to soil and tested for BASTA resistance. Those seedlings that were not BASTA resistant were eliminated from the data analysis. As expected, *pex5-1* sucrose dependence (Figure 6.3) and IBA resistance (Figure 6.4) were rescued by transformation

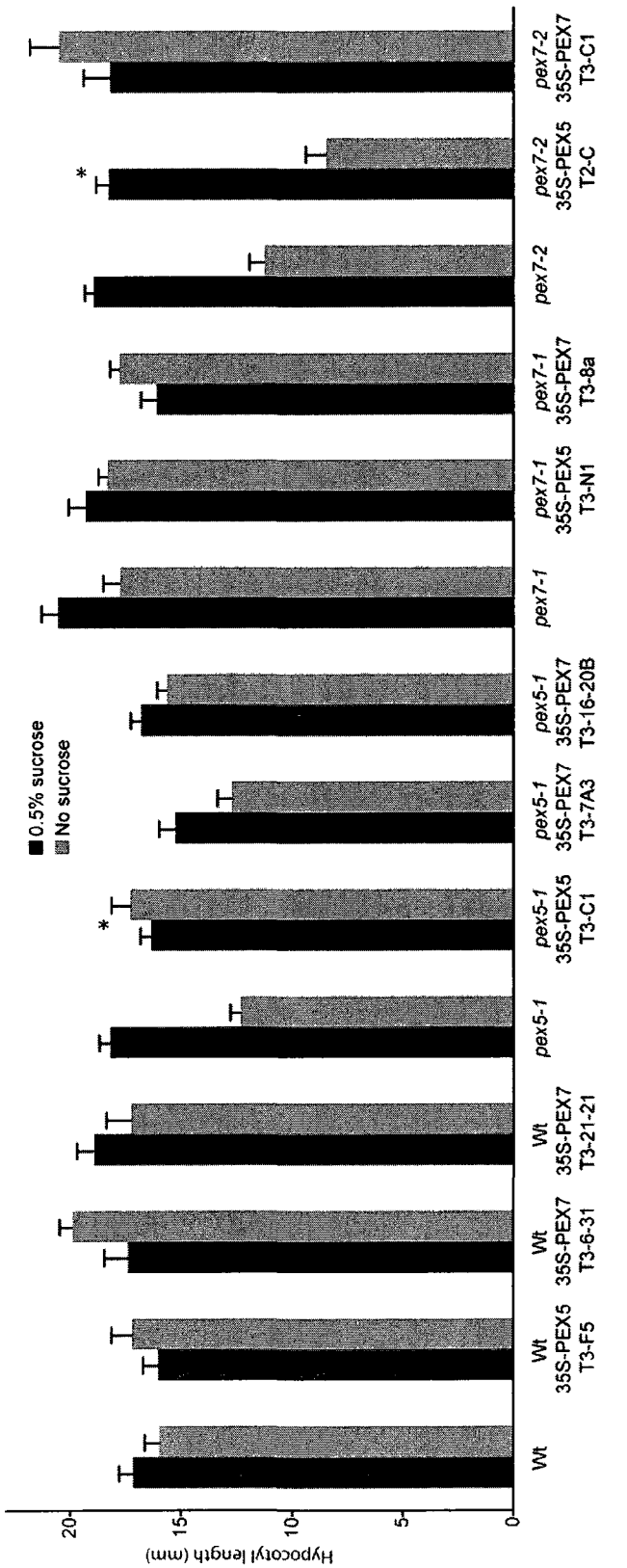

Figure 6.3. Overexpresssion lines sucrose dependence dark.

Hypocotyl lengths of seedlings grown on sucrose-free medium for 1 day in the light and 5 days vertically in darkness compared to plants grown on 0.5% sucrose. Bars show mean + SE; $n \geq 9$. Asterisks denote lines that were not homozygous for the transgene. (Only data from Basta-resistant individuals were included.)

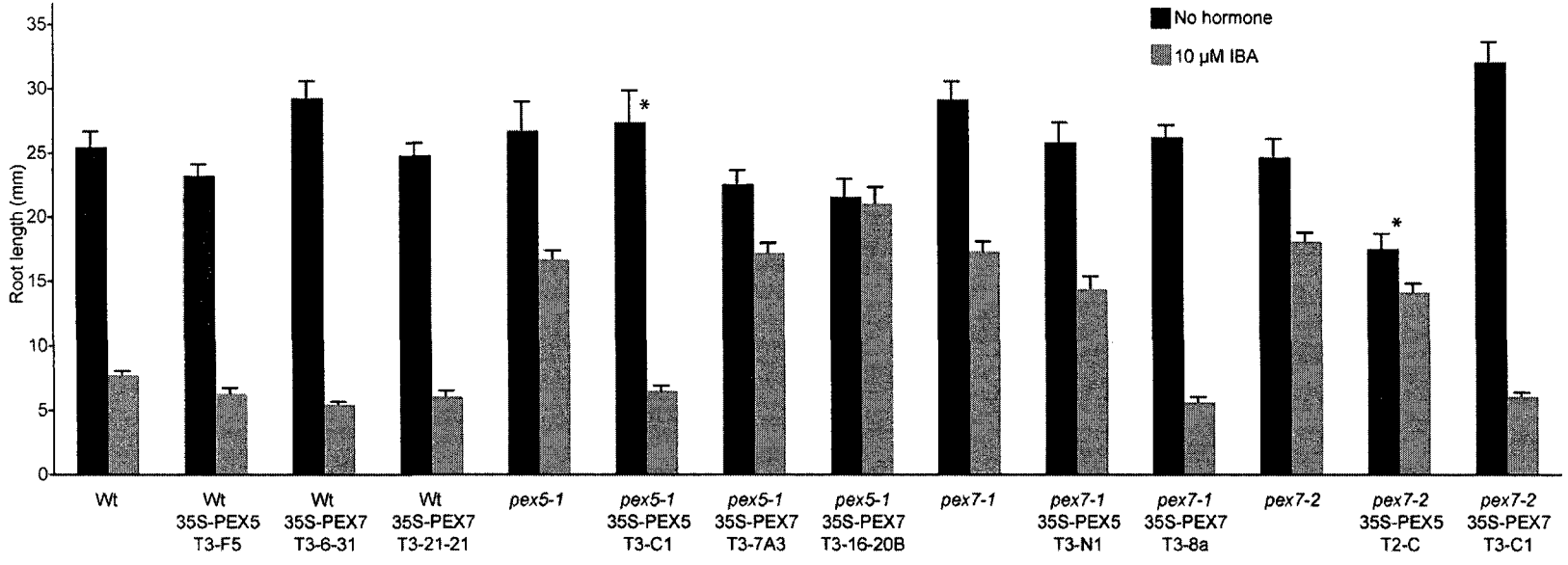

Figure 6.4. Overexpression lines on IBA.

Seedlings were grown for 8 days under yellow-filtered light on medium without hormone or supplemented with IBA were removed from the agar and roots were measured. Bars show mean + SE; $n \geq 9$. Asterisks denote lines that were not homozygous for the transgene. (Only data from Basta-resistant individuals were included.)

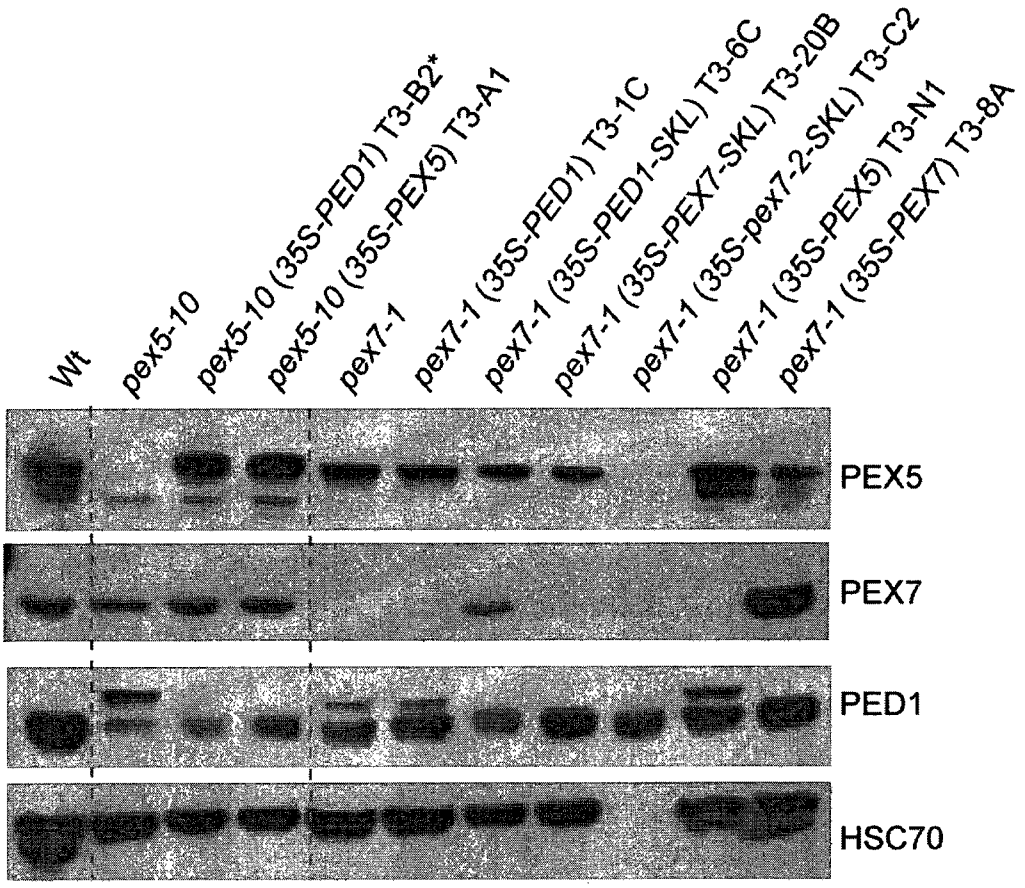

Figure 6.5. Protein accumulation in *pex5-10* and *pex7-1* overexpression lines.

Seeds were surface-sterilized prior to plating for growth on PNS. Seedlings were grown on PNS for 7 days under white light at 22°C. Each lane contains protein from 10 to 15 seedlings. Proteins were separated by SDS-PAGE and analyzed by western blotting with the indicated antibodies. *The western analysis is consistent with the possibility that this line is actually *pex5-10* (*35S-PEX5*) rather than *pex5-10* (*35S-PED1*). Future genotyping will resolve this issue.

with *35S-PEX5*. *pex5-10* (*35S-PEX5*) also displayed restored response to IBA (Figure 6.6). Together, these experiments demonstrated that the *35S-PEX5* construct was expressing functional PEX5 protein.

6.1.C. PEX5 overexpression in *pex7-1* and *pex7-2*

Light-grown *pex7* mutants are deficient in PTS1 protein import (Chapter 5), possibly because of a decrease in PEX5 accumulation in the light (Chapter 5). By restoring PEX5 levels in *pex7* mutants, we thought we might be able to rescue PTS1 import and possibly defects in IBA response and fatty acid metabolism.

Receptor levels in the light and dark. *pex7-1* and *pex7-2* (*35S-PEX5*) lines appeared to have slightly higher PEX5 levels than the untransformed mutants when grown in the light (Figure 6.1.A) although not as high as when those lines were grown in the dark (Figure 6.1.B). However, *35S-PEX5* did not restore PEX7 levels in *pex7* mutants in either the light or the dark (Figure 6.1).

PTS2 processing in the light and dark. *pex7-1* and *pex7-2* (*35S-PEX5*) lines did not have noticeably different thiolase processing or PMDH processing from untransformed *pex7* mutants in the light (Figure 6.2.A) or the dark (Figure 6.2.B), suggesting that restoring PEX5 levels in these mutants is not enough to rescue PTS2 import defects.

IBA resistance and sucrose dependence. *pex7-1* and *pex7-2* (*35S-PEX5*) lines did not have restored response to IBA (Figure 6.4). *pex7-2* (*35S-PEX5*) grew similarly to *pex7-2* in the presence and absence of sucrose (Figure 6.3). Thus, *pex7* physiological phenotypes were not restored by restoring PEX5 levels.

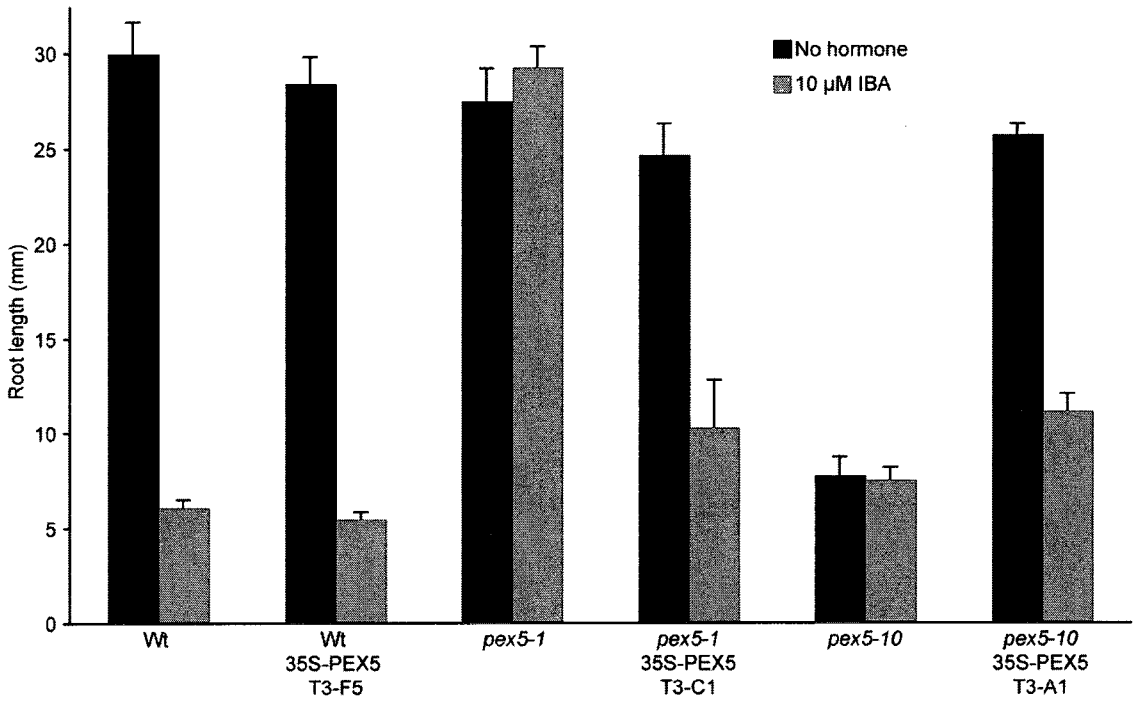

Figure 6.6. IBA resistance of *pex5* mutants is rescued by overexpression of PEX5.

Seedlings grown for 8 days under yellow-filtered light on medium without hormone or supplemented with IBA were removed from the agar and roots were measured. Bars show mean + SE; $n \geq 10$.

6.2. PEX7 overexpression

6.2.A. PEX7 overexpression in wild type

Receptor levels in the light and dark. I did not isolate a line that accumulated PEX7 to significantly higher levels than in wild type plants, despite analyzing progeny from three primary transformants (Figure 6.1 and 6.7).

PTS2 processing in the light and dark. None of the wild type (*35S-PEX7*) lines analyzed exhibited defects in PTS2 processing in the light or in the dark (Figures 6.2 and 6.8).

Physiology: IBA resistance and sucrose dependence. Wild type (*35S-PEX7*) lines exhibited normal growth with and without sucrose in the dark (Figure 6.3) and retained IBA responsiveness (Figure 6.4).

6.2.B. PEX7 overexpression in *pex7-1* and *pex7-2*

Receptor levels in the light and dark. *pex7-1* and *pex7-2* (*35S-PEX7*) lines had elevated PEX7 accumulation in the light and in the dark (Figure 6.1). PEX5 levels did not seem to be fully restored by the increase in PEX7 accumulation (Figure 6.1). This result is unexpected and this experiment needs to be repeated.

PTS2 processing in the light and dark. As expected, in light- and dark-grown *pex7* mutants overexpressing PEX7 rescued both thiolase and PMDH PTS2 processing defects (Figure 6.2).

IBA resistance and sucrose dependence. *pex7-1* and *pex7-2* (*35S-PEX7*) lines exhibit restored response to IBA in root elongation assays (Figure 6.4). *pex7-2* (*35S-PEX7*) is also no longer sucrose dependent in the dark (Figure 6.3). Together, these experiments show that the physiological and PTS2 processing defects of the *pex7-2* mutant stem from reduced PEX7 function.

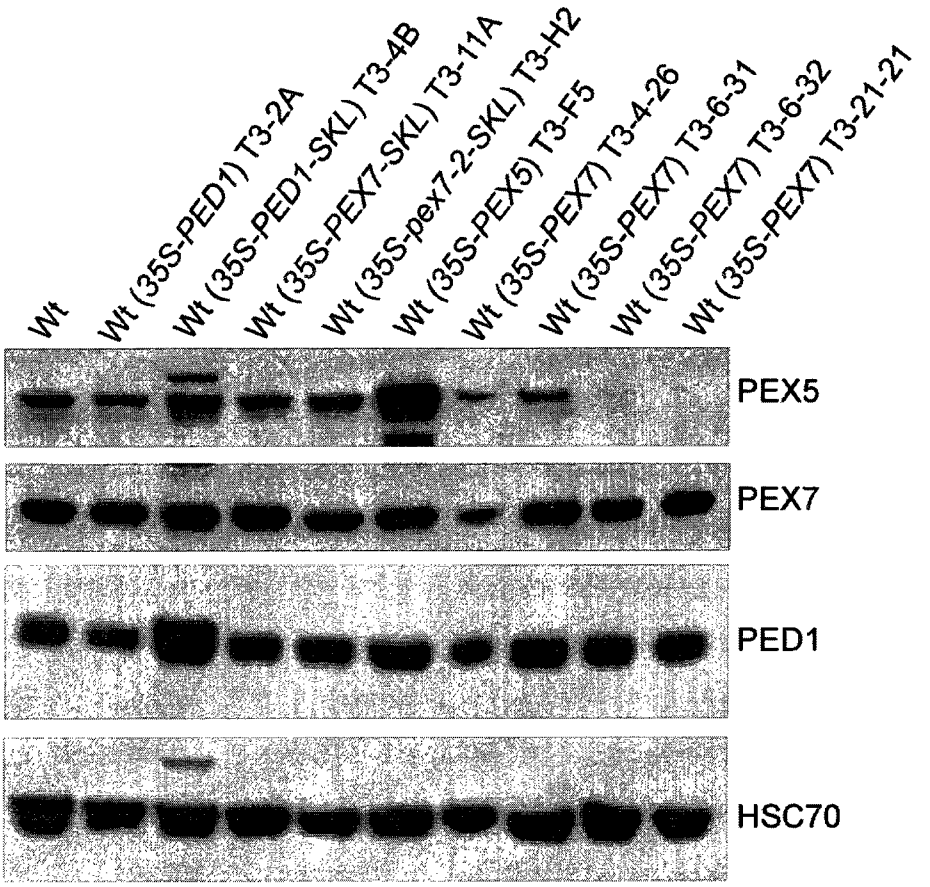

Figure 6.7. Protein accumulation in light-grown wild-type overexpression lines.

Seedlings were grown on PNS for 7 days under white light at 22°C. Each lane contains protein from 10 to 15 seedlings. Proteins were separated by SDS-PAGE and analyzed by western blotting with the indicated antibodies.

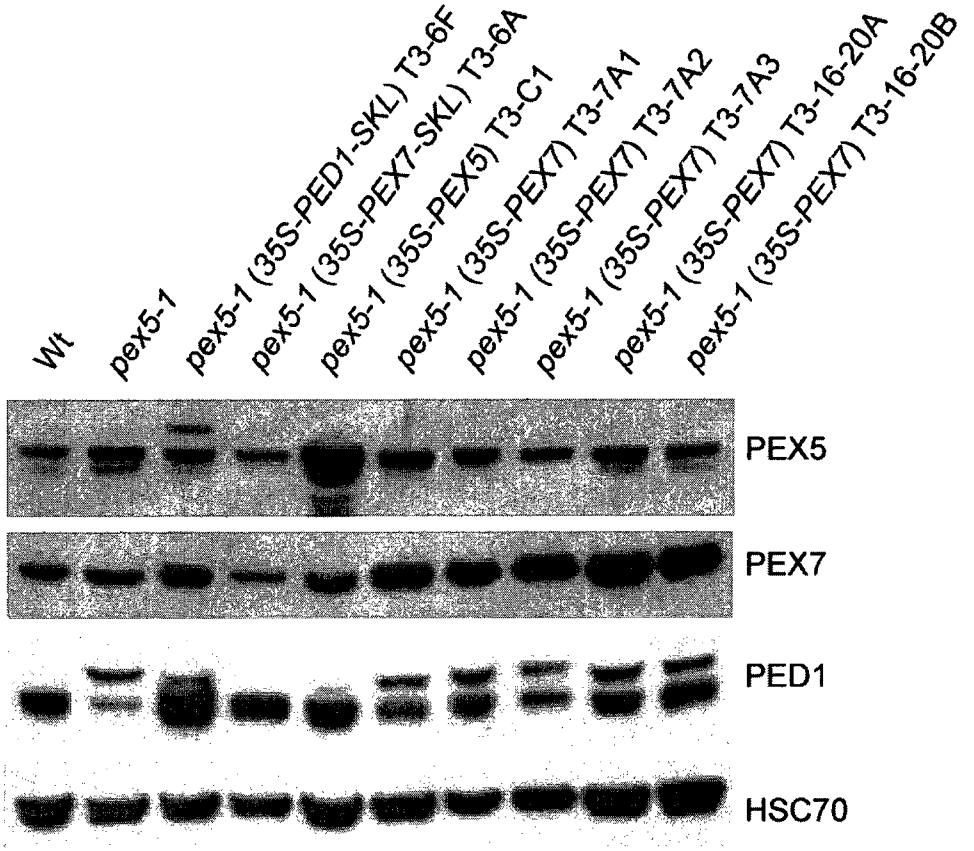

Figure 6.8. Protein accumulation in *pex5-1* overexpression lines.

Seedlings were grown on PNS for 7 days under white light at 22°C. Each lane contains protein from 10 to 15 seedlings. Proteins were separated by SDS-PAGE and analyzed by western blotting with the indicated antibodies.

6.2.C. PEX7 overexpression in *pex5-1*

Receptor levels in the light and dark. *pex5-1* (*35S-PEX7*) accumulated PEX7 to significantly higher levels than the untransformed *pex5-1* mutant in both light- and dark-grown conditions (Figures 6.1). This increase in PEX7 accumulation appeared to have no effect on PEX5 levels in *pex5-1* (Figure 6.1).

PTS2 processing in the light and dark. The ratio of processed to precursor PMDH and thiolase in *pex5-1* lines overexpressing PEX7 was higher than in untransformed *pex5-1* (Figure 6.2), suggesting that PEX7 overexpression partially rescued PTS2 processing in *pex5-1*.

IBA resistance and sucrose dependence. In two different trials, *pex5-1* IBA resistant root elongation was not (Figure 6.4) or was partially (Figure 6.11) rescued by PEX7 overexpression. This experiment needs to be repeated using a range of IBA concentrations. In addition, the *pex5-1* partial sucrose dependence in the dark was rescued upon overexpression of PEX7 (Figure 6.3), suggesting that the partial restoration of PTS2 proccessing that accompanied PEX7 overexpression was enough to fully rescue *pex5-1* sucrose dependence in the dark.

6.3. PED1 overexpression

6.3.A. PED1 overexpression in wild type

I did not obtain a wild-type line that accumulated significantly higher levels of PED1 than untransformed wild type (Figure 6.7). Wild type (*35S-PED1*) did not exhibit defects in thiolase processing (Figure 6.7), altered PEX5 and PEX7 levels (Figure 6.7), or altered IBA responsiveness in root elongation assays (Figure 6.9).

6.3.B. PED1 overexpression in *ped1-1*

ped1-1 (*35S-PED1*) had restored PED1 levels, no defects in PTS2 processing (Figure 6.10), and restored response to IBA in primary root elongation inhibition (Figure

6.9), confirming that my *35S-PED1* construct was working properly. Overexpression of 35S-*PED1* appeared to have no effect on PEX5 or PEX7 levels in *ped1-1* (Figure 6.10).

6.3.C. PED1 overexpression in *pex7-1*

PED1 levels were not elevated in *pex7-1* (*35S-PED1*) compared to *pex7-1* and PED1 processing was not rescued (Figure 6.5). PEX7 and PEX5 levels were unaffected in *pex7-1* (*35S-PED1*) (Figure 6.5). Despite the apparently unchanged PED1 protein levels, *35S-PED1* appeared to partially rescue *pex7-1* defects in IBA response (Figure 6.9).

6.4. PEX7-SKL and pex7-2-SKL overexpression

pex5-1 is deficient in PTS2 protein transport, possibly because of an altered ability of PEX5 to bind PEX7 (Woodward and Bartel, 2005). Because oligomeric proteins can be imported into the peroxisome (McNew and Goodman, 1994; Kato et al., 1999), we hypothesized that PEX7 containing a C-terminal PTS1 sequence might bind PEX5 in a different manner and that I might rescue the *pex5-1* mutant by introducing a PTS1-targeted PEX7. I overexpressed PEX7-PTS1 driven by the constitutive 35S promoter in *pex7-1*, *pex7-2*, *pex5-1*, and wild type.

Based on the results of the yeast-2-hybrid experiments in Chapter 4, I overexpressed *pex7-2*-PTS1 driven by the 35S promoter in the various *pex5* and *pex7* mutants. PEX7-PTS1 transformed into *pex7-1* and *pex7-2* were controls to determine whether a PTS1 interferes with PEX7 function and accumulation, and PEX7-PTS1 transformed into *pex5-10* was a negative control that I did not expect to rescue. If PEX7-PTS1 rescues *pex7-1* and *pex7-2* phenotypes, this result would indicate that the modified PEX7 is still functional. If PEX7-PTS1 is able to rescue *pex5-1*, but not the putative null *pex5-10* mutant, this result would suggest that targeting PEX7 for PEX5 binding by another means can restore peroxisome function.

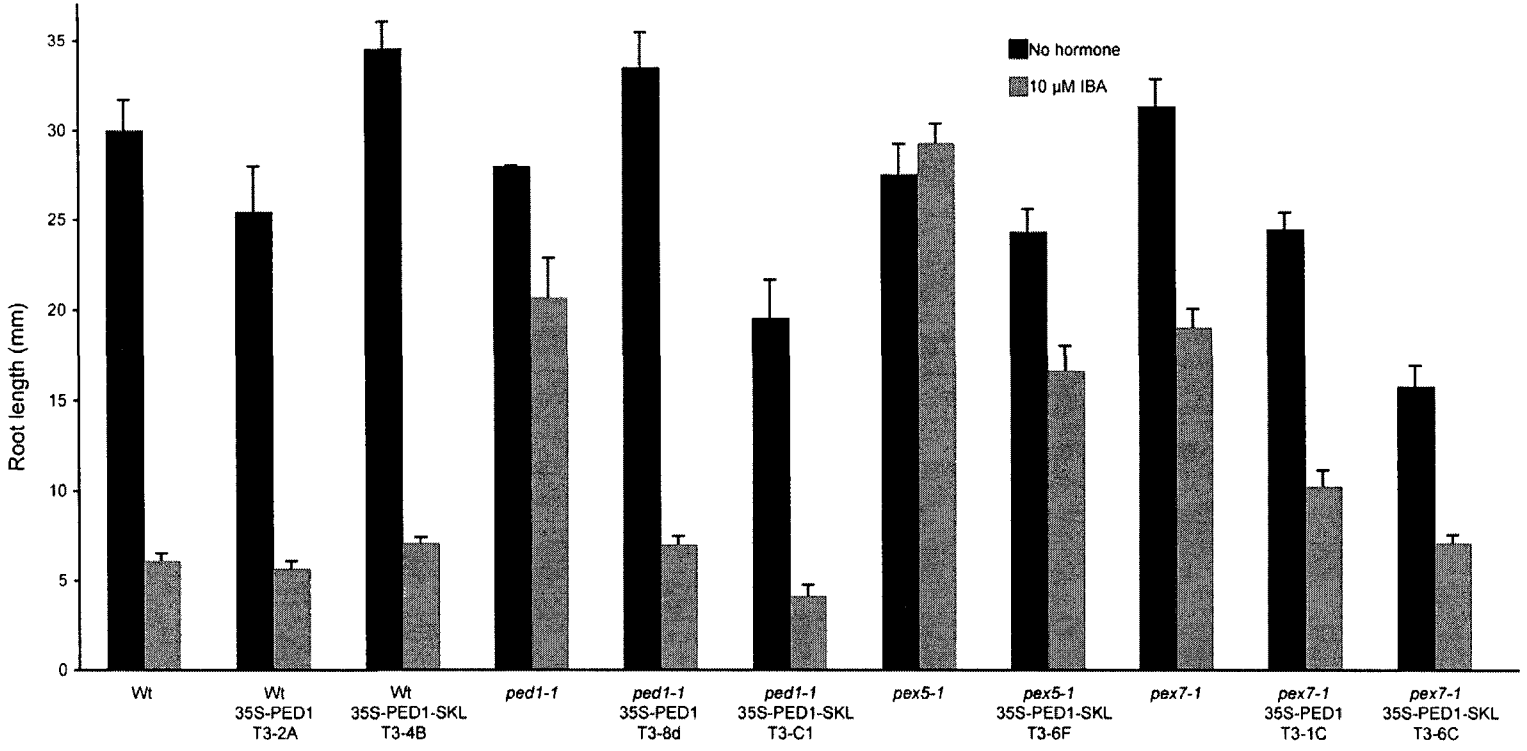

Figure 6.9. Effects of overexpressing PED1 or a PTS1-tagged PED1 on IBA response.

Seeds were surface-sterilized and plated on 10 µM IBA or a no hormone control. Seedlings were grown for eight days under yellow light at 22°C and removed from the agar for measuring. Bars show mean + SE; n≥1.

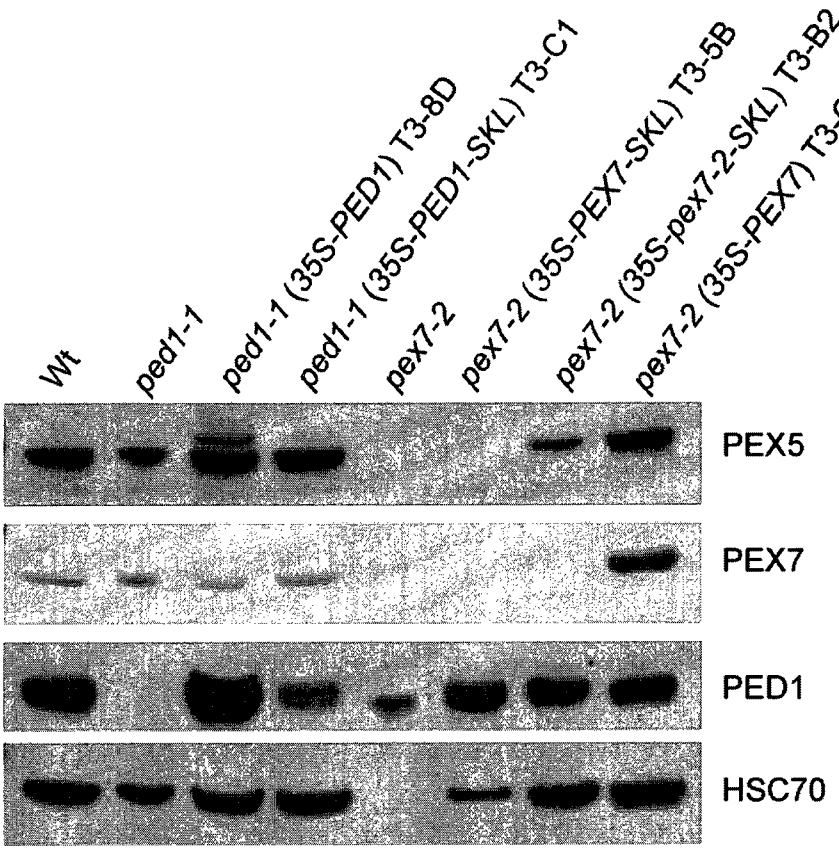

Figure 6.10. Protein accumulation in *ped1-1* and *pex7-2* overexpression lines.

Seedlings were grown on PNS for 7 days under white light at 22°C. Each lane contains protein from 10 to 15 seedlings. Proteins were separated by SDS-PAGE and analyzed by western blotting with the indicated antibodies.

6.4.A. PEX7-SKL and pex7-2-SKL overexpression in wild type

Receptor levels. In the light, *35S-PEX7-SKL* and *35S-pex7-2-SKL* did not accumulate to notably higher levels in either of the examined transformed plant lines compared to the untransformed plant lines (Figure 6.7). In addition, PEX5 protein levels were unaffected in these lines. One important factor to consider is that our PEX7 antibody recognizes the extreme C-terminus of the PEX7 protein and any alterations to the C-terminus, such as the addition of a PTS1, could cause the protein to be unrecognizable by the antibody. The PEX7 protein band that is visible in Figure 6.7 could be endogenous PEX7 and not PEX7-SKL or pex7-2-SKL.

PTS2 processing. In the light, PED1 was processed similarly to wild type in wild type (*35S-PEX7-SKL*) and wild type (*35S-pex7-2-SKL*).

IBA resistance. Wild type (*35S-pex7-2-SKL*) was unaffected in IBA primary root elongation assays. Surprisingly, wild type (*35S-PEX7-SKL*) exhibited moderate IBA-resistant root elongation (Figure 6.11). This result suggests that the C-terminal PTS1 tag interferes with wild-type PEX7 or PEX5 function.

6.4.B. PEX7-SKL overexpression in *pex5-1*

Receptor levels. *pex5-1* (*35S-PEX7-SKL*) did not overaccumulate PEX7 in the light (Figure 6.8). Once again, our PEX7 antibody may not recognize the protein encoded by the transgene, and the PEX7 seen in Figure 6.8 could be endogenous PEX7 and not PEX7-SKL.

PTS2 processing. Although PEX7 was not more abundant in *pex5-1* (*35S-PEX7-SKL*) than in *pex5-1*, this transgenic line displayed completely rescued thiolase processing (Figure 6.8). In contrast, multiple *pex5-1* (*35S-PEX7*) lines only partially restored thiolase processing (Figure 6.8).

IBA resistance. PEX7-SKL was also able to partially restore IBA responsiveness to *pex5-1* roots (Figure 6.11). This rescue appeared to be somewhat more effective than rescue by *35S-PEX7* (Figure 6.11), even though the latter lines accumulated more PEX7 than the PEX7-SKL line (Figure 6.8). These results are consistent with the possibility that pex5-1 is deficient in PEX7 binding and that this deficiency can be rescued by providing an alternate binding site.

6.4.C. PEX7-SKL and pex7-2-SKL overexpression in *pex7-1* and *pex7-2*

Receptor levels in the light. PEX7-SKL and pex7-2-SKL did not accumulate to detectable levels in either *pex7* mutant (Figure 6.5 and 6.10). PEX5 levels remained unaltered in *pex7* mutants (Figure 6.5).

PTS2 processing. Although PEX7-SKL and pex7-2-SKL failed to accumulate in *pex7* mutants (Figure 6.5 and 6.10), I observed a partial rescue of thiolase processing defects (Figure 6.5 and 6.10) in both mutants with both constructs.

IBA resistance. Additionally, both *pex7* mutants displayed partially restored responses to IBA (Figure 6.11) when either *35S-PEX7-SKL* or *35S-pex7-2-SKL* were introduced. *pex7-1* was more completely rescued than *pex7-2* (Figure 6.11).

6.5. PED1-SKL overexpression

pex5 and *pex7* mutants have defects in PTS2 import (Chapter 5) and thiolase processing (Chapter 5). pex7-2 is unable to bind PED1 in yeast two-hybrid assays (Chapter 4). These results suggest that thiolase is not being delivered to the peroxisome efficiently in *pex5* and *pex7* mutants. To determine if thiolase not entering the peroxisome is the major defect causing the molecular defects in PTS2-GFP import and thiolase processing I engineered a thiolase construct containing a C-terminal PTS1 (*PED1-SKL*). In Chapter 4, I demonstrated that PED1-SKL binds to PEX5, suggesting that the C-terminal PTS1 will provide an alternate route for PED1 into the peroxisome.

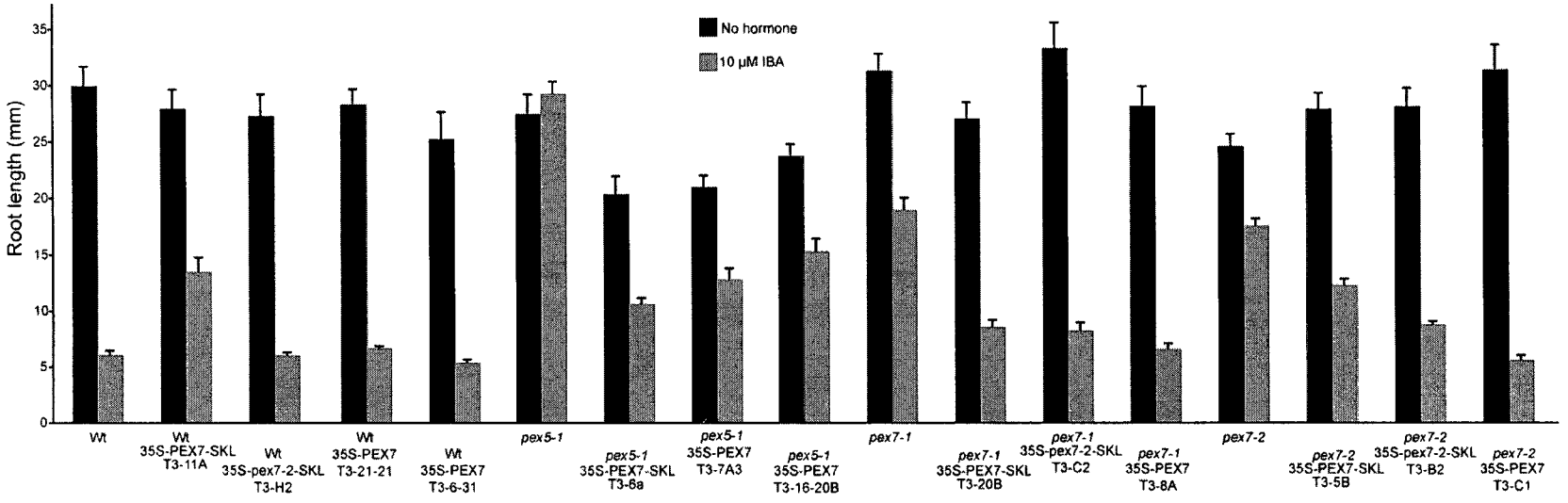

Figure 6.11. Effects of overexpressing a PTS1-tagged PEX7 or pex7-2 protein on IBA response.

Seeds were surface-sterilized and plated on 10 µM IBA or a no hormone control. Seedlings were grown for eight days under yellow light at 22°C and removed from the agar for measuring. Bars show mean + SE; n≥9.

6.5.A. PED1-SKL overexpression in wild type

Unlike *35S-PED1*, PED1-SKL accumulated to significantly higher levels than PED1 in untransformed wild type (Figure 6.7). PED1 was completely processed in wild type (*35S-PED1-SKL*). Wild type (*35S-PED1-SKL*) lines had normal PEX5 and PEX7 levels (Figure 6.7). *35S-PED1-SKL* had no effect on wild type IBA response (Figure 6.9), suggesting that my construct does not interfere with normal peroxisomal processes.

6.5.B. PED1-SKL overexpression in *ped1-1*

I was able to express PED1-SKL in light-grown *ped1-1* although PED1-SKL did not accumulate to the same level as 35S-driven PED1 in *ped1-1* (Figure 6.10). As expected, *ped1-1* (35S-PED1-SKL) did not exhibit defects in thiolase processing (Figure 6.10). I found that *ped1-1* (35S-PED1-SKL) had restored responsiveness to IBA in root elongation assays (Figure 6.9), suggesting that PED1-SKL functions similarly to PED1.

6.5.C. PED1-SKL overexpression in *pex5-1*

PED1-SKL accumulated in *pex5-1* (*35S-PED1-SKL*) overexpressed in *pex5-1* and the transgenic line seemed to have a partial rescue of thiolase processing (Figure 6.8). *35S-PED1-SKL* had no effect on receptor levels in *pex5-1* (Figure 6.8). *pex5-1* (*35S-PED1-SKL*) appeared to have partially restored response to IBA in root elongation assays (Figure 6.9).

6.5.D. PED1-SKL overexpression in *pex7-1*

35S-PED1-SKL restored thiolase processing in *pex7-1*. *pex7-1* (*35S-PED1-SKL*) had increased PEX7 compared to the untransformed mutant but PEX5 levels remained the same (Figure 6.5). *pex7-1* (35S-PED1-SKL) had a partially restored response to IBA root elongation inhibition (Figure 6.9).

6.6. Conclusions

The experiments in this chapter are preliminary; the promising experiments will need to be repeated with additional lines and more in depth analyses. Following are some tentative conclusions and areas warranting further investigation.

Although *pex5* mutants do not have PEX7 accumulation defects, overexpression of PEX7 in *pex5-1* partially rescued thiolase processing and sucrose dependence phenotypes. These results are consistent with the idea that *pex5-1* defects stem from a partial loss of PEX7 function.

When I introduced a PTS1-tagged *PEX7*, *PEX7-SKL*, into wild-type plants, I observed a decrease in IBA response, suggesting that PEX7-SKL partially interferes with peroxisome function. PEX7-SKL did not overaccumulate in wild type plants and was not detected in either *pex7* mutant in a western blot. However, *PEX7-SKL* was still able to rescue IBA response in *pex7-1* and partially rescue IBA response in *pex7-2*. *35S-PEX7-SKL* also partially rescued thiolase processing in *pex7* mutants. Additionally, PEX7-SKL overexpression, unlike PEX7, was able to fully rescue *pex5-1*, further suggesting that *pex5-1* has a PEX7 binding defect that can only be more completely overcome by allowing PEX7 to bind PEX5 in a different manner.

It was interesting that overexpression of PEX7 in *pex7* mutants appeared to rescue PTS2 processing as well as IBA response and sucrose dependence phenotypes without fully restoring PEX5 levels. If this result is confirmed, it would be interesting to assess the effects on GFP-PTS1 and PTS2-GFP import in these lines to determine whether elevated PEX7 in a background with decreased PEX5 can restore the molecular defects in import.

I did not isolate a *pex7* (*35S-PEX5*) line that accumulated PEX5 to higher levels than wild type. The defect in PEX5 accumulation is less severe in *pex7* mutants grown in the dark, and accordingly, I observed that PEX5 accumulated to slightly higher levels in

the dark in *pex7* (*35S-PEX5*) lines. It is possible that PEX5 is not easily overexpressed in *pex7* because PEX5 requires PEX7 for stability. To test this hypothesis, we have crossed the *pex7* mutants to the wild type (*35S-PEX5*) T3-F5 line, which very noticeably overaccumulates PEX5. Analysis of PEX5 levels in *pex7* (*35S-PEX5*) plants from this cross will allow us to remove any variation caused by the position of the *35S-PEX5* T-DNA insertion site.

Chapter 7: Genetic Analysis of IBA-Response Mutants

Hormone homeostasis and signaling has an essential role in the plant life cycle. This project involves the study of the hormone IBA and its conversion to IAA in the model plant *Arabidopsis thaliana.* It has been suggested that IBA is converted to IAA in a process that is similar to fatty acid β-oxidation (Fawcett et al., 1960). Several *IBA-response (ibr)* mutants have been isolated and studied with the aim of determining the steps involved in the conversion of IBA to IAA. *ibr* mutants are resistant to root elongation inhibition by IBA, but respond normally to IAA (Zolman et al., 2000). This project focused on the identification and characterization of proteins that help convert IBA to IAA.

An unresolved question about IBA β-oxidation to IAA is whether the enzymes acting in fatty acid β-oxidation are the same as those used to convert IBA to IAA. One possibility is that the enzymes used in fatty acid metabolism recognize IBA-CoA as a substrate and act directly on IBA-CoA. Another possibility is that enzymes exist that act solely on IBA-CoA and are independent of fatty acid metabolism (Figure 7.1). A piece of evidence that supports the former possibility is that *ped1*, *aim1*, and *acx* mutants are deficient not only in fatty acid β-oxidation, but also in IBA responses, suggesting there are shared factors between the two processes (Hayashi et al., 1998; Zolman et al., 2000; Adham et al., 2005). This chapter describes evidence supporting the latter possibility from the characterization of three IBA-response mutants, *ibr3*, *ibr10*, and *ibr1*. These mutants are deficient in IBA responses but lack defects in fatty acid β-oxidation. Part of the work described in this chapter has been published (Zolman et al., 2008).

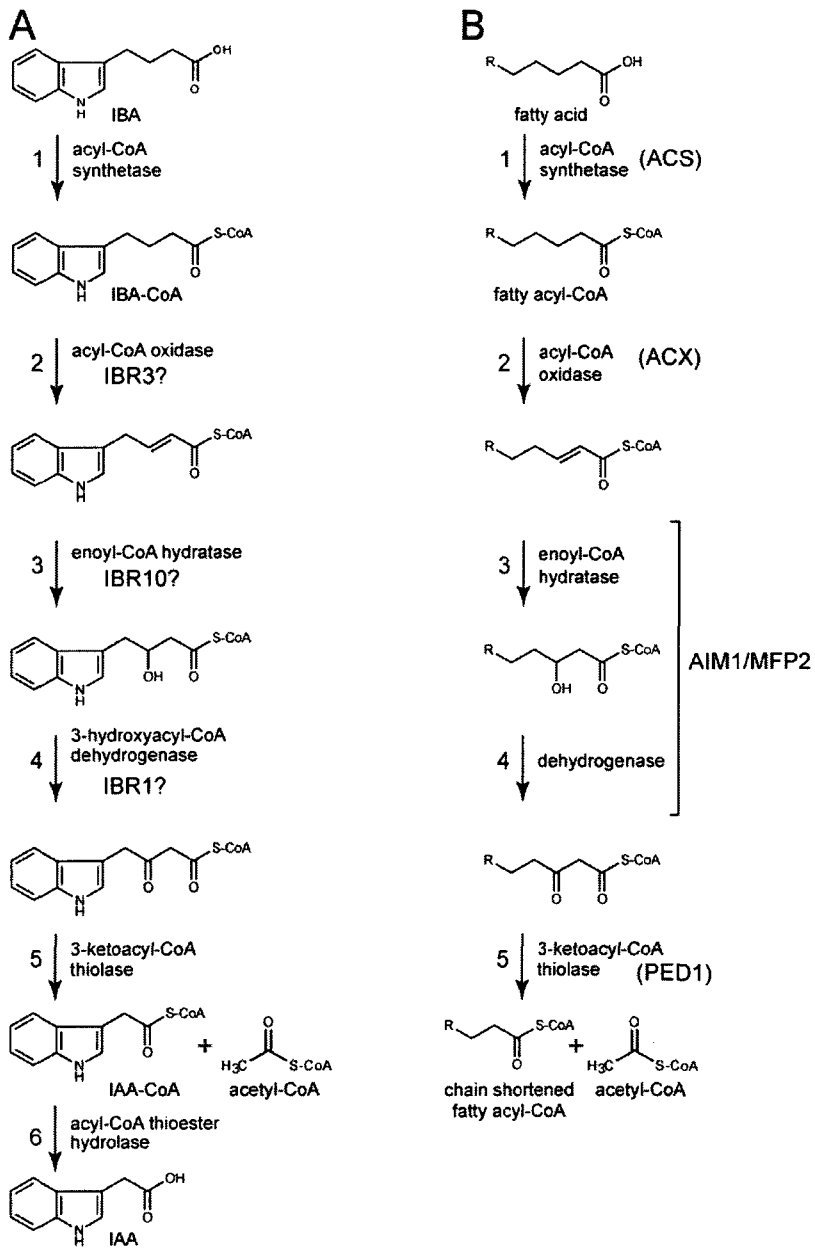

Figure 7.1. Fatty acid β-oxidation (right) versus a model for IBA β-oxidation (left).

A. A proposed pathway for IBA to IAA conversion may involve the proteins IBR3, a putative acyl-CoA dehydrogenase, IBR10, a putative enoyl-CoA hydratase, and IBR1, a putative hydroxyacyl-CoA dehydrogenase. B. Fatty acid β-oxidation is carried out by the sequential action of acyl-CoA synthetases (ACS), acyl-CoA oxidases (ACX), multifunctional proteins (AIM1/MFP2) responsible for two different enzymatic activities, and thiolases including PED1 (peroxisome defective). (Modified from Zolman et al., 2008).

7.1. *ibr3*, *ibr10*, and *ibr1* are defective in peroxisomal enzymes

Three mutants have been isolated, *ibr3*, *ibr10*, and *ibr1*, that display an IBA resistant, IAA sensitive phenotype without any apparent defect in fatty acid β-oxidation (Zolman et al., 2000; Zolman et al., 2008). These mutants are defective in proteins similar to three proteins involved in fatty acid β-oxidation: an acyl-CoA oxidase/dehydrogenase, an enoyl-CoA hydratase, and a hydroxyacyl-CoA dehydrogenase, respectively (Zolman et al., 2007; Zolman et al., 2008). Thus the IBR3, IBR10, and IBR1 proteins are candidates for catalyzing sequential steps of IBA β-oxidation (Figure 7.1).

Multiple alleles of *ibr1* were isolated by Bethany Zolman through a screen for IBA resistant root elongation (Zolman et al., 2000; Zolman et al., 2008). *ibr1* was mapped to a region of chromosome 4 (Figure 7.2.A) and found to be defective in a PTS1 enzyme similar to a short-chain dehydrogenase reductase (Figure 7.3). The focus of my efforts on this project was limited to *ibr1-2,* which has a G to A mutation that disrupts a 3' splice site (Figure 7.2.B).

Multiple *ibr3* alleles were isolated by Bethany Zolman in a screen for IBA resistant root elongation (Zolman et al., 2000; Zolman et al., 2007). *ibr3* was mapped to the top of chromosome 3 (Figure 7.2.C) and found to be defective in an enzyme similar to acyl-CoA dehydrogenases. This project focuses on characterization of *ibr3-1,* which has a G to A mutation that leads to a Glu to Lys amino acid change and a second G to A mutation that disrupts a 3' splice site (Figure 7.2.D).

ibr10 was isolated by Arthur Millius from a T-DNA mutagenized population through a screen for IBA-resistant root elongation (Zolman et al., 2008). Positional cloning revealed a 78-bp deletion south of *IBR1* on chromosome 4 (Figure 7.2.E, F) in a gene (*At4g14430*) encoding a PTS1 enzyme similar to enoyl-CoA hydratases (Figure 7.4).

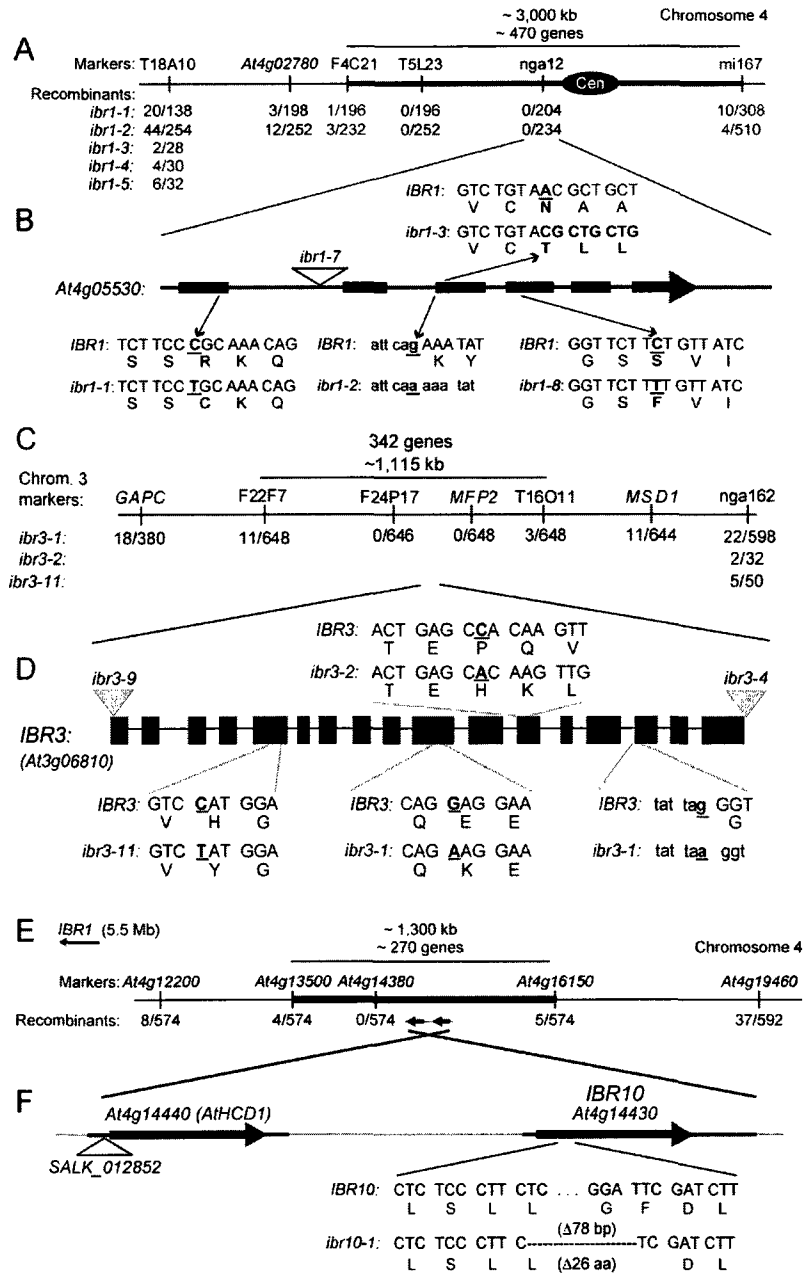

Figure 7.2. Positional cloning of IBR1, IBR3, and IBR10.

A and B. *ibr1* mutants were identified in a forward genetics screen for elongated roots on inhibitory concentrations of IBA. Recombination mapping localized the *ibr1* mutations to the top of chromosome 4. C and D. *ibr3* mutants were identified in a forward genetics screen for elongated roots on inhibitory concentrations of IBA. Recombination mapping localized the mutations to the top of chromosome 3. E and F. *ibr10-1* was identified in a forward genetics screen for elongated roots on inhibitory concentrations of IBA. Recombination mapping localized *ibr10* to chromosome 4. *At4g14440* is a close homologue of *IBR10*. Arrows show point mutations; triangles indicate positions of T-DNA insertions. (Modified from Zolman et al., 2007; Zolman et al., 2008).

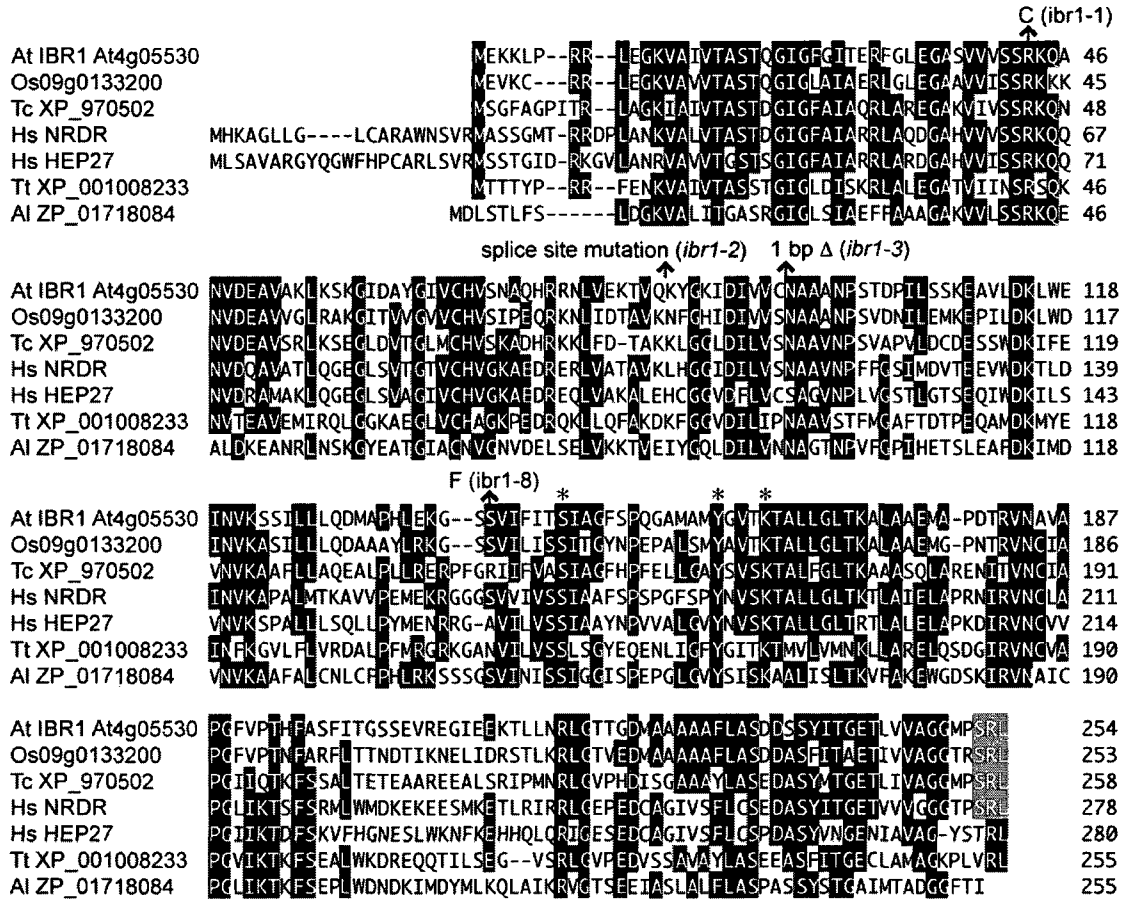

Figure 7.3. IBR1 resembles short-chain dehydrogenase/reductase enzymes.

Using the Clustal W method, an alignment was made of *Arabidopsis* (At) IBR1 with rice (Os), beetle (Tc), human (Hs), Tetrahymena (Tt), and *Algoriphagus* (Al). Conserved residues are highlighted in black. The C-terminal PTS1 is highlighted in gray. Asterisks denote the catalytic residues characteristic in SDR proteins (Kallberg et al. 2002). (Modified from Zolman et al., 2008).

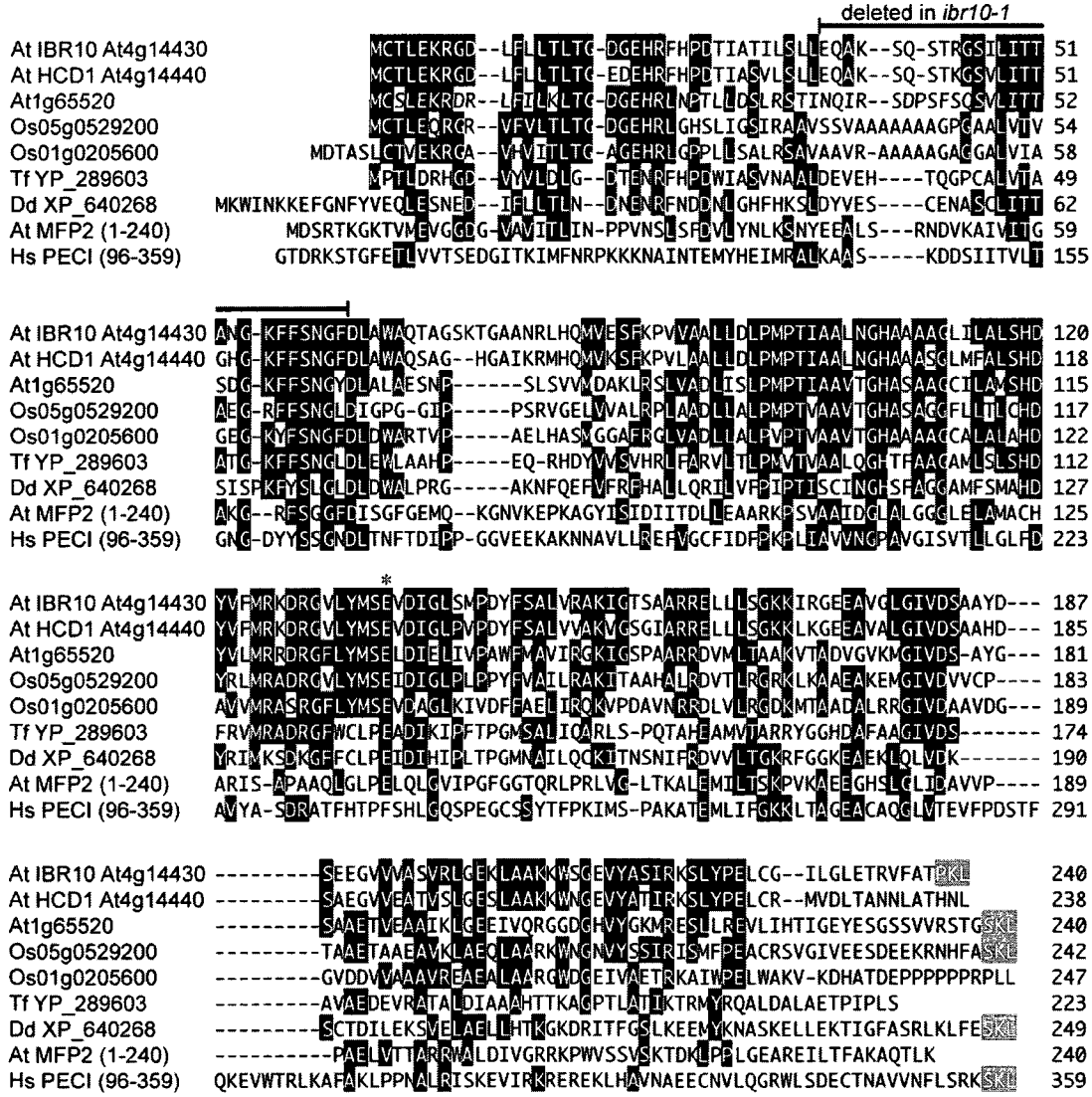

Figure 7.4. IBR10 resembles enoyl-CoA hydratases.

An alignment of IBR10 with enoyl-CoA hydratases from Arabidopsis (At), rice (Os), Thermobifida fusca (Tf), Dictyostelium (Dd), and humans (Hs) was made using the Clustal W method. Conserved residues are highlighted in black. The C-terminal PTS1 is highlighted in gray. An asterisk denotes a Glu residue important for activity in various organisms. (Modified from Zolman et al., 2008).

7.2. Complementation of *ibr10-1*

To confirm that the *ibr10-1* mutation was responsible for the IBA-resistant root elongation and lateral root initiation phenotypes, we overexpressed wild type IBR10 in *ibr10-1* using the 35S promoter from cauliflower mosaic virus. I found that *35S-IBR10* rescued both IBA-resistant root elongation and IBA-resistant lateral root formation of *ibr10-1* (Figure 7.5.A, B), indicating that the correct gene had been identified.

7.3. Mutations in *IBR10* homologs do not cause IBA resistance

The two closest homologs of *IBR10*, *At4g14440* and *At1g65520* encode proteins 80% identical and 49% identical to IBR10, respectively (Figure 7.4). At4g14440 does not contain a known PTS, whereas At1g65520 possesses a C-terminal SKL. I tested insertion mutations (SALK_012852 and SALK_036386) in the closest homologs of IBR10 for IBA-resistant root elongation and found that these mutants were not defective in IBA response (Figure 7.5.C), suggesting that the two IBR10 homologs do not have an important role in IBA response.

7.4. Phenotypic analysis of *ibr1* and *ibr10*

7.4.A. Response to auxins

To assess the *ibr* mutant phenotypes, I compared *ibr1* and *ibr10* to *ibr3* and *chy1*. I found that in root elongation assays, similar to *ibr3* and *chy1* (Zolman et al., 2001a; Zolman et al., 2007), *ibr1* and *ibr10* responded normally to the naturally occurring auxin IAA and to the synthetic auxins 2,4-D and NAA (Figure 7.6.B). When grown in the presence of IBA, *ibr1* and *ibr10* displayed more severe defects in root elongation response than the previously characterized *ibr3* mutant (Figure 7.6.A). Both *ibr1* and *ibr10* were also resistant to root elongation inhibition caused by the 2,4-D precursor 2,4-DB, similar to *ibr3* and *chy1* (Figure 7.6.B).

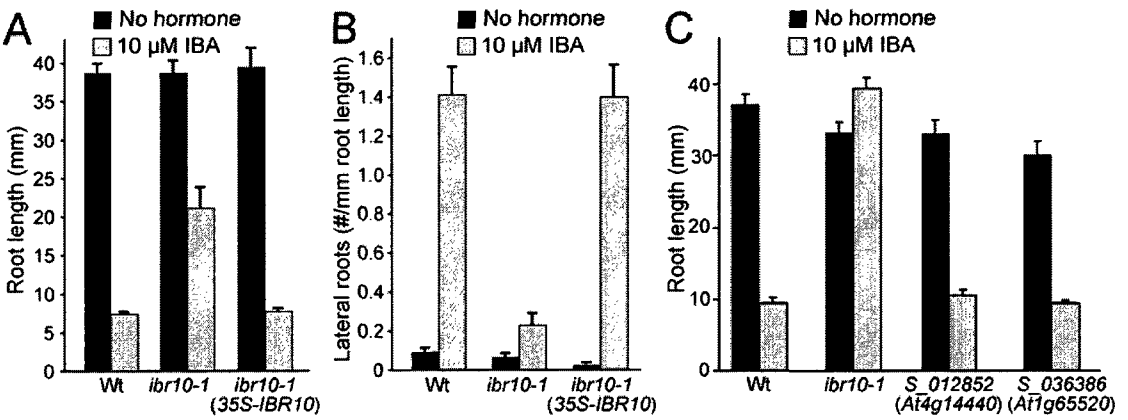

Figure 7.5. *ibr10-1* is rescued by *IBR10*.

A. Root elongation inhibition by IBA is restored in *ibr10-1* overexpressing IBR10. Bars show mean + SE ($n \geq 12$). B. Lateral root initiation by IBA is restored in *ibr10-1* overexpressing IBR10. Bars show mean + SE ($n \geq 12$). C. Mutations in IBR10 homologues do not cause IBA resistant root elongation. Bars show mean + SE ($n \geq 11$). (Modified from Zolman et al., 2008).

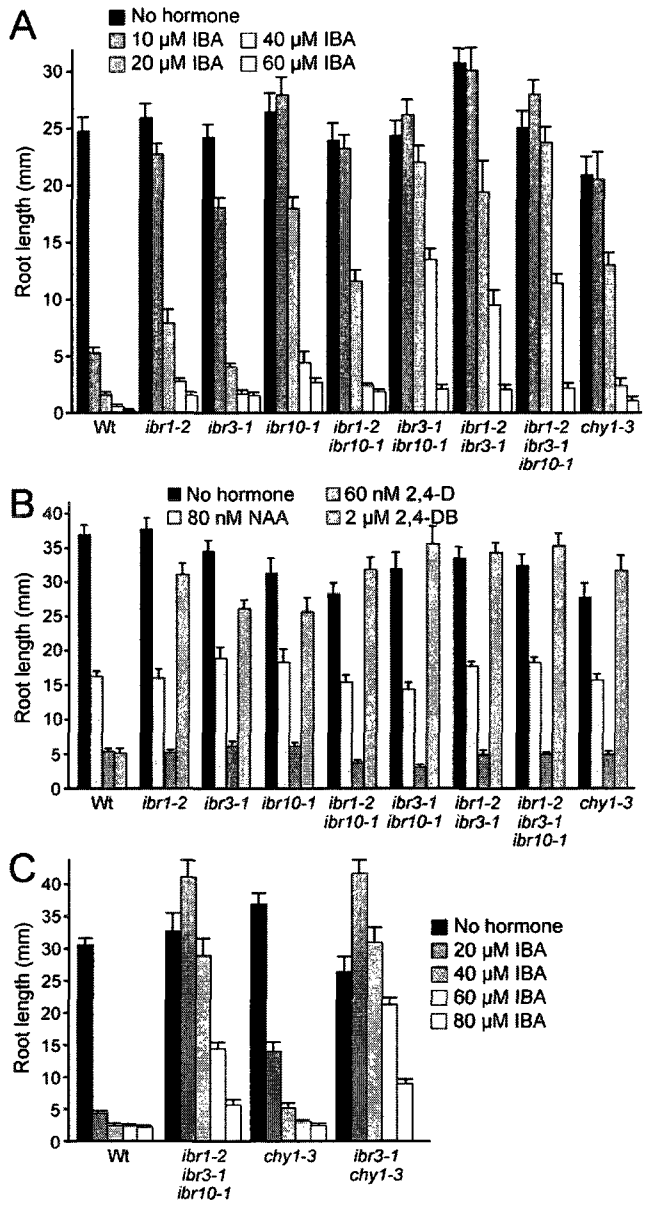

Figure 7.6. The ibr single, double, and triple mutants are resistant to 2,4-DB and IBA, but respond normally to 2,4-D and NAA.

A. *ibr* single, double, and triple mutants eventually respond to IBA at high concentrations. Seeds were stratified for 3 days at 4°C then germinated under white light for 2 days at 22°C. Germinating seeds were transferred to medium containing 0.5% sucrose (no hormone) or supplemented with IBA. Roots were measured after 8 additional days of growth under yellow-filtered light. Bars show mean + SE ($n \geq 10$). B. *ibr* mutants are resistant to 2,4-DB but respond normally to other synthetic auxins. Bars show mean + SE ($n \geq 12$). C. *ibr1 ibr3 ibr10* has enhanced IBA resistant root elongation compared to *chy1-3* but is less IBA resistant than *ibr3 chy1*. Bars show mean + SE ($n \geq 8$). (Modified from Zolman et al., 2008).

Because auxin promotes lateral root formation, I tested *ibr1* and *ibr10* for defects in lateral root formation in response to IBA and NAA. I found that although *ibr1* and *ibr10* produced lateral roots normally in response to NAA, both mutants produced significantly fewer lateral roots than wild type when grown on IBA (Figure 7.7.A).

We expressed the auxin-inducible DR5-GUS reporter (Guilfoyle, 1999) in *ibr10-1* and wild type plants to allow visualization of lateral root induction. I found that DR5-GUS was induced normally in *ibr10-1* in response to NAA treatment but exhibited a dampened response when treated with IBA (Figure 7.7.B). The specific response defects of *ibr1* and *ibr10* to IBA and not other auxins led us to conclude that both genes are important in IBA metabolism.

7.4.B. Are IBR1 and IBR10 important in other peroxisomal pathways?

Defects in fatty acid β-oxidation are typical of some peroxisomal mutants. Fatty acid β-oxidation mutants are unable to develop normally following germination without the addition of sucrose (Hayashi et al., 1998). Mutations likely to cause sucrose dependent phenotypes include mutations in fatty acid β-oxidation enzymes (Hayashi et al., 1998; Zolman et al., 2001a; Adham et al., 2005), mutations in the peroxisome import receptors (Hayashi et al., 2005; Woodward and Bartel, 2005), or mutations in other peroxisome biogenesis factors (Hayashi et al., 1998; Zolman et al., 2001b; Zolman and Bartel, 2004; Zolman et al., 2005). Because it is unclear whether the enzymes required for fatty acid and IBA metabolism overlap, I tested the *ibr* mutants for sucrose dependence. When grown in the presence or absence of sucrose, *ibr1* and *ibr10* developed normally resembling *ibr3* but unlike *chy1,* which acts indirectly in fatty acid β-oxidation (Figure 7.8.A).

CHY1 is involved not only in valine catabolism (Zolman et al., 2001a) but also in propionate and isobutyrate metabolism, as evidenced by the hypersensitive root elongation inhibition of the *chy1* mutant when treated with either compound (Lucas et al.,

2007). I found that *ibr1*, *ibr3*, and *ibr10* responded normally to isobutyrate and propionate (Figure 7.8.B), suggesting that IBR1, IBR3, and IBR10 are not involved in isobutyrate or propionate metabolism.

The sucrose independent phenotype and normal responses to isobutyrate and propionate, coupled with the IBA-specific response defects of the *ibr1* and *ibr10* mutants, together suggest that IBR1 and IBR10 are solely involved in IBA metabolism and do not participate in the other peroxisomal pathways tested.

7.4.C. Higher order mutants

Double and triple mutants are important in discovering whether two proteins have redundant or overlapping roles. I isolated an *ibr1 ibr3 ibr10* triple mutant. I compared the single, double, and triple combinations of *ibr1*, *ibr3*, and *ibr10* mutants on IBA and IAA, and tested these mutants for sucrose dependence.

Enhanced defects with progressive loss of gene function will suggest that the corresponding genes are acting in different pathways, or that the lesions only partially disrupt the pathway. Alternatively, if the multiple mutants are no more IBA resistant than the parents, this will suggest that the corresponding genes act in the same pathway.

I found that the double and triple mutants were not notably different from wild type in morphology, growth, or fertility. The double and triple mutants also responded normally to NAA and 2,4-D (Figure 7.6.B). In IBA resistance assays, the double and triple mutants were IBA resistant compared to wild type; however, like the single mutants, they did eventually respond to inhibition by IBA at high concentrations (Figure 7.6.A). Additionally, I tested the double and triple mutants for fatty acid β-oxidation defects and found that all combinations remained sucrose independent (Figure 7.8.A). Because I observed only slight enhancement of mutant phenotypes in the double and triple mutants, we concluded that IBR1, IBR3, and IBR10 may act in the same pathway.

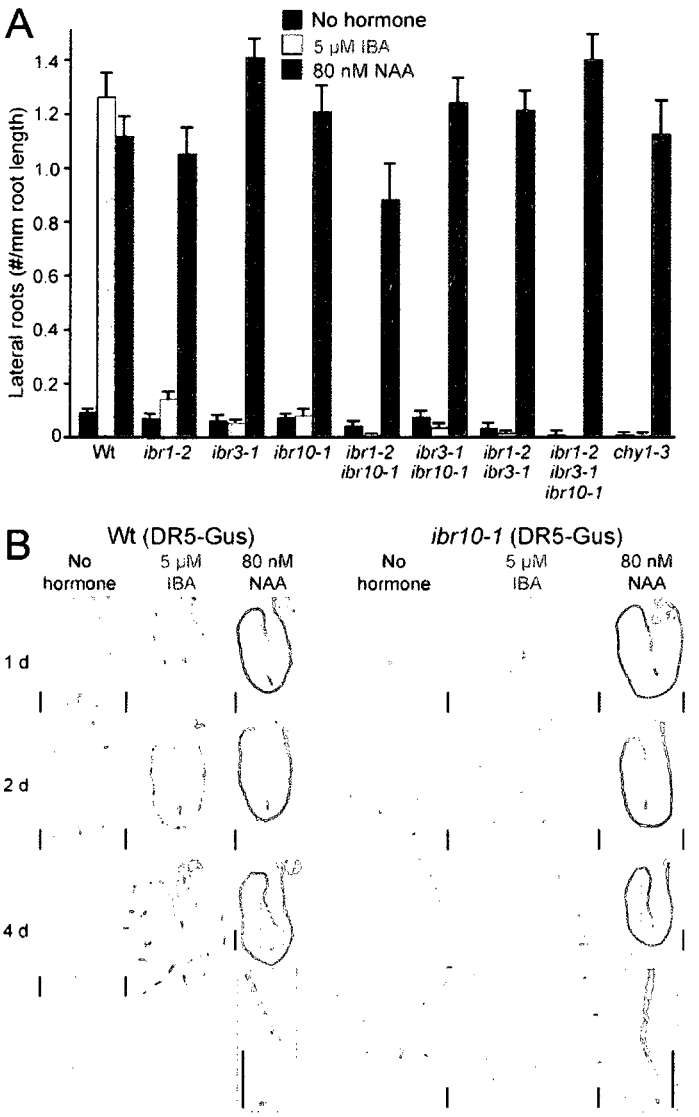

Figure 7.7. Lateral root initiation of *ibr* mutants on auxin.

A. *ibr1* and *ibr10* mutants produce normal roots in response to NAA but fail to induce lateral roots in response to IBA. Seeds were stratified 3 days at 4°C then plated on medium containing 0.5% sucrose and incubated under white light for 4 days at 22°C. Seedlings were then transferred to medium containing 0.5% sucrose with no hormone or supplemented with auxin. Roots were measured and lateral roots were counted after 4 additional days of growth. Bars show mean + SE ($n \geq 8$). B. DR5-GUS expression in response to auxin in wild type and *ibr10-1* seedlings. *ibr10-1* has normal DR5-GUS expression in NAA treated seedlings but reduced DR5-GUS expression when treated with IBA. Seedlings containing the DR5-GUS transgene were germinated on medium containing 0.5% sucrose, grown for 4 days, then transferred to medium containing no hormone, IBA, or NAA. After the indicated number of days, seedlings were removed from the medium, stained, and mounted for photography. Lateral root primordia of NAA-treated plants can be seen in the higher magnification insets. Scale bars represent 1 mm. (Figure from Zolman et al., 2008).

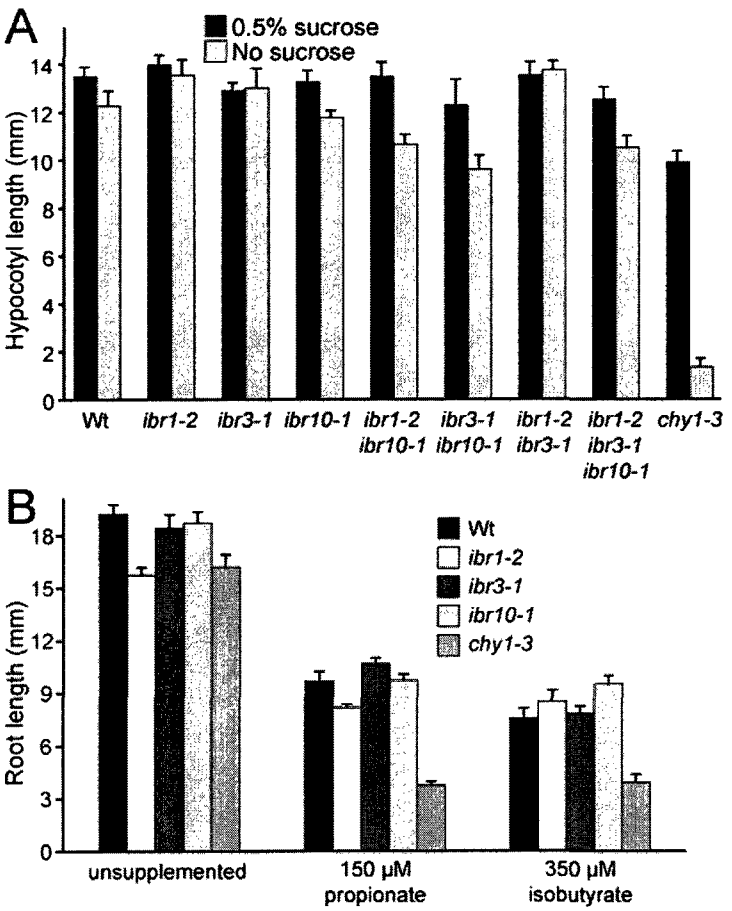

Figure 7.8. Assaying defects in alternative peroxisomal processes.

A. Hypocotyl length of seedlings grown with and without sucrose in the dark reveals that fatty acid β-oxidation is occurring normally in the single, double, and triple mutants. Seeds were stratified 4 days at 4°C prior to plating on medium with our without 0.5% sucrose. Seedlings were grown for 1 day at 22°C under white light then transferred to the dark at 22°C for 5 additional days. Bars show mean + SE ($n \geq 10$). B. Root elongation of *ibr* mutants is normal on propionate and isobutyrate. Seeds were stratified 3 days at 4°C then germinated under white light for 2 days at 22°C. Germinating seeds were transferred to medium containing 0.5% sucrose with or without 150 µM propionate or 350 µM isobutyrate. Roots were measured after 7 additional days of growth. Bars show mean + SE ($n \geq 11$). (Figure from Zolman et al., 2008).

7.5. Conclusions

IBR enzymes have homology to known fatty acid β-oxidation enzymes but because mutations in the corresponding genes do not lead to sucrose dependence, it is likely that IBR enzymes do not act in fatty acid metabolism. Additionally, *ibr* mutants are resistant to IBA and 2,4-DB but not to NAA, IAA, or 2,4-D; therefore, it is likely that IBR enzymes may act directly or indirectly in IBA to IAA conversion and the analogous process of 2,4-DB to 2,4-D conversion. *chy1* contributes to IBA responses indirectly through build-up of toxic intermediates in valine catabolism (Zolman et al., 2001a). Because *ibr* mutants respond normally to propionate and isobutyrate, we conclude that the IBR enzymes do not participate in the CHY1 pathway and it is unlikely that the IBR proteins act in the same manner as CHY1 to contribute to IBA response. Mutant phenotypes were only slightly enhanced in higher order mutants, consistent with the possibility that IBR1, IBR3, and IBR10 act in the same IBA to IAA conversion pathway, as modeled in Figure 7.1. Future biochemical analysis testing the *in vitro* activity of IBR1, IBR3, and IBR10 with the potential substrates depicted in Figure 7.1 will allow a more definitive elucidation of the roles of IBR proteins in peroxisomal processes.

Chapter 8: Conclusions and future directions

8.1. The interdependence of PEX5 and PEX7

Previous studies have shown that import of PTS2 cargo into mammalian and plant peroxisomes requires not only the PTS2 receptor PEX7, but also the PTS1 receptor PEX5 (Braverman et al., 1998; Otera et al., 1998; Hayashi et al., 2005; Woodward and Bartel, 2005; Lee et al., 2006). In this work, I have employed a new *pex7* allele, *pex7-2*, to demonstrate that the reciprocal is also true: *Arabidopsis* PEX5 and PTS1 import depend on the PTS2 receptor PEX7. The *pex7-2* mutant displayed typical peroxisome-defective phenotypes such as IBA resistance and sucrose dependence during seedling development (Chapter 3), and the *pex7-2* missense mutation disrupted interactions with both PTS2 cargo and the PTS1 receptor PEX5 in yeast two-hybrid assays (Chapter 4). I found that not only PEX7, but also PEX5 protein levels were reduced in light-grown *pex7* mutants (Chapter 5), suggesting that PEX5 depends on PEX7 for stability. Moreover, GFP-PTS1 was mislocalized to the cytosol in light-grown *pex7-2* mutants (Chapter 5), indicating that the reduced PEX5 levels that I observed in *pex7* were accompanied by a reduced efficiency of PTS1 import.

It is interesting that the more severe *pex7-2* sucrose dependence in the light compared to the dark (Chapter 3) was accompanied by more substantial defects in PEX5 and PEX7 accumulation in the light (Chapter 4). Other peroxisome-related mutants with light-enhanced sucrose dependence include *acx4*, a mutant defective in a PTS1-targeted short-chain acyl-CoA oxidase that is sucrose dependent in the light but not in the dark (Adham et al., 2005), and *pex6-1*, which displays severe sucrose dependence in the light but only partial sucrose dependence in the dark (Zolman and Bartel, 2004). These light-exacerbated phenotypes suggest that particular PEX protein roles might have varied importance in different environmental conditions. It is intriguing that PTS2 proteins are

over-represented among fatty acid β-oxidation enzymes (Kamada et al., 2003), which act to metabolize fatty acids stored in seeds immediately following germination, whereas virtually every photorespiration enzyme is a PTS1 protein. It is possible that the role of PEX7 in promoting PEX5 accumulation becomes more important in the light when there is a reduced demand for PTS2 import.

pex7-2 pex5-1 and *pex7-2 pex5-10* double mutants fail to complete embryogenesis (Chapter 3), similar to the embryo lethality observed in null alleles of the ring-finger peroxins PEX2, PEX10, and PEX12 (Hu et al., 2002; Schumann et al., 2003; Fan et al., 2005). This lethality implies that peroxisomal matrix protein import is required during *Arabidopsis* embryogenesis. Moreover, the enhanced defects observed in the *pex5 pex7* double mutants suggest that even the severe *pex7-2* and *pex5-10* mutations are not null alleles. Consistent with this possibility, thiolase processing is not completely blocked in *pex7-2* (Chapter 5), and we occasionally detect a small fraction of processed thiolase even in *pex5-10* plants (Zolman et al., 2005), suggesting that the *pex5-10* allele may produce a partially functional pex5-10 protein. Indeed, a smaller protein that cross-reacts with our PEX5 antibody, which was generated to a peptide corresponding to the PEX5 C-terminus (Zolman and Bartel, 2004), is sometimes detected in *pex5-10* extracts (Chapter 5).

I attempted to restore PEX5 levels in the *pex7* mutants, but after analyzing multiple transformants, I did not isolate a line that overaccumulated PEX5 to higher than wild type levels when grown in the light. I did observe a slight increase in PEX5 accumulation in these transgenic lines when grown in the dark (Chapter 6). PEX7 accumulation defects in the *pex7* mutants seem to be less severe in the dark (Chapter 5), and it is possible that if PEX7 is stabilized in the dark, then PEX5 also can be stabilized and accumulate to high levels. Additional western analyses with light- and dark-grown overexpression lines will illuminate this possibility. It also would be interesting to determine more directly the effect of *pex7* mutations on PEX5 stability by crossing *pex7*

to a *35S-PEX5* wild-type line that overaccumulates PEX5. Although *35S-PEX5* did not rescue the thiolase processing, sucrose dependence, or IBA responses of *pex7* mutants, I did not assess the effects on GFP-PTS1 import; it remains possible that PTS1 import defects were restored, but that the remaining PTS2 import defects caused the physiological phenotypes.

Mutations in either the *Arabidopsis* PEX5 or PEX7 receptors can cause deficiencies in PTS2 import (Hayashi et al., 2005; Woodward and Bartel, 2005). Based on the results of the yeast two-hybrid analysis discussed in Chapter 4, the *pex7-2* defects might be caused by an inability of pex7-2 to bind cargo or by an inability of pex7-2 to enter the peroxisome because of a disruption in PEX5 binding. To distinguish further between these two possibilities, I created PTS1-tagged versions of PEX7, pex7-2, and PED1 to allow an alternate route for the receptor and one of its primary cargos into the peroxisome, and introduced these constructs into the various receptor mutants. I was surprised to find that PEX7-SKL decreased IBA responsiveness in wild type while fully rescuing IBA response in *pex7-1* and partially rescuing IBA response in *pex7-2* (Chapter 6). This result suggests that PEX7-SKL can provide some PEX7 function, but that it also interferes with wild type PEX7 function. In *pex5-1*, which, based on yeast two-hybrid analyses (Chapter 4), does not seem to disrupt interaction with PEX7, PEX7-SKL partially rescued both thiolase processing and IBA response. The finding that pex7-2-SKL also rescued IBA response and partially restored thiolase processing in *pex7-1* and *pex7-2* suggests that the inability of pex7-2 to bind PEX5 is only partially contributing to the PTS2-specific phenotypes of the pex7-2 mutants. Future analysis of lines overexpressing the untagged pex7-2 protein would likely clarify this issue.

In Chapter 6, I described how overexpressing PED1 from the 35S promoter in *pex7-1* partially rescued IBA response. This was surprising because *pex7-1* has no defects in accumulating PED1. Adding an SKL to PED1 also partially rescued *pex7-1* IBA response but also fully rescued thiolase processing. It would be interesting to

overexpress PED1 in the stronger *pex7-2* and assess rescue. PED1 accumulation varies with plant age (Lingard et al., 2009) and in the future, a time course experiment with *pex7* (*35S-PED1*) lines may give further insight into the mechanisms behind this rescue.

PED1-SKL partially rescued *pex5-1* IBA response, suggesting that PEX7 cargo-binding is impaired in *pex5-1* and can be circumvented by providing PTS2 cargo an alternative means to bind PEX5. Moreover, this result suggests that peroxisomal thiolase becomes limiting for IBA β-oxidation in the *pex5-1* mutant.

One intriguing observation was that although I did not isolate wild-type lines that overaccumulated PEX7 or PED1 to much higher levels than normal, the *35S-PEX7* and *35S-PED1* constructs did drive protein overaccumulation and phenotypic rescue in *pex7* and *ped1* mutants, respectively. When we select for transformants by screening for Basta resistance, we also are selecting for healthy plants. Perhaps by selecting for healthy seedlings, I also selected for those transformants with higher overexpression, in cases when overexpression rescued the mutant phenotypes. Because wild-type growth is not enhanced by *PEX7* or *PED1* overexpression, it may be more difficult to find a wild-type line that overaccumulates these proteins.

The possibility that PTS1 import can depend on PEX7 may not be unique to plants. A recent study in trypanosomes revealed that *pex7* RNAi lines had low PEX5 levels and mislocalized not only PTS2, but also PTS1 proteins (Galland et al., 2007). Although this role cannot be universal among eukaryotes, given the lack of PEX7 and PTS2 proteins in *C. elegans* (Gurvitz et al., 2000; Motley et al., 2000), a role for PEX7 in PEX5 stabilization or accumulation provides a rationale for the continued existence of an apparent *PEX7* homolog in *Drosophila melanogaster* (Motley et al., 2000), which lacks readily identifiable PTS2 proteins (Woodward, 2005).

8.2. New insights into the nature of *pex5-1* defects

A mammalian *pex5* mutant with a mutation (Ser to Phe) analogous to the *Arabidopsis pex5-1* Ser to Leu mutation disrupts binding to PEX7 *in vitro* (Matsumura et al., 2000; Dodt et al., 2001). After molecular and physiological analysis, the defects that underlie *pex5-1* phenotypes remain unknown. *pex5-1* mutants do not display PEX5 or PEX7 protein accumulation defects (Chapter 5). Moreover, I unexpectedly found that pex5-1 did not disrupt interaction with cargo or PEX7 in the yeast two-hybrid assay (Chapter 4). Through the use of a truncated pex5-1 derivative, I eliminated the possibility that a yeast protein possessing both a PTS1 and PTS2 could be bridging the interaction of pex5-1 with PEX7 in yeast. Nito et al. (2002) demonstrated that a N-terminal PEX5 derivate lacking the pex5-1 mutation region interacts with PEX7 in a yeast two-hybrid assay less efficiently than full-length PEX5 (Nito et al., 2002). It remains possible that quantitative comparisons of pex5-1 and PEX5 interactions with PEX7 would reveal a difference.

Rather than altering interaction in a manner that disrupts binding, it is also possible that the serine to leucine change in pex5-1 creates a stronger binding to PEX7 such that PEX7 cannot be efficiently released from PEX5. Leucine is more hydrophobic than serine and this hydrophobicity may create a need to remain "hidden" within the binding pocket with PEX7. If PEX7 release from PEX5 is necessary for PEX7 to carry out its function, then this tighter binding might disrupt PTS2 import and other peroxisome processes associated with PEX7. However, my observation that PEX7 overexpression is able to partially rescue *pex5-1* phenotypes (Chapter 6) seems more consistent with the possibility that PEX7 binds pex5-1 less avidly than wild-type PEX5.

Regardless of whether pex5-1 binds more or less strongly to PEX7, I found that *35S-PEX7-SKL* was able to more fully rescue *pex5-1* phenotypes than was *35S-PEX7*.

Because providing PEX7 with an alternate means to bind PEX5 partially restores *pex5-1* phenotypes, it is likely that the *pex5-1* lesion impacts PEX7 binding or release.

In the future, it might be informative to create the Ser to Phe mutation found in the mammalian mutant (Matsumura et al., 2000) in *Arabidopsis PEX5* to determine if this residue disrupts interaction with *Arabidopsis* PEX7.

Our models for *pex5-1* defects are limited by the dearth of structural information about peroxins. The C-terminal, PTS1-binding region of *Trypanosoma brucei* PEX5 and the N-terminal domain of mammalian PEX14 are the only regions in peroxins with solved crystal structures (Sampathkumar et al., 2008; Su et al., 2009). Future crystallographic studies of peroxins, in particular of PEX5 and PEX7, may in the future clarify some of the findings reported here. For example, structural studies of PEX7 might reveal whether the pex7-2 lesion is likely to disrupt the integrity of the WD-40 structure or have more specific effects.

8.3. Additional *pex7* mutants

The two *Arabidopsis* PEX7 single mutants have relatively weak phenotypes and no presumptive *PEX7* null alleles are available in T-DNA collections. *PEX7* mutations that completely abolish PTS2 import have yet to be recovered. My analysis in Chapter 3 is consistent with the possibility that PEX7 null alleles may be embryo lethal.

TILLING (Colbert et al., 2001) has been employed to isolate point mutations in *PEX7* with the aim of recovering additional informative alleles. Five point mutations have been isolated (Chapter 1). *pex7-6* and *pex7-7* are of particular interest because they contain mutations in completely conserved residues (Chapter 1). Preliminary analysis has shown that none of the TILLING alleles have defects in thiolase processing (data not shown). However, *pex7-1* often shows completely processed thiolase while maintaining reduced PEX5 and PEX7 levels. In the future, analysis of receptor levels in these

mutants could be used to reveal whether they alter PEX7 function similarly to the previously characterized alleles.

8.4. Future studies on PEX7 and the docking complex

Beyond the questions that remain to be answered regarding PEX7 interactions with PEX5, many questions remain about how PEX7 interacts with the docking complex prior to translocation. What effect might *pex7* mutations have on PEX14 and PEX13 docking or dynamics? Preliminary western blots using an anti-PEX14 antibody did not reveal decreased PEX14 accumulation in *pex7* mutants (data not shown). It is clear that PEX5 has a dependence on PEX7, but the details of that dependence remain to be further understood. It is possible that PEX5 depends on PEX7 for docking to the peroxisome membrane. If *pex7-2* disrupts PEX5 binding, and PEX5 depends on PEX7 for function, can PEX5 still bind to PEX14? An interesting future study could involve localization studies in *pex7* mutants to determine whether the distribution of PEX5 between the peroxisome and cytosol is altered.

Because *Arabidopsis* PEX7 binds PEX13 and not PEX14 (Nito et al., 2002; Mano et al., 2006), we expect that combining *pex7* alleles with *pex13* and *pex14* alleles might be informative. Moreover, overexpressing PEX7 in *pex14* and *pex13* mutants could yield more information about the interaction between PEX7 and the docking complex.

8.5. Future Studies on PEX7 recycling

Neither *pex4-1* nor *pex6-1* have defects in PEX7 accumulation (data not shown) but both exhibit defects in thiolase processing (Zolman and Bartel, 2004; Zolman et al., 2005). Although PEX7 levels are normal in these mutants, we do not know if PEX7 localization is affected. In an effort to shed some light on how PEX7 is recycled from the peroxisome, I introduced the *35S-PEX7* construct into *pex4-1* and *pex6-1* mutants. A current graduate student in our lab, Sarah Ratzel, is currently characterizing these lines

for peroxisome-defective phenotypes. If PEX7 depends on these peroxins for recycling, then we would expect that adding excess PEX7 might magnify defects.

pex6-1 has decreased PEX5 accumulation and mutant phenotypes can be partially rescued through PEX5 overexpression (Zolman and Bartel, 2004); preliminary studies show a partial restoration of thiolase processing (S. Ratzel personal communication). Just as the dependence of PEX5 on PEX7 remains unclear, so does the dependence of PEX7 on PEX5. If PEX5 can partially rescue PTS2 defects in *pex6-1*, this might be a clue that PEX7 may depend on PEX5 for recycling.

Future analysis of *pex7 pex4* and *pex7 pex6* double mutants may provide further insight into the PEX7 recycling process. Furthermore, a yeast two-hybrid analysis to assess PEX7 and PEX5 interactions with PEX4 and PEX6 may be informative.

8.6. Final thoughts

Perhaps because the majority of peroxisomal matrix proteins are PTS1-containing proteins, PEX5 has been at the forefront of peroxisome receptor research. This study has uncovered an importance for the PTS2 receptor PEX7 in facilitating PTS1 import in *Arabidopsis* peroxisomes. Although the molecular mechanisms by which PEX7 promotes PEX5 accumulation and function remain to be determined, the tools are now in place to make progress in this area. It will be interesting to learn which other organisms share the reciprocal receptor dependence uncovered here.

Many questions remain about the roles of auxin metabolism in plant growth and development. To begin to unravel some of the complexities of auxin metabolism, I have isolated and characterized new *ibr* mutants, tested candidate genes for roles in IBA β-oxidation, biochemically characterized enzymes defective in known *ibr* mutants, and analyzed the effects of multiple mutations on IBA responses and fatty acid metabolism. My mutant screen may have uncovered novel players in the conversion of IBA to IAA. This research is enhancing our understanding of IBA metabolism in plants. Because IBA

is an important *in vivo* IAA precursor, and because IBA is widely used commercially for its ability to initiate lateral roots, this research may also proved insights for the manipulation of auxin levels in agriculturally important plants.

References

Adham, A. R., Zolman, B. K., Millius, A., and Bartel, B. (2005). Mutations in *Arabidopsis* acyl-CoA oxidase genes reveal distinct and overlapping roles in β-oxidation. Plant J *41*, 859-874.

Akiyama, N., Ghaedi, K., and Fujiki, Y. (2002). A novel *pex2* mutant: catalse-deficient but temperature-sensitive PTS1 and PTS2 import. Biochem and Biophys Research Communications *293*, 1523-1529.

Albertini, M., Rehling, P., Erdmann, R., Girzalsky, W., Kiel, J. A. K. W., Veenhuis, M., and Kunau, W. H. (1997). Pex14p, a peroxisomal membrane protein binding both receptors of the two PTS-dependent import pathways. Cell *89*, 83-92.

Asada, K. (1996). Radical production and scavenging in the chloroplasts. In Photosynthesis and the Environment (Baker, NR, ed) *Dordrecht, the Netherlands*, 123-150.

Asamizu, E., Nakamura, Y., Sato, S., and Tabata, S. (2000). A large scale analysis of cDNA in *Arabidopsis thaliana*: generation of 12,028 non-redundant expressed sequence tags from normalized and size-selected cDNA libraries. DNA Res *7*, 175-180.

Ausubel, F., Brent, R., Kingston, R. E., Moore, D. D., Seidman, J. G., Smith, J. A., and Struhl, K. (1999). Current Protocols in Molecular Biology (New York: Greene Publishing Associates and Wiley-Interscience).

Ausubel, F. M., Brent, R., Kingston, R. E., Moore, D. D., Seidman, J. G., Smith, J. A., and Struhl, K. (1995). Short Protocols in Molecular Biology, third edn: John Wiley & Sons, Inc.).

Baes, M., Huyghe, S., Carmeliet, P., Declercq, P. E., Collen, D., Mannaertsi, G. P., and Veldhoven, P. P. (2000). Inactivation of the peroxisomal multifunctional protein-2 in mice impedes the degradation of not only 2-methyl-branched fatty acids and bile acid intermediates but also of very long chain fatty acids. J Biol Chem *275*.

Baraldi, R., Bertazza, G., Predieri, S., Bregoli, A. M., and Cohen, J. D. (1993). Uptake and metabolism of indole-3-butyric acid during the in vitro rooting phase in pear cultivars (*Pyrus communis*). Acta Hort *329*, 289-291.

Bartel, B., and Fink, G. R. (1994). Differential regulation of an auxin-producing nitrilase gene family in *Arabidopsis thaliana*. Proc Natl Acad Sci USA *91*, 6649-6653.

Bell, C. J., and Ecker, J. R. (1994). Assignment of 30 microsatellite loci to the linkage map of *Arabidopsis*. Genomics *19*, 137-144.

Birschmann, I., Stroobants, A. K., van den Berg, M., Schafer, A., Rosenkranz, K., Kunau, W. H., and Tabak, H. F. (2003). Pex15p of Saccharomyces cerevisiae provides a molecular basis for recruitment of the AAA peroxin Pex6p to peroxisomal membranes. Mol Biol Cell *14*, 2226-2236.

Braverman, N., Dodt, G., Gould, S. J., and Valle, D. (1998). An isoform of Pex5p, the human PTS1 receptor, is required for the import of PTS2 proteins into peroxisomes. Hum Mol Genet *7*, 1195-1205.

Braverman, N., Steel, G., Obie, C., Moser, A., Moser, H., Gould, S. J., and Valle, D. (1997). Human *PEX7* encodes the peroxisomal PTS2 receptor and is responsible for rhizomelic chondrodysplasia punctata. Nat Genet *15*, 369-376.

Brocard, C., Kragler, F., Simon, M. M., Schuster, T., and Hartig, A. (1994). The tetratricopeptide repeat-domain of the PAS10 protein of *Saccharomyces cerevisiae* is essential for binding the peroxisomal targeting signal -SKL. Biochem Biophys Res Com *204*, 1016-1022.

Brown, L.-A., and Baker, A. (2008). Shuttles and cycles: transport of proteins into the peroxisome matrix (Review). Molecular Membrane Biology *25*, 363-375.

Brown, L. A., and Baker, A. (2003). Peroxisome biogenesis and the role of protein import. J Cell Mol Med *7*, 388-400.

Celenza, J. L., Grisafi, P. L., and Fink, G. R. (1995). A pathway for lateral root formation in *Arabidopsis thaliana*. Genes Dev *9*, 2131-2142.

Chase, C. A., Bewick, T. A., and Shilling, D. G. (1998). Differential photosynthetic electron transport and oxidative stress in paraquat-resistant and sensitive biotypes of *Solanum americanum*. Pesticide biochemistry and physiology *60*, 83-90.

Chothia, C., Hubbard, T., Brenner, S., Barns, H., and Murzin, A. (1997). Protein folds in the all-beta and all-alpha classes. Annu Rev Biophys Biomol Sruct *26*, 597-627.

Clough, S. J., and Bent, A. F. (1998). Floral dip: a simplified method for *Agrobacterium*-mediated transformation of *Arabidopsis thaliana*. Plant J *16*, 735-743.

Colbert, T., Till, B. J., Tompa, R., Reynolds, S., Steine, M. N., Yeung, A. T., McCallum, C. M., Comai, L., and Henikoff, S. (2001). High-throughput screening for induced point mutations. Plant Physiol *126*, 480-484.

Cregg, J. M., Klei, I. J. V., Sulter, G. J., Veenhuiss, M., and Harder, W. (1990). Peroxisome-deficient mutants of *Hansenula polymorpha*. Yeast *6*, 87-97.

Dammai, V., and Subramani, S. (2001). The human peroxisomal targeting signal receptor, Pex5p, is translocated into the peroxisome matrix and recycled to the cytosol. Cell *105*, 187-196.

Dodt, G., Braverman, N., Wong, C., Moser, A., Moser, H. W., Watkins, P., Valle, D., and Gould, S. J. (1995). Mutations in the PTS1 receptor gene, *PXR1*, define complementation group 2 of the peroxisome biogenesis disorders. Nature Genetics *9*, 115-125.

Dodt, G., and Gould, S. J. (1996). Multiple PEX genes are required for proper subcellular distribution and stability of Pex5p, the PTS1 receptor: evidence that PTS1 protein import is mediated by a cycling receptor. J Cell Biol *135*, 1763-1774.

Dodt, G., Warren, D., Becker, E., Rehling, P., and Gould, S. J. (2001). Domain mapping of human PEX5 reveals functional and structural similarities to *Saccharomyces cerevisiae* Pex18p and Pex21p. J Biol Chem *276*, 41769-41781.

Eastmond, P. J., Hooks, M. A., Williams, D., Lange, P., Bechtold, N., Sarrobert, C., Nussaume, L., and Graham, I. A. (2000). Promoter trapping of a novel medium-chain acyl-CoA oxidase, which is induced transcriptionally during *Arabidopsis* seed germination. J Biol Chem *275*, 34375-34381.

Elgersma, Y., Kwast, L., Klein, A., Voorn-Brouwer, T., van den Berg, M., Metzig, B., America, T., Tabak, H. F., and Distel, B. (1996). The SH3 domain of the *Saccharomyces cerevisiae* peroxisomal membrane protein Pex13p functions as a docking site for Pex5p, a mobile receptor for the import PTS1-containing proteins. J Cell Biol *135*, 97-109.

Epstein, E., and Lavee, S. (1984). Conversion of indole-3-butyric acid to indole-3-acetic acid by cuttings of grapevine (*Vitus vinifera*) and olive (*Olea europa*). Plant Cell Physiol *25*, 697-703.

Erdmann, R., Veenhuis, M., Mertens, D., and Kunau, W.-H. (1989). Isolation of peroxisome-deficient mutants of *Saccharomyces cerevisiae*. Proc Natl Acad Sci U S A *86*, 5419-5423.

Fan, J., Quan, S., Orth, T., Awai, C., Chory, J., and Hu, J. (2005). The *Arabidopsis PEX12* gene is required for peroxisome biogenesis and is essential for development. Plant Physiol *139*, 231-239.

Fawcett, C. H., Wain, R. L., and Wightman, F. (1960). The metabolism of 3-indolylalkanecarboxylic acids, and their amides, nitriles and methyl esters in plant tissues. Proc Royal Soc London, Series B *152*, 231-254.

Flynn, C. R., Mullen, R. T., and Trelease, R. N. (1998). Mutational analyses of a type 2 peroxisomal targeting signal that is capable of directing oligomeric protein import into tobacco BY-2 glyoxysomes. Plant J *16*, 709-720.

Fransen, M., Brees, C., Baumgart, E., Vanhooren, J. C. T., Baes, M., Mannaerts, G. P., and Veldhoven, P. P. (1995). Identification and characterization of the putative human peroxisomal C-terminal targeting signal import receptor. J Biol Chem *270*, 7731-7736.

Froman, B. E., Edwards, P. C., Bursch, A. G., and Dehesh, K. (2000). ACX3, a novel medium-chain acyl-Coenzyme A oxidase from Arabidopsis. Plant Physiol *123*, 733-741.

Fujibe, T., Saji, H., Watahiki, M. K., and Yamamoto, K. T. (2006). Overexpression of the *RADICAL-INDUCED CELL DEATH1 (RCD1)* gene of *Arabidopsis* causes weak *rcd1* phenotype with compromised oxidative-stress responses. Biosci Biotechnol Biochem *70*, 1827-1831.

Fujiwara, C., Imamura, A., Hashiguchi, N., Shimozawa, N., Suzuki, Y., Kondo, N., Imanaka, T., Tsukamoto, T., and Osumi, T. (2000). Catalse-less peroxisomes. Implication in the milder forms of peroxisome biogenesis disorder. J Biol Chem *275*, 37271-37277.

Fulda, M., Shockey, J., Werber, M., Wolter, F. P., and Heinz, E. (2002). Two long-chain acyl-CoA synthetases from *Arabidopsis thaliana* involved in peroxisomal fatty acid β-oxidation. Plant J *32*, 93-103.

Galland, N., Demeure, F., Hannaert, V., Verplaetse, E., Vertommen, D., Van Der Smissen, P., J. Courtoy, P., and A.M. Michels, P. (2007). Characterization of the role of the receptors PEX5 and PEX7 in the import of proteins into glycosomes of *Trypanosoma brucei*. Biochim Biophys Acta *1773* 521–535.

Gatto, G. J., Jr., Geisbrecht, B. V., Gould, S. J., and Berg, J. M. (2000). Peroxisomal targeting signal-1 recognition by the TPR domains of human PEX5. Nat Struct Biol *7*, 1091-1095.

Germain, V., Rylott, E. L., Larson, T. R., Sherson, S. M., Bechntold, N., Carde, J. P., Bryce, J. H., Graham, I. A., and Smith, S. M. (2001). Requirement for 3-ketoacyl-CoA thiolase-2 in peroxisome development, fatty acid β-oxidation and breakdown of triacylglycerol in lipid bodies of *Arabidopsis* seedlings. Plant J *28*, 1-12.

Gietz, R., and Schiestl, R. (1995). Transforming yeast with DNA. Methods Mol Cell Biol *5*, 255-269.

Gould, S. J., Keller, G. A., Hosken, N., Wilkinson, J., and Subramani, S. (1989). A conserved tripeptide sorts proteins to peroxisomes. J Cell Biol *108*, 1657-1664.

Grou, C. P., Carvalho, A. F., Pinto, M. P., Wiese, S., Piechura, H., Meyer, H. E., Warscheid, B., Sá-Miranda, C., and Azevedo, J. E. (2008). Members of the E2D (UbcH5) family mediate the ubiquitination of the conserved cysteine of Pex5p, the peroxisomal import receptor. J Biol Chem *283*, 14190-14197.

Guilfoyle, T. J. (1999). Auxin-regulated genes and promoters, In Biochemistry and Molecular Biology of Plant Hormones, P. J. J. Hooykaas, M. A. Hall, and K. R. Libbenga, eds. (Amsterdam: Elsevier), pp. 423-459.

Gurvitz, A., Langer, S., Piskacek, M., Hamilton, B., Ruis, H., and Hartig, A. (2000). Predicting the function and subcellular location of *Caenorhabditis elegans* proteins similar to *Saccharomyces cerevisiae* β-oxidation enzymes. Yeast *17*, 188-200.

Haughn, G. W., and Somerville, C. (1986). Sulfonylurea-resistant mutants of *Arabidopsis thaliana*. Mol Gen Genet *204*, 430-434.

Hayashi, H., De Bellis, L., Ciurli, A., Kondo, M., Hayashi, M., and Nishimura, M. (1999). A novel acyl-CoA oxidase that can oxidize short-chain acyl-CoA in plant peroxisomes. J Biol Chem *274*, 12715-12721.

Hayashi, M., and Nishimura, M. (2003). Entering a new era of research on plant peroxisomes. Curr Opin Plant Biol *6*, 577-582.

Hayashi, M., and Nishimura, M. (2006). *Arabidopsis thaliana*--A model organism to study plant peroxisomes. Biochim Biophys Acta *1763*, 1382-1391.

Hayashi, M., Nito, K., Toriyama-Kato, K., Kondo, M., Yamaya, T., and Nishimura, M. (2000). *At*Pex14p maintains peroxisomal functions by determining protein targeting to three kinds of plant peroxisomes. EMBO J *19*, 5701-5710.

Hayashi, M., Toriyama, K., Kondo, M., and Nishimura, M. (1998). 2,4-dichlorophenoxybutyric acid-resistant mutants of *Arabidopsis* have defects in glyoxysomal fatty acid β-oxidation. Plant Cell *10*, 183-195.

Hayashi, M., Yagi, M., Nito, K., Kamada, T., and Nishimura, M. (2005). Differential contribution of two peroxisomal protein receptors to the maintenance of peroxisomal functions in *Arabidopsis*. J Biol Chem *280*, 14829-14835.

Helm, M., Luck, C., Prestele, J., Hierl, G., Huesgen, P. F., Frohlich, T., Arnold, G. J., Adamska, I., Gorg, A., and Lottspeich (2007). Dual specificities of the glyoxysomal/peroxisomal processing protease Deg15 in higher plants. Proc Natl Acad Sci USA *104*, 11501-11506.

Hodge, V. J., Gould, S. J., Subramani, S., Moser, H. W., and Krisans, S. K. (1991). Normal cholesterol synthesis in human cells requires functional peroxisomes. Biochem Biophys Res Commun *181*, 537-541.

Hooks, M. A., Kellas, F., and Graham, I. A. (1999). Long-chain acyl-CoA oxidases of *Arabidopsis*. The Plant Journal *20*, 1-13.

Hu, J., Aguirre, M., Peto, C., Alonso, J., Ecker, J., and Chory, J. (2002). A role for peroxisomes in photomorphogenesis and development of *Arabidopsis*. Science *297*, 405-409.

Johnson, T. L., and Olsen, L. J. (2003). Import of the peroxisomal targeting signal type 2 protein 3-ketoacyl-Coenzyme A thiolase into glyoxysomes. Plant Physiol *133*, 1991-1999.

Kamada, T., Nito, K., Hayashi, H., Mano, S., Hayashi, M., and Nishimura, M. (2003). Functional differentiation of peroxisomes revealed by expression profiles of peroxisomal genes in *Arabidopsis thaliana*. Plant Cell Physiol *44*, 1275-1289.

Kato, A., Hayashi, M., and Nishimura, M. (1999). Oligomeric proteins containing N-terminal targeting signals are imported into peroxisomes in transgenic *Arabidopsis*. Plant Cell Physiol *40*, 586-591.

Kato, A., Hayashi, M., Takeuchi, Y., and Nishimura, M. (1996). cDNA cloning and expression of a gene for 3-ketoacyl-CoA thiolase in pumpkin cotyledons. Plant Mol Biol *31*, 843-852.

Kienow, L., Schneider, K., Bartsch, M., Stuible, H.-P., Weng, H., Miersch, O., Wasternack, C., and Kombrink, E. (2008). Jasmonates meet fatty acids: functional analysis of a new acyl-coenzyme A synthetase family from *Arabidopsis thaliana*. Journal of Experimental Botany *59*, 403-419.

Kindl, H. (1993). Fatty acid degradation in plant peroxisomes: Function and biosynthesis of the enzymes involved. Biochimie *75*, 225-230.

Kohalmi, S., Reader, L. J. V., Samach, A., Nowak, J., Haughn, G. W., and Crosby, W. L. (1998). Identification and characterization of protein interactions using the yeast 2-hybrid system, In Plant Molecular Biology Manual, S. B. Gelvin, and R. A. Schiperoort, eds. (Dordrecht, The Neterlands: Kluwer), pp. 1-30.

Koller, A., Snyder, W. B., Faber, K. N., Wenzel, T. J., Rangell, L., Keller, G. A., and Subramani, S. (1999). Pex22p of *Pichia pastoris*, essential for peroxisomal matrix protein import, anchors the ubiquitin-conjugating enzyme, Pex4p, on the peroxisomal membrane. J Cell Biol *146*, 99-112.

Koncz, C., Schell, J., and Rédei, G. P. (1992). T-DNA transformation and insertion mutagenesis, In Methods in Arabidopsis Research, C. Koncz, N.-H. Chua, and J. Schell, eds. (Singapore: World Scientific), pp. 224-273.

Konieczny, A., and Ausubel, F. M. (1993). A procedure for mapping *Arabidopsis* mutations using co-dominant ecotype-specific PCR-based markers. Plant J *4*, 403-410.

Koo, A. J. K., Chung, H. S., Kobayashi, Y., and Howe, G. A. (2006). Identfication of a Peroxisomal Acyl-activating Enzyme Involved in the Biosythesis of Jasmonic Acid in *Arabidopsis*. J Biol Chem *281*, 33511-33520.

Koornneef, M., Alonso-Blanco, C., and Vreugdenhil, D. (2004). Naturally Occurring Genetic Variation in *Arabidopsis Thaliana*. Annu Rev Plant Biol *55*, 141-172.

Lazarow, P. B. (2003). Peroxisome biogenesis: advances and conundrums. Curr Opin Cell Biol *15*, 489-497.

LeClere, S., and Bartel, B. (2001). A library of *Arabidopsis* 35S-cDNA lines for identifying novel mutants. Plant Mol Biol *46*, 695-703.

Lee, J. R., Jang, H. H., Park, J. H., Jung, J. H., Lee, S. S., Park, S. K., Chi, Y. H., Chan Moon, J., Lee, Y. M., Kim, S. Y. *et al.* (2006). Cloning of two splice variants of the rice PTS1 receptor, OsPex5pL and OsPex5pS, and their functional characterization using pex5-deficient yeast and *Arabidopsis*. Plant J *47*, 457-466.

Leon, S., Zhang, L., McDonald, W. H., Yates, J., 3rd, Cregg, J. M., and Subramani, S. (2006). Dynamics of the peroxisomal import cycle of PpPex20p: ubiquitin-dependent localization and regulation. J Cell Biol *172*, 67-78.

Lin, Y., Cluette-Brown, J. E., and Goodman, H. M. (2004). The peroxisome deficient Arabidopsis mutant *sse1* exhibits impaired fatty acid synthesis. Plant Physiol *135*, 814-827.

Lingard, M., Monroe-Augustus, M., and Bartel, B. (2009). Peroxisome-associated matrix protein degradation in *Arabidopsis*. Proc Natl Acad Sci U S A *106*, 4561-4566.

Lucas, K. A., Filley, J. R., Erb, J. M., Graybill, E. R., and Hawes, J. W. (2007). Peroxisomal Metabolism of Propionic Acid and Isobutyric Acid in Plants. J Biol Chem *282*, 24980-24989.

Ludwig-Müller, J., and Epstein, E. (1991). Occurrence and *in vivo* biosynthesis of indole-3-butyric acid in corn (*Zea mays* L.). Plant Physiol *97*, 765-770.

Ludwig-Müller, J., Sass, S., Sutter, E. G., Wodner, M., and Epstein, E. (1993). Indole-3-butyric acid in *Arabidopsis thaliana*. I. Identification and quantification. Plant Growth Regul *13*, 179-187.

Magidin, M. (2002) Genetic analysis of auxin homeostasis: Conjugate sensitivity and auxin supersensitivity, Ph. D., Rice University, Houston, Texas.

Mano, S., Nakamori, C., Nito, K., Kondo, M., and Nishimura, M. (2006). The *Arabidopsis pex12* and *pex13* mutants are defective in both PTS1- and PTS2-dependent protein transport to peroxisomes. Plant J *47*, 604-618.

Marzioch, M., Erdmann, R., Veenhuis, M., and Kunau, W. H. (1994). PAS7 encodes a novel yeast member of the WD-40 protein family essential for import of 3-oxoacyl-CoA thiolase, a PTS2-containing protein, into peroxisomes. EMBO J *13*, 4908-4918.

Matsumoto, N., Tamura, S., and Fujiki, Y. (2003). The pathogenic peroxin Pex26p recruits the Pex1p-Pex6p AAA ATPase complexes to peroxisomes. Nat Cell Biol *5*, 454-460.

Matsumura, T., Otera, H., and Fujiki, Y. (2000). Disruption of the interaction of the longer isoform of Pex5p, Pex5pL, with Pex7p abolishes peroxisome targeting signal type 2 protein import in mammals. Study with a novel *PEX5*-impaired Chinese hamster ovary cell mutant. J Biol Chem *275*, 21715-21721.

McNew, J. A., and Goodman, J. M. (1994). An oligomeric protein is imported into peroxisomes in vivo. J Cell Biol *127*, 1245-1257.

Michels, P., Moyersoen, J., Krazy, H., Galland, N., Herman, M., and Hannaert, V. (2005). Peroxisomes, glyoxysomes and glycosomes. Molecular Membrane Biology *22*, 133-145.

Motley, A. M., Hettema, E. H., Hogenhout, E. M., Brites, P., ten Asbroek, A. L. M. A., Wijburg, F. A., Baas, F., Heijmans, H. S., Tabak, H. F., Wanders, R. J. A., and Distel, B. (1997). Rhizomelic chondrodysplasia punctata is a peroxisomal protein targeting disease caused by a non-functional PTS2 receptor. Nat Genet *15*, 377-380.

Motley, A. M., Hettema, E. H., Ketting, R., Plasterk, R., and Tabak, H. F. (2000). *Caenorhabditis elegans* has a single pathway to target matrix proteins to peroxisomes. EMBO Rep *1*, 40-46.

Mullen, R. T. (2002). Targeting and import of matrix proteins into peroxisomes, In Plant peroxisomes: biochemistry, cell biology, and biotechnological applications, A. Baker, and I. A. Graham, eds. (The Netherlands: Kluwer), pp. 339-383.

Nair, D. M., Purdue, P. E., and Lazarow, P. B. (2004). Pex7p translocates in and out of peroxisomes in *Saccharomyces cerevisiae*. J Cell Biol *167*, 599-604.

Neer, E., Schmidt, C., Nambudripad, R., and Smith, T. (1994). The ancient regulatory-protein family of WD-repeat proteins. Nature *371*, 297-300.

Neuberger, G., Kunze, M., Eisenhaber, F., Berger, J., Hartig, A., and Brocard, C. (2004). Hidden localization motifs: naturally occurring peroxisomal targeting signals in non-peroxisomal proteins. Genome Biology *5*, R97.91-R97.10.

Niederhoff, K., Meindl-Beinker, N. M., Kerssen, D., Perband, U., Scha¨ fer, A., Schliebs, W., and Kunau, W.-H. (2005). Yeast Pex14p possesses two functionally distinct Pex5p and one Pex7p binding sites. J Biol Chem *280*, 35571-35578.

Nissen, S. J., and Sutter, E. G. (1990). Stability of IAA and IBA in nutrient medium to several tissue culture procedures. Hort Science *25*, 800-802.

Nito, K., Hayashi, M., and Nishimura, M. (2002). Direct interaction and determination of binding domains among peroxisomal import factors in *Arabidopsis thaliana*. Plant Cell Physiol *43*, 355-366.

Nito, K., Kamigaki, A., Kondo, M., Hayashi, M., and Nishimura, M. (2007). Functional Classification of *Arabidopsis* Peroxisome Biogenesis Factors Proposed from Analyses of Knockdown Mutants. Plant Cell Physiology *48*, 763-774.

Nordström, A.-C., Jacobs, F. A., and Eliasson, L. (1991). Effect of exogenous indole-3-acetic acid and indole-3-butyric acid on internal levels of the respective auxins and their conjugation with aspartic acid during adventitious root formation in pea cuttings. Plant Physiol *96*, 856-861.

Osumi, T., Tsukamoto, T., Hata, S., Yokota, S., Miura, S., Fujiki, Y., Hajikata, M., Miyazawa, S., and Hashimoto, T. (1991). Amino-terminal presequence of the precursor of peroxisomal 3-ketoacyl-CoA thiolase is a cleavable signal peptide for peroxisomal targeting. Biochem Biophys Res Commun *181*, 947-954.

Otera, H., Harano, T., Honsho, M., Ghaedi, K., Mukai, S., Tanaka, A., Kawai, A., Shimizu, N., and Fujiki, Y. (2000). The mammalian peroxin Pex5pL, the longer isoform of the mobile peroxisome targeting signal (PTS) Type 1 transporter, translocates the Pex7p-PTS2 protein complex into peroxisomes via its initial docking site, Pex14p. Journal of Biological Chemistry *275*, 21703-21714.

Otera, H., Okumoto, K., Tateishi, K., Ikoma, Y., Matsuda, E., Nishimura, M., Tsukamoto, T., Osumi, T., Ohashi, K., Higuchi, O., and Fujiki, Y. (1998). Peroxisome targeting signal type 1 (PTS1) receptor is involved in import of both PTS1 and PTS2: Studies with PEX5-defective CHO cell mutants. Mol Cell Biol *18*, 388-399.

Otera, H., Setoguchi, K., Hamasaki, M., Kumashiro, T., Shimizu, N., and Fujiki, Y. (2002). Peroxisomal targeting signal receptor Pex5p interacts with cargoes and import machinery components in a spatiotemporally differentiated manner: Conserved Pex5p WXXXF/Y motifs are critical for matrix protein import. Mol Cell Biol *22*, 1639-1655.

Otzen, M., Wang, D., Lunenborg, M. G. J., and van der Klei, I. J. (2005). *Hansenula polymorpha* Pex20p is an oligomer that binds the peroxisomal targeting signal 2 (PTS2). Journal of Cell Science *118*, 3409-3418.

Platta, H. W., Magraoui, F. E., Baumer, B. E., Schlee, D., Girzalsky, W., and Erdmann, R. (2009). Pex2 and Pex12 Function as Protein-Ubiquitin Ligases in Peroxisomal Protein Import. Mol Cell Biol.

Poupart, J., and Waddell, C. S. (2000). The *rib1* mutant is resistant to indole-3-butyric acid, an endogenous auxin in Arabidopsis. Plant Physiol *124*, 1739-1751.

Pracharoenwattana, I., Cornah, J. E., and Smith, S. M. (2005). *Arabidopsis* peroxisomal citrate synthase is required for fatty acid respiration and seed germination. Plant Cell *17*, 2037-2048.

Pracharoenwattana, I., Cornah, J. E., and Smith, S. M. (2007). *Arabidopsis* peroxisomal malate dehydrogenase functions in β-oxidation but not in the glyoxylate cycle. Plant J *50*, 381-390.

Preisig-Muller, R., and Kindl, H. (1993). Thiolase mRNA translated *in vitro* yields a peptide with a putative N-terminal presequence. Plant Mol Biol *22*, 59-66.

Purdue, P. E., Zhang, J. W., Skoneczny, M., and Lazarow, P. B. (1997). Rhizomelic chondrodysplasia punctata is caused by deficiency of human PEX7, a homologue of the yeast PTS2 receptor. Nat Genet *15*, 381-384.

Reddy, J. K., and Hashimoto, T. (2001). Peroxisomal β-oxidation and peroxisome proliferator-activated receptor α: an adaptive metabolic system. Annu Rev Nutr *21*, 193-230.

Rehling, P., Marzioch, M., Niesen, F., Wittke, E., Veenhuis, M., and Kunau, W. H. (1996). The import receptor for the peroxisomal targeting signal 2 (PTS2) in *Saccharomyces cerevisiae* is encoded by the *PAS7* gene. EMBO J *15*, 2901-2913.

Rehling, P., Skaletz-Rorowski, A., Girzalsky, W., Voorn-Brouwer, T., Franse, M. M., Distel, B., Veenhuis, M., Kunau, W. H., and Erdmann, R. (2000). Pex8p, an intraperoxisomal peroxin of Saccharomyces cerevisiae required for protein transport into peroxisomes binds the PTS1 receptor pex5p. J Biol Chem *275*, 3593-3602.

Reumann, S. (2004). Specification of the peroxisome targeting signals type 1 and type 2 of plant peroxisomes by bioinformatics analyses. Plant Physiol *135*, 783-800.

Reumann, S., Ma, C., Lemke, S., and Babujee, L. (2004). AraPerox. A database of putative Arabidopsis proteins from plant peroxisomes. Plant Physiol *136*, 2587-2608.

Richmond, T. A., and Bleecker, A. B. (1999). A defect in β-oxidation causes abnormal inflorescence development in Arabidopsis. Plant Cell *11*, 1911-1923.

Robbins, J. A., Campidonica, M. J., and Burger, D. W. (1988). Chemical and biological stability of indole-3-butryic acid (IBA) after long-term storage at selected temperatures and light regimes. J Environ Hort *6*, 33-38.

Rylott, E. L., Eastmond, P. J., Gilday, A. D., Slocombe, S. P., Larson, T. R., Baker, A., and Graham, I. A. (2006). The Arabidopsis thaliana multifunctional protein gene (MFP2) of peroxisomal beta-oxidation is essential for seedling establishment. Plant J *45*, 930-941.

Sampathkumar, P., Roach, C., Michels, P., and Hol, W. (2008). Structural Insights into the recognition of peroxisomal targeting signal 1 by *Trypanosoma brucei* peroxin 5. J Mol Biol *381*, 867-880.

Schliebs, W., Saidowsky, J., Agianian, B., Dodt, G., Herberg, F. W., and Kunau, W.-H. (1999). Recombinant human peroxisomal targeting signal receptor PEX5.

Structural basis for interaction of PEX5 with PEX14. J Biol Chem *274*, 5666-5673.

Schuhmann, H., Huesgen, P. F., Gietl, C., and Adamska, I. (2008). The DEG15 serine protease cleaves peroxisomal targeting signal 2-containing proteins in *Arabidopsis*. Plant J *148*, 1847-1856.

Schumann, U., Wanner, G., Veenhuis, M., Schmid, M., and Gietl, C. (2003). AthPEX10, a nuclear gene essential for peroxisome and storage organelle formation during *Arabidopsis* embryogenesis. Proc Natl Acad Sci USA *100*, 9626-9631.

Shockey, J. M., Fulda, M. S., and Browse, J. A. (2002). Arabidopsis contains nine long-chain acyl-coenzyme A synthetase genes that participate in fatty acid and glycerolipid metabolism. Plant Physiol *129*, 1710-1722.

Shockey, J. M., Fulda, M. S., and Browse, J. A. (2003). *Arabidopsis* contains a large superfamily of acyl-activating enzymes. Phylogenetic and biochemical analysis reveals a new class of acyl-Coenzyme A synthetases. Plant Physiol *132*, 1065-1076.

Sichting, M., Schell-Steven, A., Prokisch, H., Erdmann, R., and Rottensteiner, H. (2003). Pex7p and Pex20p of *Neurospora crassa* function together in PTS2-dependent protein import into peroxisomes. Mol Biol Cell *14*, 810-821.

Singh, T., Hayashi, M., Mano, S., Arai, Y., Goto, S., and Nishimura, M. (2009). Molecular Components Required for the Targeting of PEX7 to Peroxisomes in *Arabidopsis thaliana*. The Plant Journal *60*, 488-498.

Smith, J. J., and Rachubinski, R. A. (2001). A Role for the Peroxin Pex8p in Pex20p-dependent Thiolase Import into Peroxisomes of the Yeast *Yarrowia lipolytica*. J Biol Chem *276*, 1618-1625.

Smith, T. F., Gaitatzes, C., Saxena, K., and Neer, E. J. (1999). The WD repeat: a common architecture for diverse functions. Trends Biochem Sci *24*, 181-185.

Somerville, C. R., and Ogren, W. L. (1980). Photorespiration mutants of *Arabidopsis thaliana* deficient in serine-glyoxylate aminotransferase activity. Proc Natl Acad Sci U S A *77*, 2684-2687.

Somerville, C. R., and Ogren, W. L. (1981). Photorespiration-deficient Mutants of *Arabidopsis thaliana* Lacking Mitochondrial Serine Transhyroxymethylase Activity. Plant Physiol *67*, 666-671.

Sparkes, I. A., and Baker, A. (2002). Peroxisome biogenesis and protein import in plants, animals and yeasts: Enigma and variations? Mol Membr Biol *19*, 171-185.

Sparkes, I. A., Brandizzi, F., Slocombe, S. P., El-Shami, M., Hawes, C., and Baker, A. (2003). An Arabidopsis *pex10* null mutant is embryo lethal, implicating peroxisomes in an essential role during plant embryogenesis. Plant Physiol *133*, 1809-1819.

Stasinopoulos, T. C., and Hangarter, R. P. (1990). Preventing photochemistry in culture media by long-pass light filters alters growth of cultured tissues. Plant Physiol *93*, 1365-1369.

Stein, K., Schell-Steven, A., Erdmann, R., and Rottensteiner, H. (2002). Interactions of Pex7p and Pex18p/Pex21p with the peroxisomal docking machinery: Implications for the first steps in PTS2 protein import. Mol Cell Biol *22*, 6056-6069.

Su, J.-R., Takeda, K., Tamura, S., Fujiki, Y., and Miki, K. (2009). Crystal structure of the conserved N-terminal domain of the peroxisomal matrix protein import receptor, Pex14p. Proc Natl Acad Sci U S A *106*, 417-421.

Terlecky, S. R., Nuttley, W. M., McCollum, D., Sock, E., and Subramani, S. (1995). The Pichia pastoris peroxisomal protein PAS8p is the receptor for the C-terminal tripeptide peroxisomal targeting signal. Embo J *14*, 3627-3634.

Titorenko, V. I., and Rachubinski, R. A. (2001). The life cycle of the peroxisome. Nature Reviews *2*, 357-368.

Turner, J. E., Greville, K., Murphy, E. C., and Hooks, M. A. (2005). Characterization of *Arabidopsis* Fluoroacetate-resistant Mutants Reveals the Principal Mechanism of Acetate Activation for Entry into the Glyoxylate Cycle. J Biol Chem *280*, 2780-2787.

Urquhart, A. J., Kennedy, D., Gould, S. J., and Crane, D. I. (2000). Interaction of Pex5p, the Type 1 Peroxisome Targeting Signal Receptor, with the Peroxisomal Membrane Proteins Pex14p and Pex13p. Journal of Biological Chemistry *275*, 4127-4136.

van den Brink, D. M., Brites, P., Haasjes, J., Wierzbicki, A. S., Mitchell, J., Lambert-Hamill, M., de Belleroche, J., Jansen, G. A., Waterham, H. R., and Wanders, R. J. A. (2003). Identification of *PEX7* as the second gene involved in Refsum disease. Am J Hum Genet *72*, 471-477.

van der Krieken, W. M., Breteler, H., and Visser, M. H. M. (1992). The effect of the conversion of indolebutyric acid into indoleacetic acid on root formation on microcuttings of *Malus*. Plant Cell Physiol *33*, 709-713.

Wain, R. L., and Wightman, F. (1954). The growth-regulating activity of certain ω-substituted alkyl carboxylic acids in relation to their β-oxidation within the plant. Proc Royal Soc London, Series B *142*, 525-536.

Wanders, R. J. A., and Waterham, H. R. (2004). Peroxisomal disorders I: Biochemistry and genetics of peroxisome biogenesis disorders. Clin Genet *67*, 107-133.

Wang, D., Visser, N. V., Veenhuis, M., and van der Klei, I. (2003). Physical Interactions of the Peroxisomal Targeting Signal 1 Receptor Pex5p, Studied by Fluorescence Correlation Spectroscopy. J Biol Chem *278*, 43340-43345.

Wang, X., McMahon, M. A., Shelton, S. N., Nampaisansuk, M., Ballard, J. L., and Goodman, J. M. (2004). Multiple Targeting Modules on Peroxisomal Proteins Are Not Redundant: Discrete Functions of Targeting Signals within Pmp47 and Pex8p. Molecular Biology of the Cell *15*, 1702-1710.

Waterham, H. R., Titorenko, V. I., Haima, P., Cregg, J. M., Harder, W., and Veenhuis, M. (1994). The *Hansenula polymorpha PER1* gene is essential for peroxisome biogenesis and encodes a peroxisomal matrix protein with both carboxy- and amino-terminal targeting signals. J Cell Biol *127*, 737-749.

Wiszniewski, A. A. G., Zhou, W., Smith, S. M., and Bussell, J. D. (2008). Identification of two *Arabidopsis* genes encoding a peroxisomal oxidoreductase-like protein and an acyl-CoA synthetase-like protein that are required for responses to pro-auxins. Plant Molecular Biology *69*, 503-515.

Woodward, A. W. (2005) Genes, organelles, and molecules that influence plant development through auxin regulation, Ph.D., Rice University, Houston, TX.

Woodward, A. W., and Bartel, B. (2005). The *Arabidopsis* peroxisomal targeting signal type 2 receptor PEX7 is necessary for peroxisome function and dependent on PEX5. Mol Biol Cell *16*, 573-583.

Yamada, K., Lim, J., Dale, J. M., Chen, H., Shinn, P., Palm, C. J., Southwick, A. M., Wu, H. C., Kim, C., Nguyen, M. *et al.* (2003). Empirical analysis of transcriptional activity in the *Arabidopsis* genome. Science *302*, 842-846.

Zolman, B. K. (2002) Genetic analysis of indole-3-butyric acid response mutants in *Arabidopsis thaliana*, PhD, Rice University, Houston.

Zolman, B. K., and Bartel, B. (2004). An *Arabidopsis* indole-3-butyric acid-response mutant defective in PEROXIN6, an apparent ATPase implicated in peroxisomal function. Proc Natl Acad Sci USA *101*, 1786-1791.

Zolman, B. K., Martinez, N., Millius, A., Adham, A. R., and Bartel, B. (2008). Identification and characterization of *Arabidopsis* indole-3-Butyric Acid response mutants defective in novel peroxisomal enzymes Genetics *180*, 237-251.

Zolman, B. K., Monroe-Augustus, M., Silva, I. D., and Bartel, B. (2005). Identification and functional characterization of *Arabidopsis* PEROXIN4 and the interacting protein PEROXIN22. Plant Cell *17*, 3422-3435.

Zolman, B. K., Monroe-Augustus, M., Thompson, B., Hawes, J. W., Krukenberg, K. A., Matsuda, S. P. T., and Bartel, B. (2001a). *chy1*, an *Arabidopsis* mutant with impaired β-oxidation, is defective in a peroxisomal β-hydroxyisobutyryl-CoA hydrolase. J Biol Chem *276*, 31037-31046.

Zolman, B. K., Nyberg, M., and Bartel, B. (2007). IBR3, a novel peroxisomal acyl-CoA dehydrogenase-like protein required for indole-3-butyric acid response. Plant Mol Biol *in press*.

Zolman, B. K., Silva, I. D., and Bartel, B. (2001b). The Arabidopsis *pxa1* mutant is defective in an ATP-binding cassette transporter-like protein required for peroxisomal fatty acid β-oxidation. Plant Physiol *127*, 1266-1278.

Zolman, B. K., Yoder, A., and Bartel, B. (2000). Genetic analysis of indole-3-butyric acid responses in *Arabidopsis thaliana* reveals four mutant classes. Genetics *156*, 1323-1337.

Appendix

A. A screen for IBA resistant root elongation in a Landsberg background

In a forward genetics approach to identify mutant plants resistant to IBA, I screened the progeny of ethyl methane sulfonate (EMS) mutagenized Landsberg *erecta* (L*er*) seeds on inhibitory concentrations of IBA for enhanced root length.

Although a variety of peroxisomal mutants have been isolated over the years through forward and reverse genetics approaches (Zolman et al., 2001a; Zolman et al., 2001b; Zolman and Bartel, 2004; Adham et al., 2005; Woodward and Bartel, 2005; Zolman et al., 2005; Zolman et al., 2007; Zolman et al., 2008) there are many genes expected to contribute to peroxisome functioning in *Arabidopsis* for which mutants have yet to be identified (Figure A.1), suggesting that the screen for mutants defective in peroxisomal processes is far from saturated. Most of the mutations isolated to date have been in the Columbia accession. Different *Arabidopsis* accessions display distinct responses to stimuli such as IBA and other hormone treatments (reviewed in Koornneef et al., 2004). Isolating mutations in multiple accessions can help us further dissect peroxisome function. In this project, I attempted to isolate mutants defective in IBA response in a L*er* background. We decided to conduct the screen in a L*er* background because it is largely sequenced (http://www.tigr.org/tdb/e2k1/ath1/atgenome/Ler.shtml), and previous researchers were successful in isolating peroxisome-defective mutants in this accession (Hayashi et al., 1998).

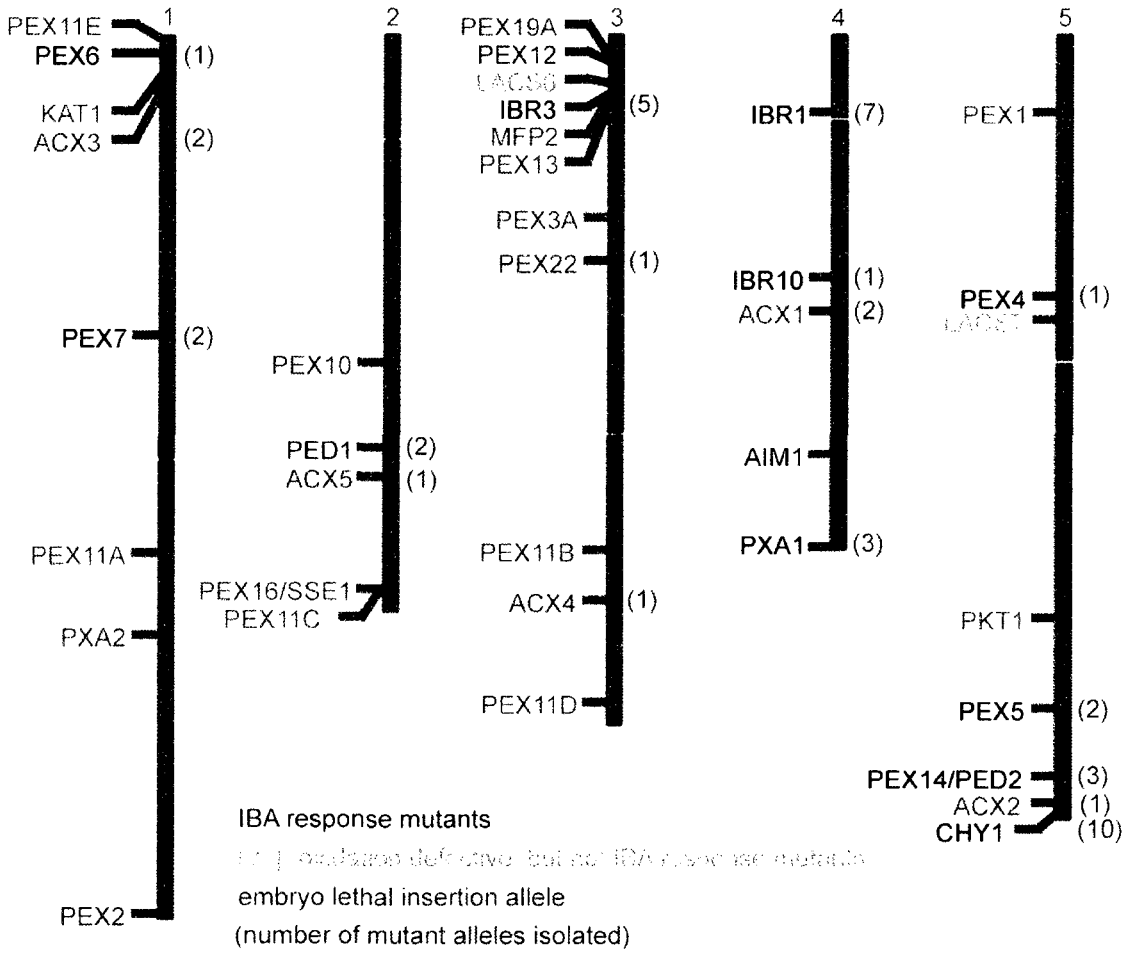

Figure A.1. Candidate genes and peroxisomal mutants identified in Arabidopsis through forward and reverse genetics.

Bars depict the five Arabidopsis chromosomes; numbers in parentheses denote number of alleles isolated in *ibr* screens in the Bartel lab.

A.1. Materials and methods

A.1.A. Phenotypic analysis

Root elongation on IBA. Surface-sterilized seeds were plated on medium supplemented with 0.5% sucrose with or without 10 μM IBA. Seedlings were grown for 8 days under yellow-filtered light at 22°C before removing seedlings for root measurements.

Sucrose dependence assays. Surface-sterilized seeds were plated on medium with or without 0.5% sucrose. Seedlings were grown 1 day under white light at 22°C then transferred to the dark and grown for an additional 5 days at 22°C before removing seedlings for hypocotyl measurements.

Lateral root assays. Surface-sterilized seeds were plated on medium supplemented with 0.5% sucrose and grown for 4 days under yellow-filtered light at 22°C. Four-day-old seedlings were transferred to medium supplemented with 0.5% sucrose with or without 10 μM IBA and grown for an additional 4 days under yellow-filtered light at 22°C.

A.1.B. PCR-based accession identification

SSLP markers and primers used to verify accession are summarized in Table A-1.

A.2. Phenotypic characterization of putative mutants from the L*er* screen

A.2.A. Mutant isolation

EMS mutagenized L*er* M2 seed pools were purchased from Lehle Seeds (Round Rock, TX). I screened 104,000 L*er* accession M2 seeds from fourteen different pools on either 20 or 25 μM IBA for IBA resistant root elongation. I isolated 50 putative mutants with a long root on IBA. Putative mutants were transferred from IBA to soil and M3 seed was harvested from the 34 surviving mutants.

Table A-1. PCR-based markers used for genotyping accessions.

Chr	Marker	Primer pairs	Enzyme	Expected Product sizes Col	Ler	Ws	Cvi
1	NAX101*	NAX101-1, TGGCGGTGTAACAAACTCATCTTC NAX101-2, AGCGGAAGCAGCAAACGAAAAG	PvuII	383	383	383	255 128
1	F6N18	F6N18-2, ATTGATTTCTAACTCCAACTCTACATAGC F6N18-4, GTTTGTGTTCTTTGTTGTTTTCTTTTAG		202	181	202	
1	T12C22	T12C22-1, ACTAGAAATTACCAGTAAGATTGTTGGCA T12C22-2, TAACTATTAGCTATGTGTCTTACAGTTCC		164	147	147	
1	LCS104	LCS104-1, CCAAGTAGGCCACCATCTCCTCTTG LCS104-2, AGGCTCACACTCAATCTGCAAACCAAAATA	EcoNI	185	165	165	165
2	NGA168	NGA168-1, GGCCTTTGGTGGCATGATATTCATCC NGA168-2, GCCTCGAATGATGAAGCATGTGC		161	145	145	
3	NAX302*	NAX302-1, AAAAGTTTGATTCCACGAGATGATGTTC NAX302-2, TTCTGGACTCTTGGTTATAAATGGAC		362 32	240 122 32		240 122 32
3	NGA172	NGA172-1, TACATCCGAATGCCATTGTTCCTATCATTG NGA172-2, AGCACATCAAGCTGCTTCCTTATAGCGTCC		170	150	150	
3	NAX301*	NAX301-1, AATTGCACCTCCACTAGCTTCATCATCTTC NAX301-2, TCTGCTGCACCTTTTAATACCTTCACAATCC	TspRI	264 93	264 93	264 93	175 93 89
4	NAX401*	NAX401-1, GACCCAACATTTCCTCTCAACCAAC NAX401-2, CTTCGTAGTGATCTTCCCGTCTCCGTCCTTG	ApoI	159 99 87	159 99 87	159 99 87	258 87
4	T18A10	T18A10-1, ATTTACTCATAAGAGGAGGAATCTGATACG T18A10-2, GACGTTAAAAACTTAAAATGTGTGGTCAGG		175	195	185	
4	F8L21	F8L21-3, AGTTTCAGAGTCATTCCAAGTGTTTATGAC F8L21-4, AGATGTTTGCCACAATATCGAAATTAATAC		285	270	255	
5	NAX501*	NAX501-1, GGTTTATGTTATTGGCCCGCTTTGTTC NAX501-2, ATCACAGCCCCACTCGTTATCCCTTC	AccI	321 63	321 63	321 63	384
5	NGA249	NGA249-F, TTACCGTCAATTTCATCGCCG NGA249-R, TGGATCCCTAACTGTAAAATCCC		125	115	115	
5	NGA129	NGA129-F, TCAGGAGGAACTAAAGTGAGGG NGA129-R, CACACTGAAGATGGTCTTGAGG		177	179	165	
5	NAX502*	NAX502-1, TGATACAGGGGACGAGTTAGTGGAAGAGC NAX501-2, AGGAGGCAATGCACCGTAAATAACACAAC	PmeI	208	165 43	165 43	208

* Newly developed markers for this study

A.2.B. Determining the background accession

While waiting for the M2 plants to produce seed, I realized that some of the plants I was working with were not phenotypically similar to Landsberg *erecta* (L*er*) plants. Although we had purchased L*er* M2 seed pools, the aerial phenotype suggested either that the seed pools were contaminated with Landsberg *ER* or that the seed pools were contaminated by a different accession. To determine which possibility had occurred, I proceeded to verify the accession of some of the mutants by genotyping at various polymorphic regions. The results are summarized in Table A-2.

By combining the data I obtained from PCR analysis with the adult phenotype of each putative mutant, I concluded that only B1132, B1137, B1143, B1153, B1169, and B1170 were in the L*er* background. B1162, B1163, and B1164 appear to be in a Col background. B1150, B1151, B1154, B1156, and B1158 were neither Col, L*er*, or Ws and will need further analysis to determine the background.

A.2.C. Responses to auxin

M3 lines were retested for IBA resistance then divided into different classes as outlined in Figure A.2 (Zolman et al., 2000).

A.2.C.1. Root elongation. I rescreened 33 of the 34 putative mutants for IBA resistant root elongation and found that 12 displayed wild type responses to IBA and 21 remained IBA resistant to root elongation inhibition (Figure A.3). Two of the mutants, B1169 and B1170, appeared to be completely resistant to the inhibitory effect of IBA at the concentration tested.

I attempted to screen putative mutant lines for IAA resistant root elongation but the IAA stock that I was working with was not efficiently inhibiting Col or L*er*. I set aside only those mutants that retained 100% or greater root length on IAA as general auxin response mutants (data not shown). 9 mutants were classified as general auxin response mutants and were not further characterized.

Table A-2. Genotyping using SSLP markers.

marker	B1132	B1137	B1139	B1143	B1150	B1151	B1153	B1154	B1156	B1158	B1162	B1163	B1164	B1169	B1170
NAX101					C/L/W	C/L/W		C/L/W	C/L/W	C/L/W					
F6N18	L	L	C/W	L	L	L	L	L	L		C/W	C/W	C/W		
T12C22		H	C	L/W				L/W							
LCS104					Cvi/W	Cvi/W		Cvi/W	Cvi/W	Cvi/W					
NGA168	L/W	L/W	C	L/W	L/W	L/W	L/W	L/W	L/W						
NAX302	L/W		C	L/W	C	C	L/W	C	C	C	C	C	C		
NGA172	L/W	L/W	C	L/W	C	C	L/W	C	C	C	C	C	C		
NAX301					C/L/W	C/L/W		C/L/W	C/L/W	C/L/W					
NAX401					C/L/W	C/L/W		C/L/W	C/L/W	C/L/W					
T18A10			C												
F8L21				L											
NAX501					Cvi/C	Cvi/C		Cvi/C	Cvi/C	Cvi/C					
NGA249	L/W	L/W	C	L/W											
NGA129	C/L		C/L		W	W	C/L		W	W	C/L	C/L	C/L		
NAX502	L/W	L/W		L/W											
Phenotype	*er-*	*er-*	*Er+*	*er-*	*Er+*	*Er+*	*er-*	*Er+*	*Er+*	*Er+*	*Er+*	*Er+*	*Er+*	*er-*	*er-*
Likely Accession	L	L	C	L	?	?	L	?	?	?	C	C	C	L	L

Each marker distinguishes between various accessions as summarized in Table A-1.
C represents Columbia accession
L represents Landsberg *erecta* accession
W represents Wassileskija accession
Cvi represents Cape Verde Islands accession
Er+ does not display the *erecta* mutation phenotype
er- displays *erecta* mutation phenotype

A.2.C.2. Lateral root initiation. I tested B1153, B1154, and B1156 for lateral root initiation by IBA (Figure A.5). I observed that all three mutants initiate lateral roots less efficiently than wild type, an observation that reinforces a deficiency in IBA responses.

A.2.D. Sucrose dependence in the dark

I tested 18 putative mutants for defects in fatty acid metabolism by growing seedlings in the dark with and without an exogenous carbon source. I found that B1169 and B1170 had reduced hypocotyl elongation when grown in the absence of sucrose (Figure A.4), suggesting that these mutants have defects in fatty acid β-oxidation.

A.3. Conclusions and future work

Twelve new *ibr* mutants have been isolated; these are summarized in Table A-3. The commercial M2 seed pools from Lehle seeds were badly contaminated with multiple accessions of Arabidopsis, as I found mutants not only in the expected L*er* accession, but also what appears to be Col-0 and a third, unidentified accession. Future work with these mutants could include additional biochemical and cell biological characterization and map-based identification of the defective genes. In preparation for mapping, 11 of the mutants in the L*er* accession have been outcrossed to Col-0.

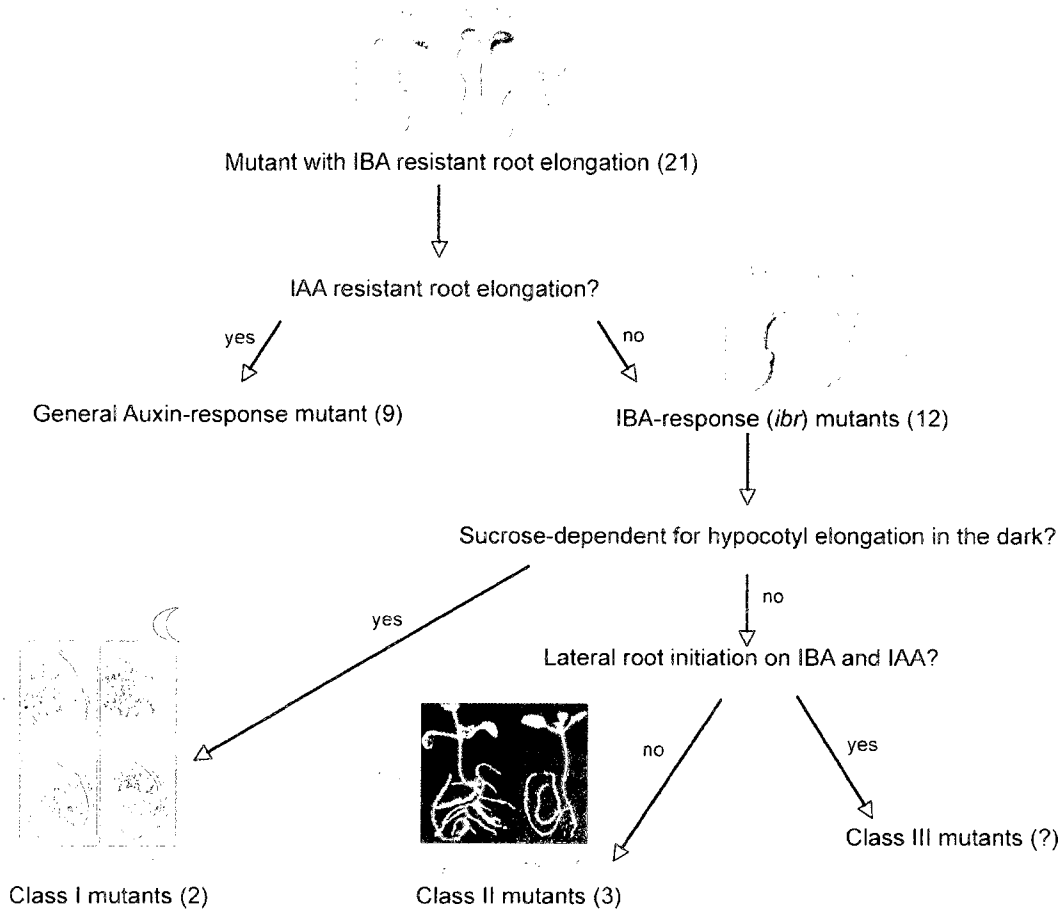

Figure A.2. Mutant classification scheme.

Second generation EMS-mutagenized seedlings were selected for IBA resistant root elongation. Progeny of the putative mutants were retested for resistance to IBA and for resistance to IAA. IAA resistant mutants were categorized as general auxin-response mutants, whereas IAA sensitive mutants were further tested for sucrose dependence in the dark. Some of the seed lines that were sucrose independent were tested for lateral root initiation on IBA and IAA. The number of mutants found in each category is indicated in parentheses.

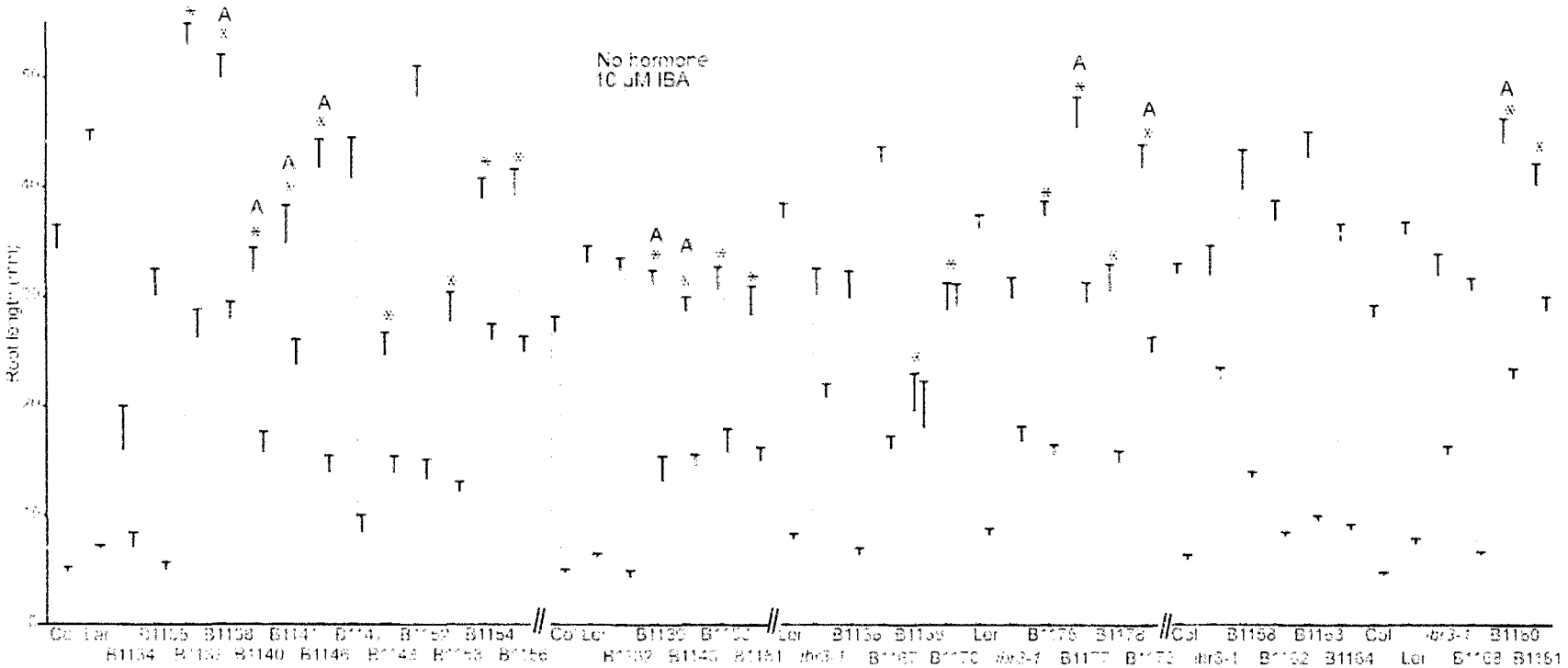

Figure A.3. Retesting mutants for resistance to IBA.

Surface-sterilized seeds were plated on medium supplemented with 0.5% sucrose with or without 10 µM IBA. Seedlings were grown for 8 days under yellow-filtered light at 22°C before removing seedlings from the agar for root measurements. Mutants classified as IBA resistant are indicated by an asterisk. Mutants classified as IAA resistant (data not shown) are indicated by an A. Breaks in the x-axis separate lines measured in separate experiments, and *ibr3-1* is an IBA-resistant control (Zolman et al., 2007). Dotted lines are for comparison to L*er* root length in each experiment. Bars show mean + SE ($n \geq 3$).

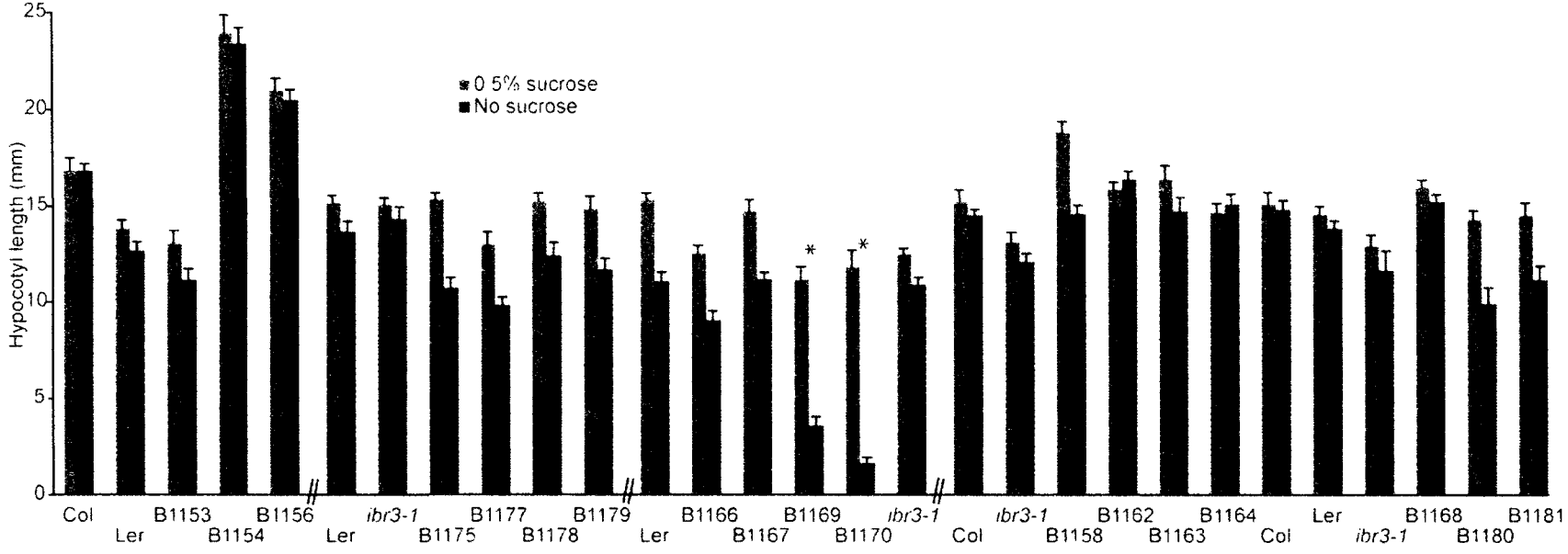

Figure A.4. Retesting mutants for sucrose dependence.

Surface-sterilized seeds were plated on medium with or without 0.5% sucrose. Seedlings were grown 1 day under whit light at 22°C then transferred to the dark for an additional 5 days. Seedlings were removed from the agar for hypocotyl measurements. Mutants classified as sucrose dependent are indicated by an asterisk. Breaks in the y-axis separate lines measured in separate experiments, and *ibr3-1* is sucrose independent control (Zolman et al., 2007). Bars show mean + SE ($n \geq 4$).

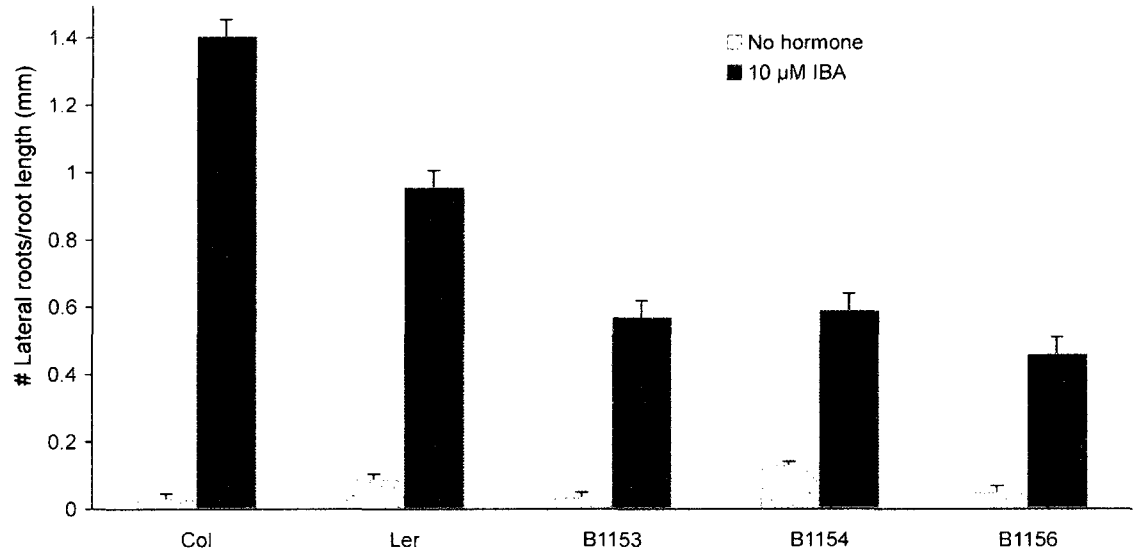

Figure A.5. B1153, B1154, and B1156 have reduced lateral root responses to IBA.

Surface-sterilized seeds were plated on medium supplemented with 0.5% sucrose and grown for 4 days under yellow-filter light at 22°C. 4-day-old seedlings were then transferred to medium supplemented with 0.5% sucrose with or without 10 µM IBA and grown for an additional 4 days. Seedlings were removed from the agar for root measurements and lateral root tallies. Bars show mean + SE ($n \geq 10$).

Table A-3. *ibr* mutant classifications (as defined in Figure A.2)

Class	Pool	Seedling phenotype	Adult phenotype	M3 genotype
Class 1				
B1169	EMS46	IBA^R, Suc^D	er-	
B1170	EMS47	IBA^R, Suc^D	er-	
Class 2				
B1153	EMS44	IBA^R, Few lats	er-	L*er*
B1154	EMS44	IBA^R, Few lats	Er+	not Ws/L*er*/Col
B1156	EMS44	IBA^R, Few lats	Er+	not Ws/L*er*/Col
Class 2 or 3				
B1137	EMS42	IBA^R	er-	
B1148	EMS43	IBA^R	er-	
B1150	EMS44	IBA^R	Er+	not Ws/L*er*/Col
B1151	EMS44	IBA^R	Er+	not Ws/L*er*/Col
B1175	EMS47	IBA^R	er-	
B1181	EMS48	IBA^R	er-	

B. Reverse genetic experiments to identify IBA-activating enzymes

The active form of auxin, IAA, can be formed from auxin precursors with longer even-numbered chain lengths, such as IBA, with a 4-carbon side chain, and indole-3-caproic acid (ICapA), with a 6-carbon side chain (Fawcett et al., 1960). Genetic analyses have provided extensive evidence that IBA to IAA conversion occurs through the action of enzymes similar to those acting in fatty acid β-oxidation (Zolman et al., 2000; Zolman et al., 2007; Zolman et al., 2008). The IBR proteins have arisen as likely candidates to carry out intermediate steps in IBA β-oxidation (Chapter 6). However, we have yet to identify a candidate likely to carry out the activation step of IBA β-oxidation (Chapter 7 Figure 7.1).

The first step of peroxisomal β-oxidation involves the activation of a precursor through the addition of a CoA group. *Arabidopsis* encodes 44 apparent acyl-activating enzymes (Shockey et al., 2003); 18 of these enzymes have an apparent peroxisome targeting signal (PTS) (Reumann, 2004). The 44 apparent acyl-CoA activating enzymes (AAE) fall into six phylogenic clades (Shockey et al., 2003), and four of these clades include proteins predicted to be peroxisomal (Reumann, 2004).

In clade I, two of 11 long chain acyl-CoA synthetases, LACS6 and LACS7 are peroxisomal enzymes that activate fatty acids (Fulda et al., 2002; Shockey et al., 2003). *lacs6* and *lacs7* do not exhibit fatty acid metabolism defects as single mutants but when combined, the double mutant is sucrose dependent (Fulda et al., 2002; Shockey et al., 2003). However, the *lacs6 lacs7* double mutant responds normally to IBA and 2,4-DB (Fulda et al., 2002; Shockey et al., 2002; Shockey et al., 2003), indicating that LACS6 and LACS7 are unlikely to act on auxin precursors.

Two of the three AAE enzymes in clade II are peroxisomal, AAE17 and AAE18 (Shockey et al., 2003; Reumann, 2004). AAE18 has been implicated in the activation of the synthetic auxin 2,4-dichlorophenoxybutyric acid (2,4-DB); *aae18* and *aae17 aae18*

mutants are 2,4-DB resistant but respond normally to IBA (Wiszniewski et al., 2008), suggesting that AAE18 and its closest homolog AAE17 do not act on IBA.

All eight of the 4-coumarate:CoA-ligase-like (4-CL-like) of clade V are predicted to be peroxisomal. OPCL1 is in clade V and has been implicated in jasmonic acid (JA) activation (Koo et al., 2006; Kienow et al., 2008). Finally, six of the 14 AAE enzymes in clade VI are predicted to be peroxisomal. This clade includes ACN1/AAE7, a peroxisomal acetyl-CoA synthetase (Turner et al., 2005). CoA ligases for naturally occurring auxin precursors, such as IBA and possibly ICapA, have not been uncovered using either forward or reverse genetic approaches.

Because several of the eight 4-CL-like proteins proteins of clade V have been implicated in activation of JA precursors (Kienow et al. 2008), and all of these enzymes are predicted to be peroxisomal (Koo et al., 2006), these enzymes are candidates for IBA-activating enzymes. However, some β-oxidation enzymes, such as LACS6 and LACS7, have redundant functions and will not easily be identified through forward genetics screens. In this project, I used reverse genetic analysis to study the role of the 4-CL-like proteins in IBA and ICapA metabolism, and uncovered two enzymes, OPCL1 and At4g05160, that may redundantly act in IBA activation.

B.1. Materials and methods

B.1.A Plant materials

Homozygous seed stocks for the 4CL-like T-DNA insertion mutants (Table B-1) are in the Columbia (Col-0) accession and were obtained from John Browse. A double

Table B-1. *Arabidopsis* genes encoding peroxisomal 4-CL-like enzymes

Protein	Locus	T-DNA Line	Genotyping primers
4CL-like protein-10	At1g20480	Unknown Salk line	Homozygous
4CL-like protein	At1g20490	No mutant	
4CL-like protein-6	At1g20500	SAIL_26_H04	Homozygous
4CL-like protein-9	At1g20510	SALK_140659	OPCL1-1 + OPCL1-2
(OPCL1)		(*opcl1-1*)	OPCL1-1 + LB1-Salk
4CL-like protein-12	At4g05160	SALK_050214	C6L9-1 + C6L9-2
			C6L9-1 + LB1-Salk
4CL-like protein	At4g19010	No mutant	
4CL-like protein-8	At5g38120	Unknown Riken	Homozygous
		line	
4CL-like protein-11	At5g63380	SALK_003233	Homozygous

mutant homozygous for *opcl1-1* and *at1g20510-1* was isolated from progeny of a cross by PCR using a T-DNA insertion primer paired with an endogenous gene primer and looking for the presence of an insertion product. The absence of the endogenous gene product using two endogenous gene primers flanking the insertion site confirmed the gene was no longer intact. For the endogenous gene PCR, I used OPCL1-1 (GATACGGCGACTTTGCTTTACTCTTCAG) paired with OPCL1-2 (GGTACCGTATCTCCGACTTTCCTCAACAG) with the *opcl1-1* DNA template and C6L9-1 (TTCTATGTTTGCTCGTAATGTGTAAGGTTTC) paired with C6L9-2 (TGATTGGCAAGTGAGAAGAAGAAGGAG) with the *at1g20510-1* DNA template. To detect the T-DNA inserts I used LB1-Salk (CAAACCAGCGTGGACCGCTTGCTGCAACTC) paired with OPCL1-1 and LB1-Salk with C6L9-1.

B.1.B. Phenotypic analysis

For phenotypic assays, seeds were surface-sterilized and plated on plant nutrient media (PN) (Haughn and Somerville, 1986) supplemented with sucrose and ICapA, IBA, or IAA as indicated. IBA was from Sigma, and ICapA was a gift of Jerry Cohen (University of Minnesota). Hormone stocks were dissolved in ethanol, and the volume of added ethanol was normalized for hormone-supplemented medium and unsupplemented controls. Seedlings were grown at 22°C under continuous yellow-filtered light (Stasinopoulos and Hangarter, 1990).

B.2. Results

B.2.A. A 4CL-like double mutant has defects in IBA response

To determine if the 4CL-like enzymes are important in IBA response as possible IBA activators, I grew the 4CL-like single mutants on IBA and IAA. I found that none of the single mutants displayed robust IBA resistant root elongation (Figure B.1), suggesting that either none of the CL-like genes are important to IBA response, or that they may

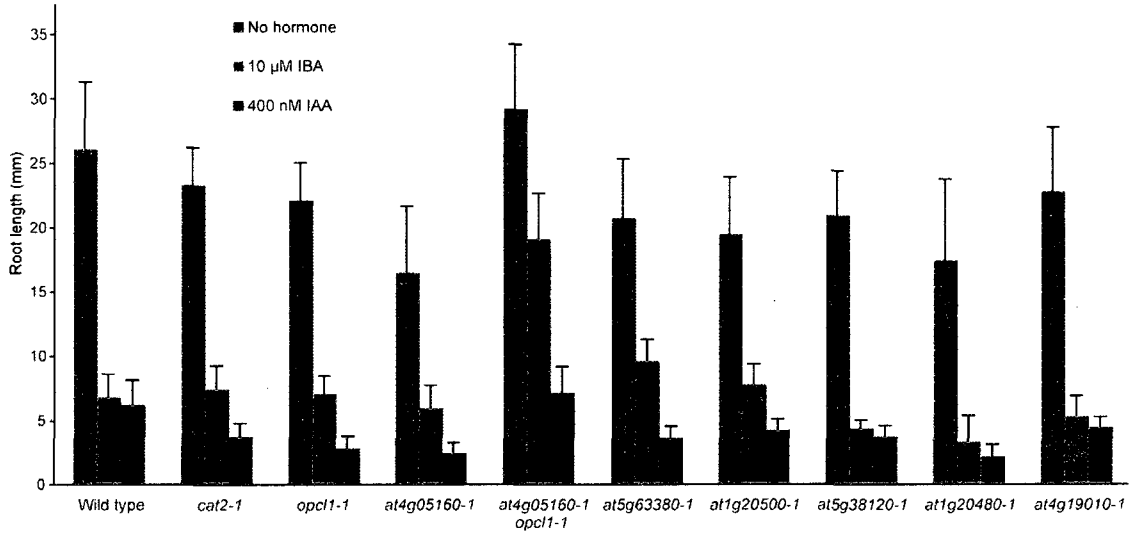

Figure B.1. A higher order CL-like mutant is resistant to IBA.

Surface-sterilized seeds were plated on medium supplemented with 0.5% sucrose containing no hormone, 400 nM IAA, or 10 µM IBA. Seedlings were grown for 8 days under yellow-filtered light before measuring. Bars show mean + SE ($n \geq 9$).

have redundant functions and impairing one gene is not enough to disrupt IBA metabolism. However, two of the single mutants (*opcl1-1* and *at4g05160-1*) showed slight IBA resistance in dose response curves (Data not shown). I therefore crossed these two mutants and isolated the double mutant.

When I assayed the *at4g05160 opcl1-1* double mutant on IBA and IAA, I found that the double mutant had a defect in root elongation inhibition by IBA and not IAA (Figure B.1), suggesting that these genes are important for IBA response.

B.2.B. Mutations in 4-CL-like genes have no effect on response to ICapA

To determine if the 4-CL-like genes have a role in the metabolism of the IAA precursor ICapA, I grew the 4-CL-like mutants on ICapA. I found that all the tested mutants responded similarly to wild type when grown in the presence of ICapA (Figure B.2) suggesting that either the 4CL-like genes are not necessary for response to ICapA or they are redundant.

B.3. Conclusions and future work

Many IBA, JA, and fatty acid β-oxidation enzymes have overlapping roles or functions (Zolman et al., 2001a; Adham et al., 2005; Kienow et al., 2008). Because 4CL-like single mutants were not IBA resistant but the 4CL-like double mutant was IBA resistant, several 4CL-like proteins may act redundantly in IBA activation.

Recently, the in vitro activities of all eight 4-CL-like enzymes were compared on various cinnamic acids, fatty acids, hormones, and hormone precursors (Kienow et al., 2008). Although At4g05160 showed highest activity with fatty acids, and OPCL1 showed highest activity with fatty acids and jasmonate precursors, these two enzymes both displayed weak activity with IBA as well (Kienow et al., 2008). It will be interesting to learn whether higher order mutants in the 4CL-like family will display a more complete block in IBA responsiveness. Regardless of the outcome of such

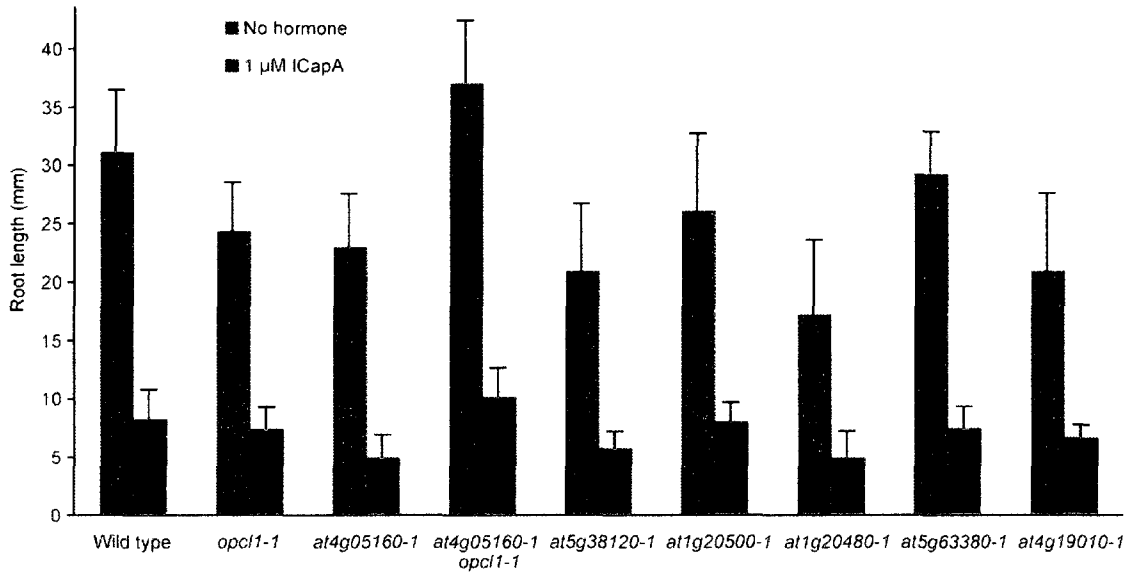

Figure B.2. Mutations in CL-like genes have no effect on root elongation inhibition by ICapA.

Surface-sterilized seeds were plated on medium supplemented with 0.5% sucrose containing no hormone or 1 μM ICapA. Seedlings were grown for 8 days under yellow-filtered light before measuring. Bars show mean + SE ($n \geq 9$).

experiments, the residual IBA responsiveness that I observe even in the double mutant strongly suggests that there is not a single enzyme dedicated to IBA activation in Arabidopsis. Instead, it appears likely that this role is shared by several enzymes, at least some of which also act on other substrates.

Interestingly, none of the single and double mutants assayed exhibited reduced responses to ICapA, suggesting either that the 4CL-like genes are not involved in ICapA activation, or that more double and higher order mutant analyses need to be completed to account for redundancy in protein function.

C. Identification and Characterization of Arabidopsis Indole-3-Butyric Acid Response Mutants Defective in Peroxisomal Enzymes.

Zolman, B. K., Martinez, N., Millius, A., Adham, R. A., and Bartel, B. (2008) Identification and Characterization of Arabidopsis Indole-3-Butyric Acid Response Mutants Defective in Peroxisomal Enzymes. Genetics 180: 237-251.

DOI: 10.1534/genetics.108.090399

Identification and Characterization of Arabidopsis Indole-3-Butyric Acid Response Mutants Defective in Novel Peroxisomal Enzymes

Bethany K. Zolman,*[,1] Naxhiely Martinez,[†] Arthur Millius,[†,2] A. Raquel Adham[†] and Bonnie Bartel[†]

**Department of Biology, University of Missouri, St. Louis, Missouri 63121 and [†]Department of Biochemistry and Cell Biology, Rice University, Houston, Texas 77005*

Manuscript received April 17, 2008
Accepted for publication July 8, 2008

ABSTRACT

Genetic evidence suggests that indole-3-butyric acid (IBA) is converted to the active auxin indole-3-acetic acid (IAA) by removal of two side-chain methylene units in a process similar to fatty acid β-oxidation. Previous studies implicate peroxisomes as the site of IBA metabolism, although the enzymes that act in this process are still being identified. Here, we describe two *IBA*-response mutants, *ibr1* and *ibr10*. Like the previously described *ibr3* mutant, which disrupts a putative peroxisomal acyl-CoA oxidase/dehydrogenase, *ibr1* and *ibr10* display normal IAA responses and defective IBA responses. These defects include reduced root elongation inhibition, decreased lateral root initiation, and reduced IBA-responsive gene expression. However, peroxisomal energy-generating pathways necessary during early seedling development are unaffected in the mutants. Positional cloning of the genes responsible for the mutant defects reveals that *IBR1* encodes a member of the short-chain dehydrogenase/reductase family and that IBR10 resembles enoyl-CoA hydratases/isomerases. Both enzymes contain C-terminal peroxisomal-targeting signals, consistent with IBA metabolism occurring in peroxisomes. We present a model in which IBR3, IBR10, and IBR1 may act sequentially in peroxisomal IBA β-oxidation to IAA.

BECAUSE the auxin indole-3-acetic acid (IAA) orchestrates many aspects of plant growth and development (Woodward and Bartel 2005b), the levels of IAA within a plant must be tightly regulated. In addition to changes in IAA biosynthesis and oxidative degradation, IAA also is transformed into alternate forms, allowing the plant to store IAA until the time and place where active auxin is needed. In one type of storage compound, IAA is conjugated to amino acids or peptides by amide bonds or to sugars by ester bonds; conjugate hydrolases break these bonds to release free IAA (Bartel *et al.* 2001; Woodward and Bartel 2005b). In a second potential storage form, the side chain of the indole moiety is lengthened by two methylene units to make indole-3-butyric acid (IBA), which can be shortened to IAA when necessary (Bartel *et al.* 2001; Woodward and Bartel 2005b).

Although both IBA and certain auxin conjugates have auxin activity in bioassays, genetic experiments suggest that in Arabidopsis this activity does not result from direct effects of the storage compounds, but rather requires release of free IAA from these precursors (Bartel and Fink 1995; Zolman *et al.* 2000). Both IAA conjugates and IBA appear to provide auxin during early Arabidopsis seedling development. In particular, mutants defective in IBA metabolism or IAA-conjugate hydrolysis have fewer lateral roots than wild-type plants, suggesting that the IAA released from storage forms plays a role in lateral root promotion (Zolman *et al.* 2001b; Rampey *et al.* 2004). Different auxin storage forms may have only partially overlapping activity or primarily regulate different physiological responses. For example, mutants with altered IBA responses have stronger rooting defects than IAA-conjugate mutants (Zolman *et al.* 2001b; Rampey *et al.* 2004).

Dedicated enzymes appear to be required to convert auxin storage forms to free IAA. A genetic approach identified a family of Arabidopsis hydrolases showing overlapping specificity in the conversion of various IAA–amino acid conjugates to IAA; mutants defective in each enzyme have altered responses to application of the corresponding conjugates (Bartel and Fink 1995; Davies *et al.* 1999; Rampey *et al.* 2004). We are taking a similar genetic approach to discover the enzymes required for conversion of IBA to IAA.

Even-numbered side-chain-length derivatives of IAA (Fawcett *et al.* 1960) and the synthetic auxin 2,4-dichlorophenoxyacetic acid (2,4-D; Wain and Wightman 1954) possess auxin activity. Wheat and pea extracts shorten these compounds in two-carbon increments (Fawcett *et al.* 1960). These results suggest that IBA,

[1]*Corresponding author:* Department of Biology, University of Missouri, R223 Research Bldg., 1 University Blvd., St. Louis, MO 63121-4400. E-mail: zolmanb@umsl.edu

[2]*Present address:* University of California, San Francisco, CA 94158.

which is structurally identical to IAA but with two additional methylene units on the side chain, and 2,4-dichlorophenoxybutyric acid (2,4-DB), the analogous elongated derivative of 2,4-D, are converted by plants to bioactive IAA and 2,4-D, respectively. The mechanism of this conversion was suggested to be similar to the two-carbon elimination that occurs during fatty acid β-oxidation (Fawcett *et al.* 1960). In this model, IBA acts as a "slow-release" form of IAA (van der Krieken *et al.* 1997), and auxin effects promoted by IBA would be limited by the β-oxidation rate.

To elucidate the proteins necessary for IBA activity, we have isolated Arabidopsis mutants with altered IBA responses. Exogenous IBA inhibits primary root elongation; mutants that cannot sense or respond to IBA have elongated roots on IBA compared to wild type (Zolman *et al.* 2000). *IBA-response* (*ibr*) mutants remain sensitive to short-chain auxins (IAA and 2,4-D), whereas general auxin-response mutants defective in auxin signaling, such as *axr2/iaa7* (Timpte *et al.* 1994; Nagpal *et al.* 2000) and *axr3/iaa17* (Leyser *et al.* 1996; Rouse *et al.* 1998), or transport, including *aux1* (Pickett *et al.* 1990; Bennett *et al.* 1996; Marchant *et al.* 1999), display reduced responses to both IBA and IAA (Zolman *et al.* 2000).

Isolation of the genes defective in *ibr* mutants has revealed a close connection between IBA metabolism and peroxisomal function. For example, mutants defective in the peroxins PEX4 (Zolman *et al.* 2005), PEX5 (Zolman *et al.* 2000), PEX6 (Zolman and Bartel 2004), PEX7 (Woodward and Bartel 2005a), and PEX12 (Fan *et al.* 2005) or in the PXA1/CTS1/PED3 transporter (Zolman *et al.* 2001b), which is required for import of peroxisomal substrates (Footitt *et al.* 2002; Hayashi *et al.* 2002; Theodoulou *et al.* 2005), are resistant to IBA. The isolation of IBA-response mutants defective in these factors, coupled with the fact that peroxisomes are the primary site of fatty acid β-oxidation in plants (Graham and Eastmond 2002; Baker *et al.* 2006), implicates peroxisomes as the subcellular location for IBA-to-IAA conversion. Mutants defective in peroxisomal biogenesis likely disrupt IBA responses by compromising the peroxisomal environment or by limiting peroxisomal import of enzymes necessary for IBA β-oxidation. Indeed, these *ibr* mutants display additional phenotypes associated with peroxisome defects, such as sucrose dependence during seedling development due to slowed β-oxidation of seed storage fatty acids (Zolman *et al.* 2000).

Other *ibr* mutants may be defective in enzymes that act in the peroxisome matrix to catalyze the β-oxidation of fatty acids, IBA, or both. In Arabidopsis, at least two genes encode related isozymes for each fatty acid β-oxidation step (Baker *et al.* 2006). Following substrate import into the peroxisome by PXA1, a CoA moiety is added by one of two long-chain acyl-CoA synthetases (LACS; Fulda *et al.* 2002, 2004). One of six acyl-CoA oxidases (ACX) catalyzes the oxidation step, adding a double bond while releasing hydrogen peroxide (Hayashi *et al.* 1999; Hooks *et al.* 1999; Eastmond *et al.* 2000; Froman *et al.* 2000; Rylott *et al.* 2003; Adham *et al.* 2005; Pinfield-Wells *et al.* 2005). Next, a multifunctional protein (MFP2 or AIM1), containing both enoyl-CoA hydratase and acyl-CoA dehydrogenase activity, forms a β-ketoacyl-CoA thioester (Richmond and Bleecker 1999; Eastmond and Graham 2000; Rylott *et al.* 2006). This substrate undergoes a thiolase-mediated retro-Claisen reaction, releasing two carbons as acetyl-CoA and producing a chain-shortened substrate that can reenter the β-oxidation spiral for continued catabolism. *PED1/KAT2* encodes the most highly expressed thiolase in Arabidopsis (Hayashi *et al.* 1998; Germain *et al.* 2001).

We recently described the *ibr3* mutant, which displays defective IBA and 2,4-DB responses but responds normally to other conditions tested (Zolman *et al.* 2007). *IBR3* (*At3g06810*) encodes a putative peroxisomal acyl-CoA dehydrogenase or oxidase that resembles the mammalian ACAD10 and ACAD11 enzymes. Because the *ibr3* mutant does not have apparent fatty acid β-oxidation defects, IBR3 may act in IBA β-oxidation to IAA (Zolman *et al.* 2007). In addition to *ibr3*, mutants defective in several fatty acid β-oxidation enzymes, including *aim1*, *ped1*, and multiple *acx* mutants, show altered responses to exogenous IBA (Zolman *et al.* 2000; Adham *et al.* 2005); whether these IBA-response defects reflect a direct enzymatic role on IBA β-oxidation intermediates or an indirect disruption of IBA-to-IAA conversion remains an open question.

Here, we describe the phenotypic characterization of *ibr1* and *ibr10*, two strong IBA-response mutants that, like *ibr3*, have no apparent defects in peroxisomal fatty acid β-oxidation. We used map-based cloning to demonstrate that *IBR1* and *IBR10* encode a short-chain dehydrogenase/reductase (SDR) family enzyme and a putative enoyl-CoA hydratase/isomerase (ECH), respectively. Both IBR1 and IBR10 have peroxisomal-targeting signals. The specific IBA-response defects of *ibr1* and *ibr10* mutants suggest that IBR1 and IBR10 are needed for the peroxisomal conversion of IBA to IAA.

MATERIALS AND METHODS

Mutant isolation: The *ibr1-1* and *ibr1-2* mutants were described previously as B1 and B19, ethyl methanesulfonate (EMS)-induced IBA-response mutants in the *Arabidopsis thaliana* Columbia (Col-0) background (Zolman *et al.* 2000). Additional screens of various mutagenized populations revealed several new mutants with IBA-resistant root elongation. *ibr1-3*, *ibr1-4*, and *ibr1-5* were isolated from the progeny of Col-0 seed mutagenized by fast-neutron bombardment (Zolman *et al.* 2007). *ibr1-8* was isolated from the progeny of EMS-mutagenized Col-0 seeds (Lehle Seeds, Round Rock, TX). *ibr10-1* was isolated by screening T-DNA insertion lines in the Col-0 accession (pool CS75075; Alonso *et al.* 2003), although our analysis indicated that the T-DNA was not linked to the IBA-resistant phenotype (data not shown). *chy1-3* (Zolman

et al. 2001a) and *ibr3-1* (Zolman *et al.* 2007) were described previously and are Col-0 alleles with point mutations in *CHY1/At5g65940* and *IBR3/At3g06810*, respectively.

The *ibr1-7* (SALK_010364), *hcd1/at4g14440* (SALK_012852), and *echic/at1g65520* (SALK_036386) mutants in the Col-0 accession were from the Salk Institute sequence-indexed insertion collection (Alonso *et al.* 2003). The three insertion mutants were genotyped using PCR amplification with a combination of genomic primers and a modified LBb1 T-DNA primer (5′-CAAACCAGCGTGGACCGCTTGCTGCA-3′; http://signal.salk.edu). The T-DNA position in *ibr1-7* was confirmed by sequencing the amplification product directly.

Higher-order mutants were generated by crossing and were identified using PCR-based genotyping. For *ibr1-2*, amplification with the oligonucleotides T1J24-8 (5′-GAAGCTTTACCTGCAG GAGAAGTATAGAGG-3′) and T1J24-12 (5′-TAAGAGATGTCT TCTGTGTTTTTGGACTCA-3′) yields a 175-bp product with one *Dde*I site in wild type that was absent in *ibr1-2*. For *ibr10-1*, amplification with At4g14430-1 (5′-ATTTGCACAATTCAACAA CAACACGATTTC-3′) and At4g14430-2 (5′-TAGCCCTAAC CAACGCCGAGAAATAATC-3′) yields a 546-bp product in wild type and a 468-bp product in *ibr10-1*. *ibr3-1* was genotyped using a derived cleaved amplified polymorphic sequence marker (Michaels and Amasino 1998; Neff *et al.* 1998) in which amplification with F3E22-22 (5′-ATGGTGCAGTCTTCCAGGG CCTAACCTAGC-3′; altered residue underlined) and F3E22-23 (5′-GTTTTGATGACGCACCTCATGGACATGCTG-3′) yields a 240-bp product with one *Alu*I site in *ibr3-1* that was absent in wild type.

Plant growth and phenotypic characterization: Surface-sterilized seeds were plated on plant nutrient (PN) medium (Haughn and Somerville 1986) solidified with 0.6% (w/v) agar and supplemented with 0.5% sucrose (PNS), hormones, kanamycin, or Basta (glufosinate–ammonium; Crescent Chemical, Augsburg, Germany) as indicated. Plates were incubated under continuous light at 22°; for auxin experiments, plates were placed under yellow filters to slow breakdown of indolic compounds (Stasinopoulos and Hangarter 1990). Seedlings were transferred to soil and grown at 18°–22° under continuous illumination.

Prior to phenotypic analyses, *ibr1-2* and *ibr10-1* were backcrossed to the parental Col-0 accession four and two times, respectively. For root elongation assays, seeds were plated on PNS supplemented with hormones at the indicated concentrations. Roots were measured after 7 or 8 days at 22° under yellow light. For some assays, seeds first were stratified for 3 days in 0.1% agar at 4° and germinated under white light for 2 days at 22° before being moved to assay plates. For lateral root assays, seeds were stratified for 3 days at 4°, grown on PNS for 4 days under yellow light at 22°, and then transferred to PNS supplemented with the indicated hormone and grown for 4 days under yellow light at 22°. To assay sucrose-dependent hypocotyl elongation, seeds were stratified for 3 days at 4° and grown on PN or PNS for 1 day under white light followed by 5 days in the dark at 22°.

ibr10-1 was crossed to Col-0 carrying a DR5-GUS transgene (Guilfoyle 1999). Lines homozygous for DR5-GUS and *ibr10-1* were selected on 12 μg/ml kanamycin and by genotyping as described above. For analysis of DR5-GUS reporter gene activation, seeds were germinated on PNS and grown for 4 days and then transferred to PNS supplemented with auxin for the indicated number of days. Histochemical localization was done by staining homozygous seedlings for 2 days at 37° with 0.5 mg/ml 5-bromo-4-chloro-3-indolyl-β-D-glucuronide (Bartel and Fink 1994).

Positional cloning and mutant complementation: *ibr1* and *ibr10* alleles were outcrossed to Landsberg *erecta tt4* (L*er*) and Wassilewskija accessions for recombination mapping. Mutations were mapped using PCR-based molecular markers (http://www.arabidopsis.org) on DNA from IBA-resistant F_2 plants. *ibr1-8* was identified as an *ibr1* allele on the basis of failure to complement *ibr1-1*. Candidate genes were PCR amplified from mutant DNA and sequenced directly using gene-specific primers.

To make the 35S-*IBR1c* construct, the *Sal*I/*Not*I insert from the 103N7T7 EST (Newman *et al.* 1994) was ligated into the 35SpBARN (Leclere and Bartel 2001) plant transformation vector cut with *Xho*I and *Not*I. An *IBR1* genomic rescue construct was made by digesting the T1J24 bacterial artificial chromosome containing *IBR1* with *Bgl*II, yielding a 4-kb fragment containing the *IBR1* coding sequence plus 1278 bp 5′ and 1118 bp 3′ of the coding region. This fragment was subcloned into the *Bam*HI site of pBluescript KS+ to give pKS-*IBR1g*. An *Eco*RI/*Xba*I fragment was subcloned from pKS-*IBR1g* into the plant transformation vector pBIN19 (Bevan 1984) cut with the same enzymes to give pBIN-*IBR1g*.

For complementation of the *ibr10* mutant, Col-0 DNA was amplified with *PfuTurbo* DNA polymerase (Stratagene, La Jolla, CA) using primers modified to add *Sal*I and *Not*I restriction enzyme sites (added residues underlined): At4g14430-5 (5′-CGT CGACCATAGACCAATCAGGATAAGGTATATTTCTCTC-3′) and At4g14430-6 (5′-GAGGCGGCCGCTGTCTCTTTCTCCCAAAAC ATGTG-3′). The purified PCR product was cloned into the PCR4-Blunt TOPO vector following the manufacturer's instructions (Invitrogen, Carlsbad, CA) to give pTOPO-*IBR10c*. The insert of pTOPO-*IBR10c* was sequenced to ensure the absence of PCR-derived mutations. The *Sal*I/*Not*I fragment from pTOPO-*IBR10c* was subcloned into *Xho*I/*Not*I-cut 35SpBARN to give 35S-*IBR10*.

Complementation constructs were introduced into *Agrobacterium tumefaciens* GV3101 (Koncz *et al.* 1992) by electroporation (Ausubel *et al.* 1999) and transformed into mutant alleles using the floral dip method (Clough and Bent 1998). Transformed T_1 seedlings and homozygous T_3 lines were identified by selecting seedlings resistant to 7.5 μg/ml glufosinate–ammonium (35S-*IBR1c* and 35S-*IBR10*) or 12 μg/ml kanamycin (pBIN-*IBR1g*).

RESULTS

***ibr1* and *ibr10* have IBA-response phenotypes:** Isolation and characterization of mutants with altered responses is a powerful method for identifying proteins involved in specific metabolic pathways. We screened mutagenized seed pools for mutants with long roots on normally inhibitory IBA concentrations. In addition to two previously described *ibr1* alleles from EMS-mutagenized pools (Zolman *et al.* 2000), we isolated an additional EMS-induced *ibr1* allele, three *ibr1* alleles from a fast-neutron mutagenized population, and a single *ibr10* allele from a T-DNA-mutagenized population (Alonso *et al.* 2003). Both *ibr1* and *ibr10* mutants were resistant to the inhibitory effects of IBA on root elongation (Figure 1A). All of the *ibr1* alleles displayed a similar level of IBA resistance (Figure 1A and data not shown) and we chose *ibr1-2* for more detailed analysis.

We examined IBA-response defects under several conditions, comparing *ibr1* and *ibr10* with the previously described *chy1-3* (Zolman *et al.* 2001a) and *ibr3-1* (Zolman *et al.* 2007) mutants. First, we examined the effects of increasing IBA concentrations on root elongation.

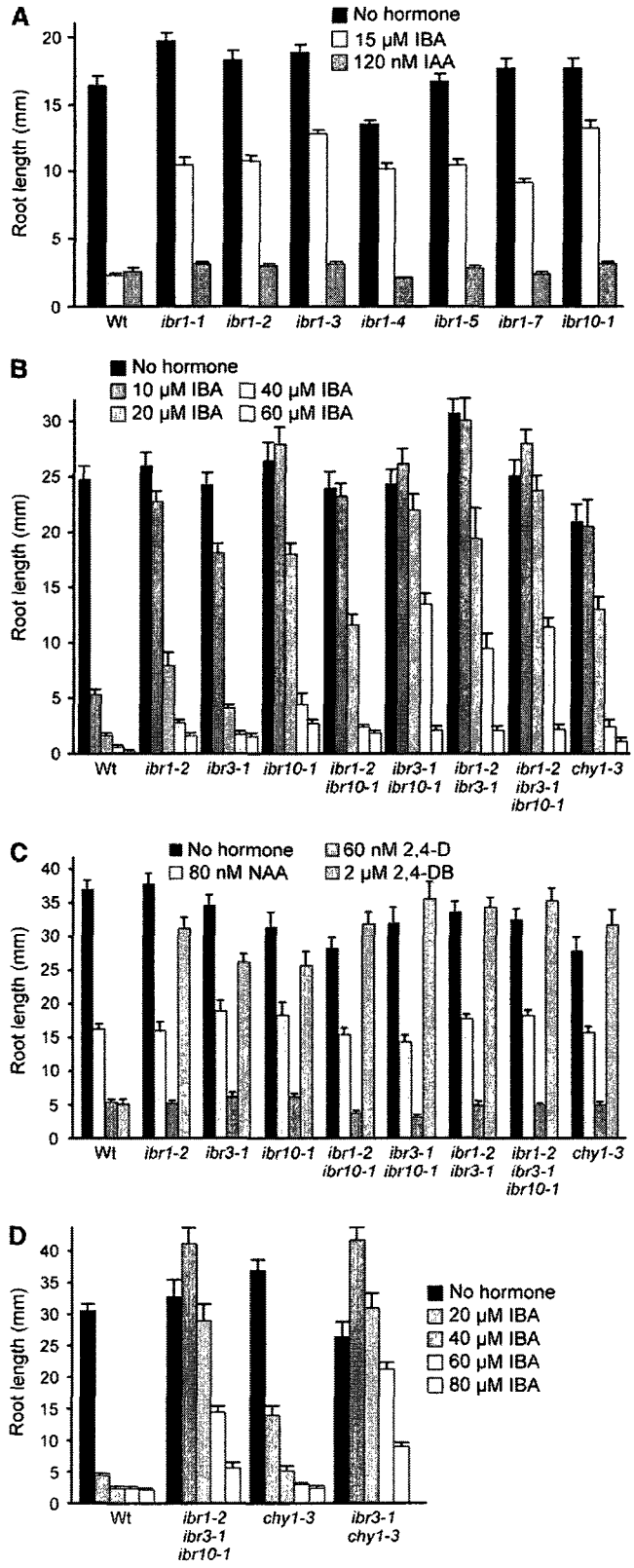

FIGURE 1.—*ibr1* and *ibr10* mutants display IBA- and 2,4-DB-resistant root elongation. (A) *ibr* mutant root elongation on IBA and IAA. Col-0 (Wt), *ibr10-1*, and six *ibr1* alleles were plated on medium containing 0.5% sucrose with no hormone, 15 μM IBA or 120 nM IAA. Root length was measured after 7 days. Error bars show standard errors of mean root lengths ($n \geq 13$). (B) *ibr* mutant root elongation in response to increasing IBA concentrations. Seeds were stratified for 3 days at 4° in 0.1% agar prior to incubation under white light for 2 days at 22°. Germinating seeds were transferred to medium containing 0.5% sucrose (no hormone) or supplemented with the indicated concentration of IBA. Roots were measured after 8 additional days of growth under yellow-filtered light. Error bars show standard errors of mean root lengths ($n \geq 10$). *ibr3-1* (ZOLMAN *et al.* 2007) is included for comparison with *ibr10* and *ibr1*. *chy1-3* (ZOLMAN *et al.* 2001a) is included as an IBA-resistant control. (C) *ibr* mutant root elongation on synthetic auxins. Roots were measured as in B. Error bars show the standard errors of mean root lengths ($n \geq 12$). *chy1-3* is included as a 2,4-DB-resistant control. (D) The *ibr1 ibr3 ibr10* triple mutant remains more IBA responsive than the *ibr3 chy1* double mutant. Root elongation was evaluated as in B. Error bars show standard errors of mean root lengths ($n \geq 8$).

Although the mutants had longer roots than wild type on intermediate IBA levels, all of the mutants responded to IBA at higher concentrations (Figure 1B). We found that *ibr1* was more IBA resistant than *ibr3* and that *ibr10* was more IBA resistant than *ibr1*, *ibr3*, and *chy1* (Figure 1B). Like *ibr3* and *chy1*, *ibr1* and *ibr10* mutants responded normally to IAA (Figure 1A) and to synthetic auxins that are not β-oxidation substrates, such as 1-naphthaleneacetic acid (NAA) and 2,4-D (Figure 1C). *ibr1* and *ibr10* mutants also were resistant to 2,4-DB (Figure 1C), a chain-elongated version of 2,4-D that may be converted to 2,4-D by β-oxidation (HAYASHI *et al.* 1998). The phenotypes of *ibr1* and *ibr10*—resistance to IBA and 2,4-DB coupled with sensitivity to IAA, NAA, and 2,4-D—closely matches the *ibr3* and *chy1* phenotypes.

In addition to assaying root elongation inhibition, we tested the *ibr1* and *ibr10* mutant responses to the stimulatory effects of exogenous auxins on lateral root proliferation. At the concentrations used in our assay, wild-type plants produced similar numbers of lateral roots in response to IBA or NAA induction. Although the *ibr1* and *ibr10* mutants produced normal numbers of lateral roots in response to NAA (Figure 2A) or IAA (data not shown) treatment, both mutants made dramatically fewer lateral roots than wild type in response to IBA stimulation (Figure 2A).

The auxin-inducible DR5-GUS reporter (GUILFOYLE 1999) is expressed in root tips and lateral root primordia, facilitating the visualization of lateral root induction. In wild-type lines carrying the DR5-GUS transgene, lateral root primordia were apparent in response to IBA induction (Figure 2B). In *ibr10-1* DR5-GUS, we found fewer lateral roots and less root staining in response to IBA (Figure 2B). In contrast, we found similar GUS induction throughout *ibr10-1* and wild-type DR5-GUS lines following NAA treatment (Figure 2B). Similar results were seen in *ibr1-2* and *ibr3-1* lines carrying the reporter (data not shown). We concluded from these experiments that, like *ibr3*, *ibr1* and *ibr10* display de-

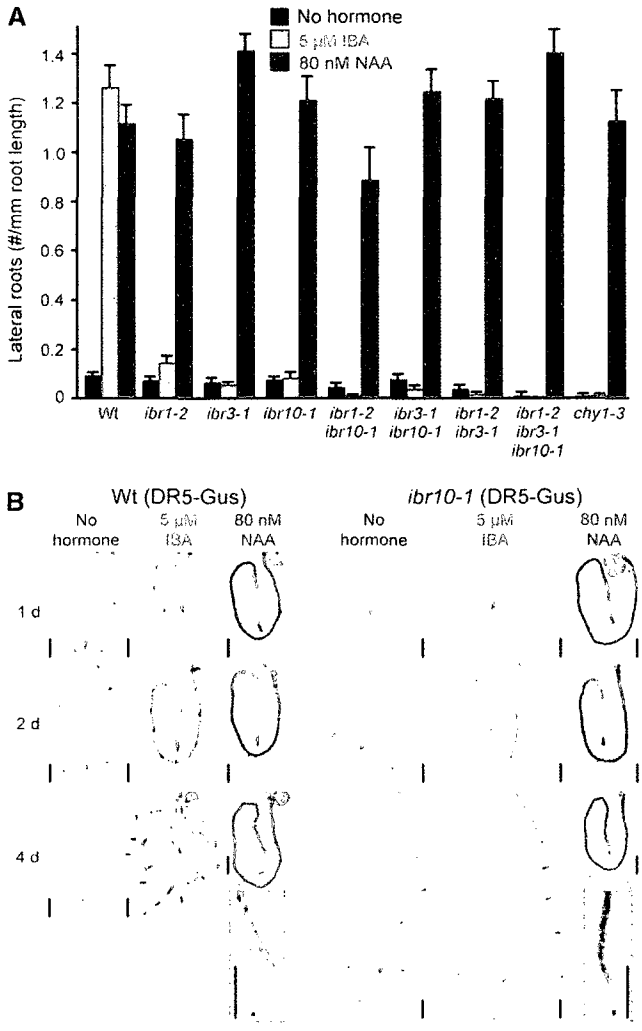

FIGURE 2.—*ibr1* and *ibr10* mutants fail to induce lateral roots in response to IBA. (A) *ibr* mutant lateral root initiation. Seeds were stratified for 3 days at 4° in 0.1% agar prior to plating on medium containing 0.5% sucrose and incubating under white light for 4 days at 22°. Seedlings then were transferred to medium containing 0.5% sucrose with no hormone or supplemented with the indicated concentration of auxin. Roots were measured and lateral roots were counted after 4 additional days of growth. Data are presented as the mean number of lateral roots per millimeter of root length and error bars show the standard error of the means ($n \geq 8$). *chy1-3* is included as an IBA-resistant control. (B) Visualization of *ibr10* lateral root initiation defects using the DR5-GUS reporter. Wild type or *ibr10* containing the DR5-GUS transgene were germinated on medium containing 0.5% sucrose and grown for 4 days and then transferred to unsupplemented medium or medium containing IBA or NAA. After the indicated number of days, seedlings were removed from the medium, stained, and mounted for photography. Lateral root primordia of NAA-treated plants can be visualized in the higher magnification insets. Bars, 1 mm.

fective responses to IBA and 2,4-DB, but maintain normal responses to other auxins.

Higher-order mutants show similar IBA-response phenotypes: Because *ibr1*, *ibr3*, and *ibr10* mutants were all incompletely defective in IBA responses (Figure 1B), we generated double and triple mutants to determine if we could further block IBA responsiveness. In root elongation assays, all of the mutant combinations were IBA resistant compared to wild type at intermediate IBA concentrations (Figure 1B). At very high IBA concentrations, all of the double and triple mutants still responded to IBA. Interestingly, at high IBA concentrations, the *ibr1 ibr3 ibr10* triple mutant was less resistant than the previously described (ZOLMAN *et al.* 2007) *ibr3 chy1* double mutant (Figure 1D). The limited enhancement of IBA resistance seen in higher-order *ibr* mutants suggests that the IBR enzymes may act in the same pathway. The stronger resistance of *ibr3 chy1* suggests that the IBR pathway may promote IBA responses independently of CHY1. *chy1* is believed to indirectly disrupt β-oxidation at the thiolase step (ZOLMAN *et al.* 2001a; LANGE *et al.* 2004).

The double and triple mutants still responded like wild type to NAA and 2,4-D and were 2,4-DB resistant (Figure 1C), consistent with the defect specific to chain-elongated auxins seen in the single *ibr* mutants. Also like the single mutants, the double and triple mutants made few lateral roots in response to IBA induction, but responded like wild type to induction by NAA (Figure 2A). Because so few lateral roots were made in the single mutants in the presence of IBA, we did not attempt to assess the significance of additive or altered effects on lateral rooting in the higher-order mutants.

Other peroxisomal pathways are not detectably disrupted in *ibr1* and *ibr10*: Previously isolated IBA-response mutants fall into two categories: those with general peroxisomal defects, including reduced rates of fatty acid β-oxidation and consequent sucrose dependence during germination, and those that are IBA resistant but appear to carry out other peroxisomal functions normally (ZOLMAN *et al.* 2000). To test whether these new IBA-response alleles had general defects in peroxisomal metabolism manifested in reduced fatty acid β-oxidation, we tested *ibr1* and *ibr10* requirements for sucrose during development. Wild-type seedlings can develop without an exogenous carbon source; early seedling growth is fueled by peroxisomal catabolism of seed storage fatty acids (HAYASHI *et al.* 1998). Mutants defective in seed oil catabolism, due to either loss of a single β-oxidation enzyme or disruption of general peroxisomal function, arrest during early seedling development. Supplementing the growth medium with sucrose, which provides the energy normally obtained from fatty acid β-oxidation, can relieve the arrest. Therefore, comparison of growth with and without exogenous sucrose can reveal defects in peroxisomal function. We found that dark-grown hypocotyls of *ibr1* and *ibr10* elongated normally in the absence of sucrose (Figure 3), suggesting that seed storage fatty acids are efficiently metabolized in both mutants. Indeed, previous gas chromatography–mass spectrometry analysis indicated that seed-storage fatty acids are metabolized

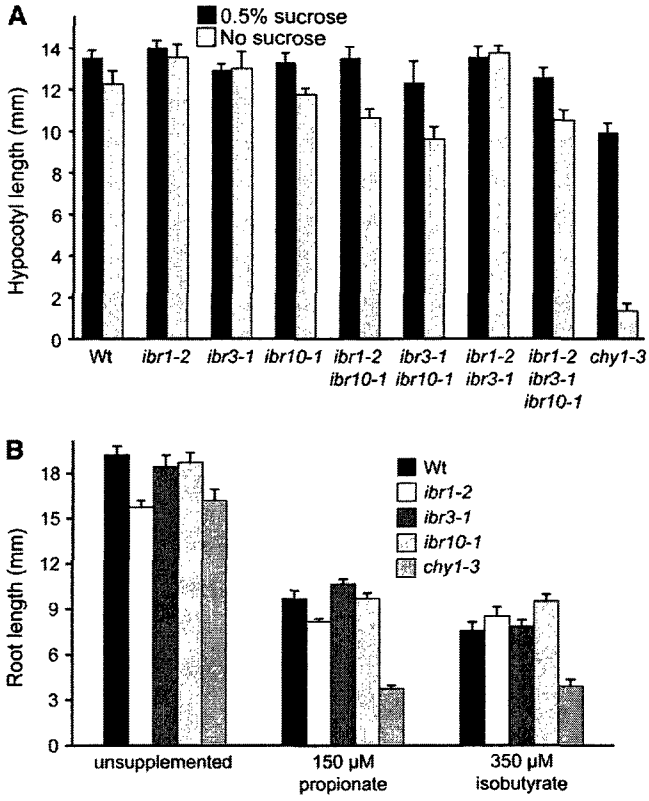

FIGURE 3.—*ibr1* and *ibr10* mutants metabolize peroxisomal substrates similarly to wild type. (A) *ibr* mutant hypocotyl elongation in the absence of sucrose. Seeds were stratified for 4 days at 4° in 0.1% agar prior to plating on unsupplemented medium or medium containing 0.5% sucrose. Plates were placed under white light for 1 day at 22° and then transferred to the dark at 22° for 5 additional days. Error bars show standard errors of mean hypocotyl lengths ($n \geq 10$). *chy1-3* (ZOLMAN *et al.* 2001a) is included as a sucrose-dependent control. (B) *ibr* mutant root elongation on propionate and isobutryate. Seeds were stratified for 3 days at 4° in 0.1% agar prior to incubation under white light for 2 days at 22°. Germinating seeds were transferred to medium containing 0.5% sucrose with or without 150 µM propionate or 350 µM isobutyrate. Roots were measured after 7 additional days of growth. Error bars show standard errors of mean root lengths ($n \geq 11$). *chy1-3* is included as a propionate- and isobutyrate-hypersensitive control (LUCAS *et al.* 2007).

normally during early seedling development in *ibr1-1* and *ibr1-2* (ZOLMAN *et al.* 2000). We also assayed the *ibr* double and triple mutants and found that none displayed sucrose-dependent growth compared to the *chy1* sucrose-dependent control (Figure 3A). We concluded that, even in combination, the *ibr1* and *ibr10* mutations do not appreciably disrupt fatty acid utilization during development.

In addition to IBA and fatty acids, peroxisomes are implicated in the metabolism of other substrates. *CHY1* encodes a peroxisomal β-hydroxybutyryl-CoA hydrolase similar to mammalian mitochondrial enzymes acting in valine catabolism (ZOLMAN *et al.* 2001a). *chy1* mutants are sucrose dependent (ZOLMAN *et al.* 2001a), resistant to IBA (ZOLMAN *et al.* 2001a) and 2,4-DB (LANGE *et al.* 2004), and display heightened sensitivity to root elongation inhibition caused by isobutyrate and propionate treatment (LUCAS *et al.* 2007). These defects are thought to result from accumulation of toxic catabolic intermediates in the mutant. To determine whether the IBR1, IBR3, or IBR10 enzymes might be involved in metabolism of propionate or the branched-chain substrate isobutyrate, we assayed responses of the *ibr* mutants to these compounds. Unlike *chy1*, the *ibr* single-mutant roots were able to elongate like wild type on isobutyrate and propionate (Figure 3B), suggesting that the IBR proteins are not needed for metabolism of these compounds.

acx1 acx5 double mutants have decreased male fertility and reduced jasmonate production, suggesting that peroxisomal ACX enzymes are important for chain shortening of jasmonate precursors (SCHILMILLER *et al.* 2007) in addition to fatty acids (ADHAM *et al.* 2005; PINFIELD-WELLS *et al.* 2005). In contrast, the *ibr1 ibr3 ibr10* triple mutant was fully fertile, suggesting that the IBR enzymes are not essential for jasmonate biosynthesis. Soil-grown *ibr1*, *ibr3*, and *ibr10* single, double, and triple mutants also were not notably different than wild type in size, morphology, or pigmentation (data not shown).

Molecular characterization of the *ibr1* mutants: Using positional information, we mapped the *ibr1* mutant defect to a 3-Mb region in the middle of chromosome 4 between the molecular markers F4C21 and mi167 (Figure 4A). Within this region are the chromosome 4 centromere and a large zone of reduced recombination (COPENHAVEN *et al.* 1999), as well as a chromosomal rearrangement between Col-0 and Ler (FRANSZ *et al.* 2000). We identified a candidate gene (*At4g05530*) within the *ibr1* mapping interval that encodes a protein in the SDR family with a C-terminal peroxisomal-targeting signal; recent proteomic analysis confirmed that the At4g05530 protein is peroxisomal (REUMANN *et al.* 2007). Because of previous connections between IBA response and peroxisomal function (see above), we hypothesized that disruption of this peroxisomal enzyme might cause the *ibr1* phenotypes.

We sequenced *At4g05530* using DNA from the *ibr1-1* mutant and identified a C-to-T mutation at position 126 (where 1 is the A of the initiator ATG), which alters an Arg to a Cys residue (Figure 4B). Figure 5 shows an alignment of similar proteins from different kingdoms; Arg126 is conserved in 25/25 IBR1 homologs. *ibr1-8* has a mutation at position 1090, which converts a Ser residue to Phe. In *ibr1-2*, we found a G-to-A mutation at position 828 that disrupts the 3′-splice junction following the second intron. The mutation changes the absolutely required G in the splice site, presumably destroying the splice site and altering the downstream protein. In *ibr1-3*, we found a 1-bp deletion at position 859, causing a frameshift in the mutant protein. The first 94 amino acids of the mutant ibr1-3 protein are

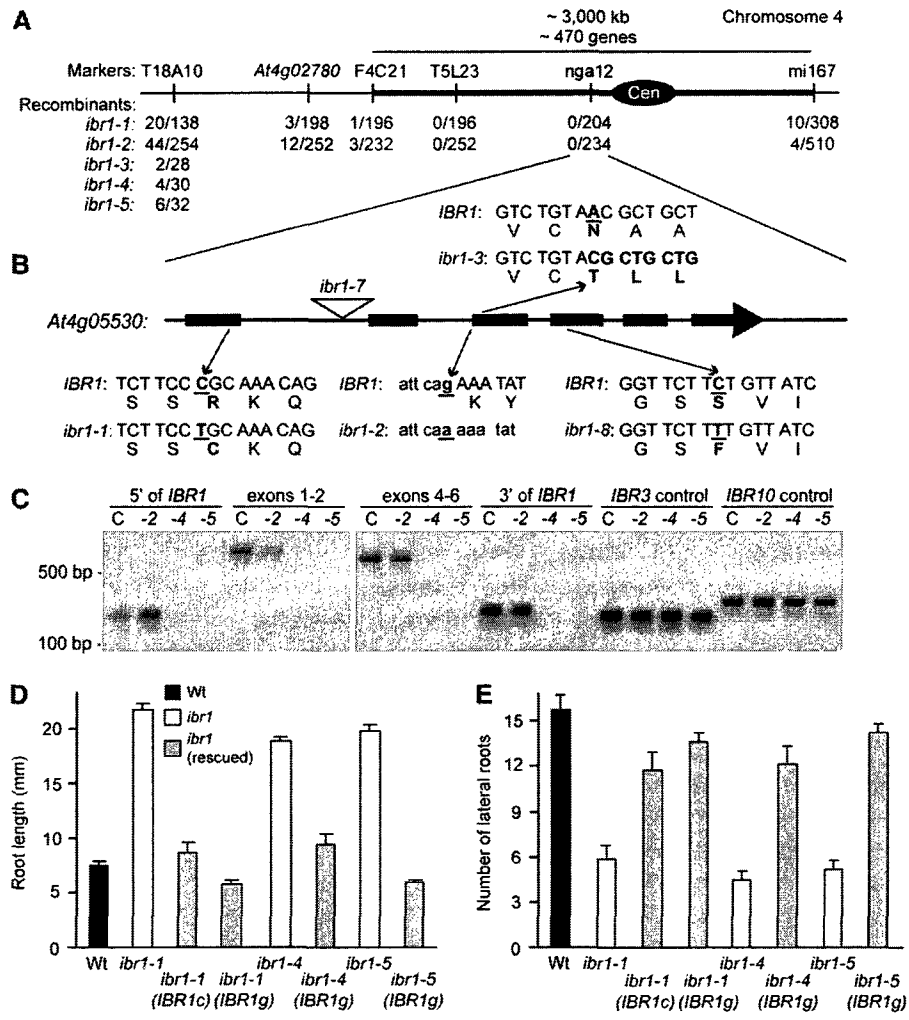

FIGURE 4.—Positional cloning of *IBR1* and complementation of *ibr1* mutants. (A) Recombination mapping of *ibr1* mutant alleles to chromosome 4. IBA-resistant F_2 plants were scored using PCR-based markers (above the bar) and the number of recombination events/total number of chromosomes scored is shown below the bar. The solid oval represents the chromosome 4 centromere. (B) Molecular lesions in *ibr1* mutant alleles. Sequence analysis of the *IBR1* (*At4g05530*) candidate gene (exons shown as solid boxes; introns shown as thin lines) using *ibr1* mutant DNA revealed a C-to-T base-pair change in *ibr1-1*, altering a conserved Arg to Cys. *ibr1-2* has a G-to-A base-pair change at the 3′ splice site of intron 2 (exon sequence is uppercase; intron sequence is lowercase). The *ibr1-3* mutant allele has a 1-bp deletion, leading to a frameshift and premature termination at amino acid 95 (see Figure 5). The position of the *ibr1-7* T-DNA insertion (SALK_010364) is shown by a triangle. *ibr1-8* has a C-to-T base-pair change, altering a Ser residue to Phe. (C) PCR analysis of the *ibr1-4* and *ibr1-5* deletion alleles. Amplification reactions were performed on Col-0 (C), *ibr1-2* (*-2*), *ibr1-4* (*-4*), and *ibr1-5* (*-5*) genomic DNA using primers upstream of *IBR1*, spanning exons 1 and 2, spanning exons 4–6, and downstream of the gene. Control reactions used primers amplifying *IBR3* and *IBR10*. (D) Rescue of *ibr1* defects in IBA-responsive root elongation inhibition by wild-type *IBR1*. Wild-type Col-0 (Wt), *ibr1-1*, *ibr1-4*, and *ibr1-5* mutants and *ibr1* lines containing either 35S-*IBR1c* (*IBR1c*) or pBIN-*IBR1g* (*IBR1g*) were germinated and grown on medium supplemented with 0.5% sucrose and 7.5 μM IBA for 8 days at 22°. Error bars indicate standard errors of the mean root lengths ($n \geq 12$). (E) Rescue of *ibr1* lateral root defects by wild-type *IBR1*. Lines used in D were assayed for lateral root production. Seeds were plated on medium with 0.5% sucrose and grown for 5 days under white light and then transferred to medium further supplemented with 10 μM IBA and grown for 4 additional days. Error bars indicate standard errors of the mean number of visible lateral roots per seedling ($n \geq 12$).

identical to IBR1, followed by 50 amino acids translated in a different frame and a stop codon; the C-terminal peroxisomal-targeting signal in this protein is lost.

The *ibr1-4* and *ibr1-5* mutants were isolated from distinct pools of fast-neutron mutagenized seeds. Both mutants appear to harbor a large deletion removing all of *IBR1*, as multiple primer sets spanning the gene did not amplify products that were present in wild-type samples (Figure 4C). Furthermore, amplification reactions using primers 1500 bp upstream or 850 bp downstream did not yield products. For both *ibr1-4* and *ibr1-5* mutant alleles, we were able to amplify genes in other regions of the genome (Figure 4C), indicating that we had successfully prepared DNA from the mutants. However, we did not explore the precise boundaries of the deletions in either *ibr1-4* or *ibr1-5* and do not know whether additional genes are affected in these alleles.

We obtained a T-DNA insertion mutant (SALK_010364) in *IBR1* from the Salk Institute collection (ALONSO *et al.* 2003). Sequence analysis confirmed that this mutant (*ibr1-7*) had an insertion at position 469 relative to the start codon, near the end of intron 1 (Figure 4B). When we compared the IBA responses of the *ibr1* alleles, we found that all were similarly defective in IBA responsiveness (Figure 1A), indicating that we are likely examining the null phenotype for this gene.

***At4g05530* complements the *ibr1* mutants:** To complement the mutant alleles, we made both a genomic construct driving *IBR1* expression from the *IBR1* 5′ regulatory region and an overexpression construct driving an *IBR1* cDNA from the constitutive 35S promoter from cauliflower mosaic virus. *ibr1-1* was rescued similarly following transformation with either the genomic or overexpression construct (Figure 4, D and E), indicating that both constructs provided sufficient pro-

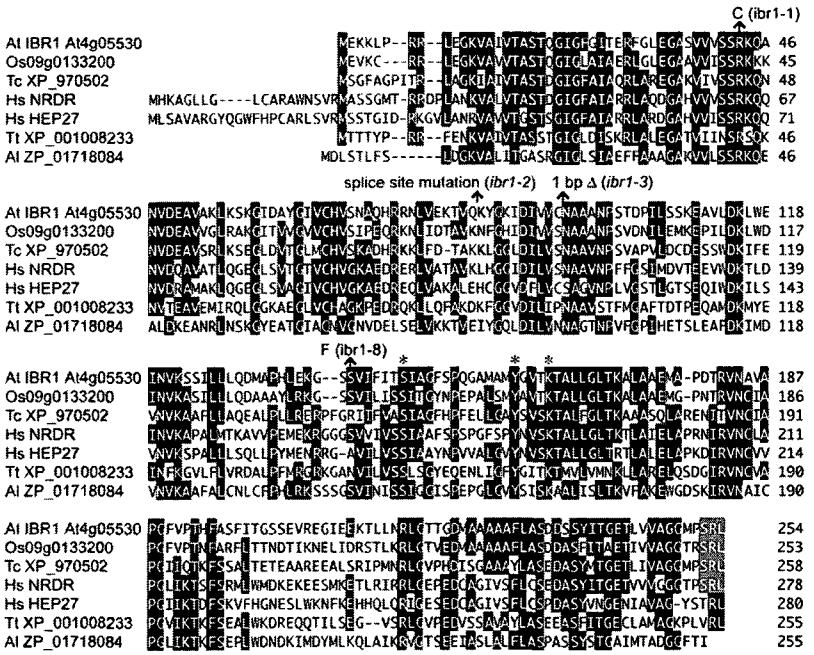

FIGURE 5.—IBR1 resembles short-chain dehydrogenase/reductase enzymes. An alignment comparing IBR1 to similar proteins from rice (Os), beetle (Tc; *Tribolium castaneum*), human (Hs), Tetrahymena (Tt), and the prokaryote *Algoriphagus* sp. PR1 (Al) was generated in the MegAlign program (DNAStar) using the Clustal W method. Amino acid residues identical in at least four sequences are against a solid background; hyphens indicate gaps introduced to maximize alignment. The *ibr1* mutations are indicated above the sequence. The C-terminal PTS1 present in IBR1 and the three closest homologs is indicated by a shaded background; HsHEP27 is not targeted to peroxisomes (PELLEGRINI *et al.* 2002). Asterisks above the sequence denote three essential residues that compose the catalytic triad characteristic of SDR proteins (KALLBERG *et al.* 2002).

tein for wild-type function and that any overexpression did not affect the response. In addition, we found that expression of genomic *IBR1* in *ibr1-3*, *ibr1-4*, and *ibr1-5* restored IBA responses in root elongation and lateral root initiation (Figure 4, D and E, and data not shown). We concluded that the IBA-response defects in *ibr1* result from disruption of the *IBR1/At4g05530* gene.

Molecular characterization of the *ibr10* mutant: We mapped the *ibr10-1* lesion to the middle of chromosome 4, 5.5 Mb below *IBR1* (Figure 6A). Within the mapping region, we identified a gene encoding a putative enoyl-CoA hydratase (*At4g14430*). The At4g14430 protein is similar to enzymes acting in fatty acid β-oxidation (Figure 7) and recently was confirmed to localize in peroxisomes (REUMANN *et al.* 2007). Sequencing this candidate gene revealed a 78-bp deletion in the *ibr10-1* mutant (Figure 6B). This deletion is predicted to remove 26 amino acids from the 240-amino-acid protein, but leave the C terminus in frame with wild-type IBR10. The deletion removes several conserved amino acids; however, a predicted active site residue and the peroxisomal-targeting signal remain in the mutant protein (Figure 7). If the mutant protein is able to fold correctly, retention of this region may be sufficient to allow partial enzyme activity. Because publicly available T-DNA insertion collections contain no insertions in the *At4g14430* coding sequence, we currently are unable to determine whether the single *ibr10-1* allele displays a null phenotype.

***At4g14430* complements the *ibr10-1* mutant:** Because we recovered only a single *ibr10* allele, we sought to confirm that the mutant phenotypes were due to *At4g14430* disruption. We created an *IBR10* overexpression construct that drives expression of *IBR10* from the cauliflower mosaic virus 35S promoter. *ibr10-1* plants transformed with the 35S-*IBR10* construct displayed restored responses to IBA in both root elongation and lateral root initiation assays (Figure 6, C and D), indicating that the identified lesion in *At4g14430* caused the IBA-response defects that we observed in *ibr10-1*.

Mutants defective in the *IBR10* homologs *At4g14440* and *At1g65520* respond normally to IBA: IBR10 has two close Arabidopsis homologs. To determine if either of these proteins contributes to IBA responses, we examined the phenotypes of insertion mutants disrupting these two genes. The closest IBR10 relative in Arabidopsis is At4g14440 (80% identical; Figure 7), which is encoded directly adjacent to *IBR10* and likely results from a recent duplication. However, At4g14440 ends with the C-terminal tripeptide "HNL," which is not a known peroxisomal-targeting signal (REUMANN *et al.* 2004). We isolated a T-DNA insertion line (SALK_012852) predicted to disrupt *At4g14440* (Figure 6B). The mutant responded like wild type to IBA (Figure 6E). We similarly examined a T-DNA insertion allele (SALK_036386) disrupting a second *IBR10* homolog *At1g65520*, which encodes a protein 49% identical to IBR10 that contains the canonical peroxisomal-targeting signal "SKL" (Figure 7). We found that this mutant also displayed wild-type IBA responsiveness (Figure 6E). We concluded that the two closest *IBR10* homologs in the Arabidopsis genome are not required for IBA-responsive root elongation inhibition.

Expression of *IBR* genes: The phenotypic similarities among the *ibr* mutants suggest that IBR1, IBR3, and IBR10 might be involved in similar processes. We used the Genevestigator database of microarray data (ZIMMERMANN *et al.* 2004) to compare the expression

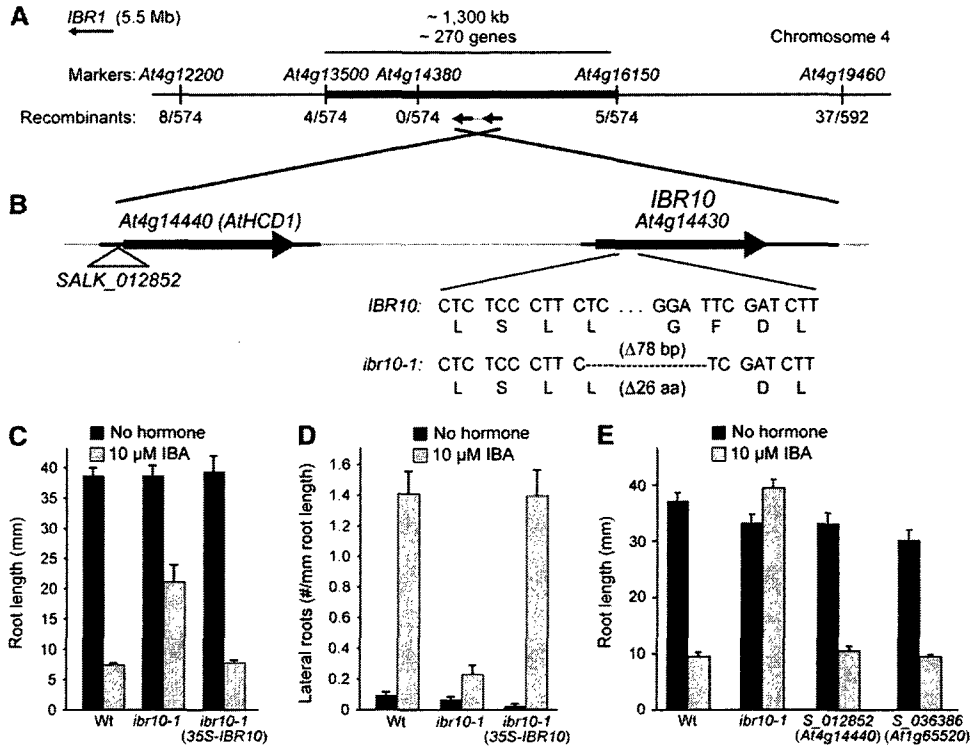

FIGURE 6.—Positional cloning of *IBR10* and complementation of the *ibr10* mutant. (A) Recombination mapping of *ibr10* to the middle of chromosome 4, south of *IBR1*. IBA-resistant F_2 plants were scored using PCR-based markers (above the bar) and the number of recombination events/total number of chromosomes scored is shown below the bar. (B) Molecular lesion in *ibr10-1*. Sequence analysis of the *IBR10* (*At4g14430*) candidate gene using mutant DNA revealed a 78-bp deletion in *ibr10-1*. This deletion removes 26 amino acids of the encoded protein (see Figure 7), but leaves the C terminus of the protein in frame. The position of the T-DNA insertion disrupting the upstream *IBR10* homolog, *AtHCD1/At4g14440*, is indicated by a triangle. (C) Rescue of *ibr10* defects in IBA-responsive root elongation inhibition by wild-type *IBR10*. Wild-type Col-0 (Wt), the *ibr10* mutant, and *ibr10* containing 35S-*IBR10* were assayed as described in the legend for Figure 1B. Error bars show standard errors of mean root lengths ($n \geq 12$). (D) Rescue of *ibr10* lateral root defects by wild-type *IBR10*. Lines used in C were assayed for lateral root production, as described in the legend for Figure 2A. Data are presented as the mean number of lateral roots per millimeter of root length and error bars show the standard error of the means ($n \geq 12$). (E) Root elongation of insertion mutants disrupting *ibr10* homologs. T-DNA insertion mutants in the *ibr10* homologs *AtHCD1/At4g14440* (S_012852) and *ECHIc/At1g65520* (S_036386) were assayed for IBA responses as described in the legend for Figure 1B. Error bars show standard errors of mean root lengths ($n \geq 11$).

patterns of *IBR1*, *IBR3*, and *IBR10* with genes encoding known fatty acid β-oxidation proteins (Figure 8). This analysis revealed that the three *IBR* genes show similar constitutive moderate-level expression in most tissues examined with apparent increases in seeds (Figure 8B). This expression pattern is similar to that of fatty acid β-oxidation genes, except that the fatty acid β-oxidation genes generally have higher expression levels (Figure 8D). In particular, *LACS6*, *LACS7*, *ACX3*, *MFP2*, and *PED1* seem to have a similar pattern as *IBR* gene expression, albeit at apparently higher levels. Interestingly, *IBR1* and *IBR3* transcripts appear to accumulate in senescing leaves, as do many of the fatty acid β-oxidation genes (Figure 8, B and D).

DISCUSSION

The isolation and characterization of two new IBA-response mutants, *ibr1* and *ibr10*, along with the map-based identification of the defective genes, revealed two novel peroxisome-targeted proteins. On the basis of mutant phenotypes and the identity of the encoded proteins, we hypothesize that IBR10 and IBR1 may act in sequential steps in the peroxisomal conversion of IBA to IAA.

IBR10 contains an ECH domain (pfam00378) and has been annotated as ECHIb (REUMANN *et al.* 2007). In a subset of characterized family members, including bacterial hydratases and a yeast isomerase, a conserved Glu residue is required for catalysis (MURSULA *et al.* 2001; WONG and GERLT 2004); this residue is present in IBR10 and retained in the ibr10 mutant protein (Figure 7). The substrates metabolized by ECH enzymes are diverse, although common structural intermediates are typical and there is strong conservation within the CoA-binding site (AGNIHOTRI and LIU 2003). Enzymes in the ECH family often act in reversible reactions and include not only isomerases and hydratases, but also napthoate synthase, carnitine racemase, and hydroxybutyryl-CoA dehydratases. In fatty acid β-oxidation, ECH family enzymes catalyze a hydration reaction to produce hydroxyacyl-CoA thioester intermediates. For example, the Arabidopsis peroxisomal MFP2 and AIM1 multifunctional proteins acting in fatty acid β-oxidation each contain an ECH domain and have enoyl-CoA hydratase activity (RICHMOND and SOMMERVILLE 2000; RYLOTT *et al.* 2006). Unlike these large multifunctional proteins, which also contain L-3-hydroxyacyl-CoA dehydrogenase and D-3-hydroxyacyl-CoA epimerase domains (RICHMOND and SOMMERVILLE 2000; RYLOTT *et al.* 2006), IBR10 is

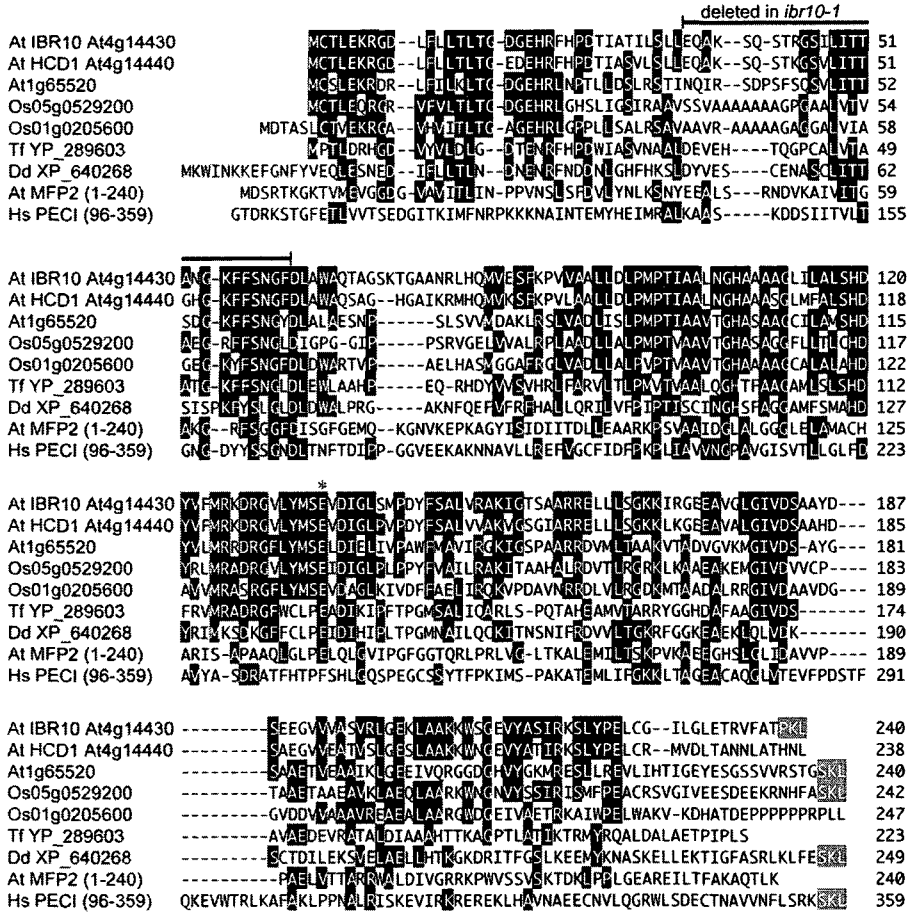

FIGURE 7.—IBR10 resembles enoyl-CoA hydratases. An alignment comparing IBR10 to similar proteins from Arabidopsis (At), rice (Os), the bacterium *Thermobifida fusca* (Tf), Dictyostelium (Dd), and humans (Hs) was generated in the MegAlign program (DNAStar) using the Clustal W method. Amino acid residues identical in at least four sequences are against a solid background; hyphens indicate gaps introduced to maximize alignment. The *ibr10-1* deletion is indicated above the sequence. The C-terminal PTS1 present in IBR10 and four of the homologs are indicated by a shaded background. The HsPECI homolog has an N-terminal extension compared to the Arabidopsis protein; for clarity, the first 95 amino acids of this protein are not shown. MFP2 is an Arabidopsis multifunctional protein acting in peroxisomal fatty acid β-oxidation that contains enoyl-CoA hydratase/isomerase activity in the first 200 amino acids of the protein (RICHMOND and BLEECKER 1999); the C-terminal domains of MFP2 are not shown. A Glu residue important for activity in a *Pseudomonas putida* hydratase (WONG and GERLT 2004), a yeast isomerase (MURSULA *et al.* 2001), and a rat ECH (HOLDEN *et al.* 2001) is indicated by an asterisk above the sequence.

a single domain protein, reminiscent of enzymes acting in mammalian β-oxidation.

Analysis of other sequenced genomes revealed single-domain IBR10 homologs in several plants, including both monocots and dicots (REUMANN *et al.* 2007). The closest IBR10 relative in Arabidopsis is *At4g14440*, which is 80% identical to IBR10 at the amino acid level but lacks a known peroxisomal-targeting signal. This IBR10 homolog, recently named AtHCD1, can act as a *h*ydroxyacyl-CoA *d*ehydratase on very-long-chain substrates in wax biosynthesis (GARCIA *et al.* 2007). An insertion mutant disrupting *AtHCD1* (SALK_012852) contains reduced wax levels and altered wax crystal morphology (GARCIA *et al.* 2007). We tested the *hcd1/at4g14440* mutant and found wild-type IBA responses (Figure 6E), suggesting that these two highly related proteins are not functionally redundant in the examined responses. A second Arabidopsis homolog, At1g65520 (ECHIc), is 49% identical to IBR10 and is peroxisomal (REUMANN *et al.* 2007); disruption of *At1g65520* also did not alter IBA responses (Figure 6E). Rice contains two clear IBR10 homologs; as in Arabidopsis, one has a predicted peroxisomal localization whereas the other does not (Figure 7).

Outside the plant kingdom, IBR10 has limited similarity (~20% identical) to a mammalian *p*eroxisomal *e*noyl-CoA *i*somerase (PECI; GEISBRECHT *et al.* 1999) that is localized in both peroxisomes and mitochondria (GEISBRECHT *et al.* 1999; ZHANG *et al.* 2002). This enzyme has $\Delta^3\Delta^2$enoyl-CoA isomerase activity (GEISBRECHT *et al.* 1999), which is required for rearranging double bonds to allow complete β-oxidation of unsaturated fatty acids. The *Saccharomyces cerevisiae* homolog, Eci1p, also has isomerase activity but lacks hydratase activity (GEISBRECHT *et al.* 1998). Human PECI has an N-terminal extension compared to the other homologs (Figure 7) that resembles acyl-CoA-binding proteins (POIRIER *et al.* 2006).

IBR1 is in the SDR family, a large group of proteins with highly variable enzymatic functions. SDR proteins can have oxidoreductase, lyase, isomerase, or related activities and act on a wide variety of substrates, including steroids, sugars, and alcohols. Each enzyme requires NAD, NADP, or FAD as an electron carrier, which typically is bound by a Rossman fold within the N-terminal region of the protein; the identity of this cofactor is used as a partial determinant of enzyme classification (KALLBERG *et al.* 2002; KALLBERG and PERSSON 2006). The C-terminal region is typically less conserved and is important for substrate interactions.

Arabidopsis IBR1 is in the dehydrogenase subcategory with different or unknown specificities (FabG/

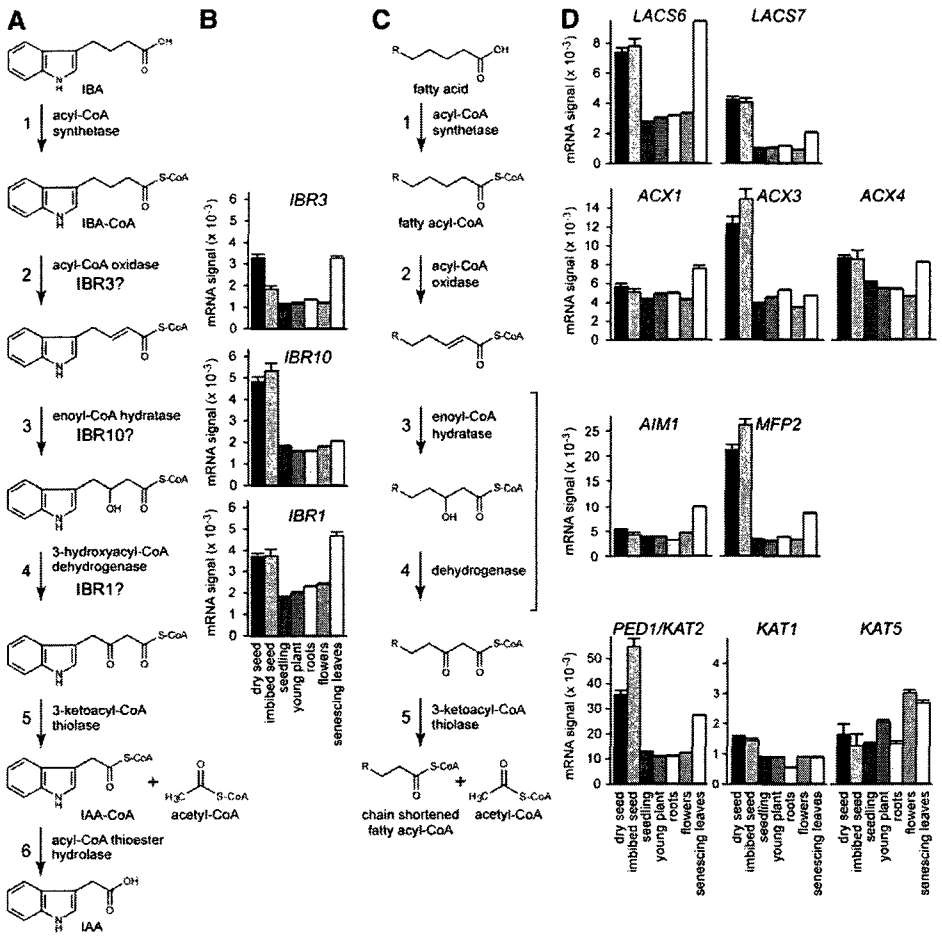

FIGURE 8.—Expression profiles of genes encoding IBR enzymes and enzymes acting in fatty acid β-oxidation. (A) A model for the conversion of IBA to IAA. General enzymatic requirements are shown to the right of the arrows along with the hypothesized positions for IBR3, IBR10, and IBR1 activity. (B) Relative expression levels (mRNA signal) for *IBR3*, *IBR10*, and *IBR1* in several Arabidopsis tissues. Genevestigator (ZIMMERMANN *et al.* 2004) data indicate that expression of the three *IBR* genes is similar among tissues. Error bars show the standard error of the mean expression levels; $n = 121$ for dry seeds, 26 for imbibed seeds, 944 for seedlings, 419 for young plants, 330 for roots, 619 for flowers, and 3 for senescing leaves. Data were retrieved from Genevestigator in June 2008. (C) Pathway of fatty acid β-oxidation, where R represents a side-chain extension of additional carbon units. In plant peroxisomes, step 1 is catalyzed by long-chain acyl-CoA synthetases (LACS6 and LACS7), step 2 is catalyzed by a family of acyl-CoA oxidases (ACX1-6), steps 3 and 4 are catalyzed by multifunctional proteins (AIM1 or MFP2), and step 5 is carried out by thiolase (PED1/KAT2, KAT1, and KAT5). (D) Relative expression levels (mRNA signal) for genes encoding fatty acid β-oxidation enzymes in several Arabidopsis tissues. Genevestigator data were collected as described in B.

COG1028 and COG4221; MARCHLER-BAUER and BRYANT 2004). On the basis of protein size and amino acid residues at conserved domains, IBR1 has been classified as a "classical" SDR (KALLBERG *et al.* 2002, 2007) and also has been annotated as SDRa (REUMANN *et al.* 2007). IBR1 has an apparent nucleotide-binding site with a predicted preference for an NADP(H) cofactor (http://www.ifm.liu.se/bioinfo/; KALLBERG and PERSSON 2006). In addition, the three SDR catalytic amino acids (KALLBERG *et al.* 2002) are conserved in IBR1 (Ser146, Tyr159, and Lys163), along with other less tightly conserved amino acid sequences indicative of SDR classification (Figure 5; KALLBERG *et al.* 2002; REUMANN *et al.* 2007).

IBR1 homologs are present in animals, bacteria, and plants. According to the classification system of KALLBERG *et al.* (2007), IBR1 is the only Arabidopsis family member in cluster 5c. Human HEP27 (also known as DHRS2) is the most characterized member of this cluster and is 45% identical to IBR1. HEP27 is a nuclear protein (PELLEGRINI *et al.* 2002) and can reduce dicarbonyl compounds, but not sugars, steroids, or retinoids (SHAFQAT *et al.* 2006). The mammalian protein NRDR (also known as DHRS4, HEP27-like, RRD, PHCR, SDR-SRL, and SCAD-SRL) is a closely related homolog that acts as a retinol dehydrogenase and a retinal reductase regulating retinoid metabolism (LEI *et al.* 2003). This enzyme has an "SRL" peroxisomal-targeting signal, like Arabidopsis IBR1, and has been shown to localize to peroxisomes using a fluorescent reporter protein (FRANSEN *et al.* 1999). Furthermore, NRDR activity has been isolated from mouse peroxisomes and increases in the presence of peroxisome proliferators (LEI *et al.* 2003). Although characterization of the human NRDR protein lends credence to the importance of IBR1 in peroxisomal metabolic pathways, retinol (vitamin A) or retinal are unlikely substrates for IBR1, as these molecules are not observed in plants (WOLF 1984).

Recent proteomic analysis of soybean peroxisomal proteins revealed GmSDR, which is 78% identical to IBR1 (ARAI *et al.* 2008), and analysis of sequenced databases identified IBR1 homologs in a variety of monocot and dicot species (REUMANN *et al.* 2007). None of the closely related IBR1 plant homologs have known substrates, although a *Solanum tuberosum* tropinone reductase (34% identical to IBR1) has been characterized (KEINER *et al.* 2002). Tropinone reduc-

tases are NADPH-dependent enzymes acting in alkaloid metabolism; these enzymes do not appear to be localized to peroxisomes. More distant Arabidopsis relatives include ABA2, which acts in ABA biosynthesis (Cheng *et al.* 2002), and the ATA1 enzyme homologous to TASSELSEED 2 (Lebel-Hardenack *et al.* 1997), involved in sex determination in maize (Delong *et al.* 1993).

We can envision both direct and indirect mechanisms by which defects in peroxisomal enzymes might reduce IBA responsiveness. In the direct model, IBR enzymes would catalyze IBA β-oxidation reactions. The specificity of the *ibr* defects and the nature of the mutated genes are consistent with the possibility that IBR1 and IBR10 act directly in the conversion of IBA to IAA (Figure 8A). Because elimination of two carbons could convert IBA to IAA, we expect that the responsible enzymes will resemble those acting in fatty acid β-oxidation. In plants, fatty acid β-oxidation occurs by addition of a CoA moiety by an acyl-CoA synthetase followed by the repeating activities of ACX, MFP, and thiolase enzymes (Figure 8C). Previously, we suggested that IBR3 might act as an IBA-CoA dehydrogenase or oxidase, carrying out the second step in IBA β-oxidation (Figure 8A, step 2; Zolman *et al.* 2007). The multifunctional proteins AIM1 (Richmond and Bleecker 1999) and MFP2 (Rylott *et al.* 2006) are isozymes with different chain-length specificities that carry out steps 3 and 4 of fatty acid β-oxidation, which involve a hydration and subsequent NAD^+-dependent dehydrogenation. AIM1 also might act in the conversion of IBA, as the *aim1* mutant is resistant to IBA (Zolman *et al.* 2000) and 2,4-DB (Richmond and Bleecker 1999). However, identification of *IBR10*, which encodes an enoyl-CoA hydratase/isomerase family member, and *IBR1*, which encodes a dehydrogenase/reductase-like protein, suggests that IBR10 and IBR1 may together provide AIM1 activity in IBA β-oxidation, either in addition to or instead of AIM1.

The activities of biochemically characterized enzymes similar to IBR1 and IBR10 fit with what would be required for IBA β-oxidation. *ibr1* and *ibr10*, along with *ibr3* (Zolman *et al.* 2007), have specific defects in IBA responses, displaying reduced responses to IBA in root elongation, lateral root initiation assays, and IBA-induced reporter gene expression, but normal responses to other forms of auxin (Figures 1 and 2). Because neither *ibr1* nor *ibr10* have phenotypes typical of fatty acid β-oxidation defects (sucrose dependence during early development; Figure 3A), the disruptions of these genes are unlikely to affect general peroxisomal function or fatty acid β-oxidation. Genetic evidence suggests that IBA-to-IAA conversion is peroxisomal; therefore, we expect enzymes catalyzing this conversion to be peroxisomally targeted. Both IBR1 ("SRL") and IBR10 ("PKL") have predicted C-terminal type 1 peroxisomal-targeting signals (Kamada *et al.* 2003; Reumann *et al.* 2004) and recent proteomic analysis of purified peroxisomes and YFP-localization studies confirm that both IBR1 and IBR10 are peroxisomal (Reumann *et al.* 2007), consistent with a role in IBA metabolism.

Rather than directly catalyzing IBA β-oxidation, IBR1 and IBR10 might act in other peroxisomal processes that, when disrupted, indirectly impede IBA metabolism. An indirect model for IBA β-oxidation disruption is not without precedent. Such a mechanism might result from accumulation of toxic intermediates, as in the *chy1* mutant (Zolman *et al.* 2001a). CHY1 encodes a β-hydroxyisobutyryl-CoA hydrolase acting in peroxisomal valine (Zolman *et al.* 2001a; Lange *et al.* 2004) or isobutyrate (Lucas *et al.* 2007) catabolism. *chy1* mutants are sucrose dependent (Zolman *et al.* 2001a), IBA resistant (Zolman *et al.* 2001a), 2,4-DB resistant (Lange *et al.* 2004), and hypersensitive to isobutyrate and propionate (Lucas *et al.* 2007). These phenotypes are thought to result from accumulation of a toxic valine catabolic intermediate that impedes thiolase activity (Zolman *et al.* 2001a; Lange *et al.* 2004). The *ibr1*, *ibr3*, and *ibr10* mutants respond like wild type to exogenous isobutyrate and propionate (Figure 3B), suggesting that the IBR proteins do not act in the CHY1 pathway.

A second potential indirect mechanism for disruption of IBA β-oxidation is decreased cofactor availability. For example, disrupting the second step of fatty acid β-oxidation (Figure 8) in certain *acx* mutants leads to accumulation of fatty acyl-CoA esters (Rylott *et al.* 2003; Pinfield-Wells *et al.* 2005). These activated, but unprocessed, substrates might deplete the CoA pool available to IBA and thereby limit IBA metabolism to IAA (Adham *et al.* 2005).

If IBR1 acts directly in IBA β-oxidation, it is curious that the protein is in the short-chain alcohol dehydrogenase/reductase family rather than resembling acyl-CoA dehydrogenases, as might be expected for an enzyme acting at this step of the pathway. However, the SDR family has a broad list of accepted substrates, perhaps indicating a catalytic pocket that could accommodate the IBA β-oxidation intermediate. Previous bioinformatic analysis led to the suggestion that IBR1 might act on β-hydroxyisobutyrate (Reumann *et al.* 2004); this model is attractive because the potential substrate lacks a CoA side chain. However, it is unclear how a block this late in valine catabolism would impede IBA responsiveness. Unlike the *chy1* mutant that is disrupted in valine catabolism, *ibr1* mutants are not sucrose dependent (Figure 3A). Moreover, in contrast to *chy1*, *ibr1* does not display increased sensitivity to isobutyrate or propionate (Figure 3B).

Ultimately, testing these competing hypotheses will require biochemical assays to determine the preferred substrates and specific activity of each enzyme. If potential substrates become available, we will be able to determine the nature of the activity of the IBR enzymes on intermediates in IBA metabolism, revealing each as a direct enzymatic player or as an indirect

participant acting in a pathway that overlaps or interferes with IBA metabolism in the peroxisome. In addition to determining the enzymatic activity of IBR1, IBR3, and IBR10, enzymes catalyzing other steps of the pathway remain to be identified. The activating enzyme that adds CoA onto IBA (Figure 8, step 1) has not been identified; LACS6 and LACS7 act on fatty acid substrates but appear not to act on IBA (FULDA *et al.* 2004). In addition, the enzyme acting in the thiolase step (Figure 8, step 5) has not been established. Although PED1 is the best-characterized and most active thiolase, two other thiolases (KAT1 and KAT5) are encoded in the Arabidopsis genome (GERMAIN *et al.* 2001; CARRIE *et al.* 2007) and could act on IBA intermediates. Furthermore, we expect that an enzyme to remove the CoA moiety (Figure 8, step 6) will be required; several thioesterases with unknown substrates are predicted to reside in the peroxisome (REUMANN *et al.* 2004) and may catalyze this reaction. Finally, IAA acts outside of the peroxisome and therefore a transporter is expected to export the active auxin; whether this transporter removes IAA or IAA-CoA also is an open question.

Although our genetic evidence in Arabidopsis suggests that IBA must be converted to IAA to exert auxin activity, IBA is proposed to promote lateral root formation in rice independently of IAA signaling (CHHUN *et al.* 2003). Interestingly, IBR3 (ZOLMAN *et al.* 2007), IBR1 (Figure 5), and IBR10 (Figure 7) all have close homologs in rice that are predicted to be peroxisomal; the conservation of these proteins hints that IBA β-oxidation may play a role in auxin metabolism in rice as well. Further examination of these proteins and IBA metabolism in a variety of plants will reveal whether different species have evolved different roles for IBA in auxin metabolism and action.

Appropriate production, transport, and storage of IAA are essential for normal plant development. Our genetic studies implicate the peroxisomal enzymes IBR1 and IBR10 as likely players in the β-oxidation of IBA to free IAA, in conjunction with the previously characterized IBR3. Continued elucidation of the regulation and mechanism of this conversion will provide a more complete understanding of inputs into the auxin pool and the control of auxin homeostasis.

We thank the Arabidopsis Biological Resource Center at Ohio State University for seeds and DNA stocks; the Salk Institute Genomic Analysis Laboratory for generating the sequence-indexed Arabidopsis T-DNA insertion mutants; and Matthew Lingard, Sarah Ratzel, Lucia Strader, and Andrew Woodward for critical comments on the manuscript. This research was supported by the University of Missouri at St. Louis start-up funds, the University of Missouri Research Board, the National Science Foundation (NSF) (IBN-0315596 and MCB-0745122), and the Robert A. Welch Foundation (C-1309). N.M. was supported in part by the Rice-Houston Alliance for Graduate Education and the Professoriate program (NSF HRD-0450363) and the National Institutes of Health (NIH) (F31-GM081911). A.M. was supported in part by an American Society of Plant Biologists' Summer Undergraduate Research Fellowship, and A.R.A. was supported by the NIH (F31-GM066373) and a Houston Livestock Show and Rodeo Fellowship.

LITERATURE CITED

ADHAM, A. R., B. K. ZOLMAN, A. MILLIUS and B. BARTEL, 2005 Mutations in Arabidopsis acyl-CoA oxidase genes reveal distinct and overlapping roles in β-oxidation. Plant J. **41:** 859–874.

AGNIHOTRI, G., and H.-W. LIU, 2003 Enoyl-CoA hydratase: reaction, mechanism, and inhibition. Bioorg. Med. Chem. **11:** 9–20.

ALONSO, J. M., A. N. STEPANOVA, T. J. LEISSE, C. J. KIM, H. CHEN *et al.*, 2003 Genome-wide insertional mutagenesis of *Arabidopsis thaliana.* Science **301:** 653–657.

ARAI, Y., M. HAYASHI and M. NISHIMURA, 2008 Proteomic analysis of highly purified peroxisomes from etiolated soybean cotyledons. Plant Cell Physiol. **49:** 526–539.

AUSUBEL, F. M., R. BRENT, R. E. KINGSTON, D. D. MOORE, J. G. SEIDMAN *et al.*, 1999 *Current Protocols in Molecular Biology.* Greene Publishing Associates and Wiley-Interscience, New York.

BAKER, A., I. GRAHAM, M. HOLDSWORTH, S. SMITH and F. THEODOULOU, 2006 Chewing the fat: beta-oxidation in signalling and development. Trends Plant Sci. **11:** 124–132.

BARTEL, B., and G. R. FINK, 1994 Differential regulation of an auxin-producing nitrilase gene family in *Arabidopsis thaliana.* Proc. Natl. Acad. Sci. USA **91:** 6649–6653.

BARTEL, B., and G. R. FINK, 1995 ILR1, an amidohydrolase that releases active indole-3-acetic acid from conjugates. Science **268:** 1745–1748.

BARTEL, B., S. LECLERE, M. MAGIDIN and B. K. ZOLMAN, 2001 Inputs to the active indole-3-acetic acid pool: *de novo* synthesis, conjugate hydrolysis, and indole-3-butyric acid β-oxidation. J. Plant Growth Regul. **20:** 198–216.

BENNETT, M. J., A. MARCHANT, H. G. GREEN, S. T. MAY, S. P. WARD *et al.*, 1996 *Arabidopsis AUX1* gene: a permease-like regulator of root gravitropism. Science **273:** 948–950.

BEVAN, M., 1984 Binary *Agrobacterium* vectors for plant transformation. Nucleic Acids Res. **12:** 8711–8721.

CARRIE, C., M. W. MURCHA, A. H. MILLAR, S. M. SMITH and J. WHELAN, 2007 Nine 3-ketoacyl-CoA thiolases (KATs) and acetoacetyl-CoA thiolases (ACATs) encoded by five genes in Arabidopsis thaliana are targeted either to peroxisomes or cytosol but not to mitochondria. Plant Mol. Biol. **63:** 97–108.

CHENG, W.-H., A. ENDO, L. ZHOU, J. PENNEY, H.-C. CHEN *et al.*, 2002 A unique short-chain dehydrogenase/reductase in Arabidopsis glucose signaling and abscisic acid biosynthesis and functions. Plant Cell **14:** 2723–2743.

CHHUN, T., S. TAKETA, S. TSURUMI and M. ICHII, 2003 The effects of auxin on lateral root initiation and root gravitropism in a lateral rootless mutant *Lrt1* of rice (*Oryza sativa L.*). Plant Growth Regul. **39:** 161–170.

CLOUGH, S. J., and A. F. BENT, 1998 Floral dip: a simplified method for *Agrobacterium*-mediated transformation of *Arabidopsis thaliana.* Plant J. **16:** 735–743.

COPENHAVEN, G. P., K. NICKEL, T. KUROMORI, M. BENITO, S. KAUL *et al.*, 1999 Genetic definition and sequence analysis of *Arabidopsis* centromeres. Science **286:** 2468–2474.

DAVIES, R. T., D. H. GOETZ, J. LASSWELL, M. N. ANDERSON and B. BARTEL, 1999 *IAR3* encodes an auxin conjugate hydrolase from Arabidopsis. Plant Cell **11:** 365–376.

DELONG, A., A. CALDERON-URREA and S. L. DELLAPORTA, 1993 Sex determination gene TASSELSEED2 of maize encodes a short-chain alcohol dehydrogenase required for stage-specific floral organ abortion. Cell **74:** 757–768.

EASTMOND, P. J., and I. A. GRAHAM, 2000 The multifunctional protein AtMFP2 is co-ordinately expressed with other genes of fatty acid β-oxidation during seed germination in *Arabidopsis thaliana* (L.). Heynh. Biochem. Soc. Trans. **28:** 95–99.

EASTMOND, P. J., V. GERMAIN, P. R. LANGE, J. H. BRYCE, S. M. SMITH *et al.*, 2000 Postgerminative growth and lipid catabolism in oilseeds lacking the glyoxylate cycle. Proc. Natl. Acad. Sci. USA **97:** 5669–5674.

FAN, J., S. QUAN, T. ORTH, C. AWAI, J. CHORY et al., 2005 The Arabidopsis PEX12 gene is required for peroxisome biogenesis and is essential for development. Plant Physiol. **139:** 231–239.

FAWCETT, C. H., R. L. WAIN and F. WIGHTMAN, 1960 The metabolism of 3-indolylalkanecarboxylic acids, and their amides, nitriles and methyl esters in plant tissues. Proc. R. Soc. Lond. Ser. B **152:** 231–254.

FOOTITT, S., S. P. SLOCOMBE, V. LARNER, S. KURUP, Y. WU et al., 2002 Control of germination and lipid mobilization by *COMATOSE*, the *Arabidopsis* homologue of human ALDP. EMBO J. **21:** 2912–2922.

FRANSEN, M., P. VAN VELDHOVEN and S. SUBRAMANI, 1999 Identification of peroxisomal proteins by using M13 phage protein VI phage display: molecular evidence that mammalian peroxisomes contain a 2,4-dienoyl-CoA reductase. Biochem. J. **340:** 561–568.

FRANSZ, P. F., S. ARMSTRONG, J. H. DE JONG, L. D. PARNELL, C. VAN DRUNEN et al., 2000 Integrated cytogenic map of chromosome arm 4S of *A. thaliana*: structural organization of of heterochromatic knob and centromere region. Cell **100:** 367–376.

FROMAN, B. E., P. C. EDWARDS, A. G. BURSCH and K. DEHESH, 2000 ACX3, a novel medium-chain acyl-coenzyme A oxidase from Arabidopsis. Plant Physiol. **123:** 733–741.

FULDA, M., J. SCHNURR, A. ABBADI, E. HEINZ and J. BROWSE, 2004 Peroxisomal acyl-CoA synthetase activity is essential for seedling development in *Arabidopsis thaliana*. Plant Cell **16:** 394–405.

FULDA, M., J. SHOCKEY, M. WERBER, F. P. WOLTER and E. HEINZ, 2002 Two long-chain acyl-CoA synthetases from *Arabidopsis thaliana* involved in peroxisomal fatty acid β-oxidation. Plant J. **32:** 93–103.

GARCIA, C., J. JOUBES, S. CHEVALIER, J. LAROCHE-TRAINEAU, B. BOURDENX et al., 2007 *AtHCD1* encodes a 3-hydroxyacyl-CoA dehydratase involved in wax biosynthesis in *Arabidopsis thaliana*, pp. 203–206 in *17th International Symposium on Plant Lipids*, edited by C. BENNING and J. OHLROGGE. Aardvark Global, East Lansing, MI.

GEISBRECHT, B. V., D. ZHU, K. SCHULTZ, K. NAU, J. C. MORRELL et al., 1998 Molecular characterization of *Saccharomyces cerevisiae* delta3, delta2-enoyl-CoA isomerase. J. Biol. Chem. **273:** 33184–33191.

GEISBRECHT, B. V., D. ZHANG, H. SCHULZ and S. J. GOULD, 1999 Characterization of PECI, a novel monofunctional delta 3,delta 2-enoyl-CoA isomerase of mammalian peroxisomes. J. Biol. Chem. **274:** 21797–21803.

GERMAIN, V., E. L. RYLOTT, T. R. LARSON, S. M. SHERSON, N. BECHNTOLD et al., 2001 Requirement for 3-ketoacyl-CoA thiolase-2 in peroxisome development, fatty acid β-oxidation and breakdown of triacylglycerol in lipid bodies of *Arabidopsis* seedlings. Plant J. **28:** 1–12.

GRAHAM, I. A., and P. J. EASTMOND, 2002 Pathways of straight and branched chain fatty acid catabolism in higher plants. Prog. Lipid Res. **41:** 156–181.

GUILFOYLE, T. J., 1999 Auxin-regulated genes and promoters, pp. 423–459 in *Biochemistry and Molecular Biology of Plant Hormones*, edited by P. J. J. HOOYKAAS, M. A. HALL and K. R. LIBBENGA. Elsevier, Amsterdam.

HAUGHN, G. W., and C. SOMERVILLE, 1986 Sulfonylurea-resistant mutants of *Arabidopsis thaliana*. Mol. Gen. Genet. **204:** 430–434.

HAYASHI, H., L. DE BELLIS, A. CIURLI, M. KONDO, M. HAYASHI et al., 1999 A novel acyl-CoA oxidase that can oxidize short-chain acyl-CoA in plant peroxisomes. J. Biol. Chem. **274:** 12715–12721.

HAYASHI, H., K. NITO, R. TAKEI-HOSHI, M. YAGI, M. KONDO et al., 2002 Ped3p is a peroxisomal ATP-binding cassette transporter that might supply substrates for fatty acid β-oxidation. Plant Cell Physiol. **43:** 1–11.

HAYASHI, M., K. TORIYAMA, M. KONDO and M. NISHIMURA, 1998 2,4-Dichlorophenoxybutyric acid-resistant mutants of Arabidopsis have defects in glyoxysomal fatty acid β-oxidation. Plant Cell **10:** 183–195.

HOLDEN, H. M., M. M. BENNING, T. HALLER and J. A. GERLT, 2001 The crotonase superfamily: divergently related enzymes that catalyze different reactions involving acyl coenzyme A thioesters. Acc. Chem. Res. **34:** 145–157.

HOOKS, M. A., F. KELLAS and I. A. GRAHAM, 1999 Long-chain acyl-CoA oxidases of *Arabidopsis*. Plant J. **20:** 1–13.

KALLBERG, Y., and B. PERSSON, 2006 Prediction of coenzyme specificity in dehydrogenases/reductases. FEBS J. **273:** 1177–1184.

KALLBERG, Y., U. OPPERMANN, H. JORNVALL and B. PERSSON, 2002 Short-chain dehydrogenase/reductases (SDRs): coenzyme-based functional assignments in completed genomes. Eur. J. Biochem. **269:** 4409–4417.

KALLBERG, Y., U. OPPERMANN, H. JORNVALL and B. PERSSON, 2007 Short-chain dehydrogenase/reductase (SDR) relationships: a large family with eight clusters common to human, animal, and plant genomes. Protein Sci. **11:** 636–641.

KAMADA, T., K. NITO, H. HAYASHI, S. MANO, M. HAYASHI et al., 2003 Functional differentiation of peroxisomes revealed by expression profiles of peroxisomal genes in *Arabidopsis thaliana*. Plant Cell Physiol. **44:** 1275–1289.

KEINER, R., H. KAISER, K. NAKAJIMA, T. HASHIMOTO and B. DRAGER, 2002 Molecular cloning, expression and characterization of tropinone reductase II, an enzyme of the SDR family in Solanum tuberosum (L.). Plant Mol. Biol. **48:** 299–308.

KONCZ, C., J. SCHELL and G. P. RÉDEI, 1992 T-DNA transformation and insertion mutagenesis, pp. 224–273 in *Methods in Arabidopsis Research*, edited by C. KONCZ, N.-H. CHUA and J. SCHELL. World Scientific, Singapore.

LANGE, P., P. EASTMOND, K. MADAGAN and I. GRAHAM, 2004 An Arabidopsis mutant disrupted in valine catabolism is also compromised in peroxisomal fatty acid beta-oxidation. FEBS Lett. **571:** 147–153.

LEBEL-HARDENACK, S., D. YE, H. KOUTNIKOVA, H. SAEDLER and S. GRANT, 1997 Conserved expression of a TASSELSEED2 homolog in the tapetum of the dioecious Silene latifolia and Arabidopsis thaliana. Plant J. **12:** 515–526.

LECLERE, S., and B. BARTEL, 2001 A library of *Arabidopsis* 35S-cDNA lines for identifying novel mutants. Plant Mol. Biol. **46:** 695–703.

LEI, Z., W. CHEN, M. ZHANG and J. L. NAPOLI, 2003 Reduction of *all-trans*-retinal in the mouse liver peroxisome fraction by the short-chain dehydrogenase/reductase RRD: induction by the PPARα ligand clofibrate. Biochemistry **42:** 4190–4196.

LEYSER, H. M. O., F. B. PICKETT, S. DHARMASIRI and M. ESTELLE, 1996 Mutations in the *AXR3* gene of *Arabidopsis* result in altered auxin response including ectopic expression from the *SAUR-AC1* promoter. Plant J. **10:** 403–413.

LUCAS, K. A., J. R. FILLEY, J. M. ERB, E. R. GRAYBILL and J. W. HAWES, 2007 Peroxisomal metabolism of propionic acid and isobutyric acid in plants. J. Biol. Chem. **282:** 24980–24989.

MARCHANT, A., J. KARGUL, S. T. MAY, P. MULLER, A. DELBARRE et al., 1999 AUX1 regulates root gravitropism in *Arabidopsis* by facilitating auxin uptake within root apical tissues. EMBO J. **18:** 2066–2073.

MARCHLER-BAUER, A., and S. BRYANT, 2004 CD-search: protein domain annotations on the fly. Nucleic Acids Res. **32:** 327–331.

MICHAELS, S. D., and R. M. AMASINO, 1998 A robust method for detecting single nucleotide changes as polymorphic markers by PCR. Plant J. **14:** 381–385.

MURSULA, A. M., D. M. F. VAN AALTEN, J. K. HILTUNEN and R. K. WIERENGA, 2001 The crystal structure of [delta]3-[delta]2-enoyl-CoA isomerase. J. Mol. Biol. **309:** 845–853.

NAGPAL, P., L. M. WALKER, J. C. YOUNG, A. SONAWALA, C. TIMPTE et al., 2000 *AXR2* encodes a member of the Aux/IAA protein family. Plant Physiol. **123:** 563–573.

NEFF, M. M., J. D. NEFF, J. CHORY and A. E. PEPPER, 1998 dCAPS, a simple technique for the genetic analysis of single nucleotide polymorphisms: experimental applications in Arabidopsis thaliana genetics. Plant J. **14:** 387–392.

NEWMAN, T., F. J. DE BRUIJN, P. GREEN, K. KEEGSTRA, H. KENDE et al., 1994 Genes galore: a summary of methods for accessing results from large-scale partial sequencing of anonymous *Arabidopsis* cDNA clones. Plant Physiol. **106:** 1241–1255.

PELLEGRINI, S., S. CENSINI, S. GUIDOTTI, P. IACOPETTI, M. ROCCHI et al., 2002 A human short-chain dehydrogenase/reductase gene: structure, chromosomal localization, tissue expression and subcellular localization of its product. Biochim. Biophys. Acta **1574:** 215–222.

PICKETT, F. B., A. K. WILSON and M. ESTELLE, 1990 The *aux1* mutation of *Arabidopsis* confers both auxin and ethylene resistance. Plant Physiol. **94:** 1462–1466.

PINFIELD-WELLS, H., E. L. RYLOTT, A. D. GILDAY, S. GRAHAM, K. JOB et al., 2005 Sucrose rescues seedling establishment but not ger-

mination of Arabidopsis mutants disrupted in peroxisomal fatty acid catabolism. Plant J. **43:** 861–872.

Poirier, Y., V. D. Antonenkov, T. Glumoff and J. K. Hiltunen, 2006 Peroxisomal [beta]-oxidation: a metabolic pathway with multiple functions. Biochim. Biophys. Acta **1763:** 1413–1426.

Rampey, R. A., S. LeClere, M. Kowalczyk, K. Ljung, G. Sandberg *et al.*, 2004 A family of auxin-conjugate hydrolases that contributes to free indole-3-acetic acid levels during Arabidopsis germination. Plant Physiol. **135:** 978–988.

Reumann, S., C. Ma, S. Lemke and L. Babujee, 2004 AraPerox: a database of putative Arabidopsis proteins from plant peroxisomes. Plant Physiol. **136:** 2587–2608.

Reumann, S., L. Babujee, C. Ma, S. Wienkoop, T. Siemsen *et al.*, 2007 Proteome analysis of Arabidopsis leaf peroxisomes reveals novel targeting peptides, metabolic pathways, and defense mechanisms. Plant Cell **19:** 3170–3193.

Richmond, T. A., and A. B. Bleecker, 1999 A defect in β-oxidation causes abnormal inflorescence development in Arabidopsis. Plant Cell **11:** 1911–1923.

Richmond, T., and S. Sommerville, 2000 Chasing the dream: plant EST microarrays. Curr. Opin. Plant Biol. **3:** 108–116.

Rouse, D., P. Mackay, P. Stirnberg, M. Estelle and O. Leyser, 1998 Changes in auxin response from mutations in an *AUX/IAA* gene. Science **279:** 1371–1373.

Rylott, E. L., C. A. Rogers, A. D. Gilday, T. Edgell, T. R. Larson *et al.*, 2003 *Arabidopsis* mutants in short- and medium-chain acyl-CoA oxidase activities accumulate acyl-CoAs and reveal that fatty acid β-oxidation is essential for embryo development. J. Biol. Chem. **278:** 21370–21377.

Rylott, E. L., P. J. Eastmond, A. D. Gilday, S. P. Slocombe, T. R. Larson *et al.*, 2006 The Arabidopsis thaliana multifunctional protein gene (MFP2) of peroxisomal beta-oxidation is essential for seedling establishment. Plant J. **45:** 930–941.

Schilmiller, A. L., A. J. K. Koo and G. A. Howe, 2007 Functional diversification of acyl-coenzyme A oxidases in jasmonic acid biosynthesis and action. Plant Physiol. **143:** 812–824.

Shafqat, N., J. Shafqat, G. Eissner, H. Marschall, K. Tryggvason *et al.*, 2006 Hep27, a member of the short-chain dehydrogenase/reductase family, is an NADPH-dependent dicarbonyl reductase expressed in vascular endothelial tissue. Cell. Mol. Life Sci. **63:** 1205–1213.

Stasinopoulos, T. C., and R. P. Hangarter, 1990 Preventing photochemistry in culture media by long-pass light filters alters growth of cultured tissues. Plant Physiol. **93:** 1365–1369.

Theodoulou, F. L., K. Job, S. P. Slocombe, S. Footitt, M. Holdsworth *et al.*, 2005 Jasmonic acid levels are reduced in COMATOSE ATP-binding cassette transporter mutants: implications for transport of jasmonate precursors into peroxisomes. Plant Physiol. **137:** 835–840.

Timpte, C., A. K. Wilson and M. Estelle, 1994 The *axr2–1* mutation of *Arabidopsis thaliana* is a gain-of-function mutation that disrupts an early step in auxin response. Genetics **138:** 1239–1249.

van der Krieken, W. M., J. Kodde, M. H. M. Visser, D. Tsardakas, A. Blaakmeer *et al.*, 1997 Increased induction of adventitious rooting by slow release auxins and elicitors, pp. 95–104 in *Biology of Root Formation and Development*, edited by A. Altman and Y. Waisel. Plenum Press, New York.

Wain, R. L., and F. Wightman, 1954 The growth-regulating activity of certain ω-substituted alkyl carboxylic acids in relation to their β-oxidation within the plant. Proc. R. Soc. Lond. Ser. B **142:** 525–536.

Wolf, G., 1984 Multiple functions of vitamin A. Physiol. Rev. **64:** 873–936.

Wong, B. J., and J. A. Gerlt, 2004 Evolution of function in the Crotonase superfamily: (3S)-methylglutaconyl-CoA hydratase from Pseudomonas putida. Biochemistry **43:** 4646–4654.

Woodward, A. W., and B. Bartel, 2005a The *Arabidopsis* peroxisomal targeting signal type 2 receptor PEX7 is necessary for peroxisome function and dependent on PEX5. Mol. Biol. Cell **16:** 573–583.

Woodward, A. W., and B. Bartel, 2005b Auxin: regulation, action, and interaction. Ann. Bot. **95:** 707–735.

Zhang, D., W. Yu, B. V. Geisbrecht, S. J. Gould, H. Sprecher *et al.*, 2002 Functional characterization of delta 3,delta 2-enoyl-CoA isomerases from rat liver. J. Biol. Chem. **277:** 9127–9132.

Zimmermann, P., M. Hirsch-Hoffmann, L. Hennig and W. Gruissem, 2004 GENEVESTIGATOR: Arabidopsis microarray database and analysis toolbox. Plant Physiol. **136:** 2621–2632.

Zolman, B. K., and B. Bartel, 2004 An *Arabidopsis* indole-3-butyric acid-response mutant defective in PEROXIN6, an apparent ATPase implicated in peroxisomal function. Proc. Natl. Acad. Sci. USA **101:** 1786–1791.

Zolman, B. K., A. Yoder and B. Bartel, 2000 Genetic analysis of indole-3-butyric acid responses in *Arabidopsis thaliana* reveals four mutant classes. Genetics **156:** 1323–1337.

Zolman, B. K., M. Monroe-Augustus, B. Thompson, J. W. Hawes, K. A. Krukenberg *et al.*, 2001a *chy1*, an *Arabidopsis* mutant with impaired β-oxidation, is defective in a peroxisomal β-hydroxyisobutyryl-CoA hydrolase. J. Biol. Chem. **276:** 31037–31046.

Zolman, B. K., I. D. Silva and B. Bartel, 2001b The Arabidopsis *pxa1* mutant is defective in an ATP-binding cassette transporter-like protein required for peroxisomal fatty acid β-oxidation. Plant Physiol. **127:** 1266–1278.

Zolman, B. K., M. Monroe-Augustus, I. D. Silva and B. Bartel, 2005 Identification and functional characterization of Arabidopsis PEROXIN4 and the interacting protein PEROXIN22. Plant Cell **17:** 3422–3435.

Zolman, B. K., M. Nyberg and B. Bartel, 2007 IBR3, a novel peroxisomal acyl-CoA dehydrogenase-like protein required for indole-3-butyric acid response. Plant Mol. Biol. **64:** 59–72.

Communicating editor: D. Voytas